CNIC-01373
CNDC-0024
INDC(CPR)-048 / L

COMMUNICATION OF NUCLEAR DATA PROGRESS

No.21 (1999)

China Nuclear Data Center

China Nuclear Information Centre

Atomic Energy Press

Beijing, June, 1999

EDITORIAL NOTE

This is the 21th issue of *Communication of Nuclear Data Progress* (CNDP), in which the achievements of last half year in nuclear data field in China are carried. It includes the measurement of differential cross sections for ^{6}Li(n,t)^{4}He reaction at 3.67 and 4.42 MeV, 14 MeV neutron activation cross section for ^{93}Nb(n,2n) ^{92}Nb, reaction, double differential cross sections for ^{39}K(n,α) ^{36}Cl reaction at 4.41, 5.46, 6.52 MeV; theoretical calculations of n+^{235}U, ^{151,153,154,155}Eu, $^{135\sim138}$Ba ^{69,71}Ga, $^{83\sim86}$Kr at E_n=0.001~20 MeV; evaluations of neutron reaction cross sections for ^{140,141,142,144}Ce, ^{63,65,Nat}Cu, ^{115}In, ^{105,108}Pα and ^{103}Rh, complete data for ^{63}Cu, and photonuclear reaction for ^{90,91,92,94,96}Zr, nuclear data sheets for A=195 and thermal-neutron captures data evaluation for A=1~19; construction of covariance matrix for absolute fission yield data measarement; thermal and fast reactor benchmark testing of ENDF/B-6.4. Also the activities on nuclear data in China are summarized.

The editors hope that our readers and colleagues will not spare their comments in order to improve this publication.

Please write to Profs. Liu Tingjin and Zhuang Youxiang
Mailing Address: China Nuclear Data Center
China Institute of Atomic Energy
P.O.Box 275 (41), Beijing 102413
People's Republic of China
Telephone: 86-10-69357729 or 69357830
Telex: 222373 IAE CN
Facsimile: 86-10-6935 7008
E-mail: tjliu @ mipsa.ciae.ac.cn or yxzhuang @ mipsa.ciae.ac.cn

EDITORIAL BOARD

CONTENTS

I EXPERIMENTAL MEASUREMENT

Differential Cross Section Measurement for $^{6}Li(n,t)^{4}He$ Reaction at 3.67 and 4.42 MeV

Zhang Guohui Tang Guoyou Chen Jinxiang
Shi Zhaomin Liu Guangzhi
(Institute of Heavy Ion Physics, Peking University, Beijing, 100871, China)

Zhang Xuemei Chen Zemin
(Department of Physics, Tsinghua University, Beijing 100084, China)

Yu. M. Dledenov M. Sedysheva G. Khuuknenkhuu
(Joint Institute for Nuclear Research, Dubna 141908, Russia)

Abstract

Using a gridded ionization chamber, the differential cross sections for $^{6}Li(n,t)^{4}He$ reaction were measured at 3.67 and 4.42 MeV. The neutrons were produced with $D(d,n)^{3}He$ reaction. Absolute neutron flux was determined through $^{238}U(n,f)$ and H(n,p) reaction. The result at 3.67 MeV is almost 90 degree symmetry but it is obviously forward peaked at 4.42 MeV in the center of mass system.

Introduction

The differential cross section data for $^{6}Li(n,t)^{4}He$ reaction are important for the study of reaction mechanism and in practical usage. Although there are some existing differential cross sections for $^{6}Li(n,t)^{4}He$ reaction, most of them were confined in keV region and at about 14 MeV. In MeV region, however, there are only few data, with large differences.

Using a gridded ionization chamber, we performed the measurement of differential cross sections for $^{6}Li(n,t)^{4}He$ reaction at 3.67 and 4.42 MeV.

1 Experimental Details

The gridded ionization chamber was described elsewhere[1]. For the present experiment, the working gas is Kr+2.37%CO_2. The distances from cathode to grid, grid to anode and anode to shield are 4.5, 2.2 and 1.1 cm, respectively.

The sample material is ^{6}LiF with the ^{6}Li abundance 91.24%. It was evaporated on a tungsten backing. The area and thickness of the sample are 15.90 cm^2 and 228.3 μg/cm^2. With the sample changer, there is also a tungsten film placed in the gridded ionization chamber for background measurement. A ^{238}U sample (1.066 mg, 2.0 cm^2) and a polyethylene film (17.84 cm^2, 23.20 mg, mass ratio of C to H 5.713) were employed inside the chamber for absolute neutron flux measurement.

Since the thermal neutron induced cross section of ^{6}Li (n,t) ^{4}He is as big as 936 b, the interference of tritium and alpha induced is very strong. Yet the Q value for ^{6}Li(n,t)^{4}He is as big as 4.786 MeV, the forward tritium or alpha events can be separated from those from thermal neutron induced tritium and alpha interference. The backward events can not be separated from thermal neutron induced interference because of the recoil of the residual nucleus. So instead of backward tritium measurement, forward alpha events were measured. In the center of mass system, one tritium event corresponds to one alpha event in opposite direction. Fig. 1 shows the two dimensional spectra of forward alpha for E_n=3.67 MeV.

For alpha measurement, the pressure was 1.05 atm* and the electrode voltages for cathode, grid and anode were −1500, 40 and 1200 V respectively. For tritium measurement the gas pressure was 4.5 atm and the voltages were −4750, 300 and 4100 V.

For tritium measurement, there is also alpha interference. Yet the interference is only confined in the region near 90 degree line, since the average free range of tritium is several times bigger than that of the alpha. For alpha measurement, since the pressure is low, tritium energy loss in the sensitivity volume is very small compared to alpha energy. Fig. 2 shows the two dimensional spectra for forward tritium measurement (E_n=4.42MeV).

A BF_3 long counter and a liquid scintillator (NE213) with n-gamma discrimination were used as relative neutron flux monitor. For tritium measurement the polyethylene film was used to calibrate absolute neutron flux, and for alpha measurement the ^{238}U sample was employed to determine absolute neutron flux. The

* 1 atm = 101 325 Pa

cross sections of H(n,p) and ^{238}U(n,f) reaction were taken from ENDF/B-6 library.

The experiment was performed at a 4.5 MV Van de Graaff accelerator of the Heavy Ion Physics, Peking University. Monoenergetic neutrons were produced through D(d,n) reaction with a deuteron gas target of 3.0 cm long and 2.0 atm in pressure separated from the vacuum tube by a molybdenum film 5 μm in thickness. The energies of the deuterons are 1.553 and 2.045 MeV and the correspondence neutron energy are 3.67±0.20 and 4.42 ±0.20 MeV. The deuteron beam was about 3.5 μA on the gas target during experiment. The chamber was placed at 0 degree to the beam line, and the distance from its cathode to the center of the neutron source was 38.0 cm. The samples were attached to the cathode.

The time for alpha or tritium event measurements is about 10 hours, and for background about 5 h. The neutron flux calibration time is about 7 h and 40 min for ^{238}U and H(n,p) respectively, corresponding to alpha and tritium event measurement.

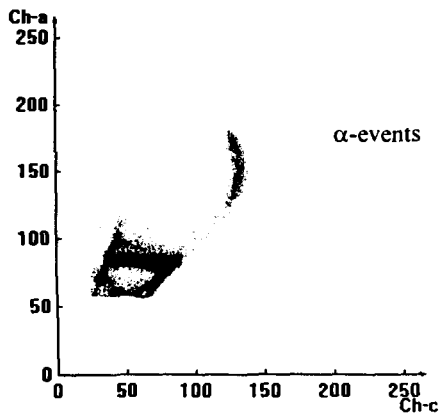

Fig. 1 The two dimensional spectra of forward alpha at E_n=3.67±0.20 MeV (Cathode channel Vs. anode channel)

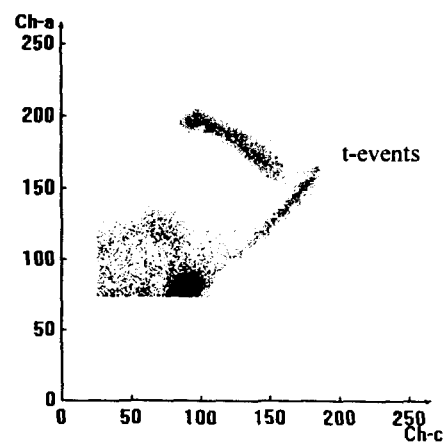

Fig. 2 The two dimensional spectra for forward tritium measurement at E_n=4.42±0.20 MeV

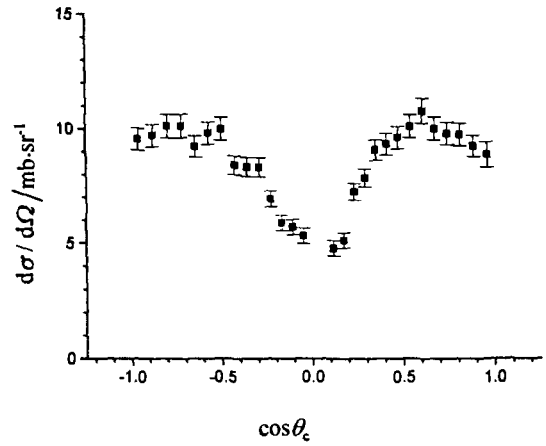

Fig. 3 Differential cross section for ^{6}Li(n,t)^{4}He reaction at E_n=3.67±0.20 MeV

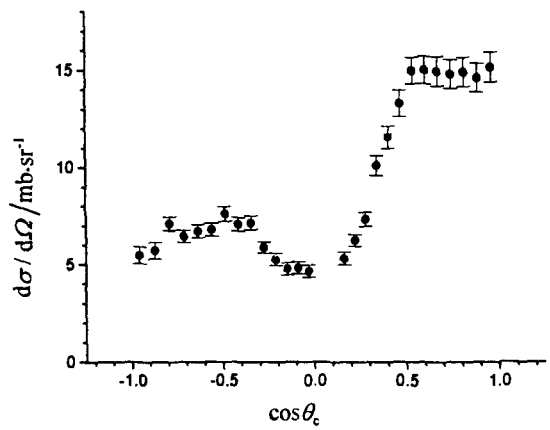

Fig. 4 Differential cross section for ^{6}Li(n,t)^{4}He reaction at E_n=4.42±0.20 MeV

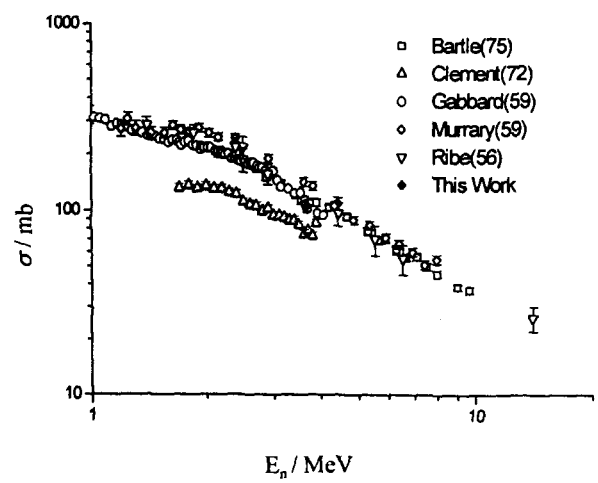

Fig. 5 The result of ^{6}Li(n,t) ^{4}He cross section compared with other measurements

2 Results and Discussion

Fig. 3 and 4 are the measured differential cross sections for tritium at 3.67 and 4.42 MeV in the center of mass system. The forward alpha data have been changed to backward tritium data. In dealing with forward tritium data, the region near 90 degree line ($\cos\theta_L$=0~0.3) were not included since there is alpha interference.

Principal sources of error include statistics for counts, background subtraction, uncertainty of $^{238}U(n,f)$ cross section and the nuclear number of the samples.

From the figures, one can see that at 3.67 MeV the differential cross section for tritium is almost symmetric about 90 degree but at 4.42 MeV it becomes obviously forward peaked. According to reference [2], in the center of mass system the angular distribution for tritium changes gradually from isotropic about eV neutron energy to strongly forward peaked at ~135 keV, and then to 90 degree symmetric near 300 keV. So, it is interesting to check how the angular distributions (or differential cross sections) change from 300 keV to 3.67 MeV, from 3.67 to 4.42 MeV and above 4.42 MeV. Our result are only at two energy points and the energy spread is somewhat big. It is considered that further study is needed.

Cross sections for $^{6}Li(n,t)^{4}He$ reaction at 3.67 and 4.42 MeV were derived from the differential data via Legendre fitting. In Fig. 5, the result was compared with existing data. It can be seen that our result is in good agreement with others, except Clement's.

The authors are indebted to China Nuclear Data Center for financial support. Dr. Zhang Guohui would like extend his thanks to Prof. Zhang Jingshang of CNDC for the helpful discussions. They also would like to thank the crew of 4.5 MV Van de Graaff of Peking University.

References

[1] Tang Guoyou, Zhang Guohui et al., INDC(CPR)-043/L(1997)

[2] H.-H.Knitter, C.Budtz-Jφrgensen, D.L.Smith et al., Nucl. Sci. Eng., 83, 229-241(1983)

Activation Cross Section Measurements for $^{93}Nb(n,2n)^{92g}Nb$ Reaction Induced by 14 MeV Neutron

Li Gongping Kong Xiangzhong Yang Jingkang
(Department of Modern Physics, Lanzhou University, Lanzhou, 730000)

Abstract

The cross section for the $^{93}Nb(n,2n)^{92g}Nb$ reaction is measured by activation method . The experimental result is 1355±149 mb at the neutron energy of 14.6±0.3 MeV. And the excitation curve of $^{93}Nb(n,2n)^{92g}Nb$ reaction is calculated by using HFTT program in neutron energy range from 9 MeV to 16 MeV .

Introduction

The cross section of the reaction $^{93}Nb(n,2n)^{92g}Nb$ induced by 14 MeV neutron, which produces a long-lived radio-nuclide, is very important to nuclear science and engineering, nevertheless, the measurement is very difficult because the half-life of ^{92g}Nb is as long as 3.2×10^{7} years. So far only a few data have been published and there are large discrepancies among them[1,2]. Therefore we measured it by the activation method at the neutron energy 14.6±0.3 MeV and compared with the data from other authors and calculated the excitation curve of $^{93}Nb(n,2n)^{92g}Nb$ reaction using HFTT program [3] in neutron energy range from 9 MeV to 16 MeV .

1 Experimental Procedure

1.1 Irradiation

The irradiation of the sample was carried out at the ZF–300–II Intense Neutron Generator of Lanzhou University with neutron yield about $(1\sim3)\times10^{12}$n/s. Neutrons were produced by $T(d,n)^{4}He$ reaction with an effective deuteron beam energy of 125 keV and a beam current of 20 mA. The thickness of T-Ti target used was 0.9 mg/cm^2.The neutron flux was monitored by using an uranium ionization chamber, the corrections were made for the variance of neutron flux during the irradiation. The sample was placed at 0° angle relative to the beam direction with a

distance about 3 cm away from the neutron source , and irradiated for about 20 h. The cross section of the reaction was determined relatively to the cross section of $^{93}Nb(n,2n)^{92m}Nb$ reaction of the sample itself. In this experiment , the sample of Nb was natural metal foil with 20 mm in diameter and 3 mm in thickness and 99.99% in purity. The weight of the sample was 2.5620 g. The neutron energy was determined by the method of cross section ratios for the reactions $^{90}Zr(n,2n)^{89m+g}Zr$ and $^{93}Nb(n,2n)^{92m}Nb$ [4]. The neutron energy was 14.6±0.3 MeV.

1.2 Activity measurement

After irradiation the activities of the sample were measured by gamma-ray spectroscopy using a coaxial HPGe detector in conjunction with an EG&G ORTEC 7450 Multichannel Analyzer and a computer. The relative efficiency of the detector was 20%, and the energy resolution was 2.7 keV at 1.33 MeV. The efficiency of the detector was calibrated by using a group of standard gamma sources, Standard Reference Material 4275 was got from the National Institute of Standard and Technology, Washington, D.C., USA. An absolute efficiency calibration curve was obtained at a distance of 20 cm from the surface of the germanium crystal. Therefore the coincidence losses can be neglected. In our case, however, we needed the efficiency at 2 cm as the actual counting position because of the weak activity of the ^{92g}Nb nuclide. So the efficiency ratios of two positions were evaluated as a function of energy. The absolute efficiency calibration curve at 2 cm was obtained from the efficiency at 20 cm and the efficiency ratio curve. The error in the absolute efficiency curve at 2 cm was estimated to be ~1.5%, while the error of the activity of the standard source was ~1%.

Because the characteristic γ ray energy of ^{92m}Nb is the same as that of ^{92g}Nb, ^{92m}Nb was measured after the sample was cooled for 39.65 days and the duration of measuring was 3.15 min. There for the influence of ^{92g}Nb upon ^{92m}Nb characteristic γ ray counts can be neglected, for the half-life of ^{92g}Nb is extremely long. Due to the low activity of ^{92g}Nb, the sample should be cooled again for six and a half years so as to avoid interference from ^{92m}Nb and any other nuclides with activity middle or short half lives. Then the cooled sample was measured again and the measuring duration was 153.8 h.

The abundance and half-lives of the residual nuclei, together with the characteristic gamma-ray energies and absolute intensities are listed in Table 1[5].

Table 1 Parameters of concerned reactions

Reaction	Abundance (%)	half-life	E_γ/keV	I_γ
$^{93}Nb(n,2n)^{92m}Nb$	100	10.15 d	934.53	99.2
$^{93}Nb(n,2n)^{92g}Nb$	100	3.2×10^7 y	934.53	100

2 Results and Discussion

The cross sections can be calculated by the following formula [6] :

$$\sigma_x = \frac{(\varepsilon I_\gamma NKSMD)_m (\lambda AFC)_x}{(\varepsilon I_\gamma NKSMD)_x (\lambda AFC)_m} \sigma_m$$

where the subscript m represents the monitor reaction and x corresponding to the measured reaction. ε is the efficiency of the full-energy peak for measured γ-ray, I_γ—absolute γ-ray intensity, N—abundance of the target nuclide, M—mass of the sample, D—counting collection factor, $D=e^{\lambda t_1}-e^{\lambda t_2}$, t_1,t_2= time intervals from the end of the irradiation to the start and end of counting, respectively, A—atomic mass, C—full—energy peak area, F–total correction factor of the activity:

$$F = f_s f_o f_g$$

where f_s, f_o , and f_g are correction factors for the self absorption of the sample at a given γ-ray energy, the effect of cascade γ-rays in the investigated nuclide and the counting geometry, respectively.

K—neutron flux fluctuation factor:

$$K = [\sum_i^L \Phi_i (1-e^{-\lambda \Delta t_i}) e^{-\lambda T_i}] / \Phi$$

where L–number of time intervals to which the irradiation time was divided, Δt_i–duration of the i'th time interval, λ–decay constant, T_i–time interval from the end of the i'th interval to the end of irradiation, Φ_i–neutron flux averaged over the sample in Δt_i, Φ–neutron flux averaged over the sample in the total irradiation time T. $S=1-e^{-\lambda T}$ growth factor of residual nuclide.

In our experiment, the measured cross section of $^{93}Nb(n,2n)^{92g}Nb$ is 1355±149 mb at neutron energy 14.6±0.3 MeV, and the standard cross section of $^{93}Nb(n,2n)$

^{92m}Nb is 459±4.9 mb [7]. The stability of the activity measurement system was very important for this work, so the error of the γ-ray activity measurement was also larger. The major experimental error of the cross section comes from the counting statistics error of the ^{92g}Nb characteristic gamma-ray full-energy peak area.

Table 2 Cross sections for ^{93}Nb(n,2n)^{92}Nb

Data sources	Neutron energy/MeV	Cross section/mb	Remarks
present work	14.6±0.3	1355±149	Experiment
L.R.Vesser et al[1]	14.7±0.15	1279±88	Experiment
M.Haring et al[2]	14.1	1350±250	Experiment
H.Vonach et al[8]	14.1	1340±50	Calculation
H.Vonach et al[8]	14.1	1333±39	Evaluation
Yao Lishan et al[9]	14.0	1322±52	Evaluation
Yao Lishan et al[9]	14.0	1013	Calculation
present work	14.6	1353	Calculation

The results of present work and others work are shown in Table 2, and plotted in Fig.1 for ^{93}Nb(n,2n)^{92g}Nb reaction. It can be seen from Fig.1 that the cross section of ^{93}Nb(n,2n)^{92g}Nb reaction increase with the increasing neutron energy and present result is in good agreement with that of M. Haring's[2] experiment, H. Vonach's[8]

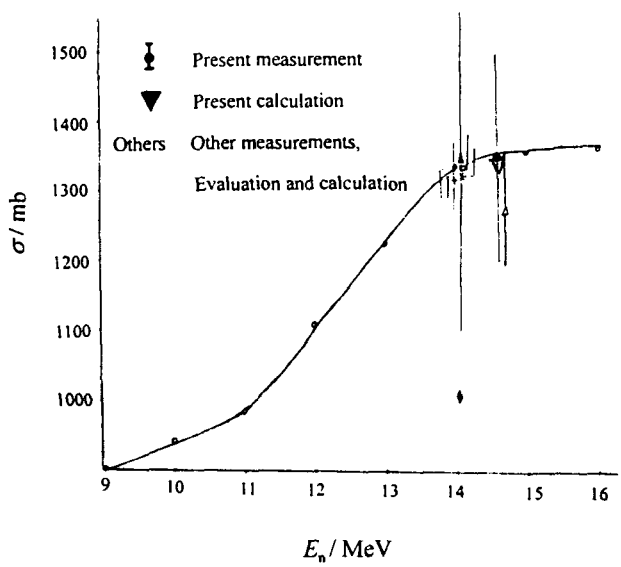

Fig. 1 The ^{93}Nb(n,2n)^{92g}Nb reaction cross section

calculation and evaluation, Yao Lishan's[9] evaluation, respectively. However L. R. Veeser's [1] experimental value is lower, but agreement with present experimental value in error range. The excitation curve of $^{93}Nb(n,2n)^{92g}Nb$ reaction was calculated using HFTT program in neutron energy range from 9 MeV to 16 MeV, and is agreement with present experimental value.

We would like to thank the group of the Intense Neutron Generator at Lanzhou University for the irradiation work and prof. Lu Hanlin for helpful comments and discussions.

Reference

[1] L.R.Veeser et al, Phy.Rev.C.16 1792-1802 (1977).

[2] M.Haring et al, Z.plysik 244, 352—357 (1971).

[3] Huang Feizeng et al, Universitis Pekinensis, (Acta Scientiarum Naturalium),25,289-299 (1989).

[4] V.E.Lewis et al, Nucl.Instrum. Method, 174,141-144 (1980).

[5] E.Browne, R.B.Firestone, Table of Radioactive Isotopes, John Wiley and Sons Prees, New York, (1986).

[6] Wang Youngchang et al, High Energy Physics and Nuclear Physics,14,919-922 (1990).

[7] Zhao Wenrong et al, NDC,CCPR. 18, (1989).

[8] H.Vonach et al, Nuclear Science and Engineering 106, 409—414(1990).

[9] Yao Lishan et al , High Energy Physics and Nuclear Physics , 11,533-542, (1987).

Measurement of Double Differential Cross Sections for $^{39}K(n,\alpha)^{36}Cl$ Reaction

Zhang Guohui Tang Guoyou Chen Jinxiang
Shi Zhaomin Liu Guangzhi
(Institute of Heavy Ion Physics, Peking University, Beijing 100871, China)

Yu. M. Gledenov M. Sedysheva G. Khuukhenkhuu
(Joint Institute for Nuclear Research, Dubna 141908, Russia)

Chen Zemin Chen Yingtang Zhang Xuemei Yuan Jing
(Department of Physics, Tsinghua University, Beijing 100084, China)

Introduction

$^{39}K(n,\alpha)^{36}Cl$ reaction data are important in nuclear engineering, nuclear medicine, astrophysics as well as in the study of nuclear mechanism. As we know, experimental data for $^{39}K(n,\alpha)^{36}Cl$ reaction are scanty and there is no double differential datum.

The double differential cross section data of $^{39}K(n,\alpha)^{36}Cl$ reaction were measured at 4.41±0.26, 5.46±0.21 and 6.52±0.16 MeV using a gridded ionization chamber (GIC).

1 Experiment

1.1 Setup

The twin GIC was constructed in Dubna, Russia, with five sample positions[1]. The electrodes area is 19×19 cm^2. In our experiment, the distances from cathode to grid, grid to anode, and anode to shield were 4.5, 2.2 and 1.1 cm, respectively. The working gas was Kr+2.73% CO_2 . For 4.41±0.26 and 5.46±0.21 MeV, the pressure of the working gas was 1.05 atm, the voltages of anode, cathode and grid were +1200, −1500 and 40 V; for 6.52±0.16 MeV they were 1.2 atm, +1400, −1800 and 20 V, respectively.

KI was chosen to be sample material, and the (n,α) interference of iodine and other potassium isotopes to ^{39}K is very little. Two KI samples 4.50 cm in diameter were placed at the same sample position, one in forward and another in backward direction. They were vacuum evaporated on tungsten backings and then attached to the cathode of the GIC. Their thickness is given in Table 1. Two tungsten backing films without samples were placed inside the GIC for background measurement.

The experiment was performed on the 4.5 MV Van de Graaff accelerator of the Institute of Heavy Ion Physics, Peking University. Monoenergetic neutrons were produced by D(d,n) reaction with a deuteron gas target 3.0 cm long and 2.4 atm in pressure separated from the vacuum system by a 5 μm Mo foil. The energy of the beam deuterons were 2.07, 2.85 and 3.77 MeV for 4.41±0.26, 5.46±0.21 and 6.52±0.16 MeV neutrons, and the beam current was about 3.5 μA during experiment. The GIC was placed 0^0 to the beam line, and the distance from the cathode of the GIC to the center of the neutron source was 39.1 cm.

To reduce the background, a collimator made of copper and iron, 12 cm in length was placed in front of the deuteron gas target.

A BF_3 long counter and a liquid scintillator detector (NE231) with n-γ discrimination were used as relative neutron flux monitor. A ^{238}U sample was placed at the same position as sample inside the GIC for the absolute neutron flux determination via $^{238}U(n,f)$ reaction by counting the fission fragments. The mass and the area of the ^{238}U sample were 1.066 mg and 2.0 cm^2 respectively.

Table 1 shows the position of the samples. The α-sources and the ^6LiF samples were used for 90^0 line determination and energy calibration.

Table 1 Sample position during experiment

	Forward	Backward
1	α-source	α-source
2	^6LiF	^6LiF
3	KI: 499.8 μg/cm^2	KI: 519.2 μg/cm^2
4	W	W
5		^{238}U

1.2 Process

The energy calibration and 90^0 line determination were performed using compound α-source and $^6Li(n_{th},t)^4He$ reaction. To deduct thermal neutrons, paraffin wax board was placed around the GIC.

For true plus background event measurement, the sample changer was turned to KI samples. Since the samples were thin and the cross sections were small, long bombarding time was needed. The measuring time was about 30 h for ture plus background events and that about 10 h for background. After measurement, we also performed energy calibration, to ensure that the system was stable. Using $^{238}U(n,f)$ reaction, the absolute neutron flux calibration was carried out. The bombarding time for ^{238}U was about 6 h. The cross section data of $^{238}U(n,f)$ reaction were taken from ENDF/B-6 library.

2 Results

Fig.1 shows the α double differential cross sections for E_n=4.41±0.26, 5.46±0.21 and 6.52±0.16 MeV at different angles (laboratory system). Fig. 2 shows the two dimensional spectra for forward α events at E_n=4.41±0.26 MeV. Fig. 3 illustrates integral cross sections compared with other experiments, they are in good agreement with others.

We use ^{238}U sample to decide the absolute neutron flux. The area of the KI sample is not the same as that of the ^{238}U sample, so their average neutron flux densities are not the same. Neutron flux density non-uniformity correction is needed to derive the neutron flux on KI sample from that on ^{238}U sample. The count loss caused by the geometrical efficiency of the GIC and the thickness of the KI sample are also corrected.

Error sources for the double differential cross section data is listed in Table 2.

Table 2 Principal source of errors

Source of uncertainty	Relative errors / %
$^{238}U(n,f)$ cross section	1.0~2.5
Interference from other K isotopes	< 1.0
Statistics for fission counts	2.5
Statistics for α counts	3. ~5.0
Background subtraction	2.0~3.0
Nuclear number of ^{238}U	3.0
Nuclear number of ^{39}K	0.5
total	< 8.0

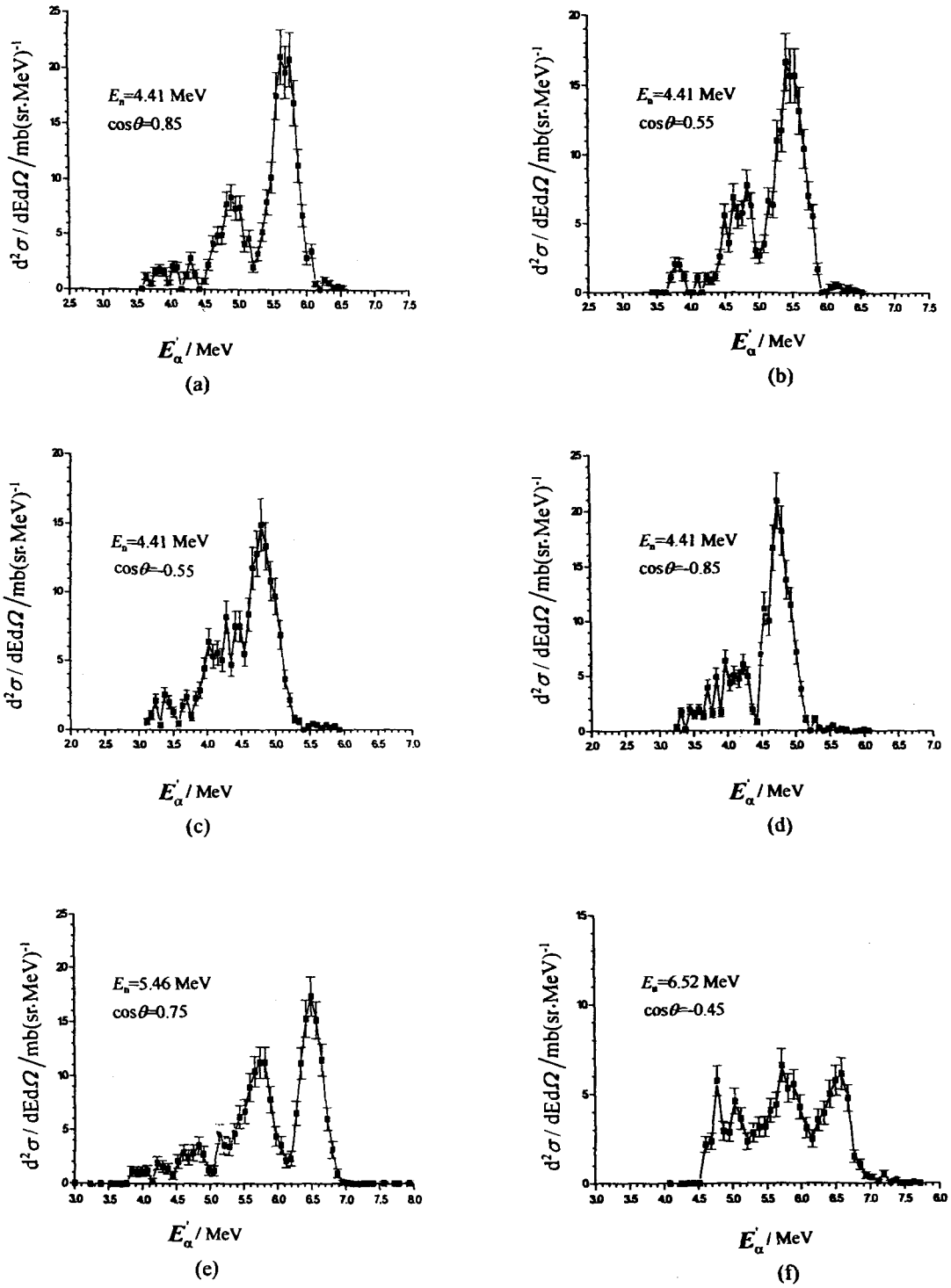

Fig. 1(a~f) The double differential cross sections of α for E_n=4.41±0.26, 5.46±0.21 and 6.52±0.16 MeV at different angles (laboratory system)

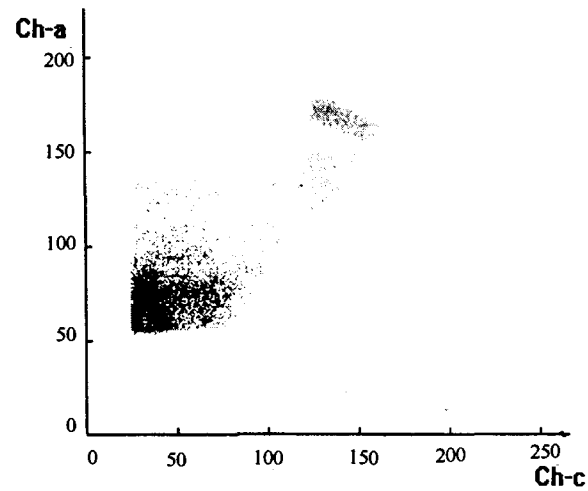

Fig. 2 The two dimensional spectra for forward α events at E_n=4.41±0.26 MeV (Cathode channel vs. anode channel)

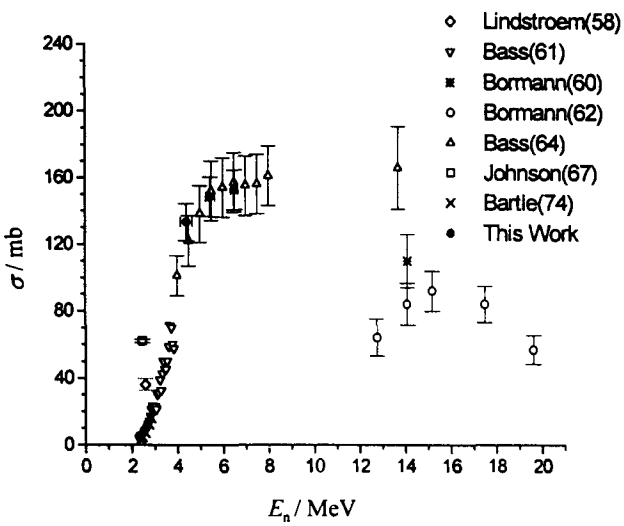

Fig. 3 $^{39}K(n,\alpha)^{36}Cl$ reaction cross section compared with other experiments

The authors would like to thank the China National Nuclear Corporation for the financial support and they appreciate the crew of 4.5 MV Van de Graaff accelerator at Peking University for their kind help.

Reference

[1] Tang Guoyou, Zhang Guohui et al., INDC(CPR)-043/L (1997)

II THEORETICAL CALCULATION

Calculations of Complete Data for n +^{235}U in the Energy Region 0.001~20 MeV

Cai Chonghai
(Department of Physics, Nankai University, Tianjin)
Shen Qingbiao Yu Baosheng
(China Nuclear Data Center, CIAE, Beijing)

Abstract

complete reaction cross sections, elastic scattering angular distributions, double differential cross sections and the γ production data of n+^{235}U in the energy region 0.001~20MeV were calculated, pretty good theoretical results in accordance with experimental data are obtained, and all calculational results are given in ENDF/B-6 format (including files,3,6,12~15).

^{235}U is a very important fissile nucleus for many kinds of thermal reactor, some kinds of fast reactor, as well as other nuclear installations. Furthermore, the fission cross section of ^{235}U is one of the standard cross sections. So very good calculation and evaluation data of its neutron reactions in the energy region 0.001~20 MeV are needed.

There are quite a lot of experimental data for σ_{tot}, σ_f and sufficient experimental data for $\sigma_{n,\gamma}$, some experimental data for $\sigma_{n,n}$, $\sigma_{n,2n}$, $\sigma_{n,3n}$, σ_{non}, σ_{el}, only one or two sets of data for $\sigma_{n,p}$ and $\sigma_{n,4n}$. There are 10 set of data for elastic scattering angular distributions from 0.5 MeV to 5.5 MeV. There are no any experimental data for other reaction cross sections, secondary neutron spectra, double differential cross sections and the γ production data. All of the experimental data were taken from EXFOR.

The Code APFO96 was used to automatically get the optimal parameters of optical potential. Because there are good evaluated values for ^{235}U in CENDL-2

given by Yu Baosheng, in this calculation we use Yu's evaluated σ_{tot}, σ_{non}, σ_{el}, $\sigma_{n,f}$ and $\sigma_{n,\gamma}$ as reference experimental data in automatically searching for the optimal optical potential parameters. The Code APFF[2] was used to automatically get the optimal fission parameters in low energy region (E less than about 4 MeV).

In this way, we get the final optimum set of optical potential parameters for neutron channel:

V_0=49.171188, V_1=0.537891, V_2=0.028673, W_0=6.905662, W_1=0.182540, U_0=0.202922, U_1=0.043414, U_2=0.001480, a_r=0.509773, a_s=0.661340, a_v=0.643472, r_r=1.272999, r_s=1.345910, r_v=1.339533.

The coupled channel optical model code ECSI was used to calculate the cross sections and angular distributions of direct inelastic scattering for 5 levels (their excited energies are 0.0462, 0.1030, 0.1707, 0.2491 and 0.3385 MeV). These direct inelastic scattering data and the optimum set of optical potential parameters for neutron channel are the input data using the kernel program FUNF[6].

The calculation formula as well as the fission parameters are some different in FUNF in comparison with APFF. Based on the program FUNF, we wrote a code ADFP[7] which can automatically search for an optimal set of fission parameters for first, second and third plateaus, respectively. The adjustable parameters in ADFP are 9 (2 level density parameters: $a_{n,\gamma}$ and $a_{n,n'}$, 3 pair energy corrections: $\Delta_{n,\gamma}$ $\Delta_{n,n'}$ and $\Delta_{n,f}$,V_f, $\hbar\omega$, K_1 for (n,f) reaction, as well as the multiplied factor Cel in $\sigma_{n,\gamma}$) for first plateau, 7 (level density parameter $a_{n,2n}$, pair energy corrections $\Delta_{n,2n}$ and $\Delta_{n,nf}$,V_f, $\hbar\omega$, K_1 for (n,n'f) reaction, as well as exciton model parameter CK) for second plateau, and 6 (level density parameter $a_{n,3n}$, pair corrections $\Delta_{n,3n}$ and $\Delta_{n,2nf}$,V_f, $\hbar\omega$, K_1 for (n,2nf) reaction) for third plateau. With ADFP, we can obtain a set of adjusted fission parameters to make $\sigma_{n,f}$, $\sigma_{n,\gamma}$, $\sigma_{n,n'}$, $\sigma_{n,2n}$, and $\sigma_{n,3n}$ in optimum agreement with experimental data.

The final parameters used are:

CK=1045.37, Cel=0.080, $\Delta_{n,p}$=1.070; $\sigma_{n,\gamma}$=28.177347, $\sigma_{n,n'}$=28.437643,

$\Delta_{n,\gamma}$=0.90714, $\Delta_{n,n'}$=0.14353, $\Delta_{n,f}$=0.463328, V_f=6.066017, $\hbar\omega$=0.864275,

K_1=6.447474 for $\sigma_{n,f}$

$a_{n,2n}$=26.3613, $\Delta_{n,2n}$=0.3634, $\Delta_{n,n'f}$=0.2595, V_f=5.8023, $\hbar\omega$=0.7546,

K_1=10.0 for $\sigma_{n,n'f}$

$a_{n,3n}$=27.8504, $\Delta_{n,2n}$=-0.0102, $\Delta_{n,2n'f}$=-0.1245, V_f=6.4611, $\hbar\omega$=0.7860,

K_1=1.0 for $\sigma_{n,2nf}$

For proton channel, some optimum parameters are changed to:

$a_r=a_s=a_v=a_{so}=0.45$, $r_r=r_{so}=1.25$, $r_s=r_v=1.20$.

The calculated σ_{tot}, σ_{non} and σ_{el} as well as their experimental data are given in Fig. 1 (a) and (b), from which we can see that calculated values are in very good accordance with experimental data except in E_n=0.1~2.0 MeV, where calculated σ_{tot} and σ_{el} are some higher than experimental data and Yu's evaluated values (otherwise we can not make both the calculated $\sigma_{n,f}$ and $\sigma_{n,n}$ in good accordance with experimental data). The calculated $\sigma_{n,f}$ as well as their experimental data are given in Fig. 2 (a) and (b), from which we can see that calculated values are in very good agreement with experimental data except in the energy region 0.05~0.7 MeV, where the calculated values are some lower than experimental data. The results of $\sigma_{n,\gamma}$ are given in Fig. 3, from which we can see that calculated values are in very good agreement with experimental data except in E_n>2.0 MeV energy region, where $\sigma_{n,\gamma}$ are of very small values. The calculated $\sigma_{n,n'}$ and $\sigma_{n,2n}$ are given in Fig. 4, from which we can see that calculated values are in pretty good agreement with experimental data. The calculated $\sigma_{n,3n}$ and $\sigma_{n,p}$, experimental $\sigma_{n,3n}$ $\sigma_{n,4n}$ and $\sigma_{n,p}$, Yu's evaluatied $\sigma_{n,3n}$ and $\sigma_{n,4n}$ are compared, in which the calculated $\sigma_{n,3n}$ are in rather good

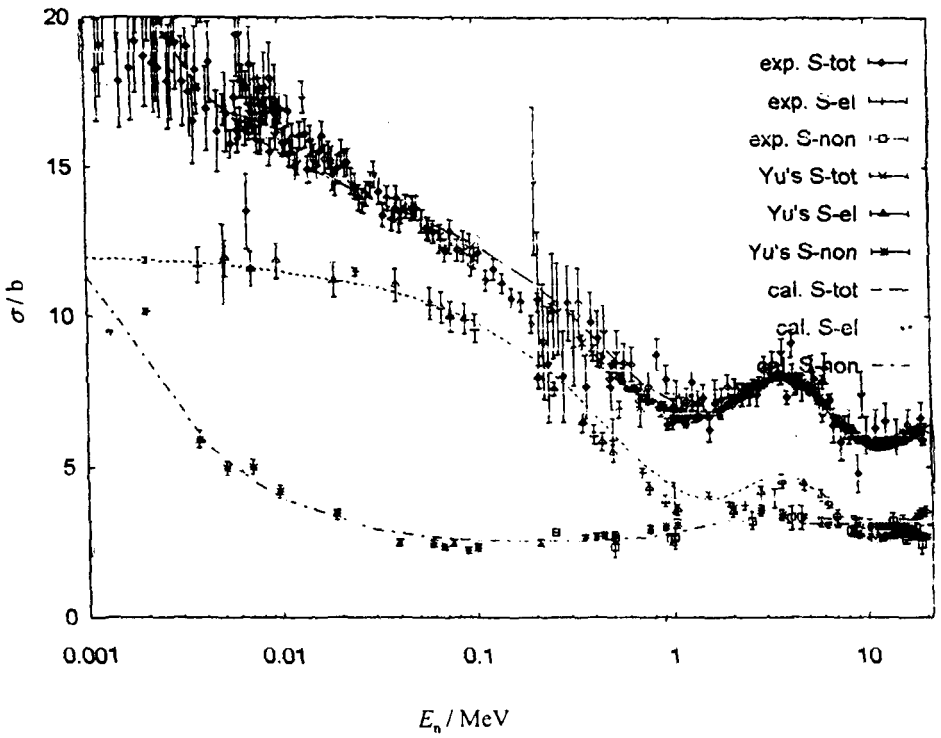

Fig. 1 (a) ^{235}U total, elastic and nonelastic cross sections

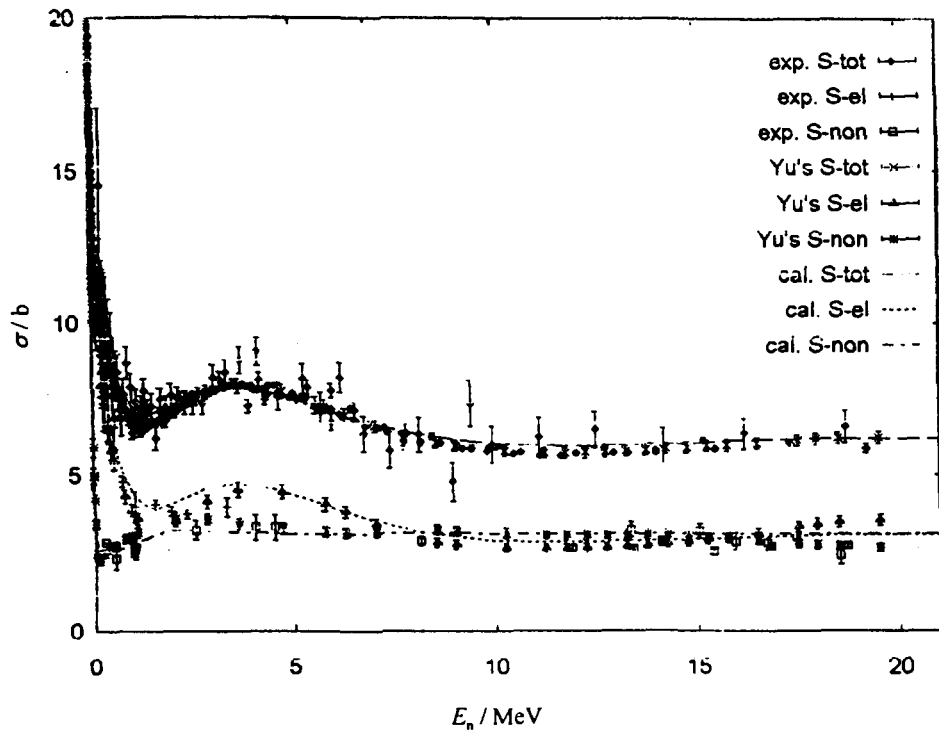

Fig. 1 (b) ^{235}U total, elastic and nonelastic cross sections

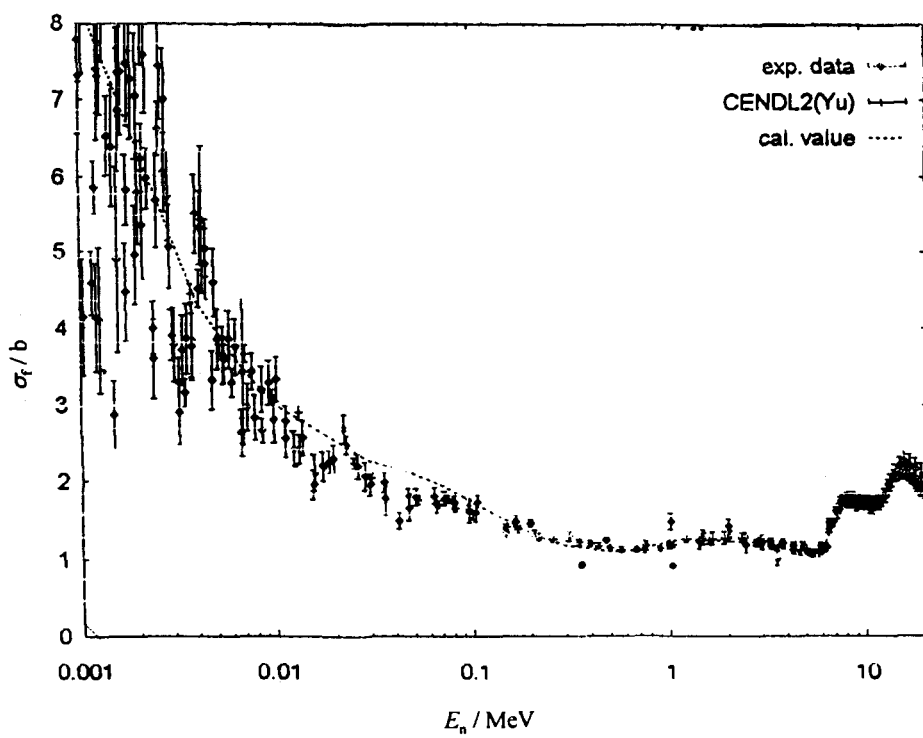

Fig. 2 (a) ^{235}U, fission cross sections

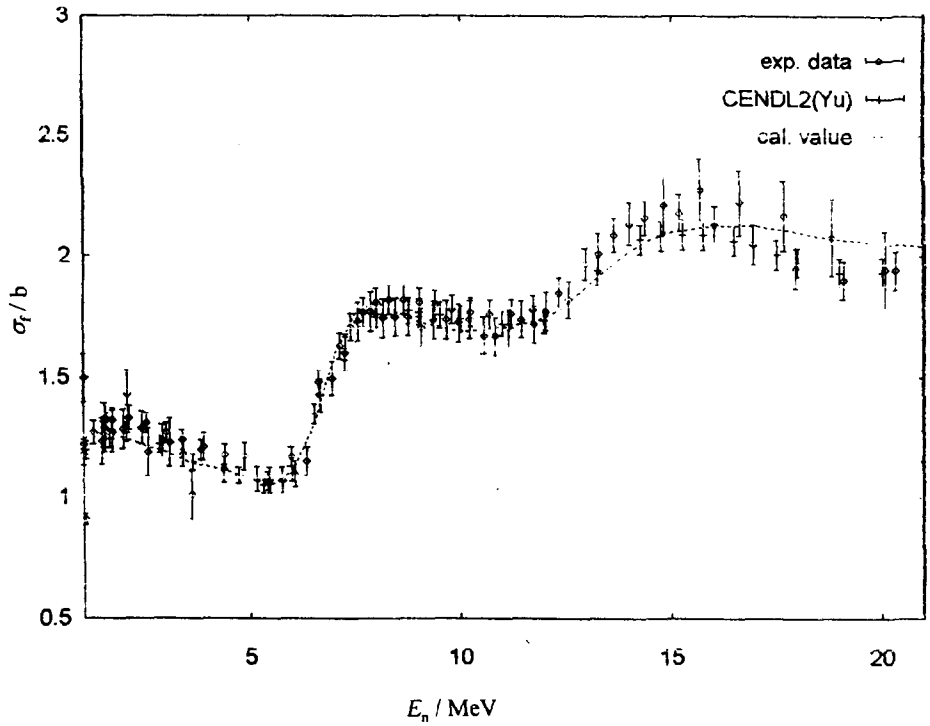

Fig. 2 (b) ^{235}U total, fission cross sections

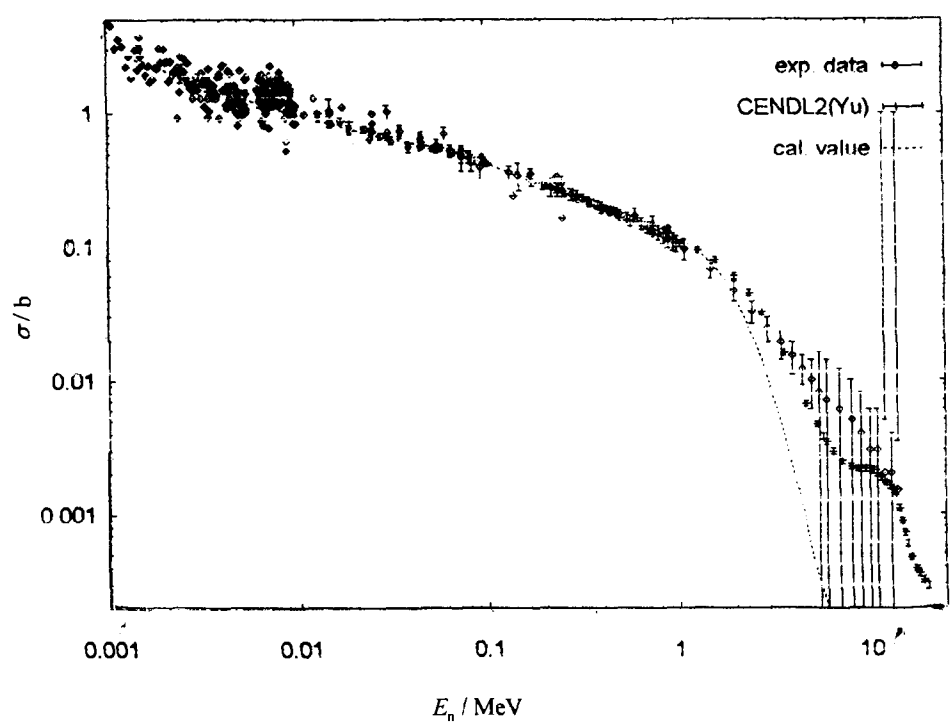

Fig. 3 ^{235}U (n,γ) cross sections

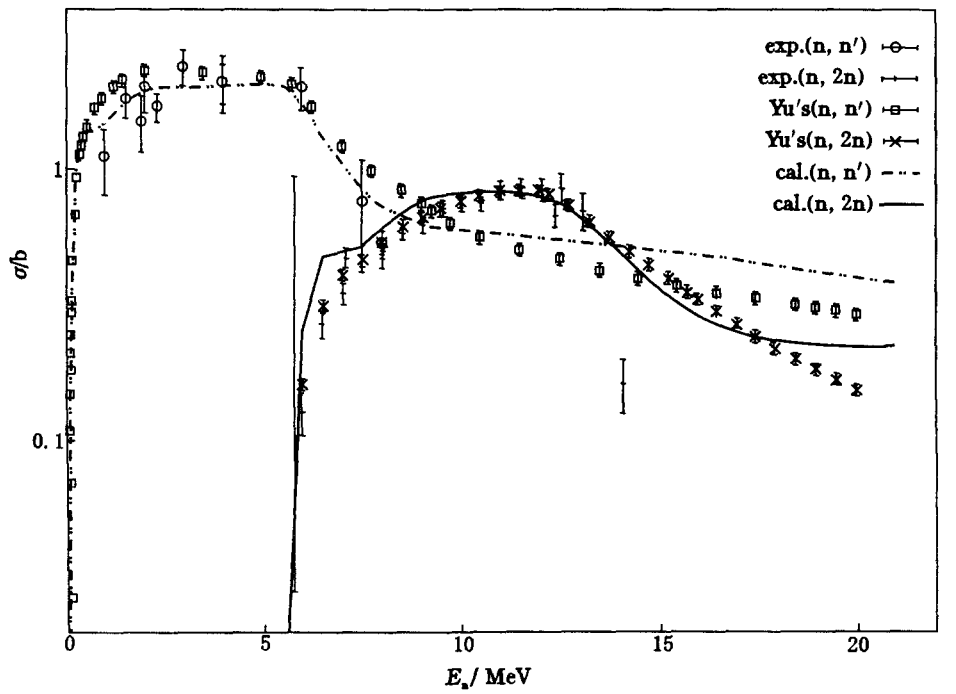

Fig. 4 ^{235}U (n,n') and (n,2n) cross sections

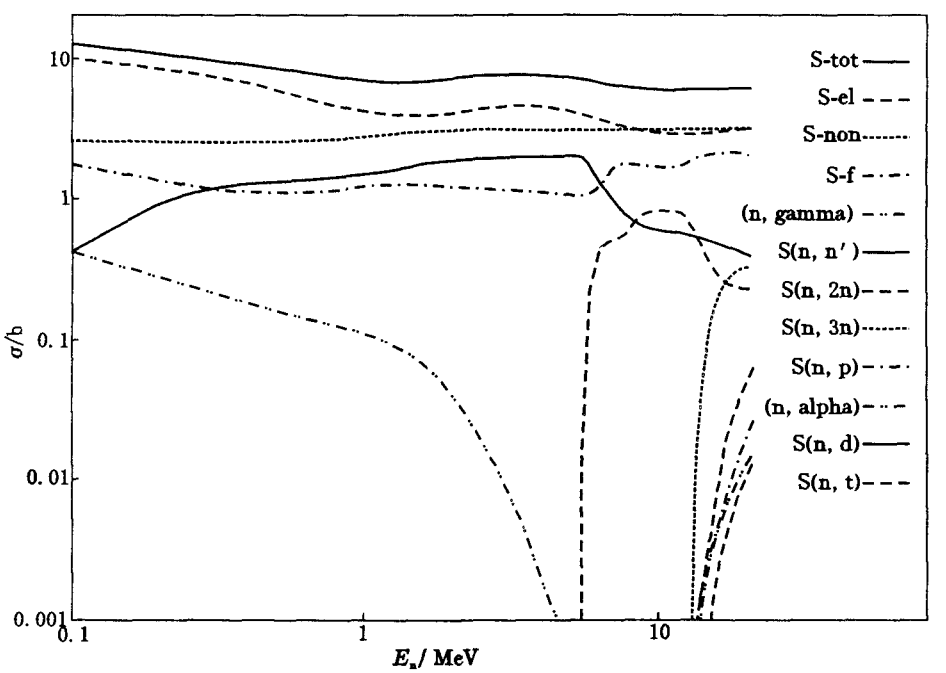

Fig. 5 All calculated cross sections of ^{235}U

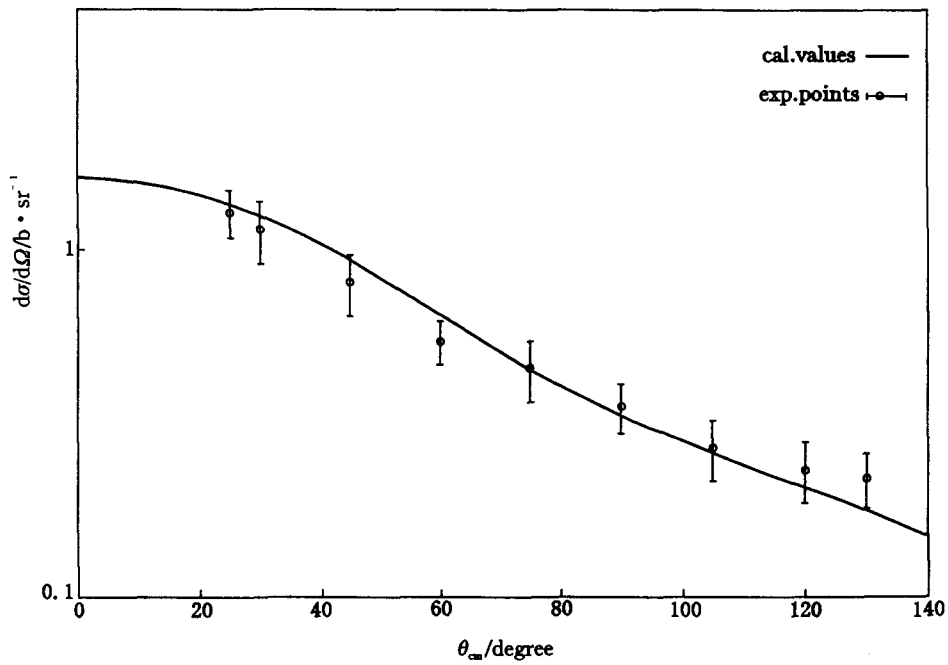

Fig. 6 (a) ^{235}U elastic differential C.S.at E_L=0.5 MeV

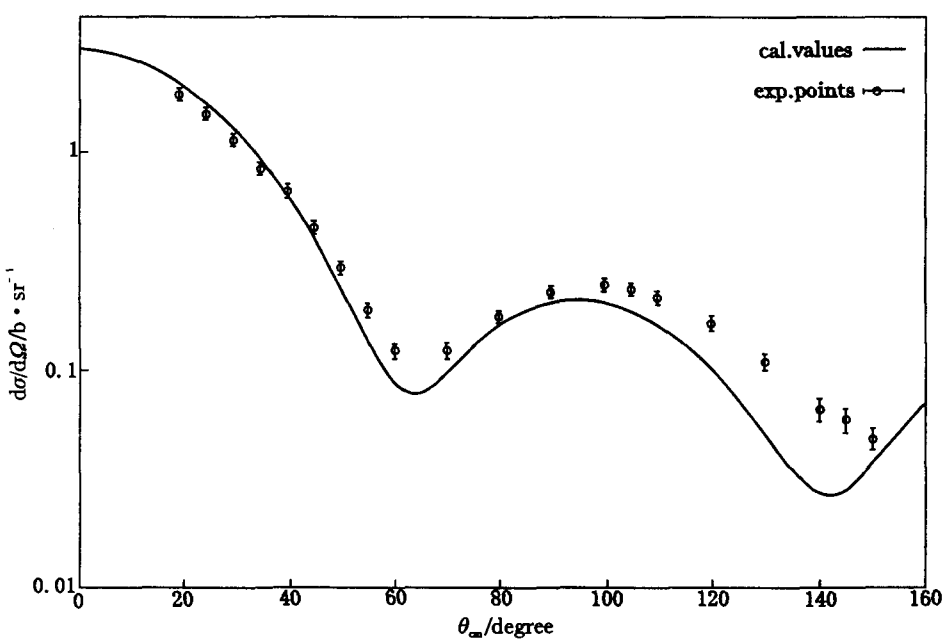

Fig. 6 (b) ^{235}U elastic differential C.S.at E_L=1.5 MeV

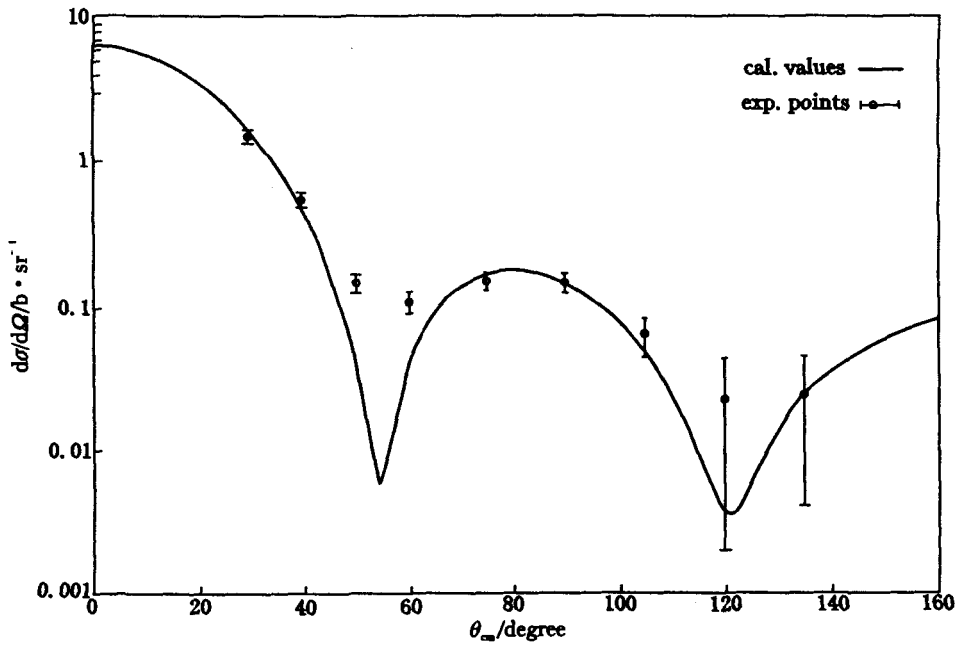

Fig. 6 (c) ^{235}U elastic differential C.S.at E_L=3.0 MeV

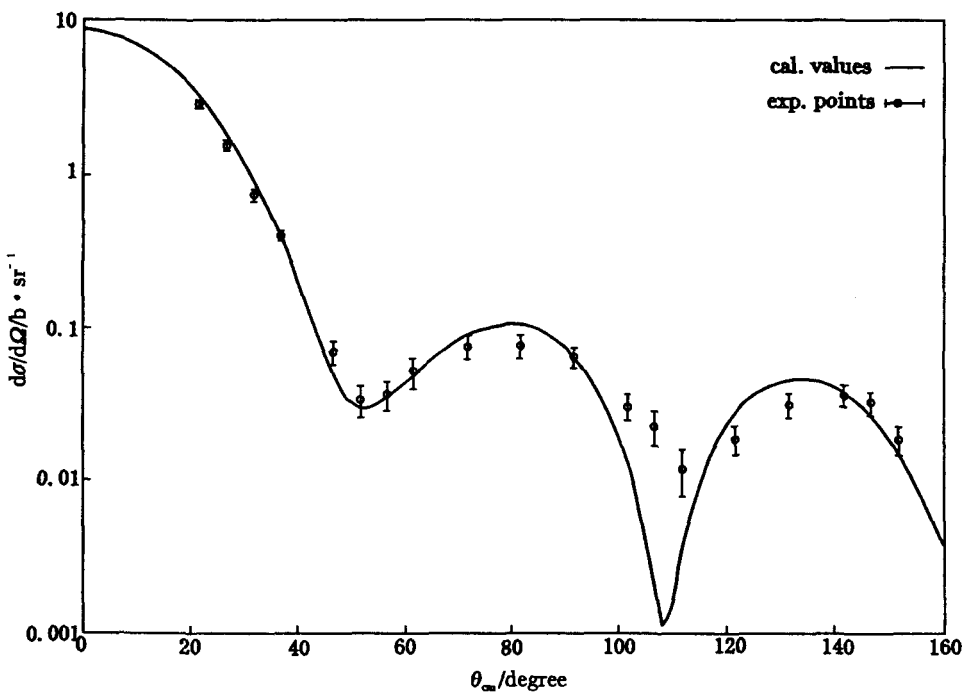

Fig. 6 (d) ^{235}U elastic differential C.S.at E_L=5.0 MeV

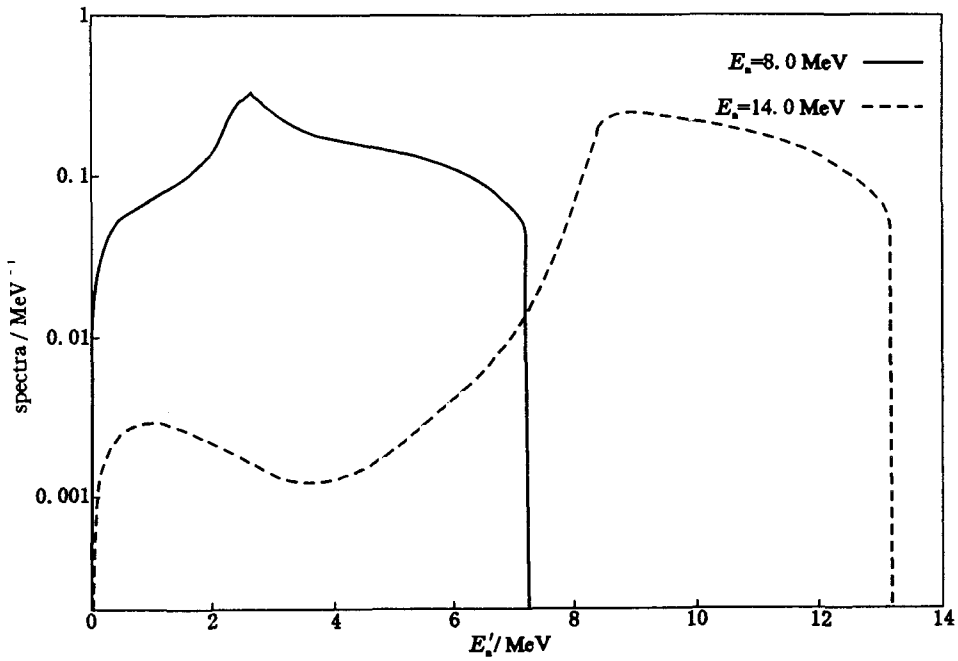

Fig. 7 (a) ^{235}U energy spectra of (n,n') (MT=91)

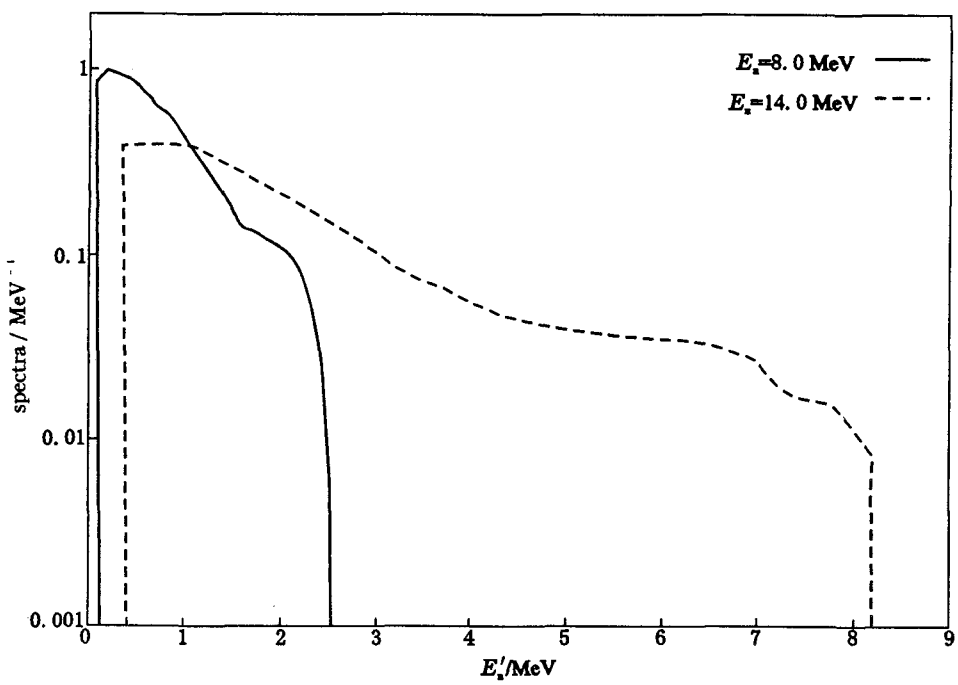

Fig. 7 (b) ^{235}U energy spectra of (n,2n)

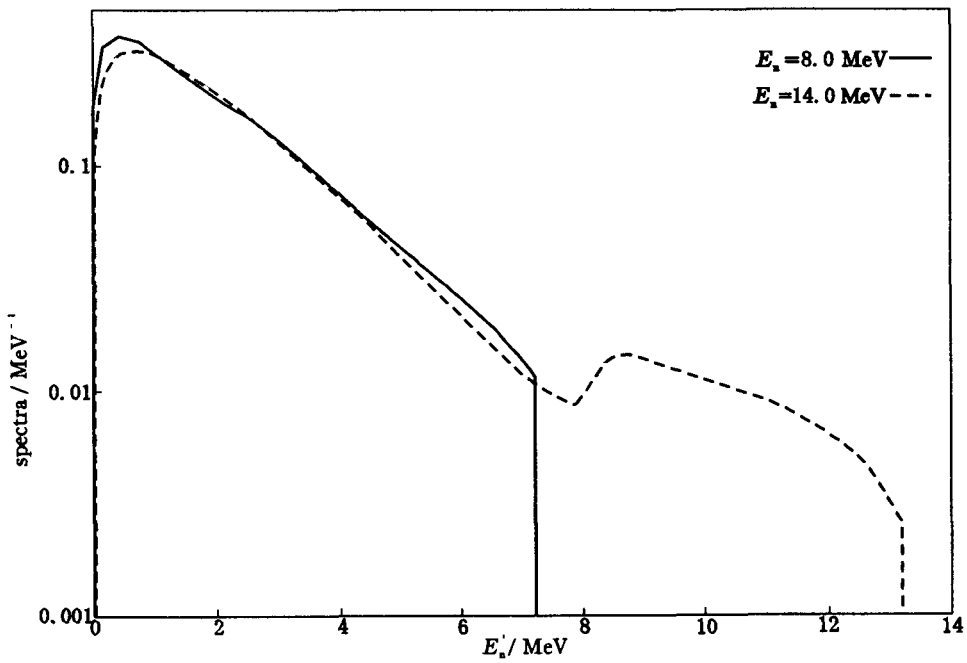

Fig. 7 (c) ^{235}U energy spectra of fission

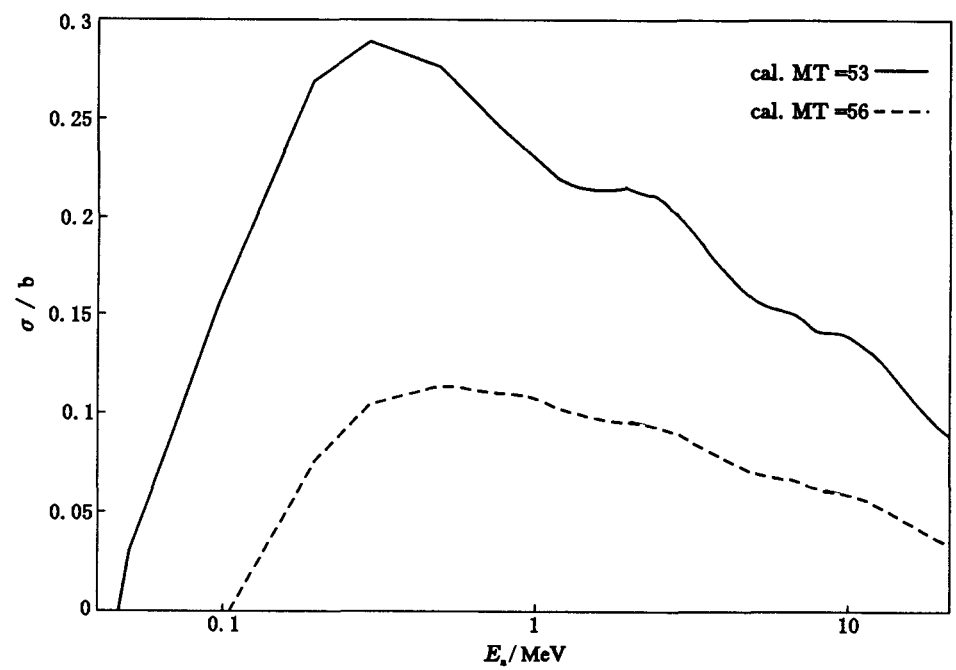

Fig. 8 (a) ^{235}U (n,n') of MT=53.56

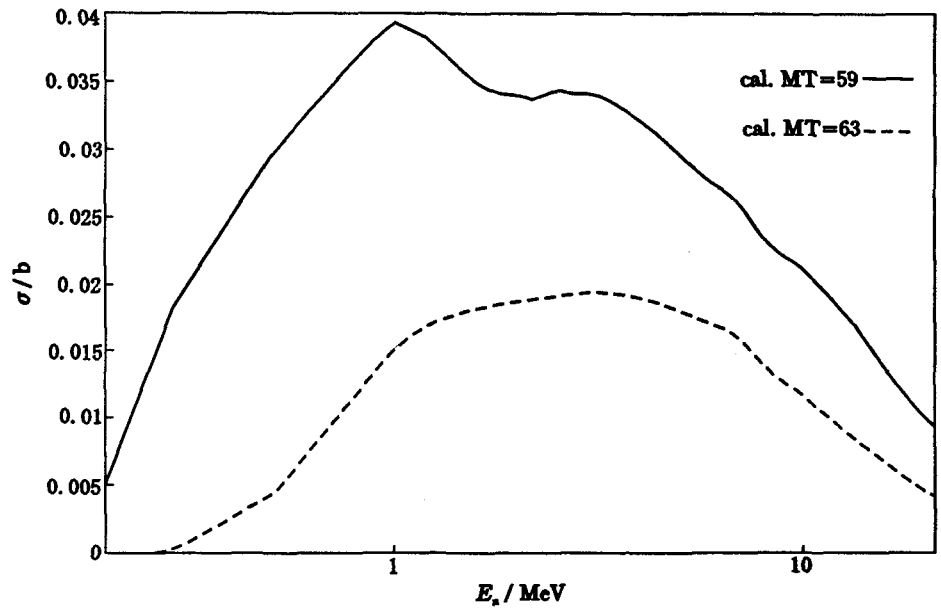

Fig. 8 (b) ^{235}U (n,n') of MT=59.63

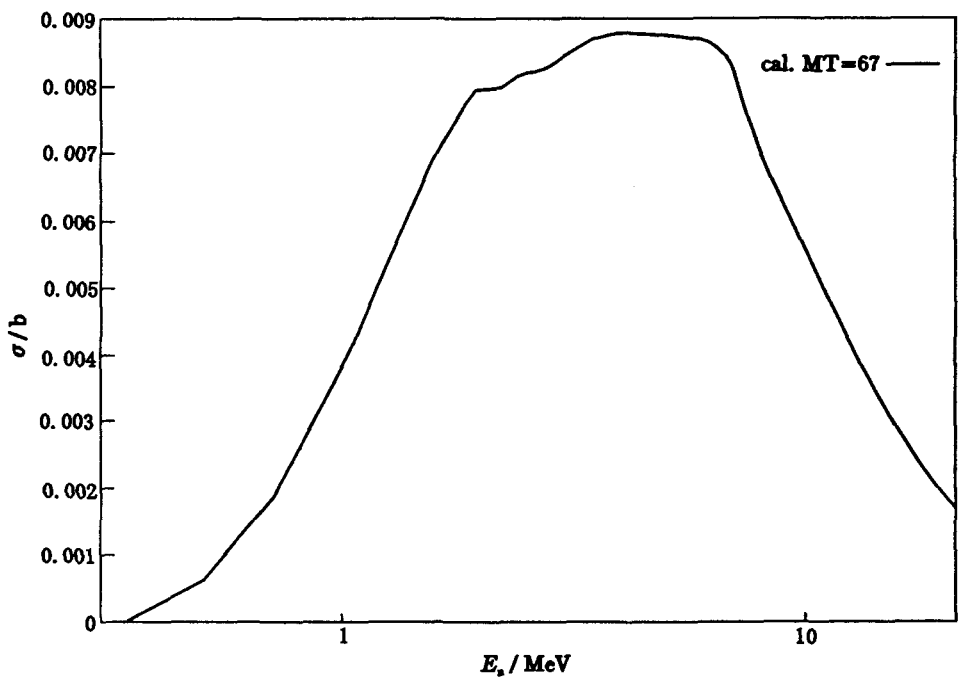

Fig. 8 (c) ^{235}U (n,n') of MT=67

agreement with experimental data, for E_n>18 MeV, the calculated $\sigma_{n,3n}$ include the small values of $\sigma_{n,4n}$ and $\sigma_{n,3nf}$, the calculated $\sigma_{n,p}$ cuve is through the only one experimental point (in calculation, the sensitive parameter is $\Delta_{n,p}$: from 0.49 to 1.070). All kinds of the calculated cross sections are plotted in Fig. 5. Some elastic scattering angular distributions are given in Fig. 6 (a), (b), (c) and (d), respectively, from which we can see that calculated values are in pretty good agreement with experimental data except near valleys of the oscillatory curves for higher energy points. The calculated secondary neutron spectra of continuous inelastic scattering, (n,2n) reaction and total fission at 8.0 MeV and 14.0 MeV are plotted in Fig. 7 (a), (b) and (c), respectively. These secondary neutron spectra are of reasonable shapes in physics. Figs. 8 (a), (b), and (c) show the calculated (n,n') excitation functions of the discrete levels mentioned above.

References

[1] Shen Qingbiao, APFO96, a code for automatically searching for a set of optimal optical potential parameters of fission nucleus (unpublished)

[2] Cai Chonghai, APFF, A code for automatically searching for a set of optimal fission parameters of fission nucleus in first fission (unpublished)

[3] Cai Chonghai, ASFP, Communication of Nuclear Data Progress 3, 26(1990)

[4] Cai Chonghai, FUP1, Communication of Nuclear Data Progress 3, 29(1990)

[5] J.Raynal, IAEA SMR-9/8, International Atomic Energy Agency (1970); P.G. Young and E.D.Arthur, Nuclear Data for Science and Technology, Mito Conference, 1988, p.603

[6] Zhang Jingshang, FUNF, a code for comprehensive calculations of fission nucleus based on unified model, CNDC, CIAE (unpublished)

[7] Cai Chonghai and Zang Jingshang, ADFP, A code for automati cally searching for a set of optimal fission parameters of fission nucleus for first, second and third plateaus (unpublished)

Evaluation and Testing of Coupled Channel Optical Potentials and Its Parameters for n+$^{238\sim242}$Pu and ^{241,242}Am

Wang Shunuan
(China Institute of Atomic Energy, Beijing 1024513)

Abstract

Several sets of coupled channel optical potentials and its parameters for n+ $^{238\sim242}$Pu and ^{241,242}Am below 20 MeV are analyzed and evaluated by direct and compound inelastic scattering cross sections and angular distributions carried out by coupled channel optical model and semi-classical statistical model calculations. The potentials and its parameters recommended to be used in CENDL-3 calculations are presented and discussed.

Several sets of coupled channel optical potentials and its parameters for actinide nuclei below 20 MeV which could be found in the literature have been tested and evaluated in the present work by direct and compound inelastic scattering cross sections and angular distributions carried out by coupled channel optical model calculation codes of ECIS95[1], PRECIS[2] and semi-classical statistical calculation code of FUNF[3]. The parameter sets are: Madland-Young(M-Y) [4], A. Tudora et al.(Tudora) [5,6], ENDF/B-6[7], JENDL-3.2[8], CENDL-2[9] and others. In the theoretical analysis, there are three main reaction models used: a coupled channel optical model to describe direct reaction contributions to inelastic scattering from collective states (ground state rotational band) by using ECIS95 code, Hauser-Feshbach statistical theory to calculate compound nucleus contributions to the reaction by using FUNF code below ~5.5 MeV and the pre-equilibrium theory employed to include the non-equilibrium effects at incident above ~5.5 MeV also by using FUNF code.

The set of parameters provided by M-Y has been evaluated in the previous paper[10]. The set of parameters provided by A. Tudora et al. [5,6] is for actinide nuclei in the energy range of 0.001~20MeV. In CENDL-2 calculations, the deformed optical potential parameters were adjusted by a coupled channel optical model code in which the hexadecapole deformation (β_4) was not taken into account. The

parameters used can be found in Ref. [9].

General ECIS95 and FUNF theoretical calculations for n+$^{238\sim242}$Pu and ^{241,242}Am below 20 MeV in the present work by means of these three sets parameters mentioned above point out that the contributions to the direct inelastic neutron scattering cross sections at 10~20 MeV is about 0.4~0.6 b. Generally speaking, this is too much compared with the inelastic neutron scattering cross sections data evaluated results of ENDF/B-6, JENDL-3.2, CENDL-2 and other evaluated data files.

In ENDF/B-6 and JENDL-3.2 for n+^{239}Pu evaluations, the ECIS code was used for the coupled channel deformed optical model calculations. The first six states of ^{239}Pu ground state rotational band ($1/2^+$, $3/2^+\cdots11/2^+$) were coupled in the calculations. The optical model and deformation parameters used in the calculations are as the following:

$$
\begin{aligned}
&V=46.2-0.3E_n \\
&W_s=3.6+0.4E_n \qquad E_n \le 7 \text{ MeV} \\
&W_s=6.4-0.1(E_n-7) \qquad E_n > 7 \text{ MeV} \\
&W_v=-1.2+0.15E_n \qquad E_n \ge 8 \text{ MeV} \\
&V_{so}=6.2 \qquad\qquad\qquad\qquad (\text{MeV})
\end{aligned}
$$

$$
\begin{aligned}
&\beta_2=0.21 \qquad \beta_4=0.065 \\
&r_v=1.26 \qquad a_v=0.615 \\
&r_s=1.24 \qquad a_s=0.5 \\
&r_{so}=1.12 \qquad a_{so}=0.47 \qquad (\text{fm})
\end{aligned}
$$

The above parameters used in ENDF/B-6 also in JENDL-3.2 are actually complete the same as used in ENDF/B-5.2[11]. In ENDF/B-5.2[11] the calculated elastic and inelastic scattering angular distributions for 0.7 MeV incident neutrons are compared with experimental data of Haouat et al.[12] for the ground state rotation band members of ^{239}Pu. Overall, the agreement with experiment is good at energy range below 3.4 MeV.

From above analysis it can be seen clearly that the deformed optical model parameters used in ENDF/B-6 or JENDL-3.2 (same as ENDF/B-5.2) for ^{239}Pu were: 1) generalized energy range from 3.4 MeV up to 20 MeV; 2) changed the surface absorbing imaginary potential parameters W_s at E_n >7 MeV; and 3) introduced a volume absorbing imaginary potential W_v at $E_n \ge 8$ MeV. It has been understood

well by the present ECIS95 and FUNF codes calculations for n+^{239}Pu below 20 MeV that it could not only fit well to the total, elastic and inelastic cross sections below 3.4 MeV as well as inelastic scattering angular distributions for 0.7 MeV incident neutrons compared with experimental data of Haouat et al.[12] for the ground state rotation band members of ^{239}Pu, but also could provide reasonable inelastic cross sections at range of 7~20 MeV (see Fig. 1), and fission cross sections at 7~10 MeV in good agreement with experimental data (see Fig. 2). Thus this set of coupled channel optical potential parameters are recommended to CENDL-3 n+^{239,241}Pu and n+^{241}Am calculations below 20 MeV.

In n+$^{240, 242}$Pu calculations of ENDF/B-6 and JENDL-3.2, the coupled channel optical potential used were taken from Ref. [13,14]. The parameters are shown as follows:

V=49.82-0.3E_n-27$(N-Z)/A$
W_s=5.52+0.4E_n -9$(N-Z)/A$ $E_n \leq 10$ MeV
W_s=9.52-9$(N-Z)/A$ $E_n \geq 10$ MeV
V_{so}=6.2 (MeV)

r_v=1.26 a_v=0.63
r_s=1.26 a_s=0.52
r_{so}=1.12 a_{so}=0.47 (fm)

n+^{240}Pu	β_2=0.2	β_4=0.062	
n+^{242}Pu	β_2=0.204	β_4=0.051	
n+^{238}Pu	β_2=0.196	β_4=0.073	(by ^{240,242}Pu systematics)

In Refs. [13,14], the geometrical parameters and the energy dependence of the real and imaginary potentials have been obtained by fit to ^{238}U and ^{232}Th experimental data, mainly the total cross sections and the scattering angular distributions at 2.5 MeV and 3.4 MeV[15]. The deformation parameters chosen were derived[15] from calculations based on the Nilsson model and the method of Strutinsky as described by Moller[16].

This set of parameters has been tested for ^{238,240,242}Pu by using ECIS95 and FUNF codes in the present work. The calculated results show that the direct mechanism contributions to the inelastic scattering cross section $\sigma_{n,n'}$ at E_n=7~10 MeV is too high so that the $\sigma_{n,n'f}$ is too low compared with the experimental data of fission cross

sections at the same energy range of E_n=7~10 MeV (see cross line in Fig. 3~4 as an example) and also the $\sigma_{n,2n}$ cross section is a little lower at the same energy range of E_n=7~10 MeV compared with Evaluated Data Files, where the calculated nonelastic cross sections are reasonable, and open channels are only the (n,n'), (n,n'f) and (n,2n) reactions. As it is seen from the above analysis, it seems to us that the set of parameters provided in Refs. [13,14] were generalized from 3.4 MeV to 10 MeV with a little crudely made. After careful long deliberation and testing calculations based on ECIS95 and FUNF codes for n+$^{238, 240, 242}$Pu in the present work and adapting the reminding of understanding the set of parameters used in ENDF/B-6 and JENDL-3.2 for n+^{239}Pu evaluations and recommended to be used in CENDL-3 calculations for n+$^{239, 241}$Pu and n+^{241}Am, a new set of coupled channel optical potential parameters has been recommended to CENDL-3 calculations for n+^{238,240,242}Pu, which is as the following:

V=49.82-0.3E_n-27$(N-Z)/A$

W_s=5.52+0.4E_n -9$(N-Z)/A$ $E_n \leq 7$ MeV

W_s=5.7+0.1 E_n $E_n \geq 7$ MeV

W_v =-1.2+0.15E_n $E_n \geq 8$ MeV

V_{so}=6.2 (MeV)

r_v=1.26 a_v=0.63

r_s=1.26 a_s=0.52

r_{so}=1.12 a_{so}=0.47 (fm)

n+^{240}Pu	β_2=0.2	β_4=0.062	
n+^{242}Pu	β_2=0.204	β_4=0.051	
n+^{238}Pu	β_2=0.196	β_4=0.073	(by ^{240,242}Pu systematics)

For completeness, the set of parameters can be described as: 1) All the parameters for V, all the parameters for W_s below 7 MeV(not below 10 MeV as in Refs. [13,14]), all geometrical parameters, and all quadrupole deformation β_2 and hexadecapole deformation β_4 are taken as the same as in Refs. [13,14]; 2) All the parameters for W_s above 7 MeV and W_v at $E_n \geq 8$ MeV are taken as the same as in ENDF/B-6 and JENDL-3.2 or Ref. [11] for n+^{239}Pu. This means that the energy range has been generalized from 3.4 MeV up to 20 MeV, the surface absorbing imaginary potential parameters of W_s at E_n>7 MeV have been changed, and a

volume absorbing imaginary potential W_v at $E_n \geq 8$ MeV has been introduced. By means of this set of parameters the testing calculations results of ECIS95 and FUNF for n+$^{238, 240, 242}$Pu, generally speaking, are in agreement with experimental data and ENDF/B-6, JENDL-3.2 and other evaluated data files (see the circle line in Fig. 3~4 as an example). Thus this set of parameters could be recommended to CENDL-3 calculations for n+$^{238, 240, 242}$Pu evaluations. Also, the parameters for n+ ^{242}Pu have been used for the CENDL-3 calculation of n+ ^{242}Am by using ECIS95 and FUNF codes and the satisfied calculated results are obtained.

It can be concluded as a whole in the present paper that several sets of coupled channel optical model parameters for actinide nuclei which could be found in the literature have been tested and evaluated. A new set of coupled channel optical potentials and its parameters for n+$^{238\sim242}$Pu and ^{241,242}Am below 20 MeV are obtained, which can be recommended to be used in CENDL-3 calculations. By using this new set of parameters, the calculated results, in general terms, not only could be in agreement with experimental data below 3.4 MeV, but also could be in agreement with experimental data in energy range between 7 and 10 MeV as well as in energy range between 10 MeV and 20 MeV in agreement with experimental data evaluated data files of ENDF/B-6, JENDL3.2 and others.

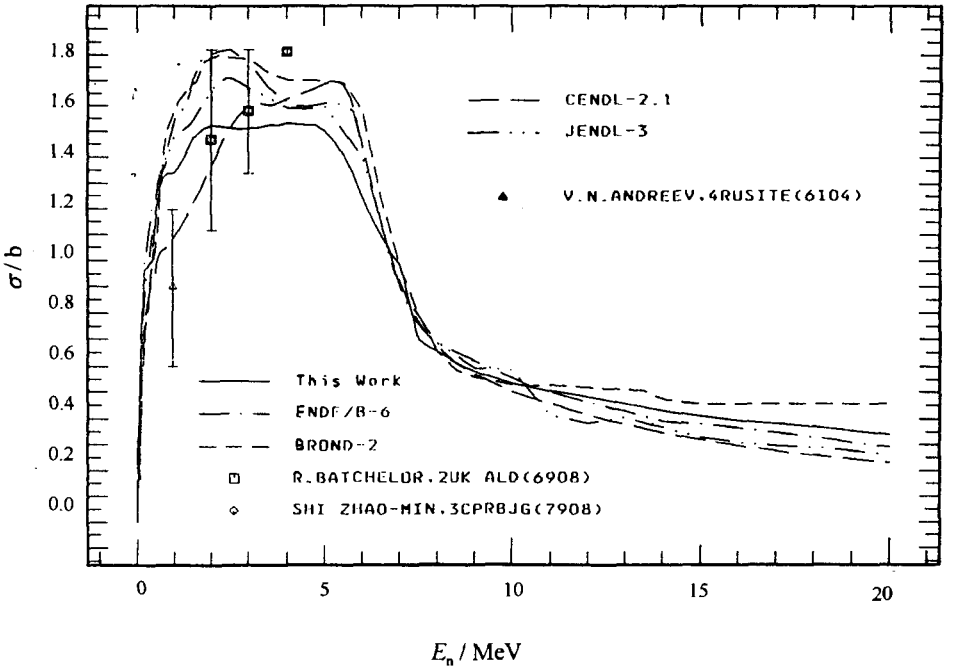

Fig. 1 ^{239}Pu (n,inl) reaction cross sections

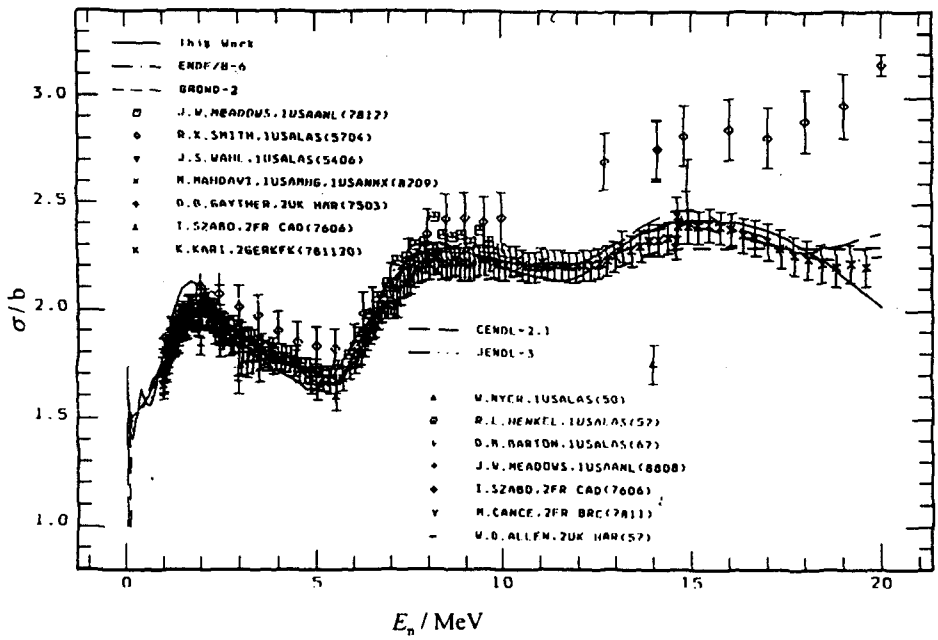

Fig. 2 ^{239}Pu (n,f) reaction cross sections

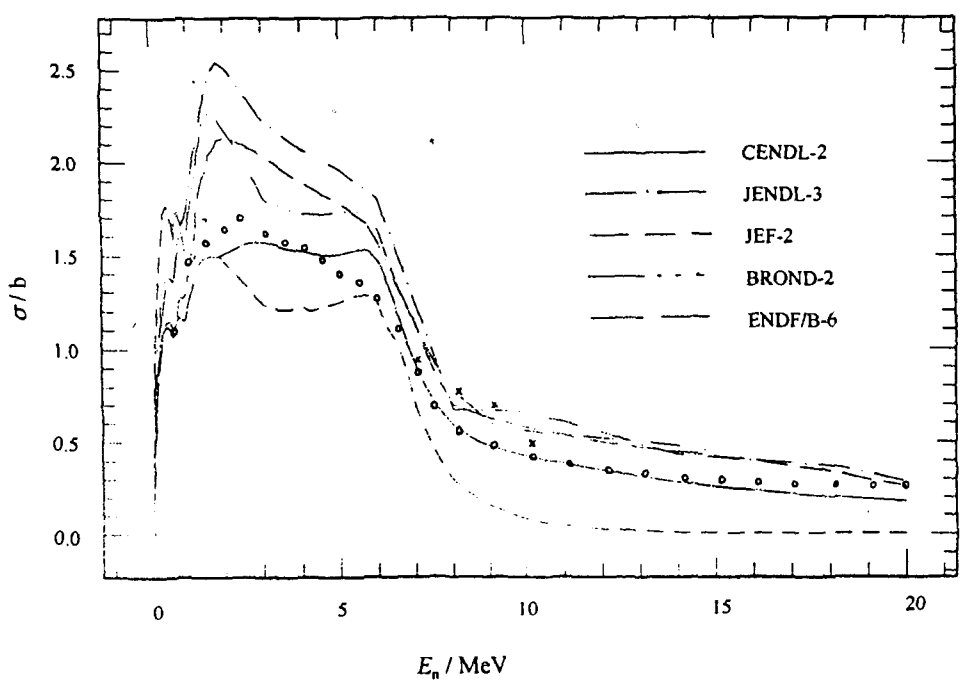

Fig. 3 ^{240}Pu (n,inl) reaction cross sections

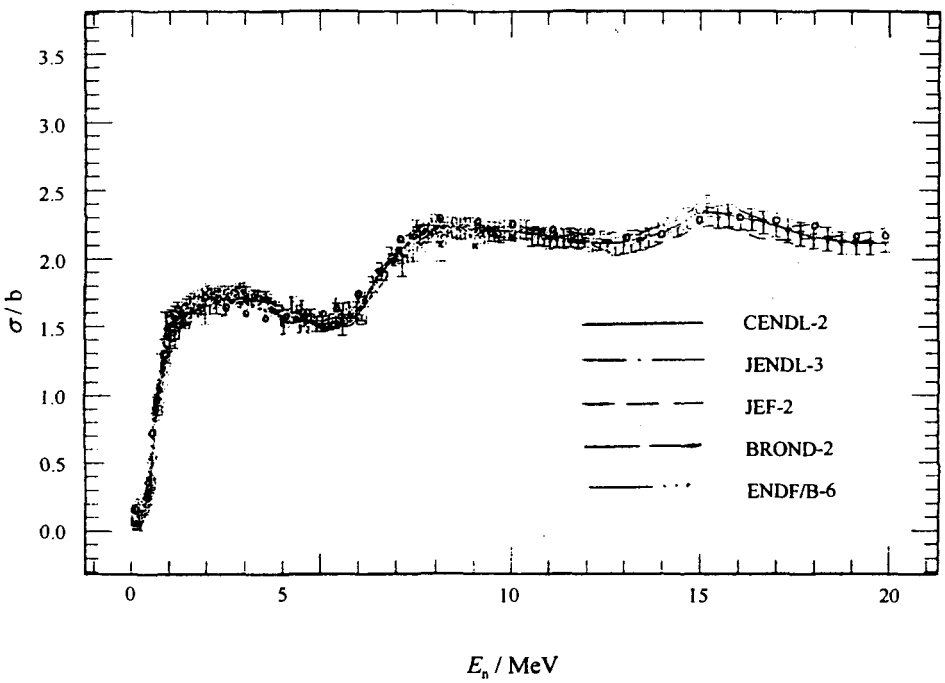

Fig. 4 ^{240}Pu (n,f) reaction cross sections

References

[1] J. Raynal, "Notes on ECIS94", CEA Scaclay Report No CEA-N-2772, 1994(unpublished).

[2] B.V. Carlson, "The Optical Model ECIS95", Workshop on Nuclear Reaction Data and Nuclear Reactors-Physics, design and Safety, 15 Apr.-17 May 1996, Miramare Trieste,Italy.

[3] Zhang Jingshang, FUNF code, CNDC,1996.

[4] D.G. Madland and P.G. Young, "Neutron-Nucleus Optical Potential for the Actinide Region", International Conference on Neutron Physics and Nuclear Data for Reactors and Other Applied Purposes, 1978 Sep. 25-29, Harwell, OECD/NEA UKAEA, p.49(1978); and late on series publications.

[5] Anabella Tudora, "Neutron Optical Deformed Parametrization for the Actinide Region", Abstract Book, p132, International Conference on Nuclear Data for Science and Technology, May 19-24, 1997 Trieste, Italy.

[6] Anabella Tudora, Private Communications.

[7] ENDF /B-6, file1.

[8] JENDL-3.2, file1.

[9] CENDL-2 , file1; Yan Shiwei et al., Commu. of Nuclear Data Progress, No.12,14(1994).

[10] Wang Shu Nuan, Commu. of Nuclear Data Progress, No.19,39(1998).

[11] E.D. Arthur, P. G. Young, D. G. Madland, and R. E. MacFarlane, Nuclear Science and Engineering, 88,56-70(1984).

[12] G.Haouat, J.Lackkar, Ch.Lagrange, J.Jaryetal.,Nuclear Science and Engineering,81,491-511(1982).

[13] Lagrange Ch and Jary J., NEANDC(E) 198"L" (1978).

[14] J.Jary, Ch. Lagrange and C. Philis, BNL-50991.P.83, Brookhaven National Lab., 1979.

[15] G.Haouat et al., NEANDC(E) 180 "L"-INDC(FR) 13/L (1977); NEANDC(E) 196 "L"-INDC(FR) 29/L.

[16] P. Moller, S.G. Nilsson, J. R. Nix, Nucl. Phys., A229(1974).

CN0101607

Theoretical Calculations of All Reactions for n+^{151}Eu, ^{153}Eu, ^{154}Eu and ^{155} Eu in E_n=0.001~20 MeV

Ge Zhigang

(China Nuclear Data Center, Beijing 102413)

Abstract

All reaction cross sections, secondary neutron spectra and elastic scattering angular distributions of n+^{151}Eu, ^{153}Eu, ^{154}Eu and ^{155}Eu in E_n=0.001~20 MeV were calculated. Pretty good theoretical results in accordance with experimental data were obtained, and all calculated results are given in ENDF/B-6 format.

Introduction

The natural element Eu, and its two stable isotopes, ^{151}Eu, ^{153}Eu, the abundance of which are 47.8% and 52.2%, respectively, the isotopes ^{154}Eu, ^{155}Eu are in the list of fission product nuclei evaluation for the CENDL-3. For convenience in plotting and description, the theoretical calculations of ^{151}Eu, ^{153}Eu, ^{154}Eu and ^{155}Eu are presented in this paper only. The construction and evaluation of natural Eu will be given in another article.

1 Theories and Parameters

There are some experimental data of total cross section σ_{tot} in energy range of 0.01~20 MeV for natural element Eu only, and abundant experimental data of $\sigma_{n,\gamma}$ in 0.01~4 MeV for ^{151}Eu and ^{153}Eu. Some experimental data of (n, 2n), (n, 3n) and (n, α) for ^{151}Eu and ^{153}Eu were obtained. All of the experimental data were taken from EXFOR. There are no experimental data for cross sections of other reaction channels, the elastic scattering angular distributions and secondary neutron spectra for n+^{151}Eu and n+^{153}Eu, and no experimental data for the reactions of n+^{154}Eu and n+^{155}Eu.

APOM94[1] code is used to automatically get the optimal parameters of optical potential for neutron channel for the four isotopes, respectively. Because there are no experimental data of the total cross sections and elastic scattering angular distributions of the four isotopes for automatically searching for the optical potential parameters, so the total cross sections for natural element Eu are used for searching the optical potential parameters for the four isotopes, with consideration of the data in other major evaluated nuclear data libraries. The final four sets of optimal parameters of optical potential for neutron channel used for the calculations were obtained after running the code APOM94 many times. The four sets of optical potential parameters are given in following Table.

	^{151}Eu	^{153}Eu	^{154}Eu	^{155}Eu
V_0	51.04378510	51.21009445	51.88004303	52.09600449
V_1	0.09244935	0.00574570	0.15004063	-0.06914829
V_2	-0.01070987	-0.00095847	-0.00474381	-0.00624844
W_0	8.45973969	8.63384914	9.81712723	8.46111774
W_1	-0.25837353	-0.10639114	-0.41546440	-0.19751523
U_0	-0.88266772	-1.42412972	-1.10963917	-0.56393069
U_1	0.31419012	0.24145548	0.33803535	0.31578040
U_2	-0.00244746	0.00319253	0.00217205	-0.00107335
a_r	0.79667264	0.79445076	0.76087022	0.78165203
a_s	0.60663128	0.61468774	0.56889051	0.57991177
a_v	0.36452791	0.68183136	0.42661604	0.75336719
r_r	1.18268061	1.18258035	1.18438399	1.18354356
r_s	1.29964125	1.29023612	1.24069023	1.26744556
r_v	1.18279791	1.24763703	1.62670541	1.31773865

The contributions of the direct inelastic scattering were gotten in this work by using the DWBA model with the code DWUCK4[2]. The selections of the discrete levels, which are taken into account of DWUCK4, and their related input parameters

are considered according to their contributions. The discrete levels of all targets were taken from CENPL[3].

SUNF[4] is a kernel code in this work. The optimum set of optical potential parameters and the direct inelastic scattering distributions mentioned above are taken as the input data of SUNF code, and all related nuclear model parameters are taken from CENPL. The adjusting of related input parameters of SUNF are necessary according to related experimental data. For the cases whithout any experimental data, the related reactions or the behaviors of neighboring nuclei are considered in the calculations. Other major evaluated nuclear data libraries are considered as references during all calculations, and the comparisons with other evaluated nuclear data libraries were performed too.

2 Calculation Results and Analyses

In this paper, the comparisons of calculated results for those reaction channels that have the experiments are presented only. The Fig. 1 and Fig. 2 show the comparisons of neutron total cross sections for the n+^{151}Eu and n+^{153}Eu between calculated results and the experimental data of natural element Eu, and the calculated results are in pretty good agreement with the experiments. For the ^{151}Eu(n,γ) ^{152}Eu and ^{153}Eu(n,γ)^{154}Eu reactions (the Fig. 3 and Fig. 4 show the calculated results) are also in good agreement with the experiments. The comparisons of cross sections of 2n, 3n and α emissions for the n+^{151}Eu and n+^{153}Eu are plotted in Fig. 5 to Fig. 8. For those no experimental data cases, the calculated cross sections are analyzed and compared with other major evaluated nuclear data library. So the results are also reasonable in physics. Fig. 9 and Fig. 10 show the elastic scattering angular distributions for ^{151}Eu and ^{155}Eu, they are of reasonable shapes in physics. As an example, all kinds of calculated cross sections of n+^{151}Eu is presented in Fig. 11, from which we can see that all reaction cross sections are of reasonable shapes in physics.

Summary

As the results showed above, most theoretical calculations can describe the experiments well enough for the reactions n+^{151}Eu, ^{153}Eu, ^{154}Eu and ^{155}Eu in E_n=0.001~20 MeV. So the theoretical calculations can be used for the evaluation activities of CENDL-3, and as a reference to the experiments.

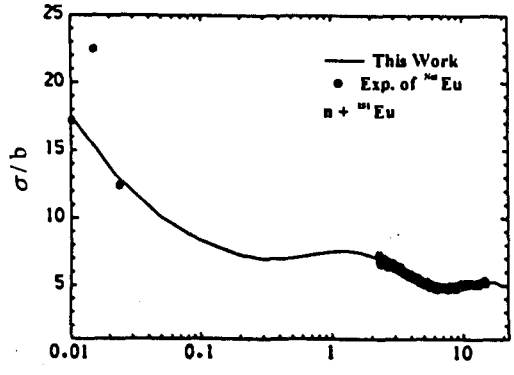

Fig. 1 Comparison of σ_{tot} ^{151}Eu between (calculated) and ^{Nat}Eu (measured)

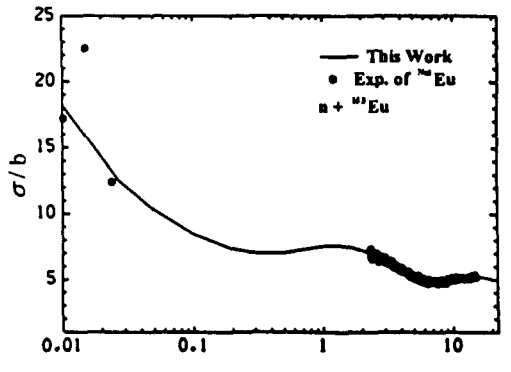

Fig. 2 Comparison of σ_{tot} ^{153}Eu between (calculated) and ^{Nat}Eu (measured)

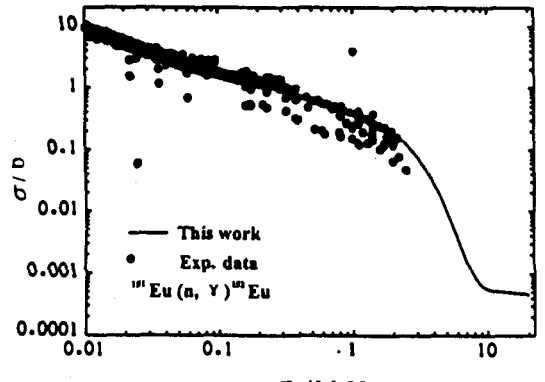

Fig. 3 Comparison of $\sigma_{n,\gamma}$ ^{151}Eu between (calculated) and ^{Nat}Eu (measured)

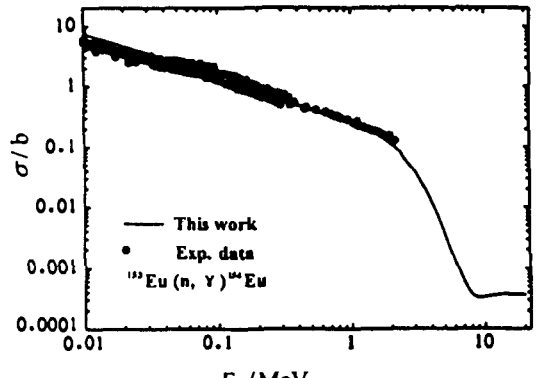

Fig. 4 Comparison of $\sigma_{n,\gamma}$ ^{153}Eu between (calculated) and ^{Nat}Eu (measured)

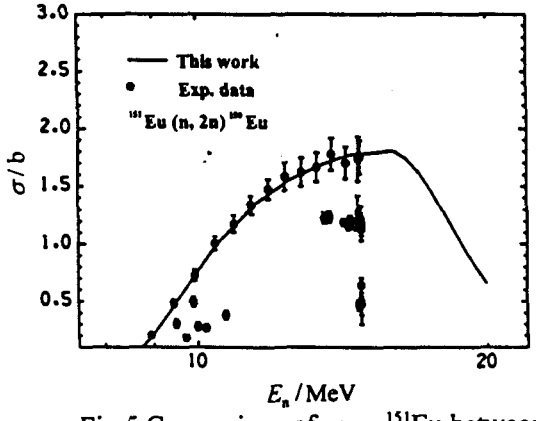

Fig.5 Comparison of $\sigma_{n,2n}$ ^{151}Eu between (calculated) and ^{Nat}Eu (measured)

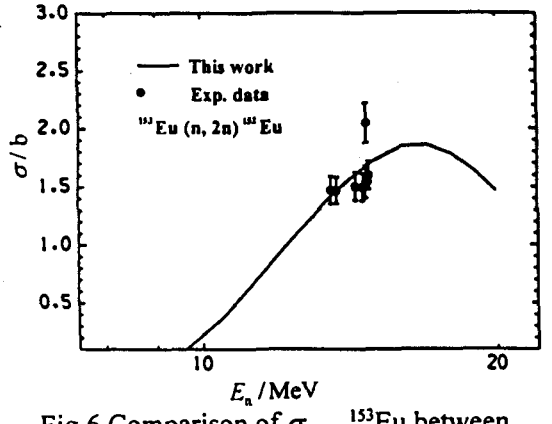

Fig.6 Comparison of $\sigma_{n,2n}$ ^{153}Eu between (calculated) and ^{Nat}Eu (measured)

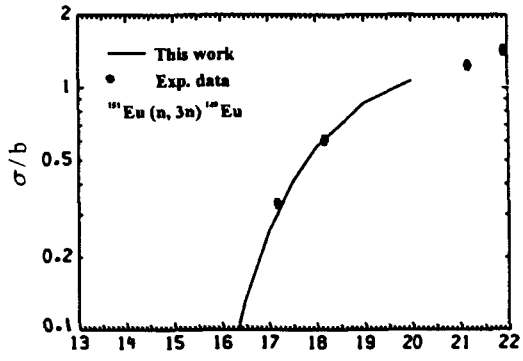

Fig.7 Comparison of $\sigma_{n,2n}$ ^{151}Eu between (calculated) and ^{Nat}Eu (measured)

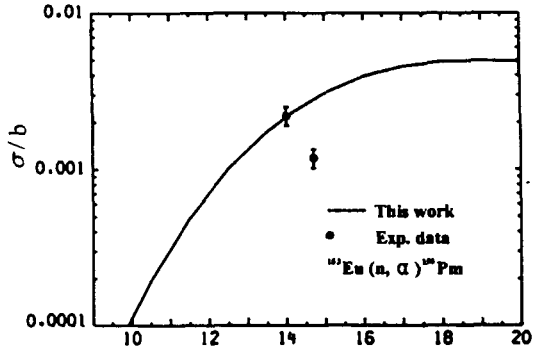

Fig.8 Comparison of $\sigma_{n,2n}$ ^{153}Eu between (calculated) and ^{Nat}Eu (measured)

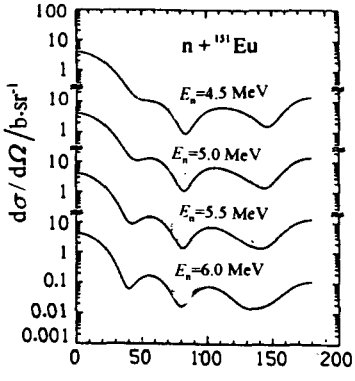

Fig. 9 The neutron elastic scattering angular distribution of n+^{151}Eu

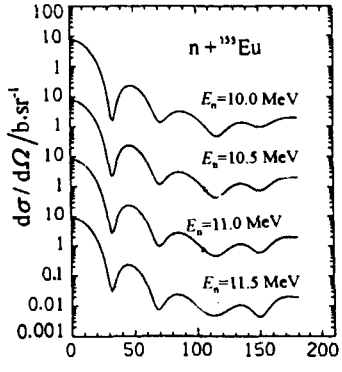

Fig. 10 The neutron elastic scattering angular distribution of n+^{155}Eu

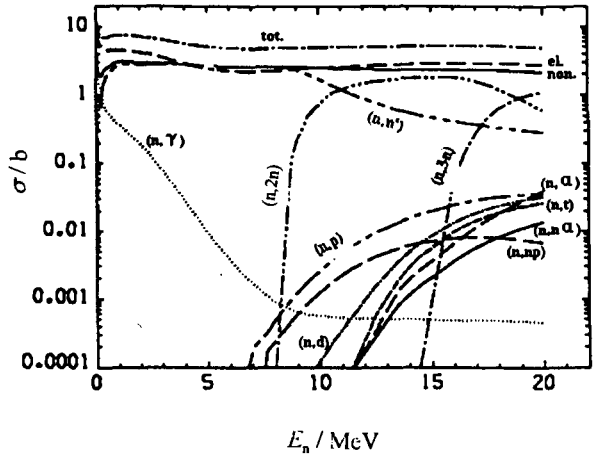

Fig. 11 The all calculated reaction section cross sections of n+^{151}Eu

References

[1] Shen Qingbiao, Commun. Nucl. Data Progress, 7, 43 (1992).

[2] P. D. Kunz, "Distorted Wave Code DWUCK4", University of Colorado.

[3] Su Zongdi et al., Chin. J. Nucl. Phys., 8, 149(1986); INC(CPR)-2, 1986.

[4] Zhang Jingshang, Commun. Nucl. Data Progress, 17 and 18, (1994).

Calculations of a Complete Data Set for n +^{83}Kr,^{84}Kr,^{85}Kr and ^{86}Kr in the Energy Region 0.001~20 MeV

Cai Chonghai

(Department of Physics, Nankai University, Tianjin)

Complete reaction cross sections, secondary neutron spectra and elastic scattering angular distributions of ^{83}Kr,^{84}Kr,^{85}Kr and ^{86}Kr in the energy region 0.001~20 MeV are calculated, theoritical results are in ENDF/B-6 in prety good accordance with experimenttal data.

The natural Kr has 6 stable isotopes: ^{84}Kr, ^{86}Kr, ^{82}Kr, ^{83}Kr, ^{80}Kr and ^{78}Kr, the abundances of which are 57.0%, 17.3%, 11.6%, 11.5%, 2.25% and 0.35%, respectively. However, the four isotopes in the lists of fission product nuclei are ^{84}Kr, ^{86}Kr, ^{83}Kr and ^{85}Kr; however ^{85}Kr is unstable in this work. There are abundant experimental data of σ_{tot} for ^{86}Kr, sufficient experimental data of σ_{tot} for natural element; sufficient experimental data of $\sigma_{n,\gamma}$ for ^{83}Kr, ^{84}Kr and natural element. There are no experimental data for any other reaction cross sections, elastic scattering angular distributions, and secondary neutron spectra. All of the experimental data are taken from EXFOR. The universal optical potential parameters for six channels used in calculations are given in Table 1 of Ref. [1].

First, the code APMN was used to automatically get the optimal parameters of optical potential for neutron reaction channels. There are abundant experimental σ_{tot} for ^{86}Kr, no experimental σ_{tot} for ^{84}Kr, ^{83}Kr and ^{85}Kr; and there are no experimental σ_{non} and elastic scattering angular distributions for all of these four isotopes. So the experimental σ_{tot} for ^{86}Kr are used to determine the optical potential parameters for ^{86}Kr. The experimental σ_{tot} for natural element are used to determine the optical

potential parameters for ^{84}Kr, and the same set of optical potential parameters are also used for calculations of ^{83}Kr and ^{85}Kr.

The final set of optical potential parameters for neutron channel used for calculations of ^{86}Kr is:

V_0=52.40768	V_1=0.55490	V_2=0.01613	V_4=0.07053
W_0=5.08673	W_1=0.21558		
U_0=2.82197	U_1=0.17652	U_2=0.00303	
a_r=0.64840	a_s=0.30067	a_v=0.66464	
r_r=1.25900	r_s=1.23472	r_v=1.19023	

The final same set of optical potential parameters for neutron channel used for calculations of ^{84}Kr, ^{83}Kr and ^{85}Kr is:

V_0=57.70444870	V_1=0.33543086	V_2=0.00571270	V_4=0.79289758
W_0=3.89204335	W_1=0.53332782		
U_0=0.02145672	U_1=0.11249849	U_2=0.00104736	

Secondary, the DWBA code DWUCK4[3] was used to calculate the cross sections and angular distributions of 10 levels for ^{84}Kr, 3 levels for ^{86}Kr, 8 levels for ^{85}Kr and 1 level for Kr in direct inelastic scattering. These direct inelastic scattering data and the above corresponding optimum set of optical potential parameters are taken as the input data of the kernel program SUNF[4]. Through adjusting the parameter Ce1(the multiplied factor in $\sigma_{n,\gamma}$) in the input data of SUNF for ^{84}Kr and ^{83}Kr, respectively, the cross sections $\sigma_{n,\gamma}$ for ^{84}Kr and ^{83}Kr are in optimum agreement with their experimental data, respectively.

The Ce1 values used are 0.31 for ^{84}Kr, 0.4 for ^{83}Kr, 1.0 for ^{85}Kr and ^{86}Kr.

Ck(the parameter for exciton model, 950.0) are not changed for all of these four isotopes. The optical potential parameters for charged particles channels and the energy level density parameters are also not changed (kept the input values) for all of these four isotopes. In order to make the calculated $\sigma_{n,2n}$ reasonable in physics, the pair energy corrections are changed as follows:

$\Delta_{n,2n}$ from 2.67 to 0.37 MeV, $\Delta_{n,3n}$ from 1.00 to 0.20 MeV for ^{83}Kr;

$\Delta_{n,2n}$ from 1.10 to 0.20 MeV, $\Delta_{n,3n}$ from 2.67 to 0.37 MeV for ^{84}Kr;

$\Delta_{n,2n}$ from 2.70 to 0.30 MeV, $\Delta_{n,3n}$ from 1.10 to 0.20 MeV for ^{85}Kr;

$\Delta_{n,2n}$ from 0.82 to 0.20 MeV, $\Delta_{n,3n}$ from 2.70 to 0.30 MeV for ^{86}Kr;

The calculated σ_{tot} , σ_{non} and σ_{el} , for ^{84}Kr, ^{86}Kr, ^{83}Kr and ^{85}Kr as well as the experimental σ_{tot} for ^{86}Kr and natural element are given in Fig. 1(a) to (c), from which we can see that the calculated σ_{tot} are in pretty good accordance with experimental data. The results of $\sigma_{n,\gamma}$ for ^{84}Kr, ^{86}Kr, ^{83}Kr and ^{85}Kr are given in Fig. 2 (a) and (b), from which we can see that the calculated values are also in pretty good agreement with experimental data. The calculated $\sigma_{n,n}$ and $\sigma_{n,2n}$, for ^{84}Kr, ^{86}Kr, ^{83}Kr and ^{85}Kr are given in Fig. 3 (a) and (b), their values are reasonable in physics, though there are no experimental data to compare with. All kinds of the calculated cross sections are plotted in Fig. 4 (a) to (d) for ^{84}Kr, ^{86}Kr, ^{83}Kr and ^{85}Kr, respectively. The calculated secondary neutron spectra of continuous inelastic scattering at E_n=8.0(or 8.5, 9.0) MeV and E_n=14.0 MeV are plotted in Fig. 5 (a) to (d) for ^{84}Kr, ^{86}Kr, ^{83}Kr and ^{85}Kr, respectively. The calculated secondary neutron spectra of (n,2n) reaction at E_n=14 MeV and E_n=20.0 MeV are ploted in Fig. 6 (a) and (b) for ^{84}Kr and ^{86}Kr at E_n=8.5(or 8.0) MeV and E_n=14.0 MeV in Fig. 6 (c) and (d) for ^{83}Kr and ^{85}Kr, respectively. These secondary neutron spectra are of reasonable shapes in physics.

The anthor would like to thank Yu Baosheng and Zhuang Youxiang for their helpful disscussions and suggestions.

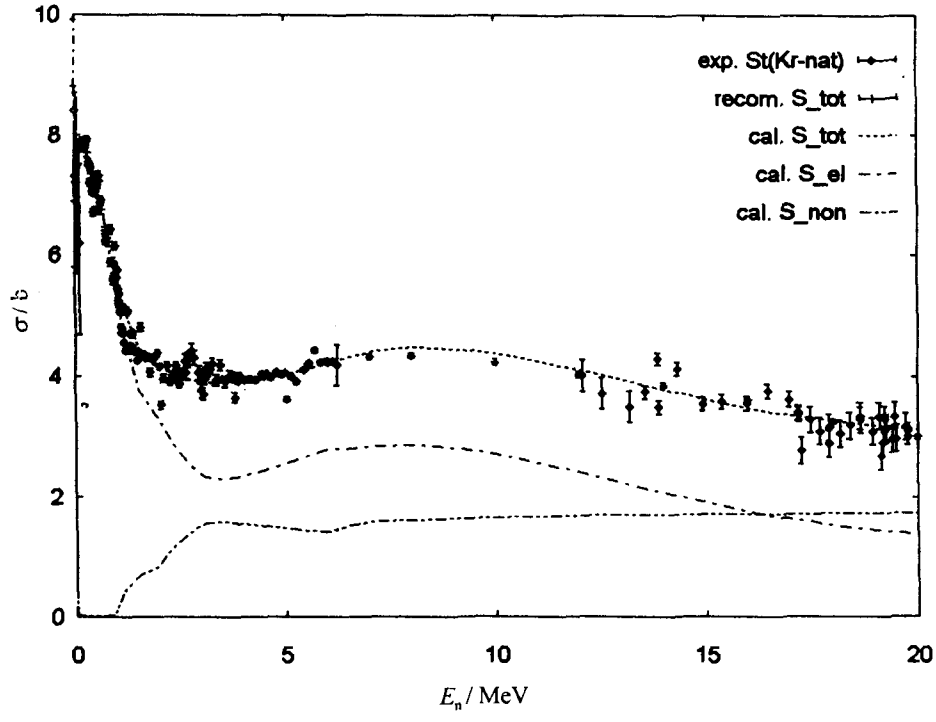

Fig. 1(a) ^{84}Kr total, nonelastic and elastic cross sections

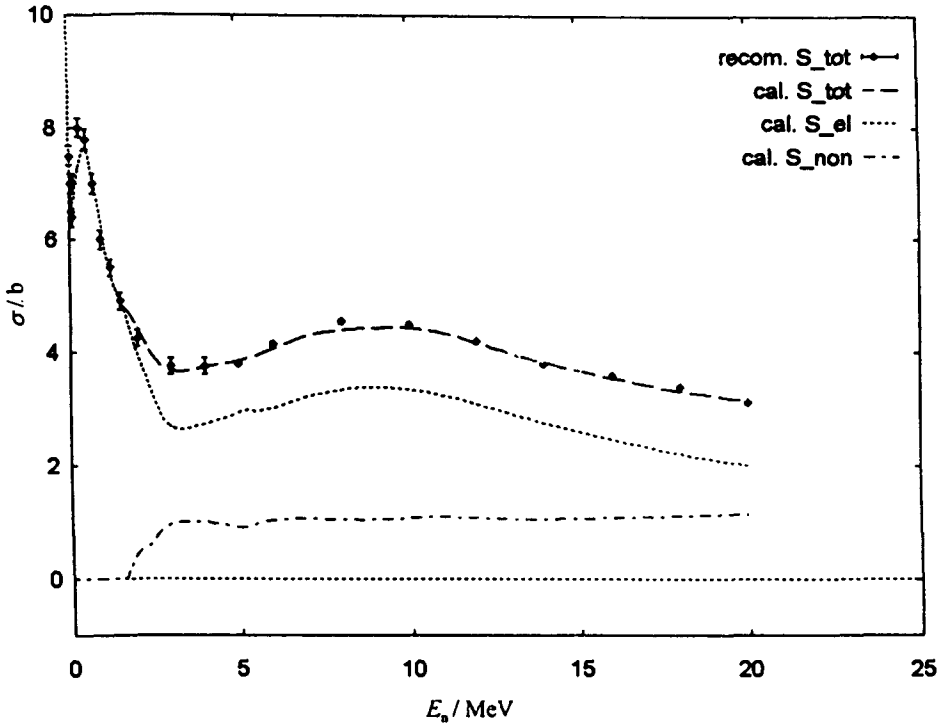

Fig. 1(b) ^{86}Kr total, nonelastic and elastic cross sections

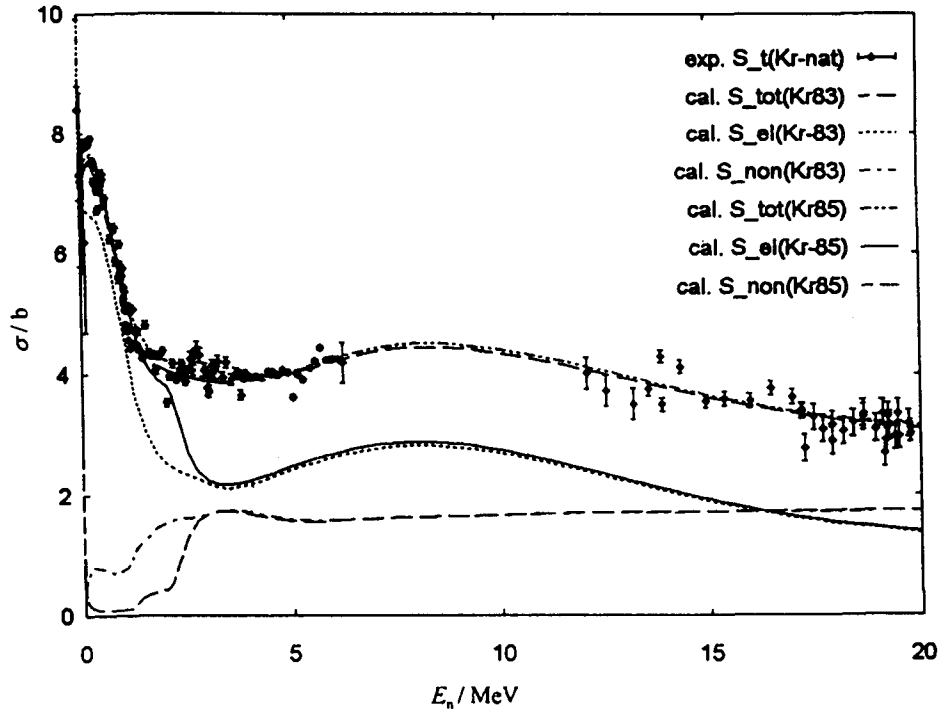

Fig. 1(c) ^{83,85}Kr total, nonelastic and elastic cross sections

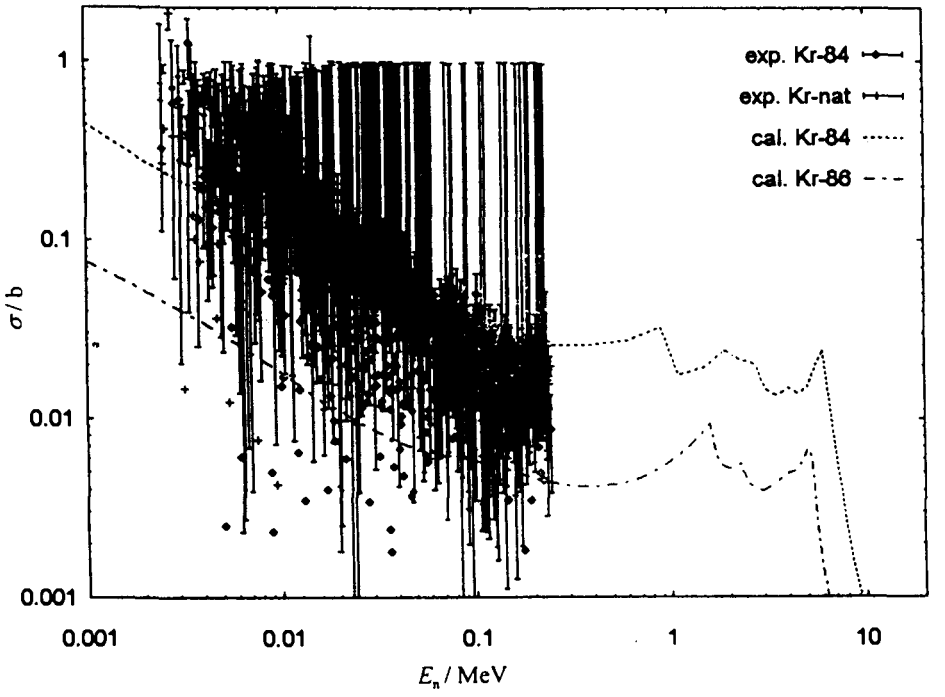

Fig. 2(a) ^{84,86}Kr (n,gamma) cross sections

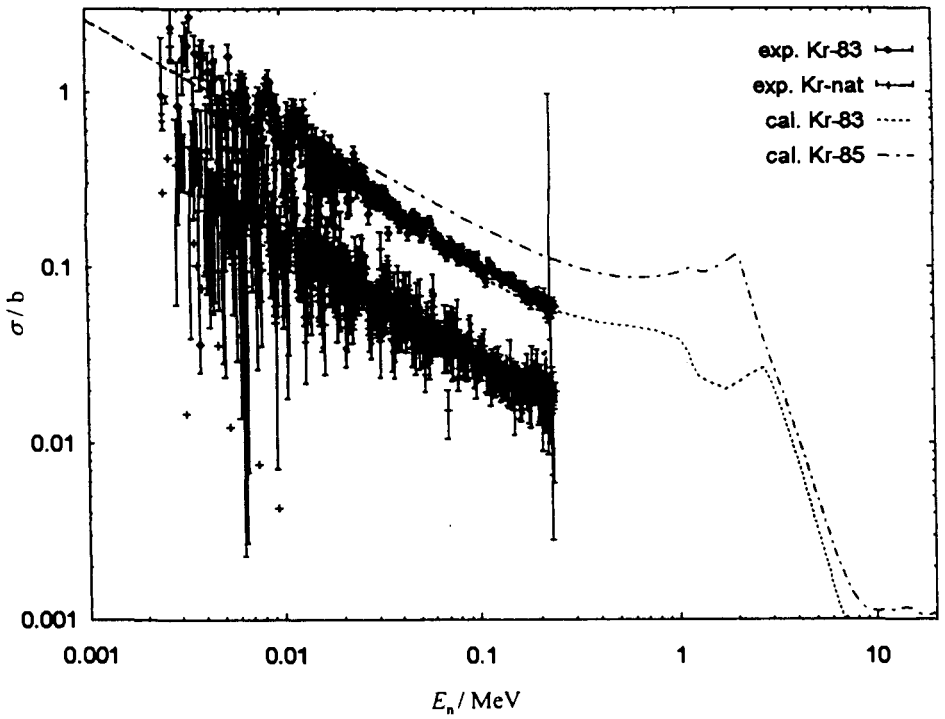

Fig. 2(b) ^{83,85}Kr (n,gamma) cross sections

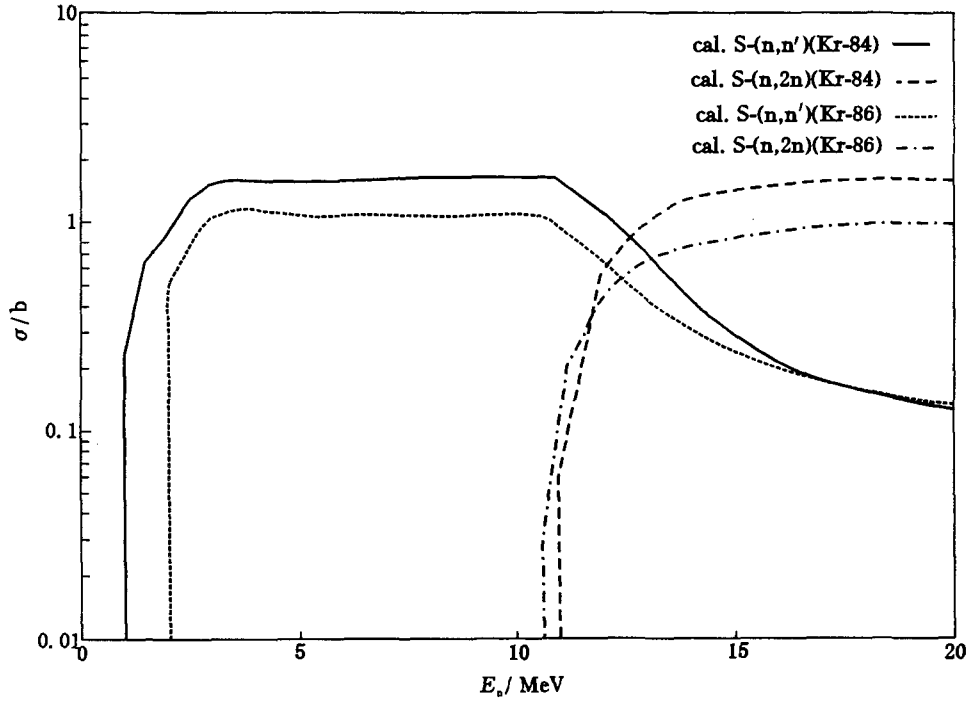

Fig. 3(a) ^{84,86}Kr (n,n') and (n,2n) cross sections

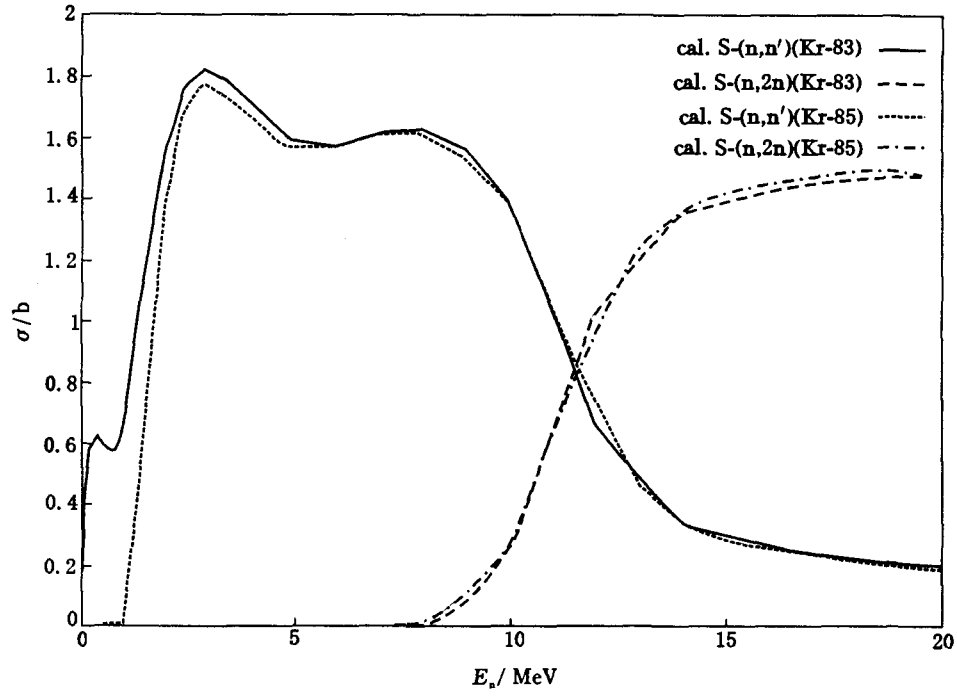

Fig. 3(b) ^{83,85}Kr (n,n') and (n,2n) cross sections

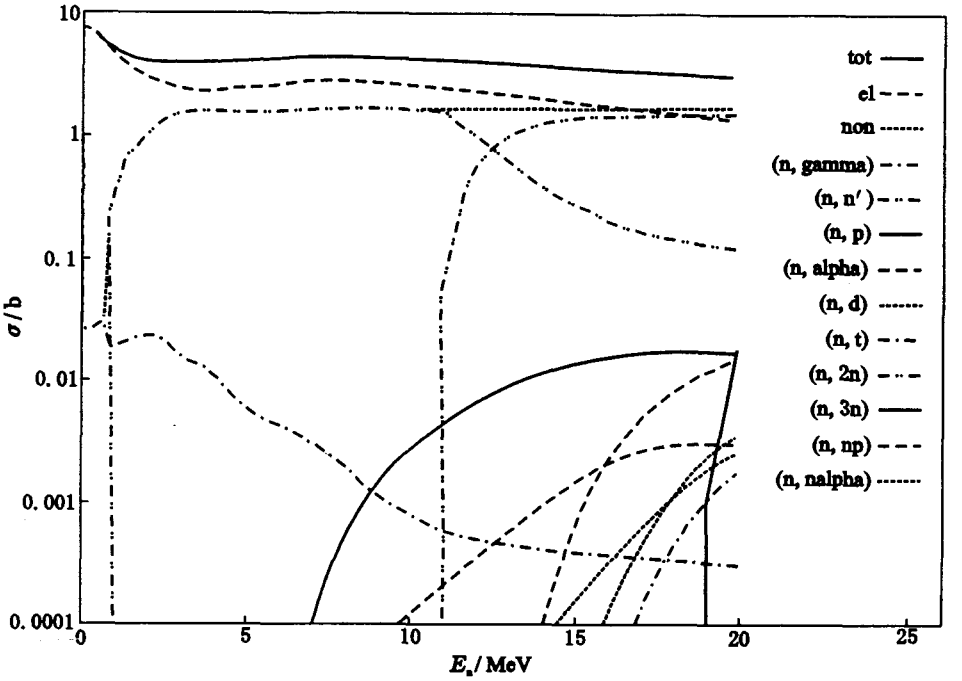

Fig. 4 (a) All calculational cross sections of ^{84}kr

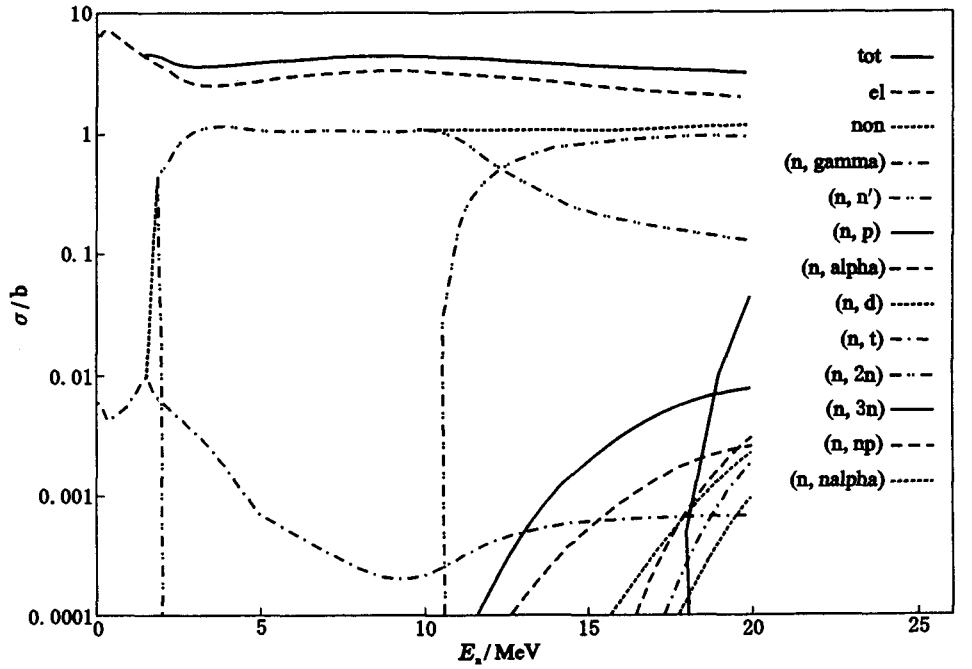

Fig. 4 (b) All calculational cross sections of ^{86}kr

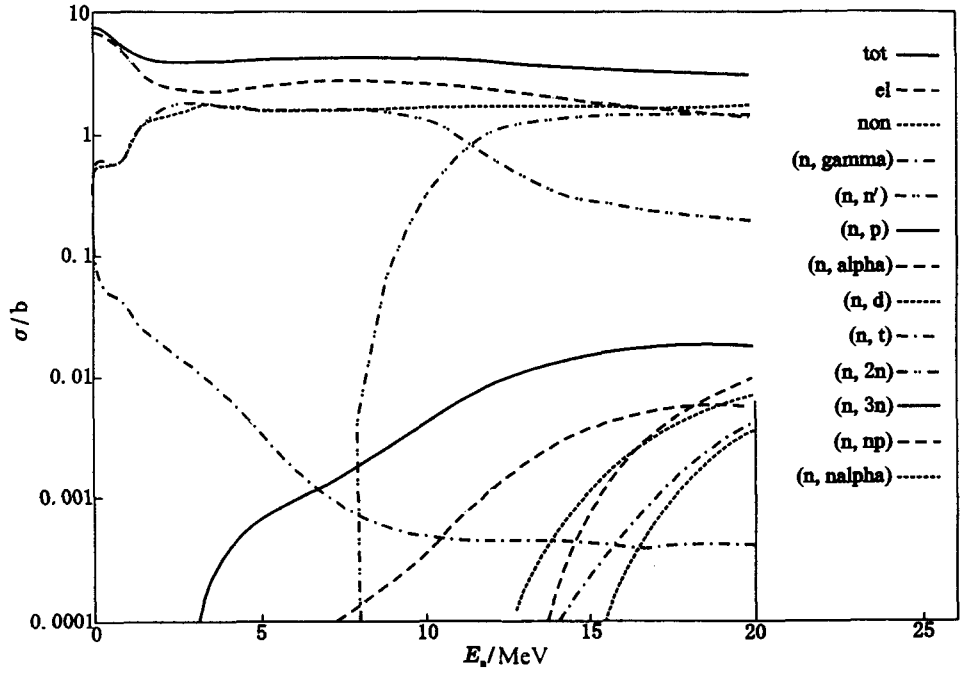

Fig. 4 (c) All calculational cross sections of ^{83}kr

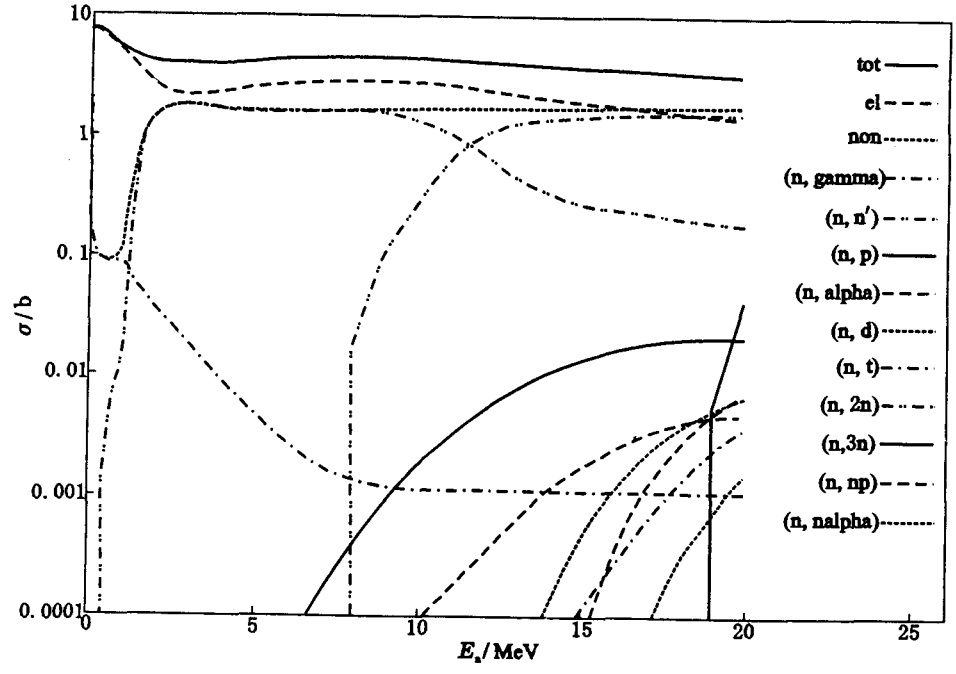

Fig. 4 (d) All calculational cross sections of ^{85}kr

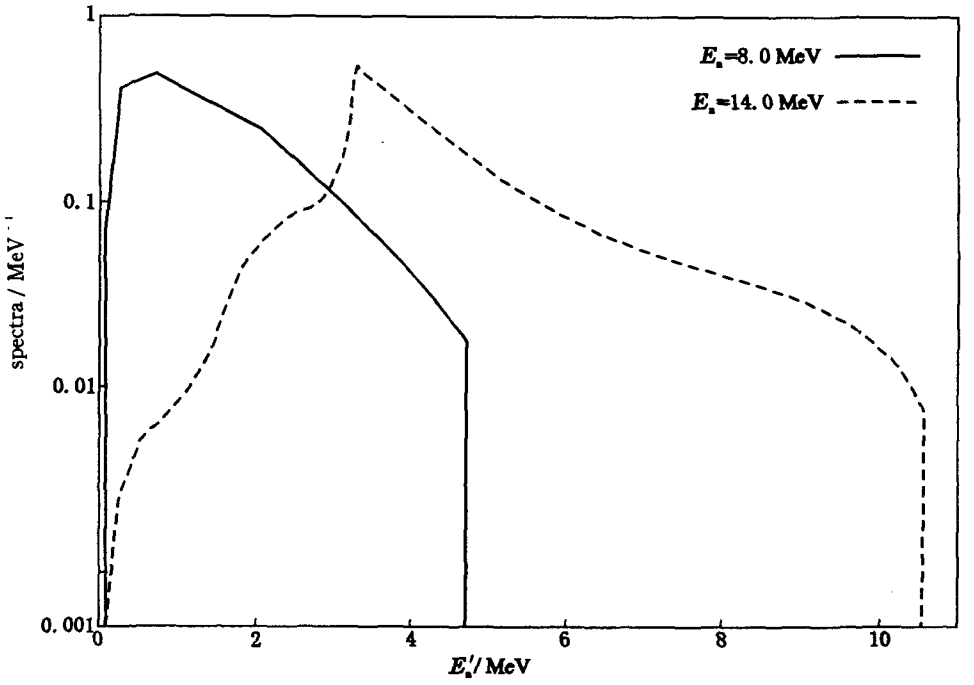

Fig. 5 (a) ^{84}kr (n,n') secondary neutorn spectra (MT=91)

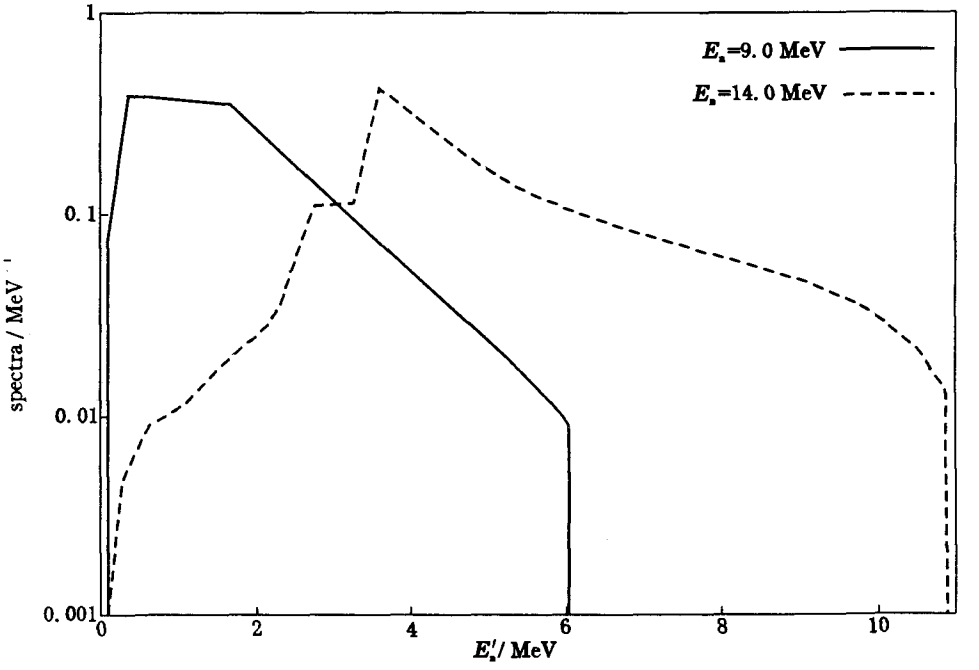

Fig. 5 (b) ^{86}kr (n,n') secondary neutorn spectra (MT=91)

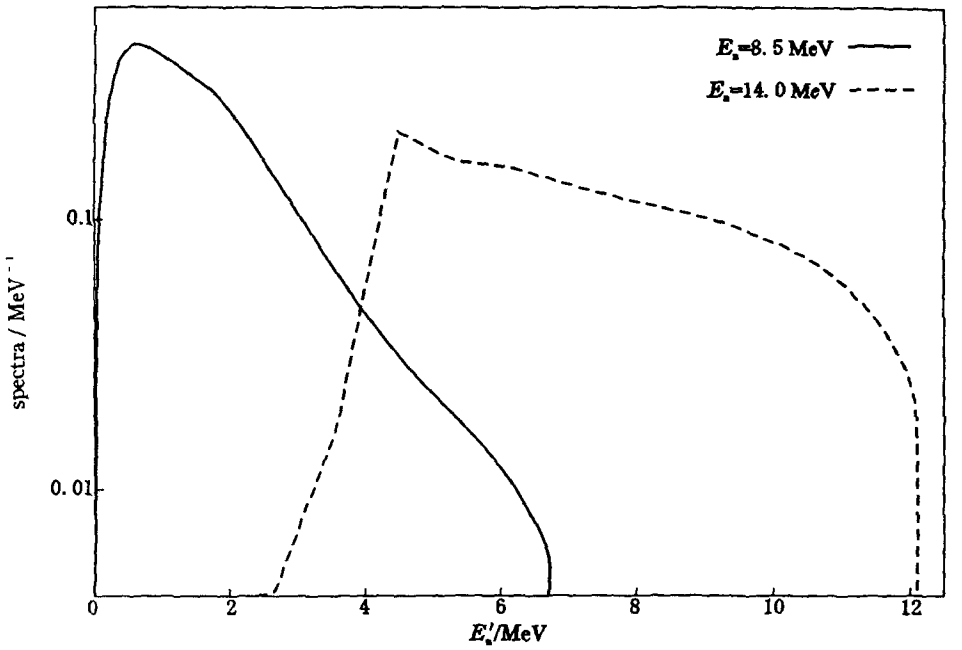

Fig. 5 (c) ^{83}kr (n,n') secondary neutorn spectra (MT=91)

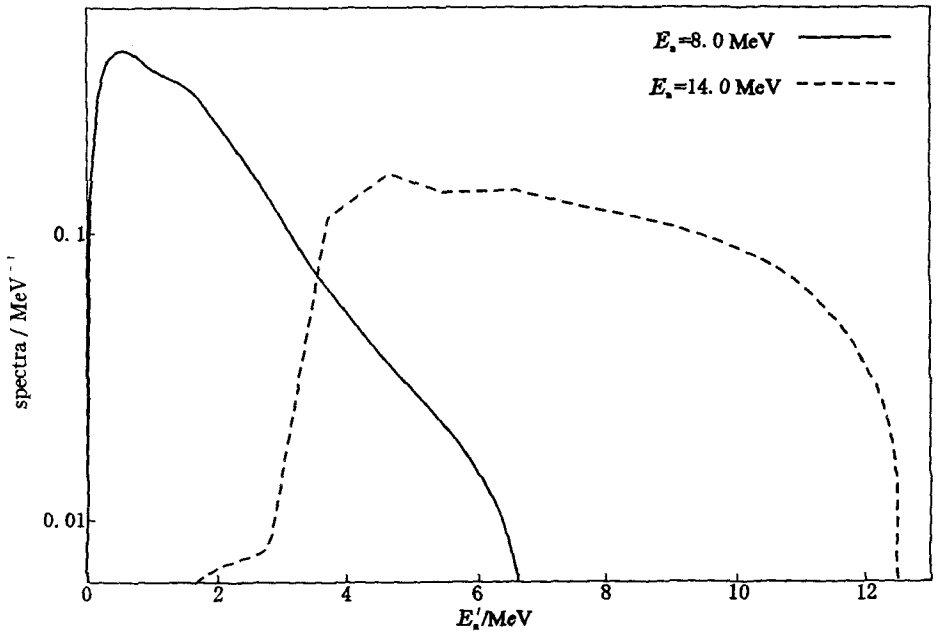

Fig. 5 (d) ^{85}kr (n,n') secondary neutorn spectra (MT=91)

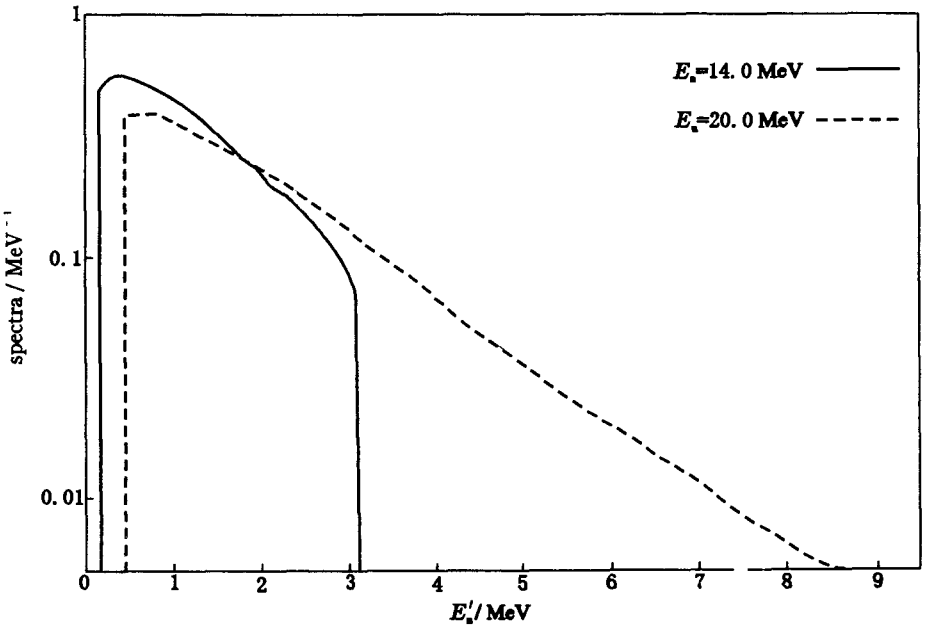

Fig. 6 (a) ^{84}kr (n,2n) secondary neutorn spectra

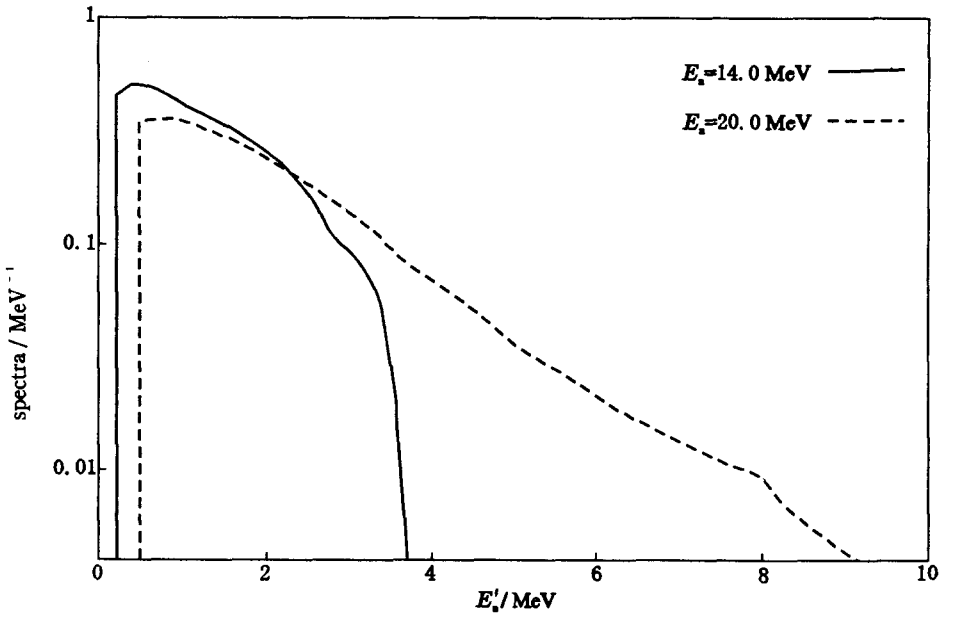

Fig. 6 (b) ^{86}kr (n,2n) secondary neutorn spectra

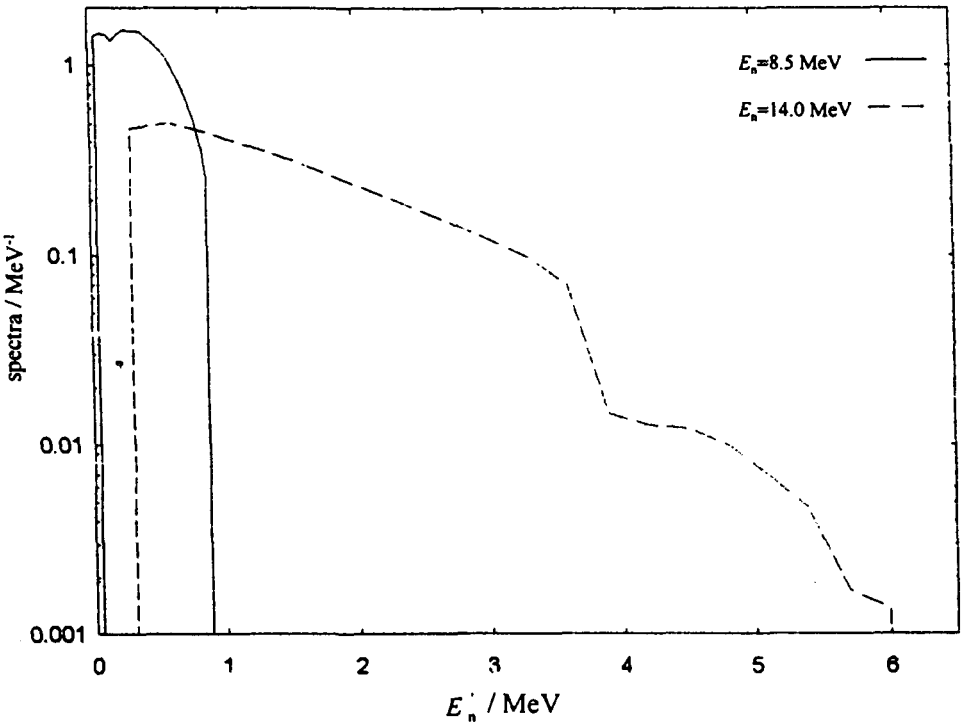

Fig. 6 (c) ^{83}kr (n,2n) secondary neutorn spectra

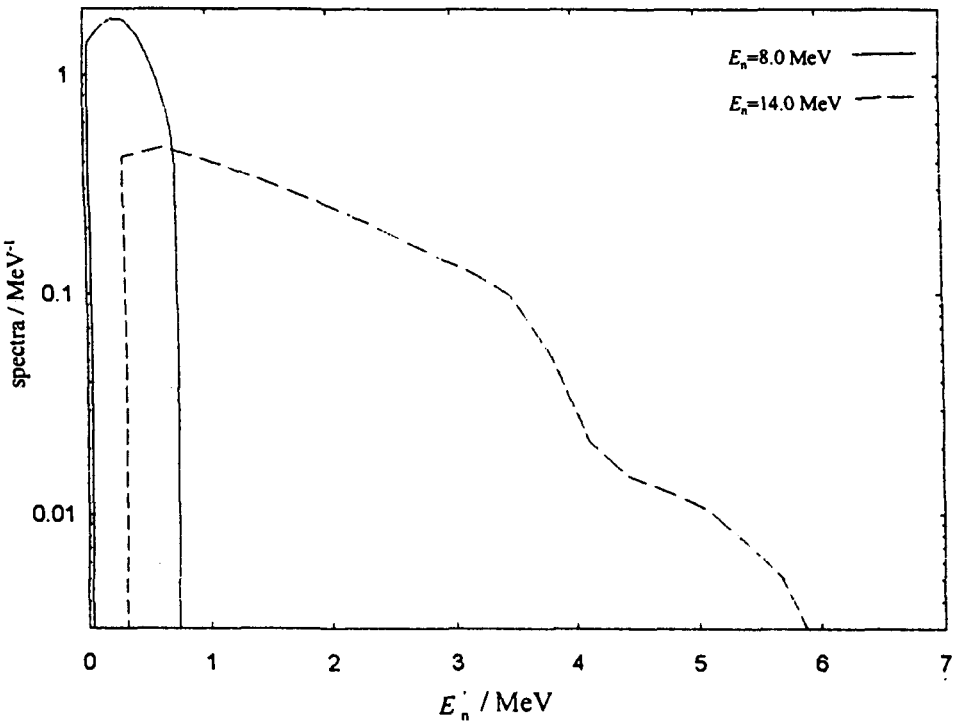

Fig. 6 (d) ^{85}kr (n,2n) secondary neutorn spectra

References

[1] Cai Chonghai and Shen Qingbiao, Calculations of Complete Data for n +89Y in E_n=0.001-20 MeV, Commun. Nucl. Data Progress, 20, 39(1998);

[2] Shen Qingbiao, APMN, a code for automatically searching for a set of optimal optical potential parameters of many medium and heavy nucleus (unpublished);

[3] P.D. Kunz, DWBA code DWUCK4, University of Colorado, USA (unpublished);

CN0101609

Calculation and Analysis of n+^{69,71}Ga Reaction

Zhang Songbai Yu Baosheng

(China Nuclear Data Center, CIAE)

Zhang Zhenjun

(Department of Physics, Northwest University, Xi'an)

Abstract

Ga is an important nucleus in nuclear science and engineering. However, its experimental data are less and the calculation is necessary. Based on the available experimental data of ^{69,71,Nat}Ga and the nuclear reaction semi-classical theory code SUNF, neutron induced reaction cross sections, angular distributions and the energy spectrum were calculated for ^{69,71}Ga at incident neutron energy below 20 MeV. The calculated results were compared with the experimental data.

1 Codes and Parameters

The calculation of n+^{69,71}Ga reaction was made with a set of codes UNF[1], APOM[2] and DWUCK[3].

Based on the experimental data from EXFOR library and recent information, using the code APOM94, the best neutron optical potential parameters were searched automatically by fitting relevant experimental total cross sections[4~7],

nonelastic scattering cross sections (because of no experimental data, they were replaced by ^{Nat}Cu from the ENDF/B-6) and elastic scattering angular distributions. The obtained optimum neutron optical potential parameters of ^{69,71}Ga are as follows:

V= 52.5716-0.4902E+0.007317E^2-24$(N-Z)/A$

W_s= max{0.0, 4.7933+0.6651E-12$(N-Z)/A$}

W_v= max{0.0, -1.5615+0.2188E-0.04927E^2}

U_{so}=6.2

r_r=1.2730 r_s=1.2679 r_v=1.3509 r_{so}=1.2730

a_r=0.6265 a_s=0.4864 a_v=0.6975 a_{so}=0.6265

Using this set of neutron optical potential parameters, the direct inelastic scattering cross sections were calculated by using code DWUCK4. Then, adjusting the charged particle optical potential parameters and level density parameters, all cross sections of n+^{69,71}Ga reactions were calculated by code SUNF.

2 Calculated Results and Analysis

The calculated results of the neutron total cross sections and nonelastic cross sections for n+^{69,71}Ga reactions are in good agreement with the experimental data of n+^{Nat}Ga reaction. The comparison between the theoretical results and experimental data of ^{69}Ga(n,γ)^{70}Ga ,^{71}Ga(n,γ)^{72}Ga reactions are given in Fig.1 and 2, respectively. Both of them are a little higher than experimental data in energy region 1~2 MeV and the calculated results of ^{69}Ga(n, γ)^{70}Ga in 2~3 MeV is lower than experimental data, but they are in the error range. The cross sections of ^{71}Ga(n, p) ^{71}Zn, ^{69}Ga(n, α) ^{66}Cu, ^{71}Ga(n, α) ^{68}Cu reactions are given in Figs. 3 to 5, respectively . They are all in good agreement with the experimental data. The comparison of the theoretical results and experimental data of ^{69}Ga(n,2n) ^{68}Ga and ^{71}Ga(n,2n) ^{70}Ga are given in Fig.6 and 7, respectively . It is shown in Fig. 6 that the calculated results of ^{69}Ga(n,2n)^{68}Ga are somewhat lower. However, taking account of the newest data measured by Zhang Guohui[8], the calculated results are reasonable. The ^{71}Ga(n,2n)^{70}Ga calculated results are in agreement with the experimental data. Fig.8 and 9 shows the all calculated cross sections of n+^{69}Ga and n+^{71}Ga ,respectively.

The authors would like to extend our thanks to Shen Qingbiao, Liu Tong, Zhang Jingshang, Zhang Guohui, Tang Guoyou, Rong Jian and all the other members of CNDC for their kind help and good suggestions.

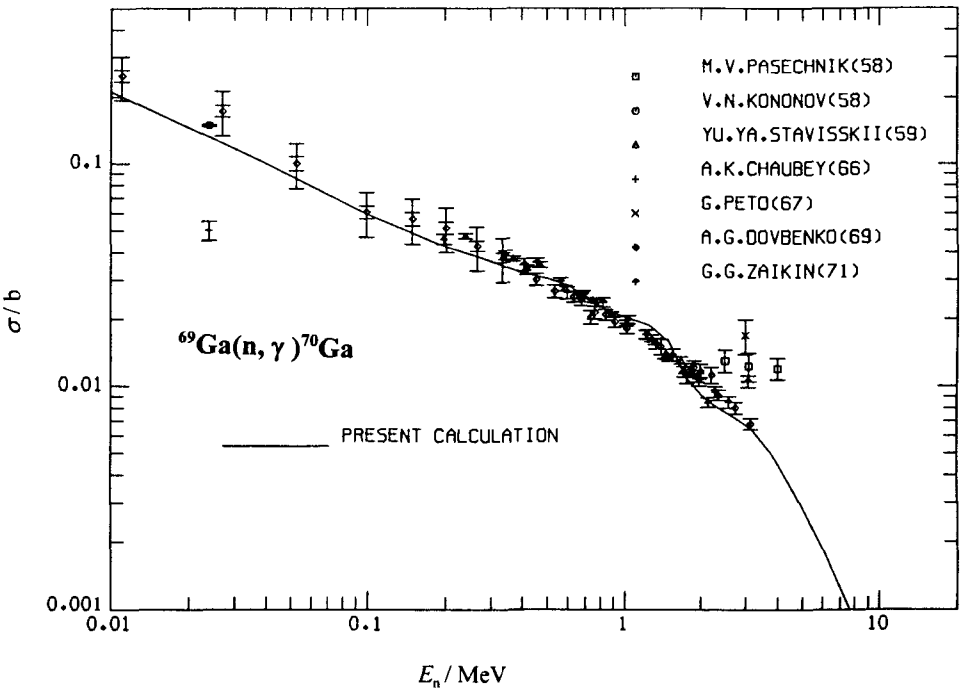

Fig. 1 The cross sections of ^{69}Ga(n, γ)^{70}Ga reaction

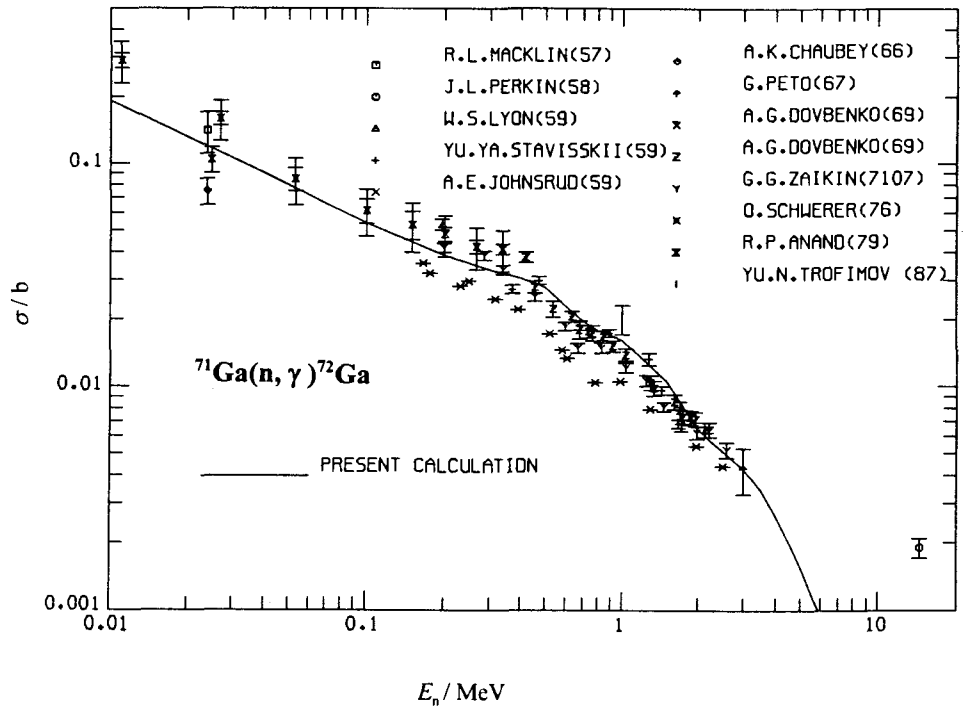

Fig. 2 The cross sections of ^{71}Ga(n, γ)^{72}Ga reaction

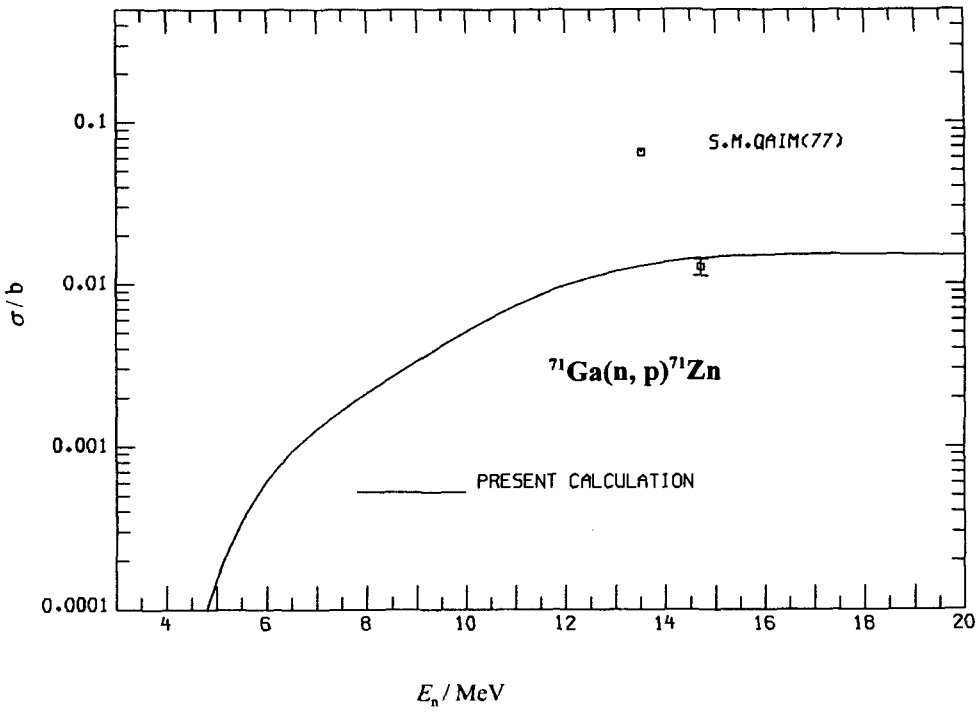

Fig. 3 The cross sections of ^{71}Ga(n, p)^{71}Zn reaction

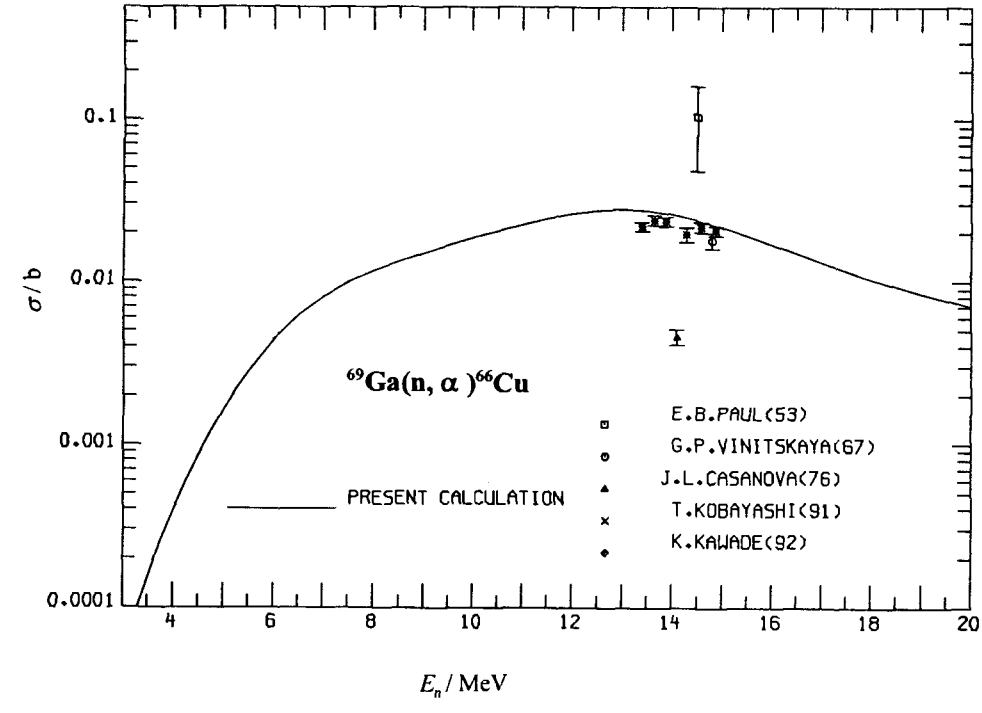

Fig. 4 The cross sections of ^{69}Ga(n, α)^{66}Cu reaction

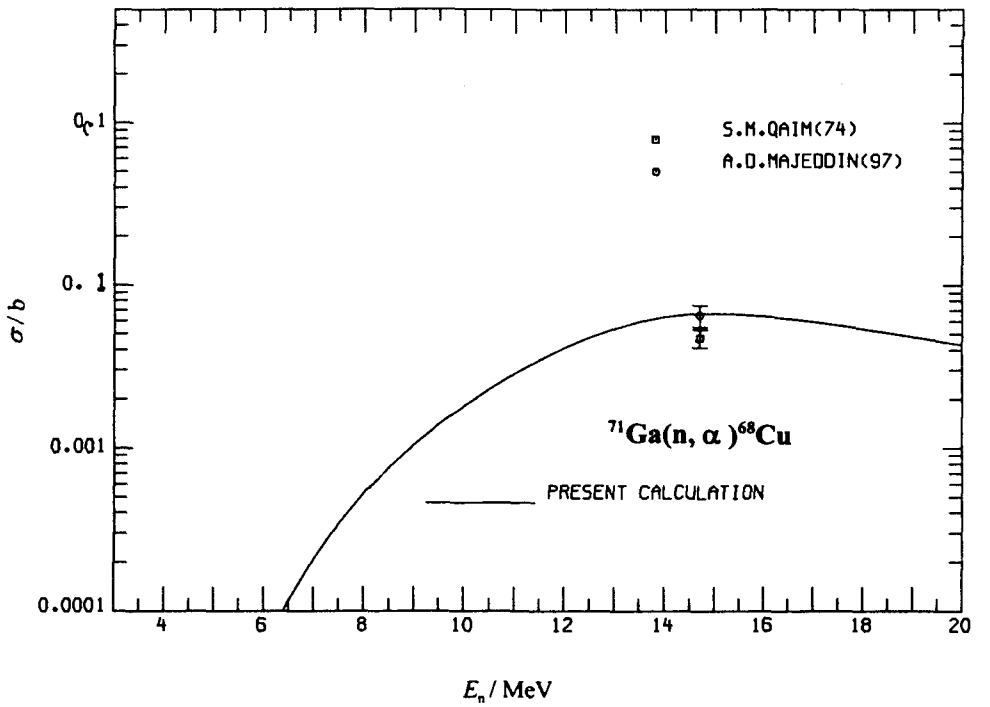

Fig. 5 The cross sections of ^{71}Ga(n, α)^{68}Cu reaction

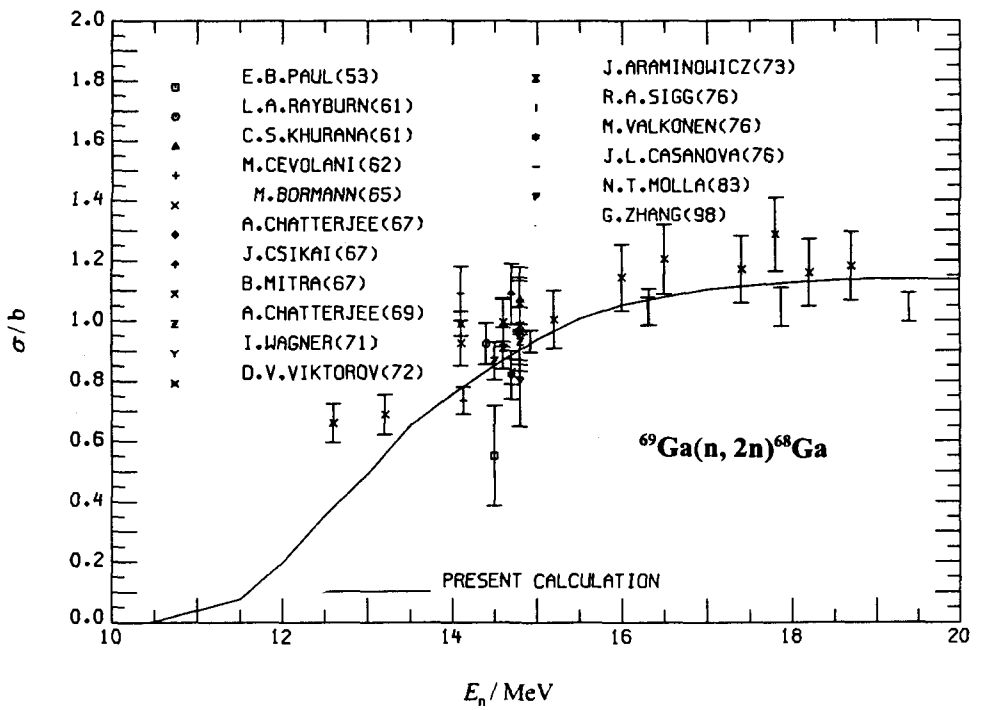

Fig. 6 The cross sections of ^{69}Ga(n,2n)^{68}Ga reaction

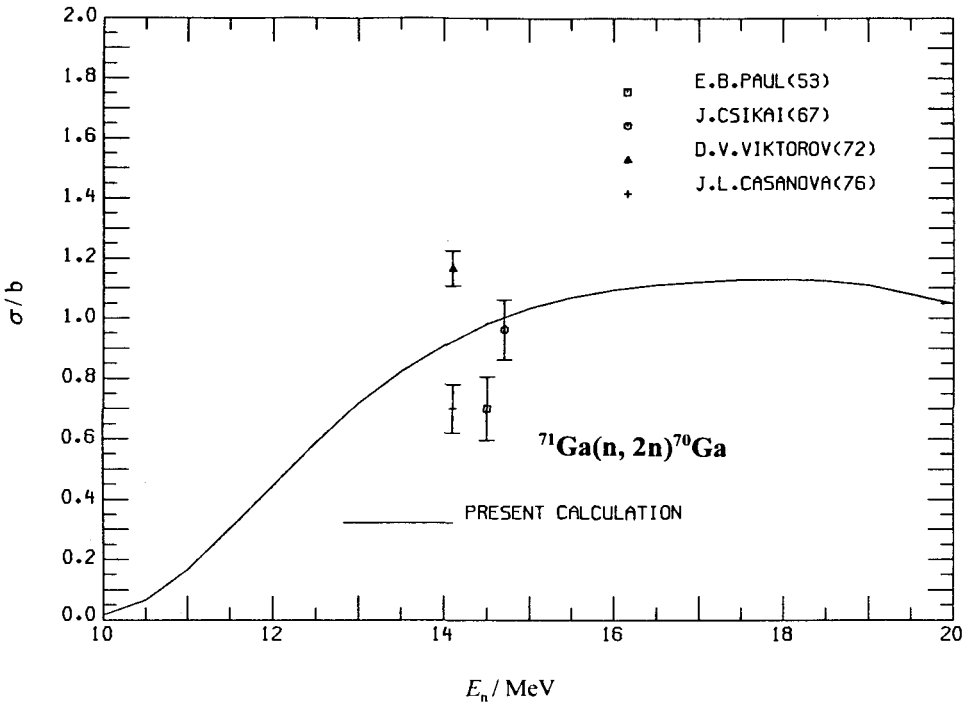

Fig. 7 The cross sections of ^{71}Ga(n,2n)^{70}Ga reaction

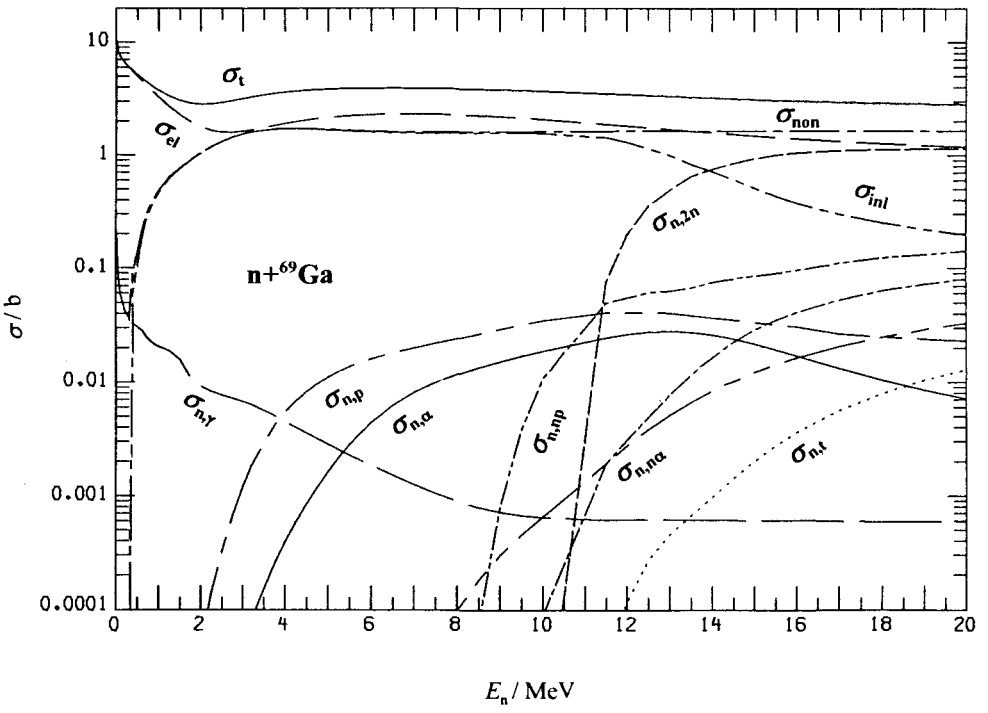

Fig. 8 The cross sections of n+^{69}Ga reaction

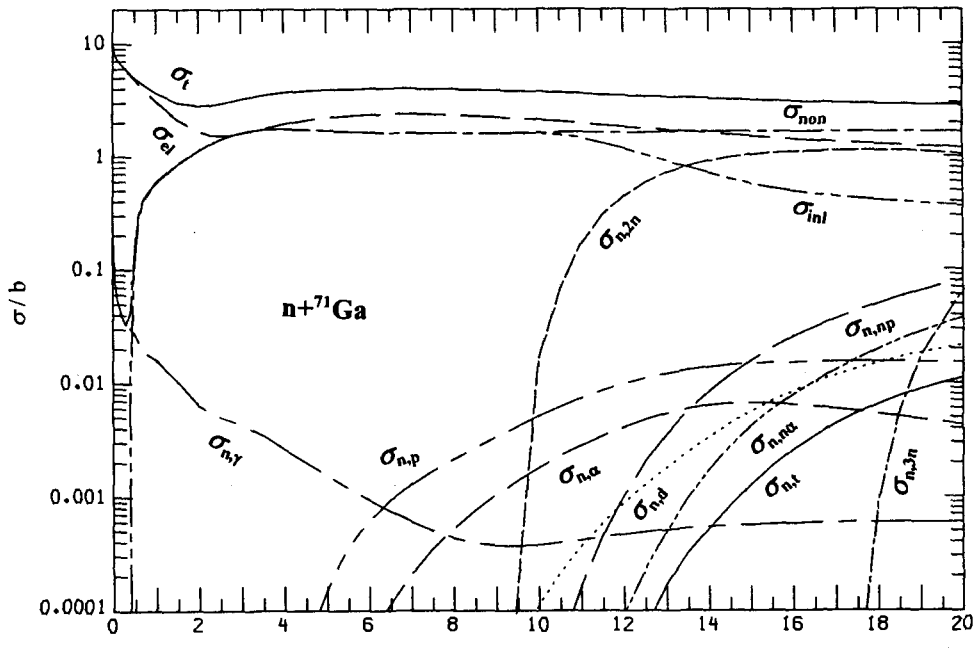

Fig. 9 The cross sections of n+^{70}Ga reaction

References

[1] Zhang Jingshang, Commu. of Nucl. Data Prog., 7, 14(1992)

[2] Shen Qingbiao ,Commu. of Nucl. Data Prog., 7, 43(1992)

[3] P.D.Kunz, "Distorted Wave Code DWUCK4", University of Colorado

[4] D.G.Foster Jr el al., J, PR/C, 3, 576(1971)

[5] J.M.Peterson el al., J, PR, 120, 521(1960)

[6] Bratenahl el al., J, PR110, 927(1958)

[7] J.Cabe el al., W, CABE(1965)

[8] Zhang Guohui, private communication, 1999

III DATA EVALUATION

Evaluation of Complete Neutron Nuclear Data for ^{63}Cu

Ma Gonggui Wang Shiming
(Institute of Nuclear Science and Technology, Sichan University, Chengdu, 610064)

Introduction

Cu is a very important structure material in nuclear fusion engineering. The evaluated neutron nuclear data include total, elastic, non-elastic, total inelastic, inelastic cross sections to 17 discrete levels, inelastic continuum, (n,2n), (n,n'α)+(n, αn'), (n,n'p)+(n,pn'), (n,p), (n,d), (n,t), (n,^{3}He), (n,α),(n,2p) and capture cross sections. The angular distributions of secondary neutron, the double differential cross sections (DDCS), the gamma-ray production data and the resonance parameters are also included. The data are given in the energy range 10^{-5} eV to 20 MeV. The evaluation is based on both experimental data measured up to 1998 and calculated data with program UNF[1]. The evaluated data have been adopted into CENDL-3 in ENDF/B-6 format.

The level scheme is given in Table 1, selected from the new data of Ref. [2]. The binding energy of emitted final particle are given in Table 2.

1 Resonance Parameter

The resolved resonance parameters were taken from ENDF/B-6 in the energy region 10^{-5} keV to 99.5 keV. Thermal cross sections are 9.6 b, 5.1 b and 4.5 b for (n, tot), (n, n) and (n,γ) reactions , respectively.

2 Neutron Cross Section

The comparison of experimental data with evaluated ones are shown in Fig.1～13. It can be seen that the present evaluation is in agreement with the experimental data.

Table 1 Inelastic discrete levels (Abundance 69.17%)

E_l/ MeV	J^π	E_l/ MeV	J^π	E_l/ MeV	J^π	E_l/ MeV	J^π
0.0	1.5^-	1.5470	1.5^-	2.0926	3.5^-	2.4972	1.5^-
0.6697	0.5^-	1.8612	3.5^-	2.2079	4.5^-	2.5064	4.5^+
0.9621	2.5^-	2.0112	1.5^-	2.3366	2.5^-	2.5120	0.5^-
1.3270	3.5^-	2.0622	0.5^-	2.3380	1.5^-		
1.4120	2.5^-	2.0814	2.5^-	2.4048	3.5^+		

Table 2 Binding energy of emitted final particle for ^{63}Cu MeV

reaction	n,γ	n,n′	n,p	n,α	n, ^{3}He	n,d	n,t
channels	n,2n	n,n′p	n,n′α	n,pn′	n,2p	n, αn′	n,3n
^{63}Cu	0.0	7.9160	7.1996	6.2011	17.444	11.816	16.155
	10.854	6.1246	5.7766	6.8411	11.275	7.4915	8.8942

2.1 Total Cross Section

Above the resolved resonance region, there are still some small structure in the energy range (99.5 keV~4.0 MeV) and become smooth in the energy range 4.0～20 MeV. In the energy range from 99.5 keV to 1.12 MeV, the data were mainly taken from Pandey's experimental data[3]. In the energy range from 1.2 MeV to 4.5 MeV, the data were mainly taken from Guenther's experimental data of ^{Nat}Cu[4]. In the smooth energy range from 4.0 MeV to 20 MeV, they were obtained from Larson's experimental data of ^{Nat}Cu[5]. A plot of these data and the evaluated data is shown in Fig. 1.

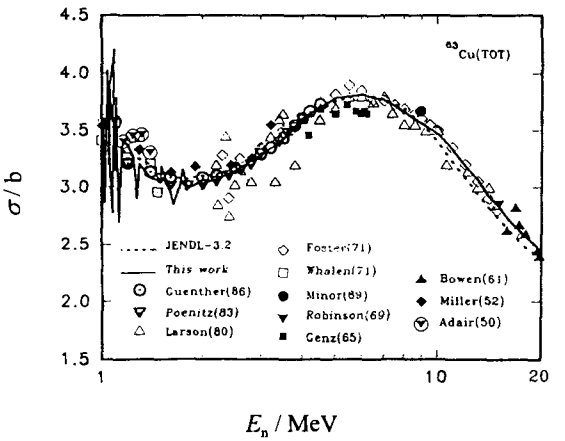

Fig. 1 Total cross section for ^{63}Cu

2.2 Elastic Scattering Cross Section

Above the resolved resonance region, the elastic scattering cross section was obtained by subtracting the sum of cross sections of all the non-elastic processes from the total cross section. In general, the agreement between the calculated cross section and the available experimental data of El-Kadi[6] and Kinney[7] is good (See Fig. 2).

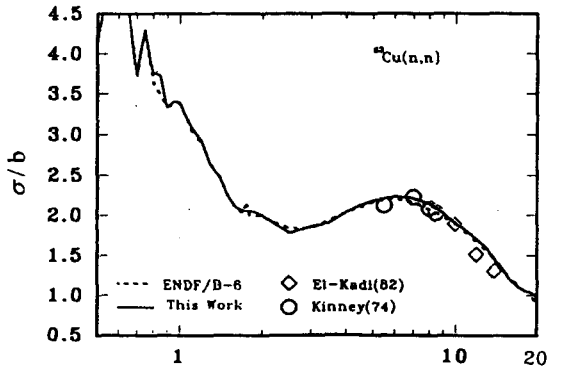

Fig. 2 Elastic scattering cross section for ^{63}Cu

2.3 Non-Elastic Scattering Cross Section

This cross section represents the sum of all cross sections of (n,n'), (n,2n),(n,γ), (n,p), (n,d), (n,t), (n,^{3}He), (n,α), (n,n'α), (n,n'p) and (n,2p) reactions.

2.4 Total Inelastic Cross Section

The experimental data by Shi Xiamin[8] and Joensson[9] around 14.5 MeV were used to normalize the corresponding model calculated results (See Fig. 3).

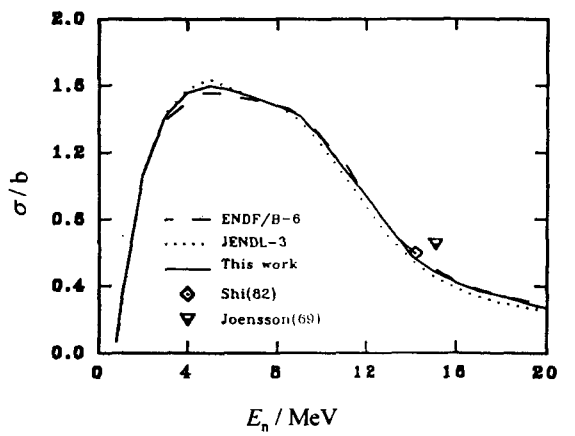

Fig. 3 Inelastic scattering cross section for ^{63}Cu

2.5 Inelastic Cross Section to the Discrete Levels and the Continuum

The inelastic scattering cross section to 17 discrete levels were calculated by using UNF code. For 0.6697 and 0.9621 MeV levels, the data were obtained by fitting experimental data measured by Guenther[4], Kinney[7], Almen-Ramstrom[10] and Holmqvist[11]. A plot of these data and the evaluated data are shown in Fig. 4. For 1.327, 1.412, 1.547 and 1.8612 MeV level, the calculated results are in good agreement with the concerned experimental data. For others, the data were taken from calculated results.

The continuum part was obtained by subtracting the cross section of inelastic scattering to 17 discrete levels from the total inelastic.

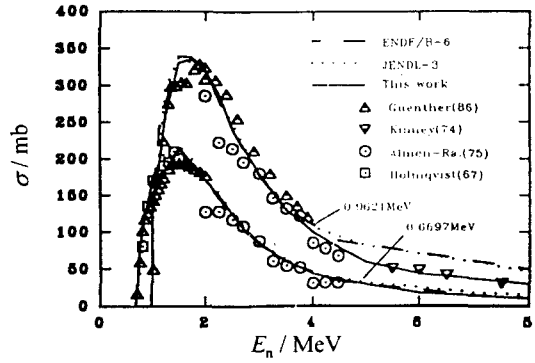

Fig. 4 Inelastic cross section of ^{63}Cu excited states

2.6 (n,2n) Cross Section

For (n,2n) reaction, the experimental data were measured by Gruzdevich, Mclane, Ghanbari, Ryves, Jarjis, Majumder, Mogharrab, Andreev, Bardolle, Rayburn, Koehler,Glover and Fowler in the energy range from threshold to 20 MeV. The evaluated data were obtained by spline function fitting these data (See Fig. 5).

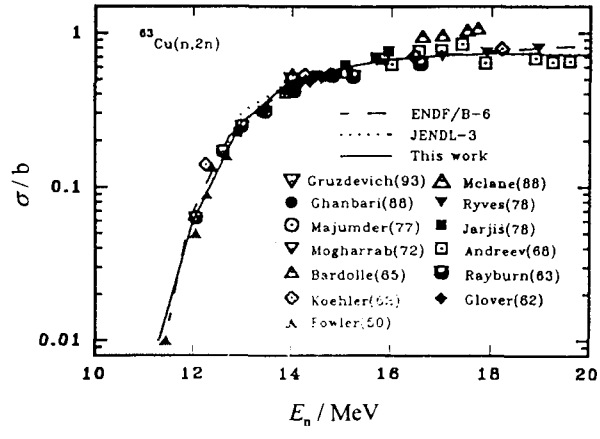

Fig. 5 ^{63}Cu (n,2n) cross section

2.7 (n,p) Cross Section

For (n,p) reaction, the experimental data[12~24] were measured by Greenwood and Qaim [25,26] at 15.0 and 14.7 MeV, respectively. They are quite discrepant. The evaluated data were taken from theoretical calculated results(See Fig. 6).

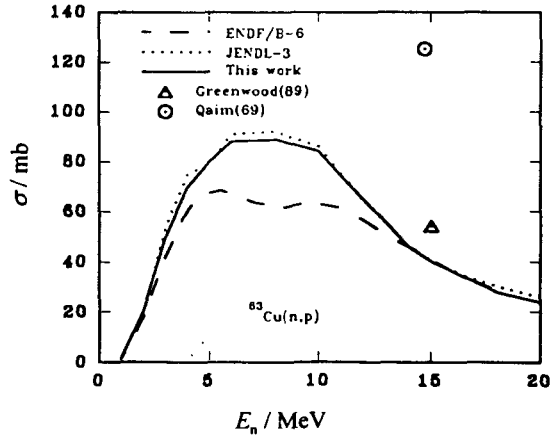

Fig. 6 ^{63}Cu (n,p) cross section

2.8 (n,n'p)+(n,pn') Cross Section

The experimental data were measured by Joensson, Colli[27] and Allan[28] around 14 MeV. The evaluated data were obtained by calculated results, they were nomalized to 250 mb at 14.1 MeV, measured by Colli[27] (See Fig. 7).

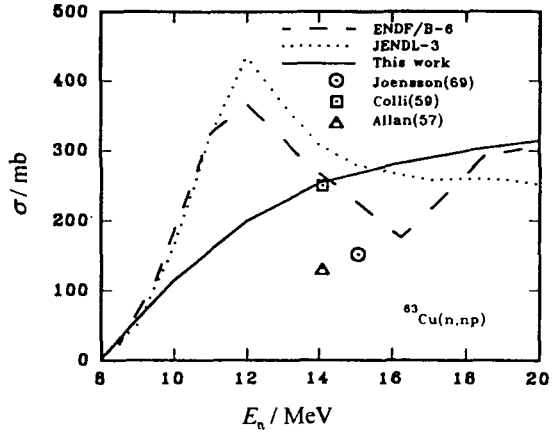

Fig. 7 ^{63}Cu (n,np) cross section

2.9 (n,α), (n,n'α+n, αn') Cross Section

For (n, α) reaction, the experimental data were measured by Zhao Wenrong, Majdeddin, Filatenkov, Lu Hanlin, Meadows, Csikai, Ikeda, WangYongchang[29~36], Greenwood, Winkler, Paulsen, Garuska, Artem and Cserpak[37~41], respectively. The

evaluated data were obtained by spline function fitting experimental data in the energy range from threhold to 20 MeV (See Fig. 8).

The (n,n' α) + (n, αn') cross section was taken from the model calculation due to lack of the experimental data.

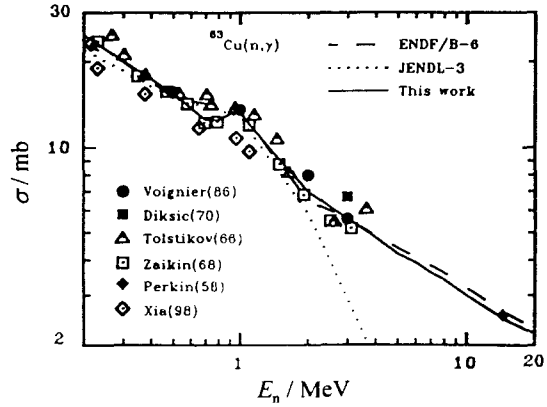

Fig. 8 ^{63}Cu (n,α) cross section

2.10 Capture Cross Section

Above resonance energy and up to 3 MeV, the evaluvated data were obtained by spline function fitting experimental data, measured by Voignier, Diksic, Tolstikov, Zaikin and Xia Yijun[42~46] in the energy range from 99.5 keV to 3.0 MeV. Above 3.0 MeV, calculated data were nomalized to Perkin's[47] experimental data at 15.0 MeV (See Fig. 9).

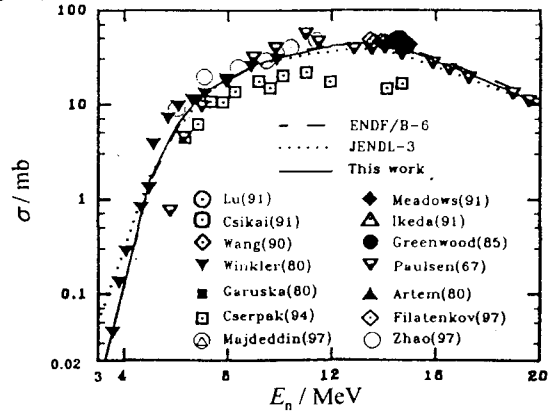

Fig. 9 ^{63}Cu (n,γ) cross section

2.11 (n,d) Cross Section

The experimental data were measured by Ahmad[48] and Grimes[49] in the energy range from 9 to 14.8 MeV. The experimental data by Grimes on 14.8 MeV energy point were used to normalize the model calculated results (See Fig. 10).

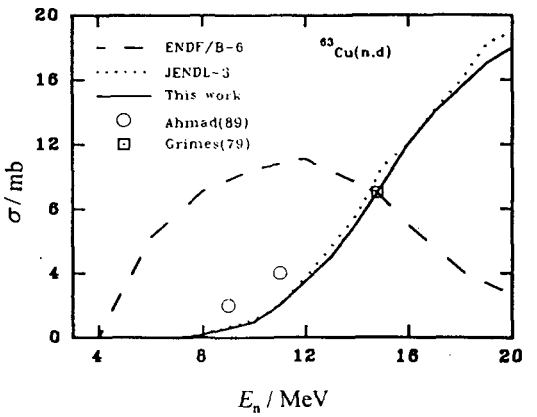

Fig. 10 ^{63}Cu (n,d) cross section

3 Secondary Neutron Angular Distributions

For elastic scattering, the experimental data measured by El-Kadi, Kinney, Guenther, Holmqvist, Tsukada[50], Smith, Gorlov[51] and Bucher[52] were used to adjust the parameters in the calculations with optical model. The calculated results in good agreement with the experimental data and used for recommended data. An example is given in Fig. 11.

The discrete inelastic angular distributions (MT=51-67) were obtained from theoretical calculation results. The angular distributions for (n,2n),(n,n'α),(n,n'p) and continuum inelastic(MT = 16, 22, 28, 91) were assumed to be isotropic.

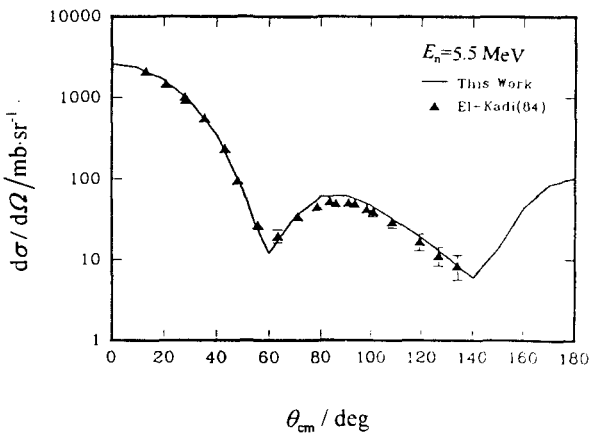

Fig. 11 Elastic scatter angular distributionof ^{63}Cu

4 The Double Differential Cross Section and γ-Ray Production Data

The double differential emission cross section (MF= 6, MT= 16, 22, 28, 91, 103, 104, 105, 106, 107, 111) and γ-ray production data (MF= 12, 13, 14, 15) were taken from the calculation results. An example of the secondary spectrum is given in Fig. 12.

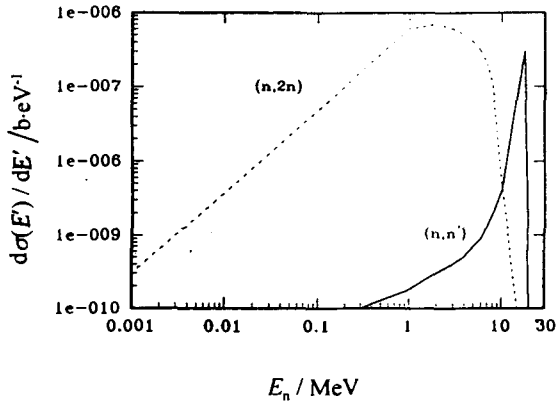

Fig. 12 ^{63}Cu (n,2n) and (n,n') continuous secondary neutron spectrum at 20.0 MeV

5 Theoretical Calculation

An automatically adjusted optical potential code (APOM)[53] was used for searching a set of optimum neutron spherical optical potential parameters. ECIS95 code[54] of coupled channel was used to calculate the direct inelastic scattering for excited levels as the input data of UNF. UNF code, including optical model, Hauser-Feshbach statistical model and exciton model, was used to calculate the data of files 3, 4, 6, 12, 13, 15, which requires following input parameters: optical potential, level density, giant dipole resonance[55] and nuclear level scheme. These parameters were adjusted on the basis of experimental data in the neutron energy range from 1 keV to 20 MeV.

5.1 Optical Model, Level Density and Giant Dipole Resonance Parameters

Optical potential parameters are given in Table 3. The level density and pair correction parameters are given in Table 4. The giant dipole resonance parameters are shown in Table 5, the symbols CSG, EE and GG are the peak cross section, resonance energy and full width at half maximum, respectively.

Table 3 Optical model potential parameters*

	Depth / MeV		Radius / fm	Diffuseness / fm
	V_o=55.563	W_o=16.076	X_r=1.1856	A_r=0.7457
	V_1=–0.4573	W_1=–0.3529	X_s=1.413	A_s=0.2569
Neutron	V_2= –0.00179	W_2=–35.467	X_v=1.413	A_v=0.2569
	V_3=–27.0387	U_o=–0.8459	X_{so}=1.1856	A_{so}=0.7457
	V_4=0.0	U_1=0.2384	X_c=1.0	
	V_{so}=3.41	U_2=0.0		

* Note: $V_r(E)=V_o+V_1E+V_2E(2)+V_3(A-2Z)/A+V_4Z/A(1/3)$;

$W_s(E)=W_o+W_1E+W_2(A-2Z)/A$;

$U_v(E)=U_o+U_1E+U_2E(2)$.

5.2 The Coupled Channel Calculation

The Legendre Coefficients (L. C.) of direct elastic scattering to ground state and direct inelastic scattering to excited states were calculated with coupled channel code ECIS95 to 18 levels by Han[56] in the required input format of UNF.

Table 4 Level density parameters and pair correction values of 11 excess nuclei *

	n,γ	n,n'	n,p	n,α	n, ^{3}He	n,d	n,t	n,2n	n,n'α	n,2p	n,3n
L	7.76	7.16	7.45	7.75	8.20	7.34	7.86	6.73	7.20	8.80	6.18
P	–0.18	1.3	2.5	–0.25	1.2	2.5	1.25	–0.15	1.22	–0.28	1.32

* Note: $L=[0.00880(s(z)+s(n))+Q_b]A$; $P=P(n)+P(z)$;

Q_b=0.142 or 0.12 (spherical or deformation).

Table 5 The giant dipole resonance parameters (single peak)

CSG / b	0.075, 0.075, 0.034, 0.026, 0.026, 0.034, 0.034, 0.075, 0.026, 0.026, 0.075
EE / MeV	16.7, 16.7, 16.3, 16.37, 16.37, 16.3, 16.3, 16.7, 16.37, 16.37, 16.7
GG / MeV	6.89, 6.89, 2.44, 2.56, 2.56, 2.44, 2.44, 6.89, 2.56, 2.56, 6.89

6 Concluding Remarks

Due to the new experimental data have been available for recent years, the evaluated data have been considerably improved especially for cross sections of

total, (n,2n), (n,α), tota inelastic reactions and inelastic scattering to some discrete levels.

Acknowledgments

The authors wish to thank Prof. Liu Tingjin and Liang Qichang for their help with this work.

References

[1] Zhang Jingshang. Nucl. Sci. Eng., 1993, 114; 55-63
[2] Nuclear Data Sheets, 1993,69:768; 1992,67:283; 1992,67:297; 1991,64:1991,62:626.
[3] M.S.Pandey et al., Private Communication and Phys. Rev., c15,600(1977)
[4] P.Guenther et al., Nucl. Phys., A448, 280(1986)
[5] D.C.Larson et al., BNL-NCS-51245(1980), 80BNL277, EXFOR-12882.011
[6] El-Kadi et al., Nucl. Phys., A390, 509(1982)
[7] W.Kinney et al., ORNL-4908(1974)
[8] Shi Xiamin et al., C. Nucl. Phys., 4(2):120(1982)
[9] B.Joensson et al., Arkiv for Fysik, 39,295(1969)
[10] E.Almen-Ramstrom et al., Atomnaya Energiya, 503(1975)
[11] B.Holmqvist et al., AE-150(1964)
[12] O.T.Gruzdevich et al., Ins. of Phys. and Power Eng., Obninsk,Russia(1993)
[13] V.Mclane et al., Neutron Cross Sections, vol.2, Boston(1988)
[14] F.Ghanbari et al., Annals of Nucl. Energy, 13,301(1986)
[15] T.V.Ryves et al., Metrologia, 14(3),127(1978)
[16] R.A. Jarjis et al., Jour. of Physics, Part G, 4,3,445(1978)
[17] Majumder et al., BOS, 40,81(1977)
[18] R.Mogharrab et al., AKE, 19,107(1972)
[19] M.F.Andreev et al., Yadernaya Fizika, 7(4),745(1968)
[20] G.Bardolle et al., J. CR, 261,1266(1965)
[21] L.A. Rayburn et al., Phys. Rev., 130,731(1963)
[22] D.R.Koehler et al., Nucl. Phys., 11667(1962)
[23] R.N. Glover et al., Nucl. Phys., 29,309(1962)
[24] J.L. Fowler et al., Phys. Rev., 77,787(1950)
[25] L.R.Greenwood et al., ASTM-STP-1001(1989);DOE-ER-006-21(1985)
[26] S.M.Qaim et al., Nucl. Phys., A283,269(1977)

[27] L.Colli et al., Nuovo Cimento, 13,730(1959)
[28] D.L.Allan et al., Proc. of the Phys. Society(London),A70,195(1957)
[29] Zhao Wenrong et al., Proc. of Tenth National Conf. of Nucl. Phys., p.157, Qingdao, Aug., 1997
[30] A.D.Majdeddin et al., INDC(HUN)-031(1997)
[31] A.A.FFilatenkov et al., INDC(CCP)-402(1997)
[32] Lu Hanlin et al., CNDP, No.13, 102(1995); Private Communication(1994)
[33] J.W.Meadows et al., INDC(NDS)-286(1993)
[34] J.Csikai et al., INDC-263-91(1991)
[35] Y.Ikeda et al., INDC-263-91(1991)
[36] Wang Yongchang et al., Chin. J. High Energy Phys. and Nucl. Phys.,14,919(1990)
[37] G.Winkler et al., Nucl. Sci. Eng., 76,1,30(1980)
[38] A.Paulsen et al., Zeitschrift fuer Physik,205,226(1967);NUK,10,91(1967)
[39] V.Garuska et al., EXFOR Data No.30553004(1980)
[40] O.I.Artem et al., Atomic Energy, 49,195(1980)
[41] F.Cserpak et al., Phys. Rev.,C49,1525(1994)
[42] J.Voignier et al., Nucl. Sci. Eng., 93,43(1986)
[43] M.Diksic et al., J. of Inorganic and Nucl. Chem., 36, 477(1974)
[44] V.A.Tolstikov et al., Atomic Energy, 21(1), 45(1966)
[45] G.G.Zaikin et al., Atomic Energy, 25,526(1968)
[46] Xia Yijun et al., Private communication(1998)
[47] Perkin et al., PPS,72,505(1958)
[48] Ahmad et al., Grimes(1986)
[49] S.M.Grimes et al., Phys. Rev., C19,2127(1979)
[50] K.Tsukada et al., 2nd IAEA Conf. on Nucl. Data for Reactors, Helsiki, Finland, 2,305(1970)
[51] G.V.Gorlov et al., Jadernaja Fizika, 8(6),1086(1968)
[52] W.Bucher et al., Phys. Lett., B58,277(1975)
[53] Shen Qingbiao et al., APOM-Acode for searching optical model parameters, CNDP, No.7, 43(1993)
[54] B.V.Carlson, The optical model ECIS95, Miramare-Trieste, Italy(1996,4,15-5,17)
[55] Zhuang Youxiang et al.,A new set of level density parameters for Fermi Gas model, Chinese Physics, 8, 721-727(1988)
[56] Han Yinlu, Private communlcation (1998)

Evaluation of Activation Cross Sections for Fission Product Nuclides of ^{140,141,142,144}Ce below 20 MeV

Yu Baosheng
(China Nuclear Data Center, CIAE)

Zhang Zhengjun
(Depart. of Physics, Northwest University, Xi'an)

Abstract

The activation cross sections were evaluated for fission product nuclides of ^{140,141,142,144}Ce below 20 MeV to provide data for reactor design. Evaluation was made on the basis of experimental data up to 1998 and nuclear mode calculation. The experimental data for ^{140,142}Ce(n, 2n), ^{140,142}Ce(n, γ) from threshold energy to 20 MeV and ^{140,142}Ce(n, p), ^{142}Ce(n, α) reactions at some energys points were adopted in this work. The evaluated data of ^{140,141,142,144}Ce were compared with other evaluated data from ENDF/B-6, JENDL-3 and BROND-2 Libraries.

Introduction

Ce is a rare-earth element and important fission product nuclides. Its various kinds of reaction cross sections are required for activation analysis and estimation of radiation damage in reactor technology. However, there are some discrepancies in present evaluated nuclear data libraries. The (n, 2n) and (n, γ) iterative reactions for Ce isotopes are one of activation cross sections for the generation of long-lived important radionuclides ^{142}Ce with the half-life 5×10^{16} years in reactor. The measurements for ^{140,142}Ce(n,2n) and ^{140}Ce(n, p) reactions were performed at CIAE. In this work, the activation cross sections for ^{140,142}Ce(n,2n), (n,3n), (n, γ) and some emission charged particle (n,x) reactions below 20 MeV were evaluated based on experimental and theoretical data. The evaluated results are compared with the experimental and other evaluated data from ENDF/B-6 and JENDL-3.

1 Evaluation and Analysis of Experimental Data

For ^{140,142}Ce(n, 2n)^{140,141}Ce reactions, there are experimental data[1~12] available from threshold energy to 18 MeV. They are shown in Table 1.

Table 1 Collected experimental data and relevant information for ^{140,42}Ce(n, 2n) reactions

Year	Author	E_n /MeV	Sample	Detector	n flux	Comments
1960	R.G.Wille	14.8	Natural	Ge(LI)	^{65}Cu(n,2n)^{64}Cu	Measured only for ^{142}Ce
1967	P.Cuzzocrea	14.0	Natural	GEMUC	^{63}Cu(n,2n)^{62}Cu	Measured only for ^{142}Ce
1968	J.Csikai	14.8	Natural	Ge(Li)	^{1141}Pr(n,p)^{141}Ce	
1968	W.Dilg	14.7	Natural	Ge(Li)	^{27}Al(n,α)	
1968	B.Bormann	14.88 (13.0~20.0)	Natural	Ge(Li)	^{1}H(n, n)^{1}H	
1970	W.D.Lu	14.4	CeO_2	Ge(Li)	^{56}Fe(n, p)^{55}Mn	
1971	A.Bari	14.8	Natural	Ge(Li)	^{27}Al(n,α)	
1974	S.M.Qaim	14.7	Natural	Ge(Li)	^{27}Al(n,α) ^{75}As(n,2n)^{71}As	
1976	O.Schwerer	14.6	Natural	Ge(Li)	^{27}Al(n,α)	Measured only for ^{142}Ce
1978	S.L.Sothras	14.8	Natural	Ge(Li)	^{56}Fe(n,p)^{55}Mn	
1985	Teng Dan	14.68 (12.0~18.0)	Natural	Ge(Li)	ASSOP	Measured only for ^{140}Ce
1998	Zhao Wenrong	8.9,9.8	Natural	Ge(Li)	^{27}Al(n,α)	Measured only for^{140}Ce

ASSOP : Associated α Particles

GEMUC : Geiger-Mueller Couter

1.1 ^{140,142}Ce(n,2n)^{139,141}Ce Reactions

1.1.1 ^{140}Ce(n,2n)^{139}Ce Reaction

The cross section of ^{140}Ce(n,2n)^{139}Ce reaction is very useful for activation indicator application and waste disposal assessment of fusion reactor materials due to 137.6 days half-life of ^{139}Ce. At present evaluation, much emphasis is on recommending accurate activation cross sections based on the newest measured and theoretically calculated data below 20 MeV. The data measuring were performed in CIAE in 1985 and 1998, using neutron source from T(d,n)^{4}He, D(d,n)^{3}He reactions in neutron regions of 12~18 and 9~10 MeV at Cockcroft-Walton and Tandem accelerator (CIAE) respectively.

Most measurement for (n, 2n) reaction has been performed around 14 MeV because of the availability of intense source of mono-energy neutron of this energy from Cockrofe-Walton accelerator. The measured data for (n,2n) reaction around 14

MeV were collected, selected and renormalized to a common set of decay data and reference cross sections. Calculated cross section from the renormalized selected data at 14.6 MeV consists with the measured data of Teng Dan[8] . The recommended value at 14.6 MeV is 1777±37 mb

Below 11 MeV, the activities of the measured products were considered for the effects of low energy neutrons at CIAE. When the neutron of 9 and 10 MeV were produced by the $D(d,n)^3He$ reaction using a gas target, several kind of low energy neutron were also produced from the breakup neutron of deuteron, the multi-scattering of the main neutron, target structure materials. For activation cross-section measurements, the monitor reaction were selected as the same for threshold and very similar shape for excitation function as possible with the investigated reaction. In this way, the effect of low energy neutron can be reduced strongly. And in this way, the data for $^{140}Ce(n, 2n)^{139}Ce$ reaction were measured by Zhao Wenrong[9] at CIAE in 1998.

Between 15 and 20 MeV, the measured data performed by Teng Dan[8] from 12 to 18 MeV at CIAE can be as the basis of evaluated data. Other measured data[3] from 13.0 to 20.0 MeV were used, but the absolute values were re-normalized to the evaluated value at 14.6 MeV.

For the evaluated experimental data of (n,2n) reaction, the data measured by Zhao Wenrong[9] performed at CIAE in 1998 could be used to guide theoretical calculation,

1.1.2 $^{142}Ce(n, 2n)^{141}Ce$ reaction

The existing measured data were collected and selected. Most of them are in the energy region from 12 to 18 MeV and around 14 MeV . By using the same method as ^{140}Ce, the data were evaluated and renormalized by using a same set of decay data and reference cross sections. The recommended value at 14.6 MeV is 1902±35 mb.

The experimental data, especially the measured data from Teng Dan[8] , Zhao Wenrong[9] and M. Bormman[3] could be used to guide theoretically calculation.

1.2 $^{140,142}Ce(n, \gamma)^{141,142}Ce$ reaction

For the $^{140,142}Ce(n,\gamma)$ $^{141,142}Ce$ reactions, there are experimental data[12,13~22] available from 0.023 to 2.0 MeV and around 14.6 MeV, they are shown in Table 2.

1.2.1 $^{140}Ce(n, \gamma)$ reaction

The data were measured at 23 keV by R. L. Macklin [13] with Sb-Be neutron source in 1957 and K.Siddappa [14] with monoenergetic filtered neutron beam facility at a reactor in 1974, respectively. But there exist large differene between two measured

data. In order to resolve the discrepancy, the measurement conditions were modified and measured again by R. P. Anand [15], who works in the same group with R. L. Macklin . The previous data by R.L.Macklin [13] were superseded.

Table 2 Collected experimental data and relevant information for $^{140,142}Ce(n, \gamma)$ reactions

Year	Author	En	Detector	n flux	comment
1957	R.L.Macklin	0.024 MeV	NaI	$^{127}I(n, \gamma)$	Sb-Be Neutron Source
1958	J.L.Perkin +	14.5 MeV	GEMUC	T(d, α)	Associated Particles Method
1959	W.S.Lyon +	195.0 keV	NaI	$^{127}I(n, \gamma)$	Rb-Th Neutron Source Activation Method
1966	A.K.Chaubey +	24.0 keV	GEMUC	$^{127}I(n, \gamma)$	Sb-Be Neutron Source Activation Method
1967	G.Peto +	3.0 MeV	GEMUC	$^{27}Al(n, \alpha)$	
1974	K.Siddappa	23.0- keV	NaI	$^{127}I(n, \gamma)$	
1976	O.Schwerer +	14.6 MeV	Ge(Li)	$^{27}Al(n, \alpha)$	Activation Method
1979	R.P.Anand	25.0 keV	NaI	$^{127}I(n, \gamma)$	Monoenergy filtered neutron beam ; activation
1979	A.R.D.Musgrove *	3.0-80.0 keV	SCIN	$^{6}Li(n, t)\alpha$	Time-of-flight Method
1987	YU.N.Trofimov	1.0 MeV	Ge(Li)	$^{197}Au(n,\gamma)$	Activation
			$^{115}In(n, n')$ Method		
			$^{115}In(n, \gamma)$		
1987	YU.N.Trofimov +	2.0 MeV	Ge(Li)	$^{197}Au(n,\gamma)$	Activation Method
1989	YU.N.Trofimov	0.5~2.0 MeV	Ge(Li)	$^{197}Au(n,\gamma)$	Activation Method

SCIN (Liquid Scintillator) * Only Measured ^{140}Ce

GEMUC : Geiger-Mueller Couter + Only Measured ^{142}Ce

During 1976~1989, the data of $^{140}Ce(n,\gamma)$ reaction were measured by Yu.N.Trofimov[17,18] with activation mecthod (Ge(Li) detector) in energy region 0.5 ~2.0 MeV and by A.R.D. Musgrove[16] with SCIN detector and time-of-flight method in energy region 3.0~80 keV. Both the data are in good agreement.

1.2.2 $^{142}Ce(n, \gamma)^{143}Ce$

The data were measured by some authors [13~15,17~22]. Most of them consist with each other within errors expected for the data measured by using Sb-Be or Rb-Be neutron source, they are ~10% systematically higher than others in energy region 23~25 keV. Other two sets of data[12, 19] were measured around 14 MeV. The data[19] at 14.5 MeV, measured by using Geiger-Mueller detector, was a estimated maximum value. The measured value[12] at 14.6 MeV with Ge(Li) detector are perfect.

The measured data by R.L. Macklin[13], K. Siddappa [14], J.L. Perkin[19], A.K. Chaubey[20] and W.S. Lyon[22] are rejected due to the systematically higher data.

In summary, the measured data by Yu. N. Trofimov [18] in energy region of 0.5~2.0 MeV, by A.R.D. Musgrove[16] in energy region 3.0~80 keV , by R.P.Anand[15] in energy region 24 keV and O. Schwerer[12] at 14.6 MeV were adopted. Based on them, the evaluated data were obtained from 0.023 to 2.0 MeV. The earlier measured data were only used as reference in the theoretical calculation.

1.3 ^{140}Ce(n, p) and (n, α) reactions

For ^{140}Ce(n,p)^{140}La reaction, there are experimental data only around 14.7 MeV measured at 9 laboratories. The early measured data were performed by R.G.Wille[10] , P. Cuzzocrea[11] , R.F. Coleman[23] and E. Havlik[24], respectively. Among them, the measured data by R.G. Wille[10] , P. Cuzzocrea[11], using the Geiger-Mueller detector, and R.F. Colenman[23], using proportional counter, are higher than others. With Ge(Li) detector, the data were measured two times by A. Bari[26] in different laboratories, respectively. Both data are in good agreement within errors. In order to check further discrepancy of previous measured data, the cross sections were measured by Teng Dan[8] at China Institute of Atomic Energy in energy region 13.5 to 14.8 MeV with the same method in 1985, the results are consistant with the measured data by S.M.Qaim[25] and A. Bari[26] . At present work, the measured values by Teng Dan[8], A.Bari[26] and S.M.Qaim[25] were used as references for theoretically calculation.

For ^{142}Ce(n, p)^{142}La reaction, the reason why the measured data [10,11,23] with large fluctuation around 14 MeV are forsaken in this work. The data measured by O.Schwerer[12] and M. Qaim[25] were recommended as references for theoretically calculation.

For ^{142}Ce(n, α)^{139}Ba reaction, before 1970 there are only 4 experimental data with large errors and very scattering around 14 MeV, which were measured by R.G.Wille[10], P. Cuzzocrea[11], R.F. Coleman[23] and V.N. Levkovskij[28]. The highest value is 2 times larger than the lowest one. The reason is that there is no enough particle discrimination character when using mica end-window Geigermuller counter.

After 1970, there are only 3 points experimental data, around 14 MeV from W.D. Lu[4], L. Chaturverdi[27] and A. Bari[26], they are consistent with each other within errors. The measured data by L. Chaturverdi[27] and A. Bari[26] using Ge(Li) detector were recommended.

For other ^{140,142}Ce(n,x) reactions, there are no measured data, the cross sections must be calculated theoretically.

2 Theoretical Calculation and Recommendation

2.1 ^{140,142}Ce

The theoretical calculation were performed with UNF code[30], based on the available total cross sections of ^{nat}Ce, nonelastic scattering cross sections were evaluated by us from (n, γ), (n,2n) etc. for ^{140,142}Ce in energy region 0.023~18 MeV. Because there are no experimental data of elastic angular distributions of Ce, the data of neighbor's nuclides were used.

A set of neutron optical potential parameters of Ce was used as input preliminary data and the parameters for ^{140,142,Nat}Ce was obtained in the energy region 0.001~20 MeV by using automatically searching code APOM [29].

$$V = 53.04642 - 0.09897E - 0.015369E^2 - 24(N-2)/A$$
$$W_s = \max\{0.0,\ 6.8171 + 0.64088E - 12.0(N-Z)/A\}$$
$$W_v = \max\{0.0,\ -1.56148 + 0.2188E - 0.07471E^2\}$$
$$W_{so} = 6.2$$
$$r_r = 1.20238 \quad r_s = 1.33344 \quad r_v = 1.31037 \quad r_{so} = 1.20239$$
$$a_r = 0.78622 \quad a_s = 0.38591 \quad a_v = 0.58002 \quad a_{so} = 0.786224$$

Using these data and adjusted level density and giant dipole resonance parameters, the cross sections of ^{140,142}Ce(n,2n), (n,3n),(n,γ) and (n x) reactions were calculated. The calculated data can reproduce the measured data well.

The recommended cross sections for (n, γ) were given based on the measured and theoretically calculated data. The cross sections of resonance energy region were taken from ADL-3I and obtained from fitting values of evaluated experimental data in enery region 0.023~2 MeV. The recommended activation cross sections for ^{140,142}Ce (n,2n),(n, γ) reactions are shown in Fig. 1~4.

The thresholds of these (n,x) reactions are above ~8 MeV. The calculated cross sections are of the order of a few ten-mb or less, generally much less. They were in agreements with existing experimental data. For the (n, α) and (n, p) reactions, the calculated curve could close or pass the data measured around 14 MeV. The recommended activation cross sections for (n,x) reactions are shown in Fig. 5~7.

2.2 For ^{141,144}Ce

Because ^{141,144}Ce are radionuclides, there are no available measured data. The theoretical calculation were performed with UNF code [30]. A set of neutron optical

potential parameters and the relevant level density and giant dipole resonance parameters of ^{141,144}Ce were used.

The cross sections of all reactions by neutron induced on ^{140,141,142,144}Ce were recommended and shown in Fig. 8~11.

3 Summary

The activation cross sections were evaluated for fission product nuclides of ^{140,141,142,144}Ce. Evaluation was made on the basis of the new and accurately measured data up to 1998 and nuclear model calculation. The recommended data could reproduce the existing measured data for ^{140,142}Ce(n, 2n), (n, γ), (n, p),(n,) reactions .

For the ^{140,142}Ce(n,2n)^{139,141}Ce reactions, the cross sections were scarce in ENDF/B-6 and BROND-2 libraries. In present work, the cross sections were evaluated by adopting the newest measured data from CIAE. The evaluated data are better than the other libraries.

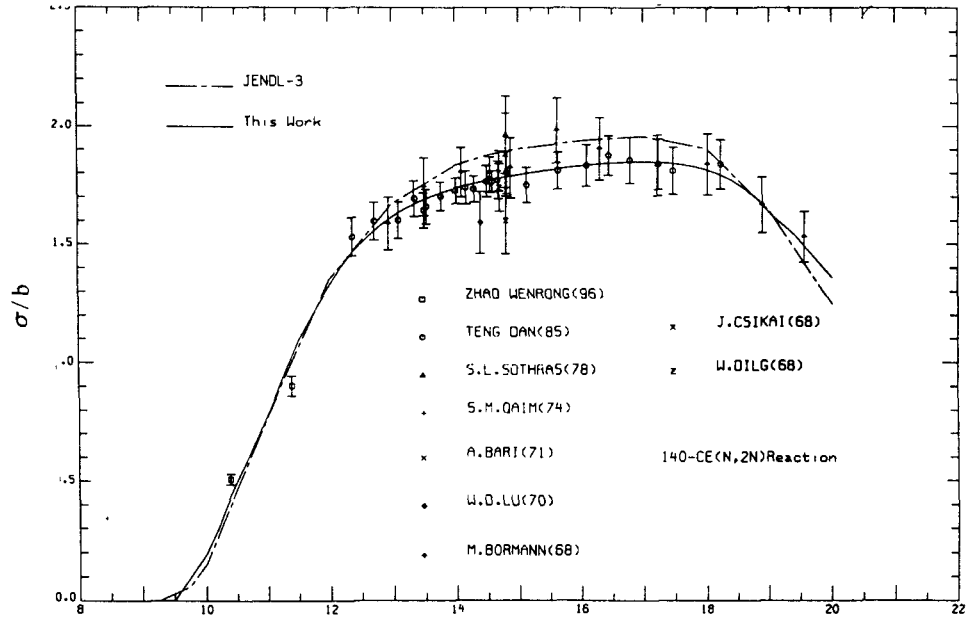

E_n / MeV

Fig. 1 Comparison of evaluated and measured data for ^{140}Ce(n,2n)^{139}Ce reaction

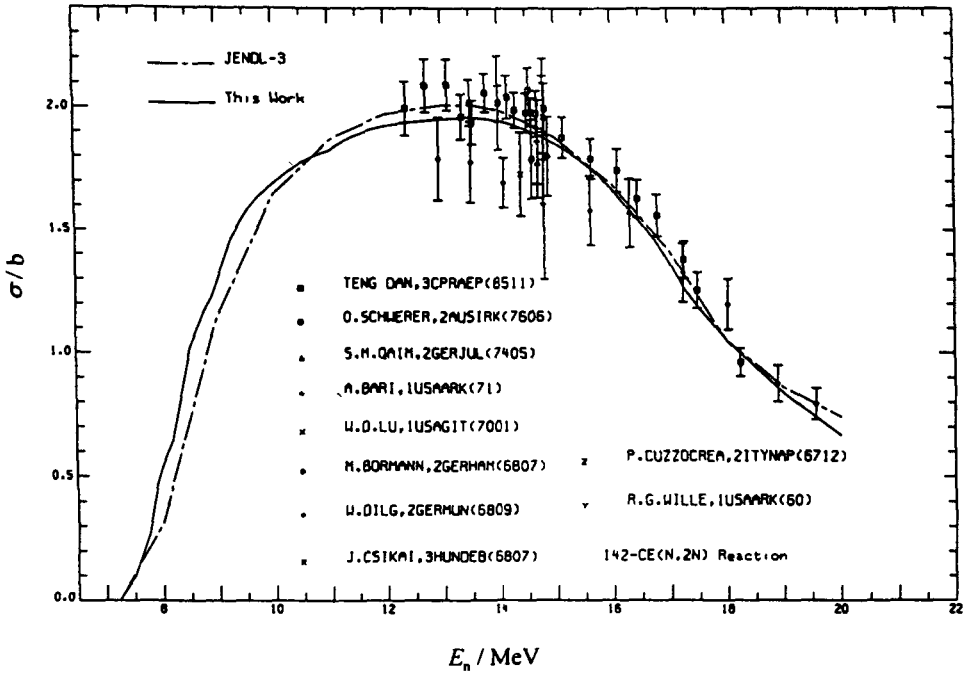

Fig. 2 Comparison of evaluated and measured data for $^{142}Ce(n,2n)^{141}Ce$ reaction

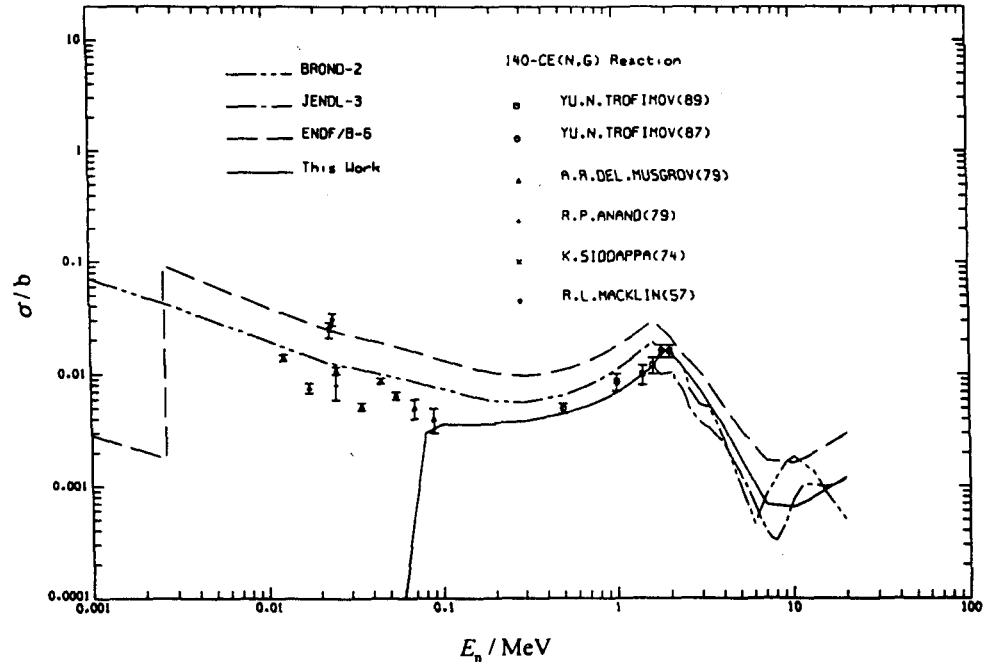

Fig. 3 Comparison of evaluated and measured data for $^{140}Ce(n,\gamma)^{141}Ce$ reaction

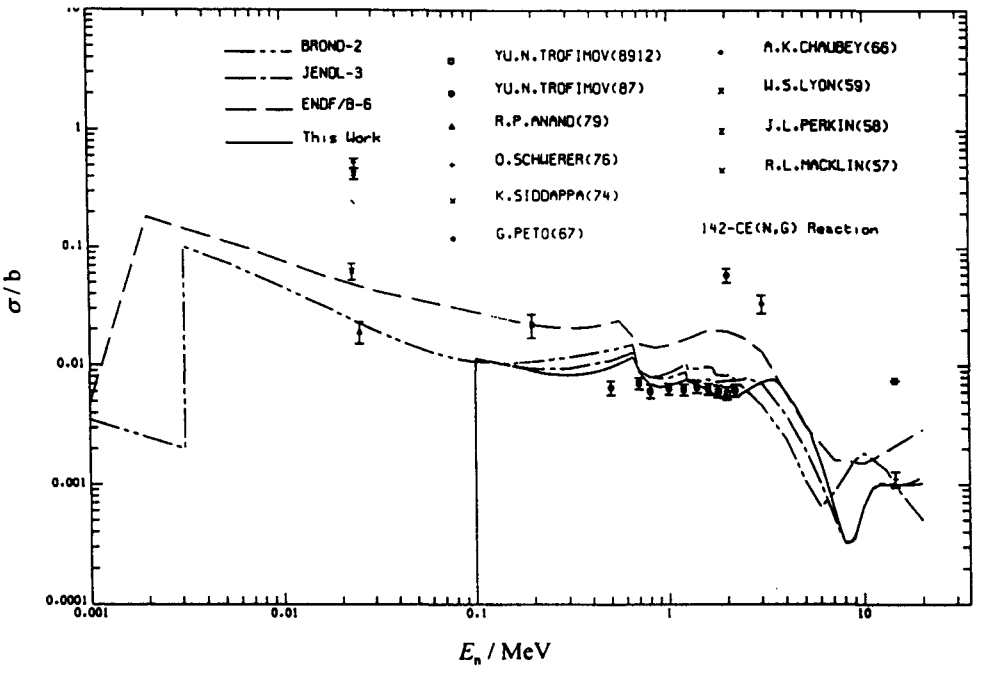

Fig. 4 Comparison of evaluated and measured data for $^{142}Ce(n,\gamma)^{143}Ce$ reaction

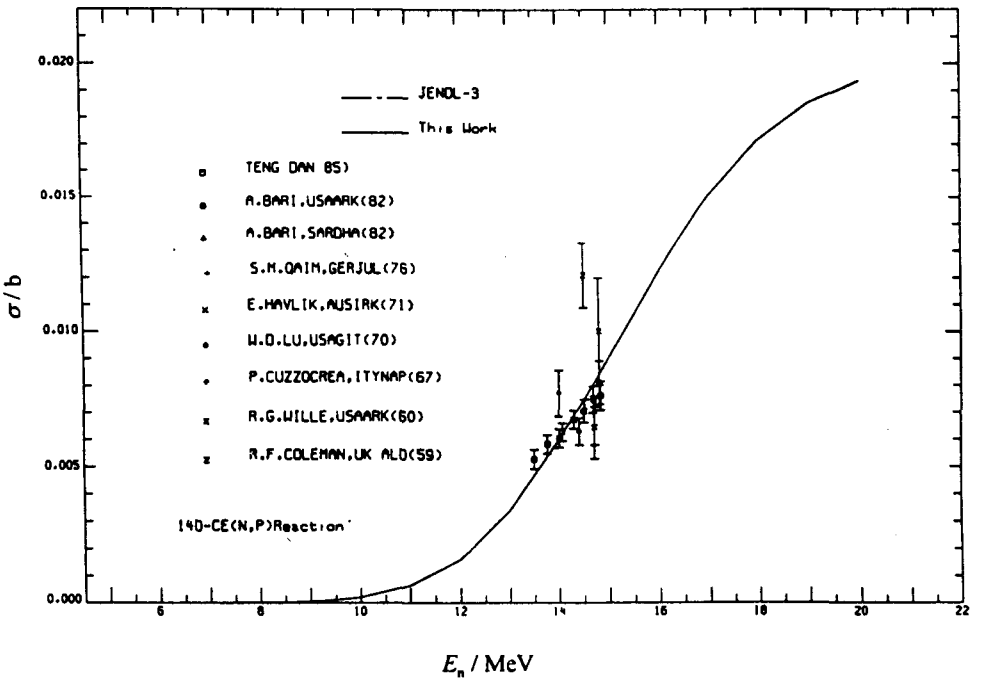

Fig. 5 Comparison of evaluated and measured data for $^{140}Ce(n,p)^{140}La$ reaction

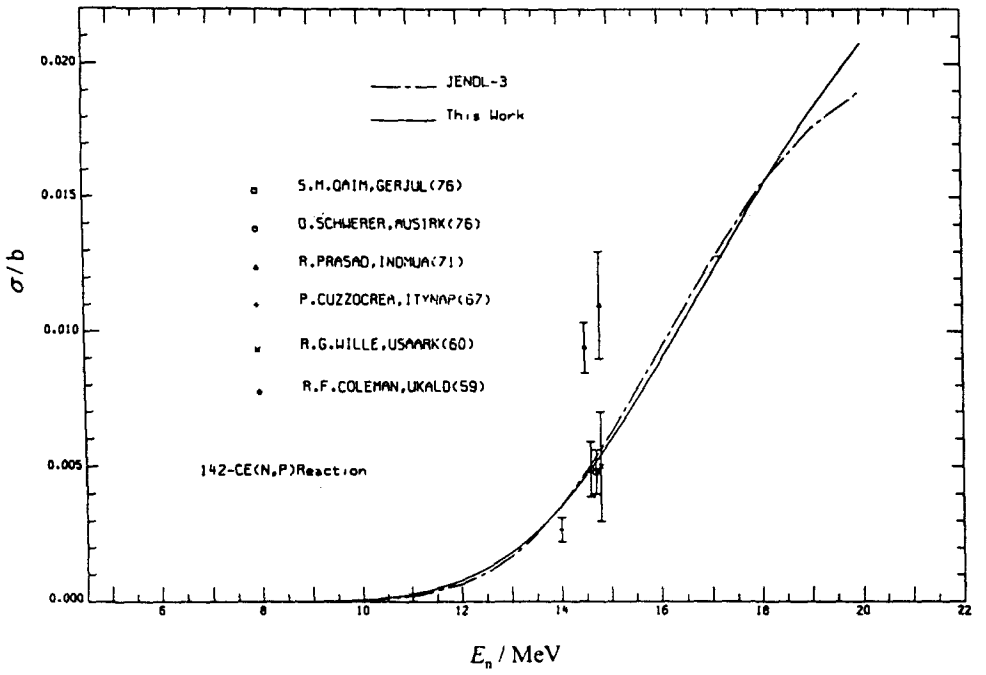

Fig. 6 Comparison of evaluated and measured data for $^{142}Ce(n,p)^{142}La$ reaction

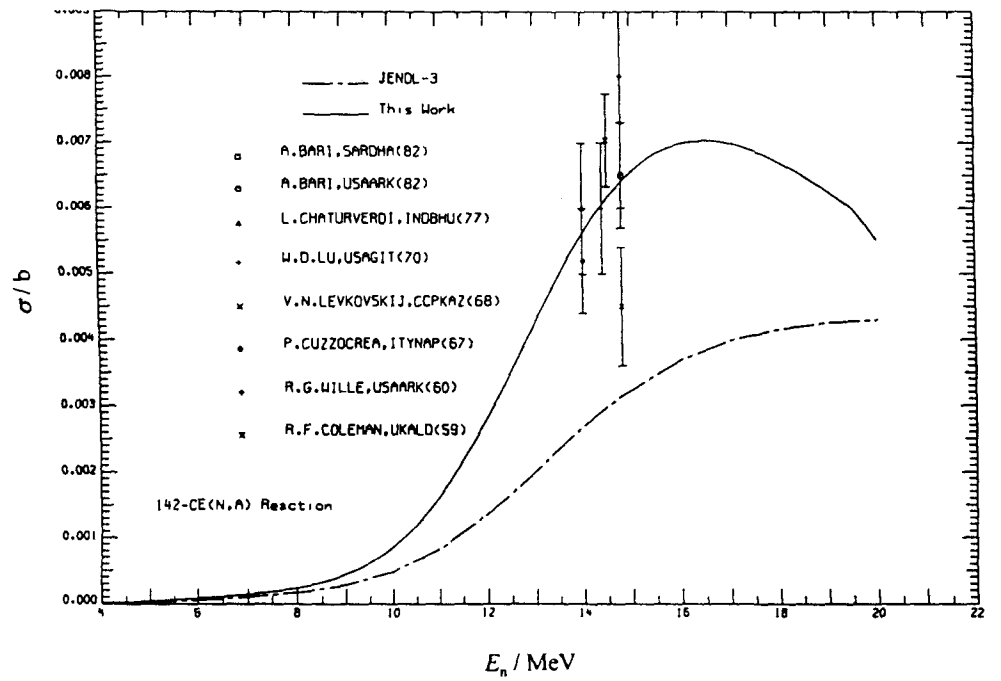

Fig. 7 Comparison of evaluated and measured data for $^{142}Ce(n,\alpha)^{139}Ba$ reaction

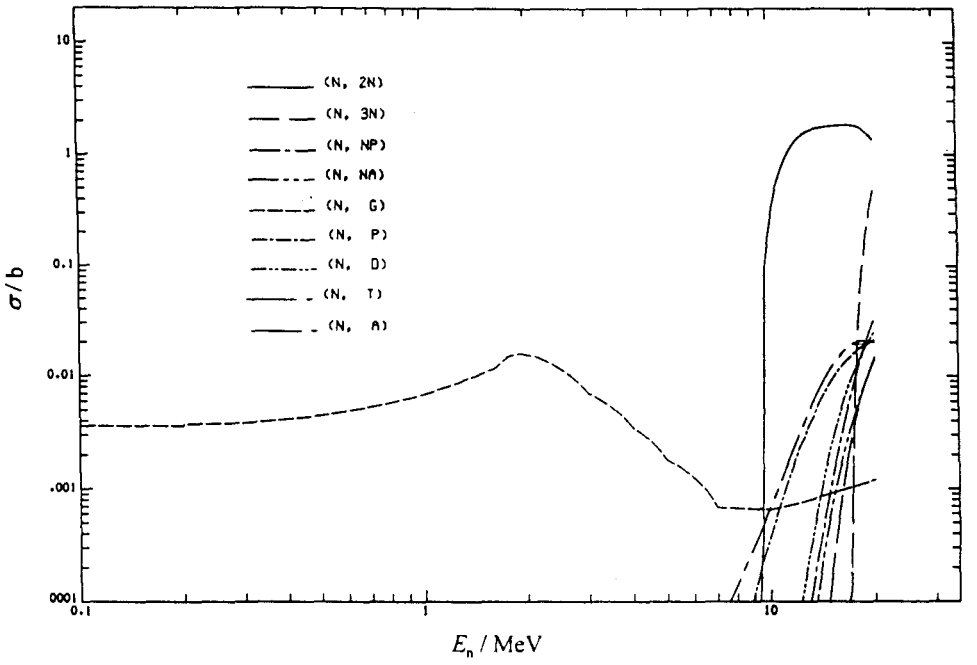

Fig. 8 Evaluated data for ^{140}Ce

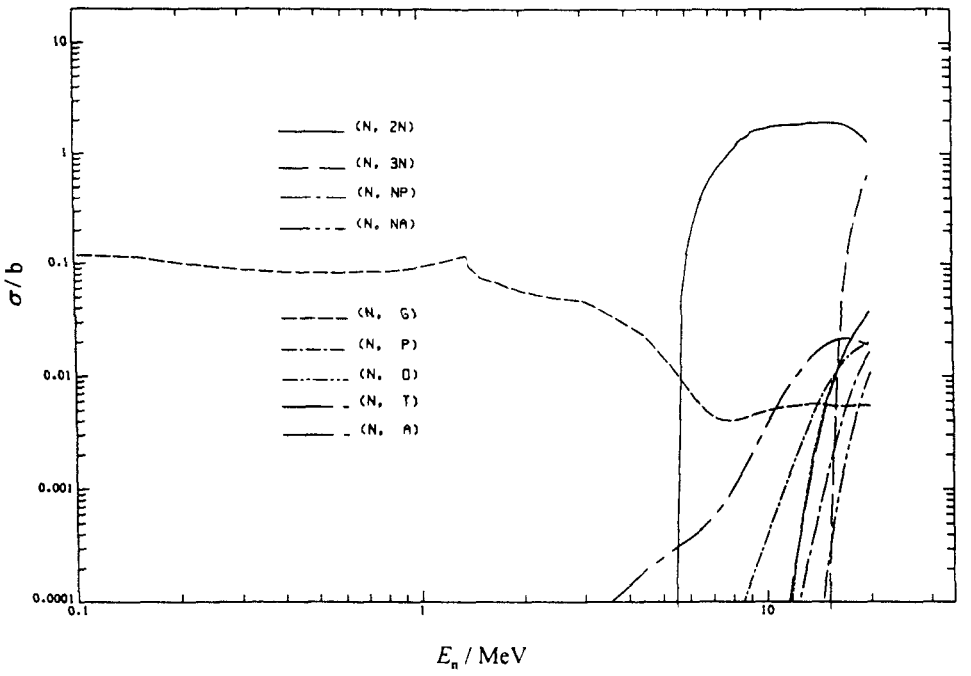

Fig. 9 Evaluated data for ^{141}Ce

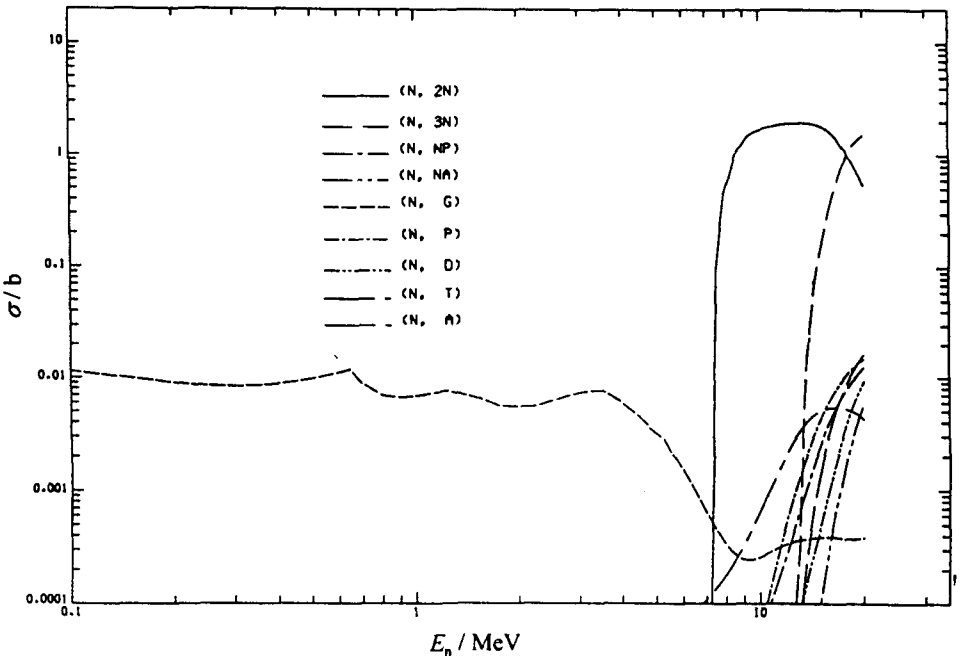

Fig. 10 Evaluated data for ^{142}Ce

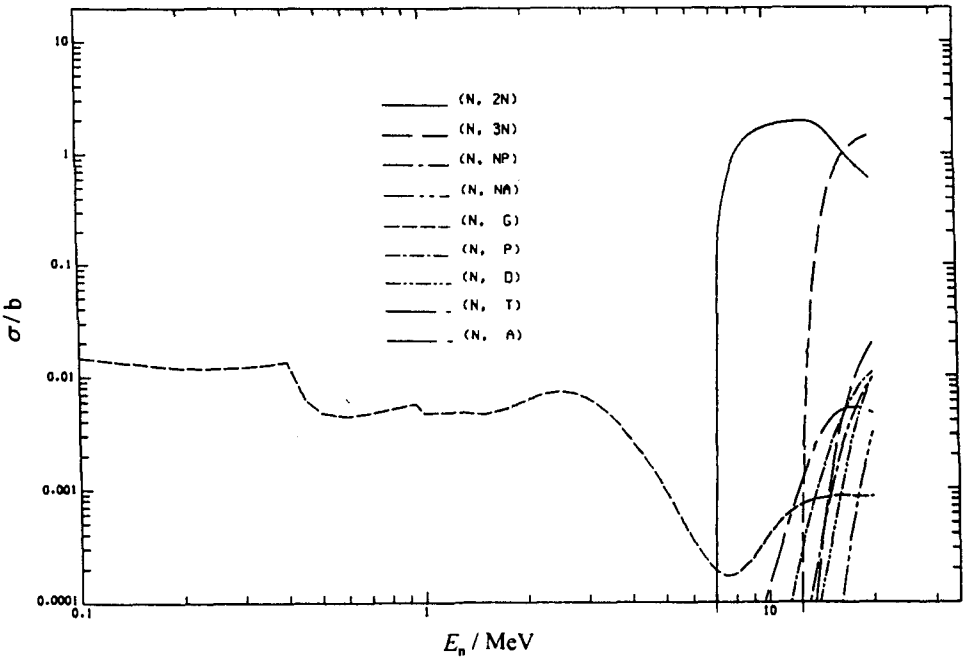

Fig. 11 Evaluated data for ^{144}Ce

Acknowledgments

The authors are indebted to CNNC (China National Nuclear Corporation) and CIAE for their supports, and thank Drs. Lu Hanlin , Zhao Wenrong , Shen Qingbiao and Liu Tong for their kind help and suggestions.

References

[1] J.Csikai et al., J.AHP,24,233(1968)
[2] W.Dilg et al., Nucl. Phys./A,118,9(1968)
[3] M.Bormann et al., Nucl. Phys./A,115,309(1968)
[4] W.D.Lu et al., Phy. Rev./C, 1,350(1970)
[5] A.Bari et al., Exfor Data N0.10431044(1971)
[6] S.M.Qaim et al., Nucl. Phys./A,224,319(1974)
[7] S.L.Sothras etal., J. JIN,40,585(1978)
[8] Teng Dan et al., J.China Nuclear Physics,7,307(1985)
[9] Zhao Wenrong et al., CNDC-0022,7(1998)
[10] R.G.Wille et al., Phy.Rev., 118,242(1960)
[11] P.Cuzzocrea et al., J.NC/B,52,476(1967)
[12] O.Schwerer et al., Nucl. Phys./A,264,105(1976)
[13] R.L.Macklin et al., Phys. Rev./C,107,504(1957)
[14] K.Siddappa et al., Exfor Data N0.30502003(1974)
[15] R.P.Anand et al., Nucl. Sci. and Eng.,82,230(1982)
[16] A.R.D.Musgrove et al., NC/A,50,274(1979)
[17] Yu.N.Trofimov et al., Conf. Kiev,3,331(1987)
[18] Yu.N.Trofimov et al., J. YK.,4,36(1989)
[19] J.L.Perkin et al., EXFOR Data 21438021(1958)
[20] A.K.Chaubey et al., Phy.Rev.,152,1055(1966)
[21] G.Peto et al., JNE,21,797(1967)
[22] W.S.Lyon et al., Nucl.Phy./A,264,105,(1976)
[23] R.F.Coleman et al., EXFOR Data 21440012(1959)
[24] E.Havlik et al., EXFOR Data 20509008(1971)
[25] S.M.Qaim et al., RRL,25,335(1976)
[26] A.Bari et al., J.JRC,75,189(1982)
[27] L.Chaturverdi et al., INDC(SEC)-61(1977)
[28] N.V.Levkovskij et al., J.YF,8,7,(1968)
[29] Shen Qingbiao et al., Commun. of Nucl. Data Prog.,7,14(1992)
[30] Zhang Jingshang et al., Commun. of Nucl. Data Prog., 7,43(1992)

Evaluation of Activation Cross Sections for (n,2n) and (n,γ) Reactions on $^{63, 65, Nat}Cu$

Ma Gonggui
(Institute of Nuclear Science and Technology, Sichuan Univ., Chengdu 610064)

Introduction

Copper is a very important structure material in nuclear fusion engineering. The neutron activation cross section are very useful in fusion research and other applications such as radiation safety, environmental, material damage and neutron dosimetry. More efforts are required to identify and resolve the differences and discrepancies in the existing activation cross sections from different laboratories.

The natural copper consists of two stable isotopes, i.e. ^{63}Cu, ^{65}Cu. The reaction *Q*-Values and abundances are listed in Table 1.

Table 1 Isotopic reaction Q-values and abundances

isotope	*Q*-Value/MeV(n,2n)	*Q*-Value/MeV(n,γ)	abun./%
63	10.854	7.916	69.17
65	9.9047	7.067	30.83

The cross sections of (n,2n) and (n,γ) for $^{63,65,Nat}Cu$ are recommended based on the latest experimentally measured data and theoretically calculated results[1] from threshold up to 20 MeV. The evaluated cross sections are given in Figs. 1~6 with experimental data and compared with other evaluated data. The present work was done for CENDL-3.

1 ^{63}Cu (n,2n) ^{62}Cu Reaction

For (n,2n) reaction, the experimental data were measured by Gruzdevich(93), Mclane(88), Ghanbari(86), Ryves(78), Majumder(77), Jarjis(78), Mogharrab(72), Andreev(68), Bardolle(65), Rayburn(63), Koehler(62), Glover and Fowler(50)[2~14] in the energy range from threshold up to 20.0 MeV, respectively. The evaluated data

were obtained by fitting experimental data from threshold energy to 20.0 MeV. The comparison of experimental data with evaluated ones is shown in Fig. 1.

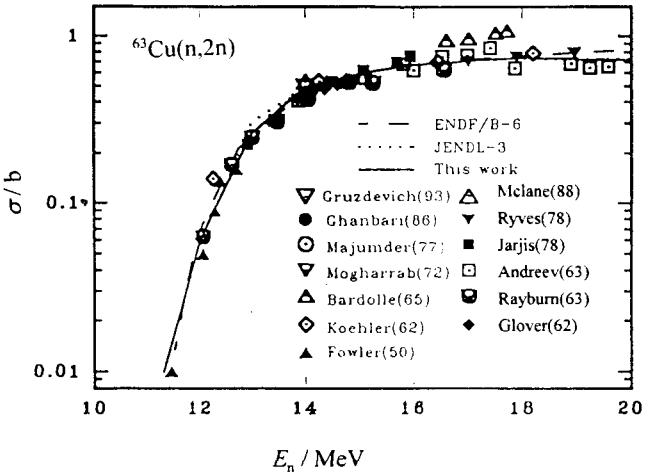

Fig. 1 ^{63}Cu (n,2n) cross section

2 ^{65}Cu (n,2n) ^{64}Cu Reaction

The experimental data were measured by Molla(94), Ghanbari(86), Winkler(83), Csikai(82), Ryves(78), Mannhart(75), Araminowicz(73), Robertson(73), Mogharrab(72), Qaim(72), Santry(65) and Prestwood(61)[14,15~25] from 10 to 20 MeV, respectively. The evaluated data were obtained by fitting experimental data from threshold energy to 20 MeV. The evaluated results are shown in Fig. 2.

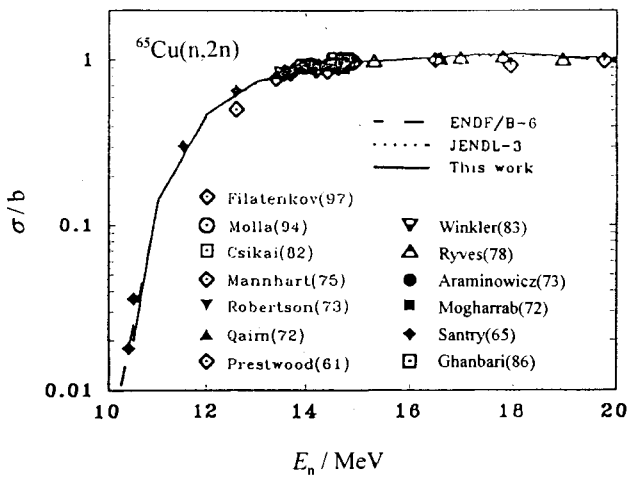

Fig. 2 ^{65}Cu (n,2n) cross section

3 ^{63}Cu (n, γ) ^{64}Cu Reaction

The experimental data were measured by Voignier(86), Diksic(70), Tolstikov(66), Zaikin(68), Perkin(58) and Xia Yijun(98)[26~31] from 0.1 MeV to 14.5 MeV. The evaluated data were obtained by fitting experimental data from 0.1 to 14.5 MeV. The recommended data were taken from calculated result, and normalized to the fitting experimental datum of 2.52 mb at 14.5 MeV. The comparison of experimental data with evaluated ones is shown in Fig. 4.

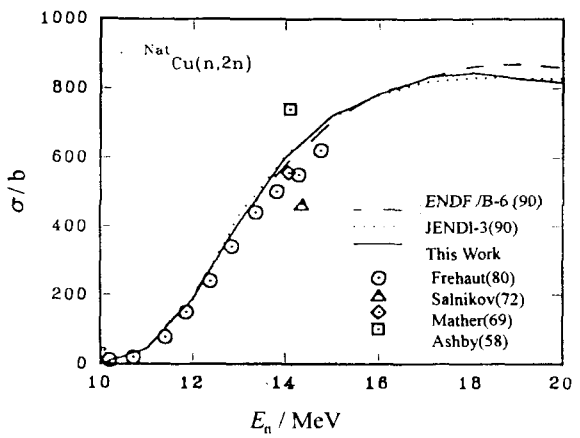

Fig. 3 ^{Nat}Cu (n,2n) cross section

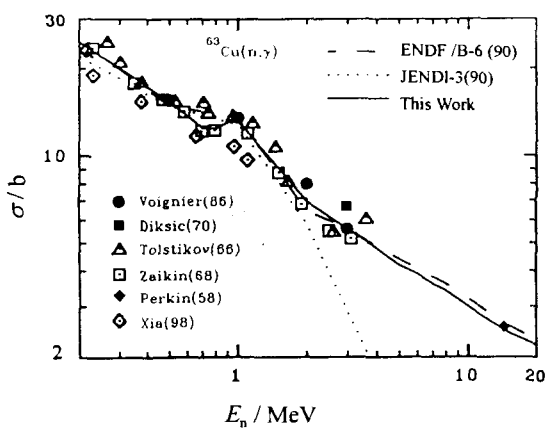

Fig. 4 ^{63}Cu (n,γ) cross section

4 ^{65}Cu (n, γ) ^{66}Cu Reaction

The experimental data were measured by Mclane(88), Voignier(86), Zaikin(68), Colditz(68), Peto(67), Tolstikov(64), Stavisskii(61), Lyon(59)[3,27,29,30,32~35] and Johnsrud(59)[36] from 0.1 to 14.5 MeV. The evaluated data were obtained by fitting

experimental data from 0.1 to 14.0 MeV. Above 14 MeV, the recommended data were taken from calculated result, and normalized to the fitting experimental datum of 0.47 mb at 14.0 MeV. The comparison of experimental data with evaluated ones is shown in Fig. 5.

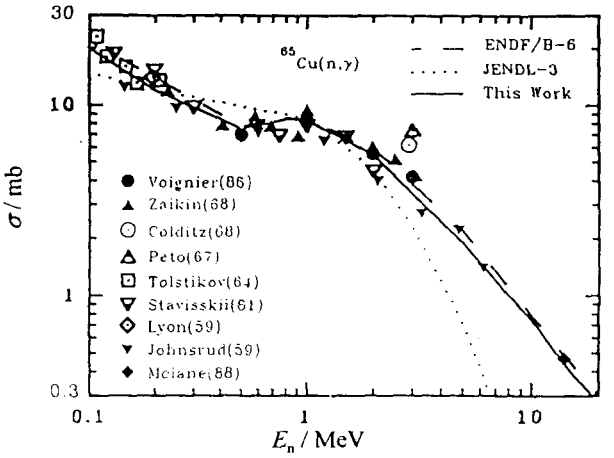

Fig. 5 ^{65}Cu (n,γ) cross section

5 The (n,2n) and (n, γ) Reaction for Natural Copper

For (n,2n) reaction, the experimental data were measured by Frehaut(80), Salnikov(72), Mather(69) and Ashby(59)[37~40] from 10.19 to 14.76 MeV. For (n,γ) reaction, the experimental data were measured by Voignier(86), Diven(60) and Stavisskij(63)[27,41~42] from 0.1 to 3.0 MeV. The recommended data were obtained from summing the isotopic data weighted by the abundance. The comparison of present evaluated data with experimental data and other evaluated data is shown in Fig. 3, 6.

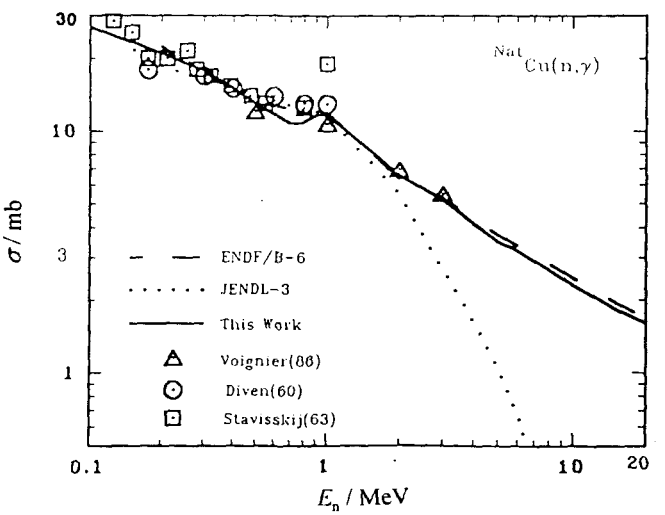

Fig. 6 ^{Nat}Cu (n,γ) cross section

6 Summary

^{63,65,Nat}Cu (n,2n) and (n,γ) cross sections were evaluated and compared with ENDF/B-6 and JEENDL-3. The recommended data could reproduce experimental data very well.

References

[1] Zhang Jingshang. Nucl. Sci. Eng., 114, 55 (1993)

[2] O.T.Gruzdevich et al., Ins. of Phys. and Power Eng., Obninsk,Russia(1993)

[3] V.Mclane et al., Neutron Cross Sections, vol.2, Boston(1988)

[4] F.Ghanbari et al., Annals of Nucl. Energy, 13,301(1986)

[5] T.V.Ryves et al., Metrologia, 14(3),127(1978)

[6] R.A. Jarjis et al., Jour. of Physics, Part G, 4,3,445(1978)

[7] Majumder et al., BOS, 40,81(1977)

[8] R.Mogharrab et al., AKE, 19,107(1972)

[9] M.F.Andreev et al., Yadernaya Fizika, 7(4),745(1968)

[10] G.Bardolle et al., J. CR, 261,1266(1965)

[11] L.A. Rayburn et al., Phys. Rev., 130,731(1963)

[12] D.R.Koehler et al., Nucl. Phys., 11667(1962)

[13] R.N. Glover et al., Nucl. Phys., 29,309(1962)

[14] J.L. Fowler et al., Phys. Rev., 77,787(1950)

[15] N.I.Molla et al., Nucl.Data for Sci. and Tech., p.938(1994), Gatlinburg,U.S.A.

[16] Winkler et al.,ANE,10(11),801(1983)

[17] Csikai et al., 82ANTWER,414(1982)

[18] T.V.Ryves et al., MET,14(3),127(1978)

[19] Mannhart et al., ZP,A272,279(1975)

[20] Araminowicz et al., INR-1464,14(1973)

[21] Robertson et al., JNE,27,531(1973)

[22] R.Mogharrab et al., AKE,19,107(1972)

[23] S.M.Qaim et al., Nucl. Phys., A185,614(1972)

[24] D.C.Santry et al., CJP,44,1183(1965)

[25] R.J.Prestwood et al., Phys.Rev., 121,1438(1961)

[26] Xia Yijun et al., Private communication(1998)

[27] J.Voignier et al., Nucl. Sci. Eng., 93,43(1986)

[28] M.Diksic et al., J. of Inorganic and Nucl. Chem., 36, 477(1974)

[29] V.A.Tolstikov et al., Atomic Energy, 17,505(1964); 21(1), 45(1966)
[30] G.G.Zaikin et al., Atomic Energy, 25,526(1968)
[31] Perkin et al., PPS,72,505(1958)
[32] Colditz et al., OSA,105,236(1968)
[33] G.Peto et al., Jou. of Nucl. Ener., 21,797(1967)
[34] Yu.Ya.Stavisskij et al., Atomic Energy, 10,508(1961)
[35] Lyon et al., Phys. Rev., 114,1619(1959)
[36] Johnsrud et al., Phys. Rev., 116,927(1959)
[37] J.Frehaut et al., 80BNL, 399(1980)
[38] Salnikov et al., Yadernye Konstanty, 7,102(1972)
[39] Mather et al., AWRE-O-47/69(1969)
[40] Ashby et al., Phys. Rev., 111,616(1958)
[41] B.C.Diven et al., Phys. Rev., 120,556(1960)
[42] Yu.Ya.Stavisskij et al., Atomnaya Energiya,15(4),323(1963)

Evaluation of Neutron Cross Sections for ^{115}In

Zhao Jingwu Su Weining
(Department of Physics, Nanjing University, Nanjing, 210093)

Introduction

This is a new evaluation for neutron cross sections of ^{115}In. The experimental data mainly taken from EXFOR, and the recommended data are compared with ENDF/B-6, JENDL-3.2 and JEF-2.

1 Total Cross Section

There are only two experimental data at one energy point[1,2] for ^{115}In. The experiment data[3~14] for natural In were taken to evaluate the total cross section for ^{115}In(Fig. 1).

2 Elastic Scattering Cross Section

In the energy range from 0.1 MeV to 20 MeV, the elastic scattering cross section was obtained by subtracting the non-elastic cross section from the total cross section.

3 Non-elastic Scattering Cross Section

This cross section is the sum of all cross section of nonelastic channels.

4 Total Inelastic Cross Section

This cross section is the sum of all inelastic cross section to 10 discrete levels and continuum one.

5 Inelastic Cross Section to the Discrete Levels and Continuum

The inelastic scattering cross section to 10 discrete levels and continuum part were calculated with SUNF code.

6 (n,2n) and (n,3n) Cross Section

For (n,2n) reaction, there are only the cross section of isomeric[15~22] and ground[23,24] state. The experimental data of ground state is only at 14 MeV energy point, and are very small compared with isomeric state, so the isomeric one can be taken as total (n,2n) cross section. The comparison between the isomeric state and recommended data is shown in (Fig. 2).

Due to no experiment data, the (n,3n) cross section was recommended with calculated result.

7 (n,p), (n,n'p)+(n,pn') Cross Section

For (n,p) reaction, the experiment data of [25~29] are divergent. The weighted means is taken to normalize calculated (n,p) cross section at 14 MeV energy point (See Fig. 3).

Due to no experiment data for (n,n'p)+(n,pn'), the cross section were taken from calculated result.

8 (n,α), (n,n'α)+(n, αn') Cross Section

For (n, α) reaction, the experiment data of [30~36] are divergent. The weighted means is taken to normalize calculated (n,α) cross section at 14 MeV energy point (See Fig. 4).

Due to no experiment data for (n,n'α)+(n, αn') reaction, the cross section was taken from calculated result.

9 (n,t), (n,^{3}He) and (n,d) Cross Section

Only one set of data measured by Woelfle[37] was taken to evaluate (n,t) cross section(See Fig. 5).

Due to no experiment data, the (n,^{3}He) and (n,d) cross sections were taken from calculated result.

10 Capture Cross Section

There are three sets of experiment data[38~40] for ^{115}In. The data[41~47] for natural nucleus were taken to evaluate the cross section for ^{115}In (See Fig. 6).

The present evaluated result was shown in Fig. 7 for all reactions.

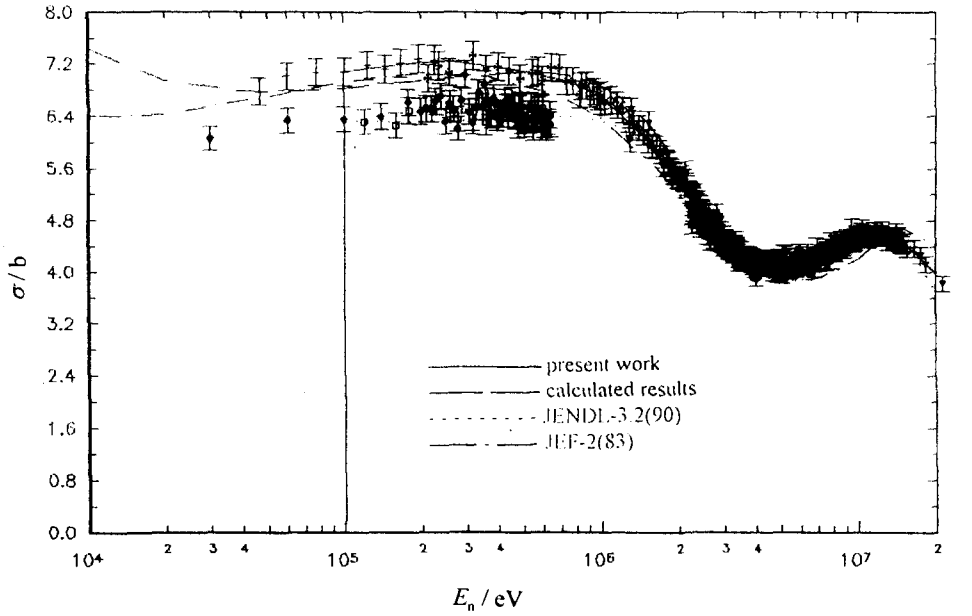

Fig. 1 Total cross section

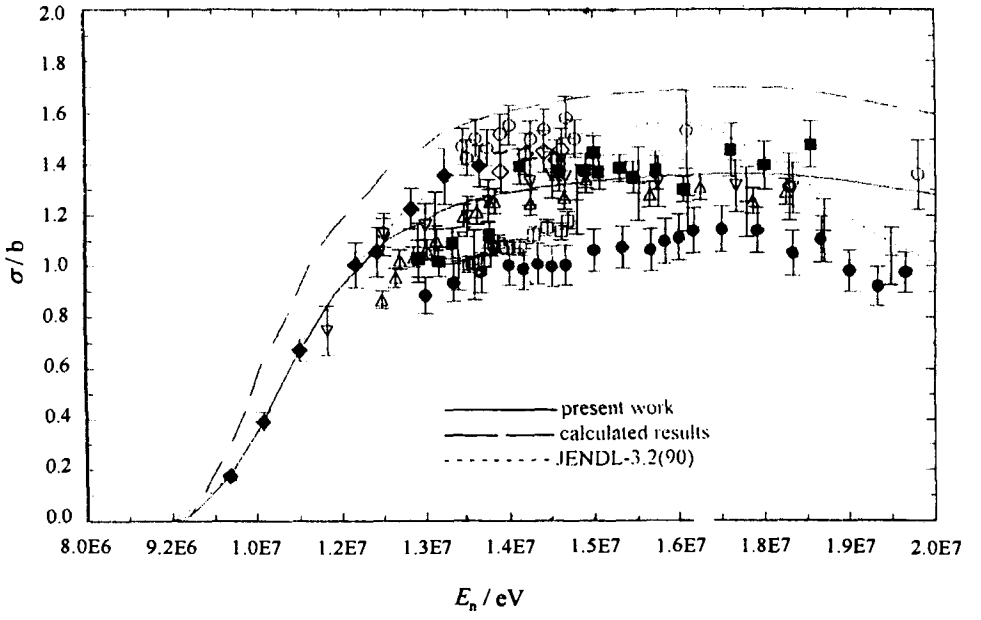

Fig. 2 (n,2n) cross section

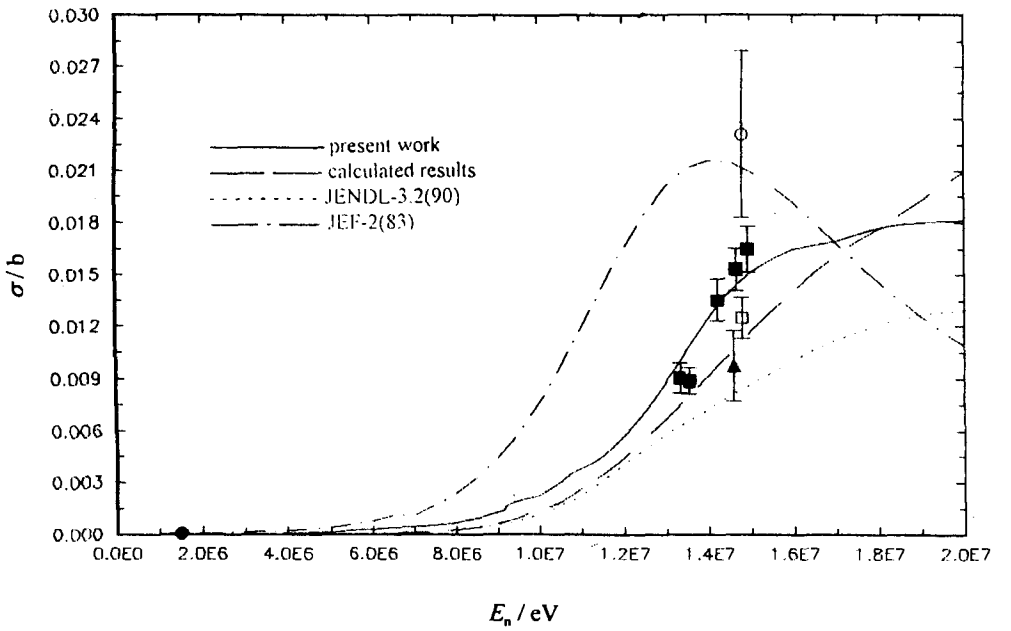

Fig. 3 (n,p) cross section

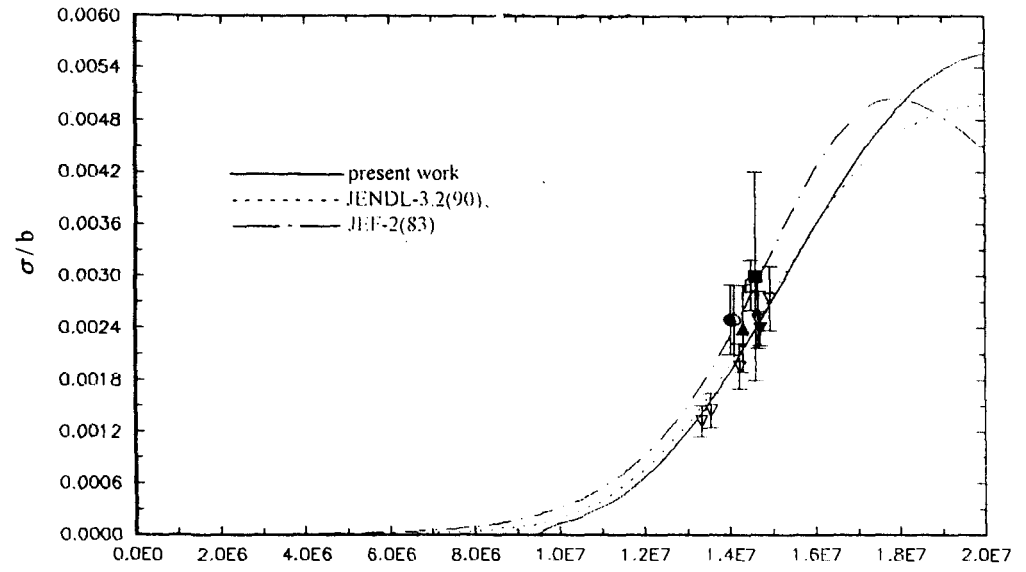

Fig. 4 (n,α) cross section

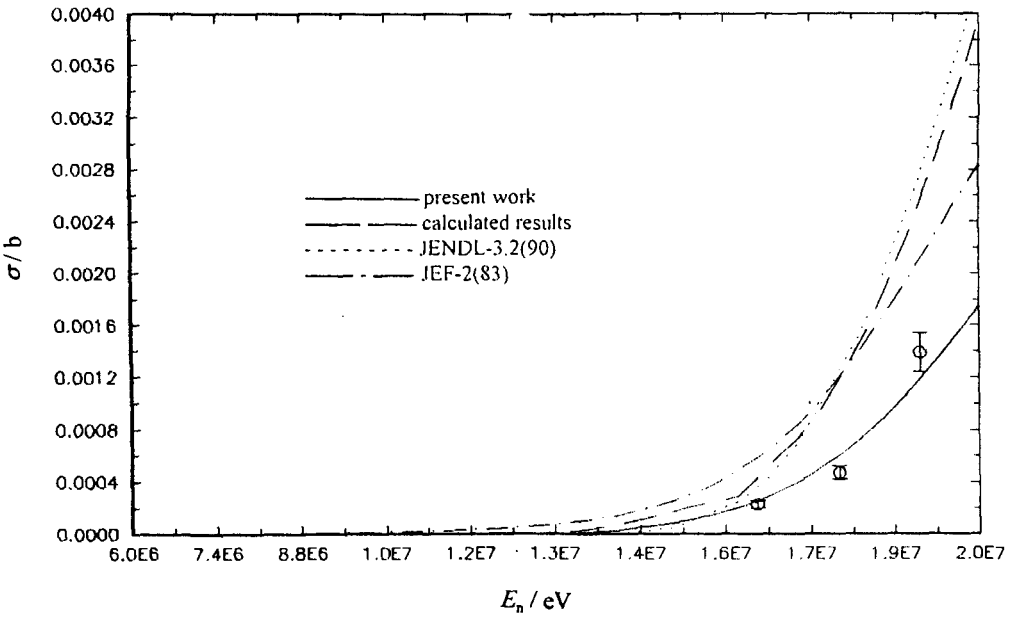

Fig. 5 (n,t) cross section

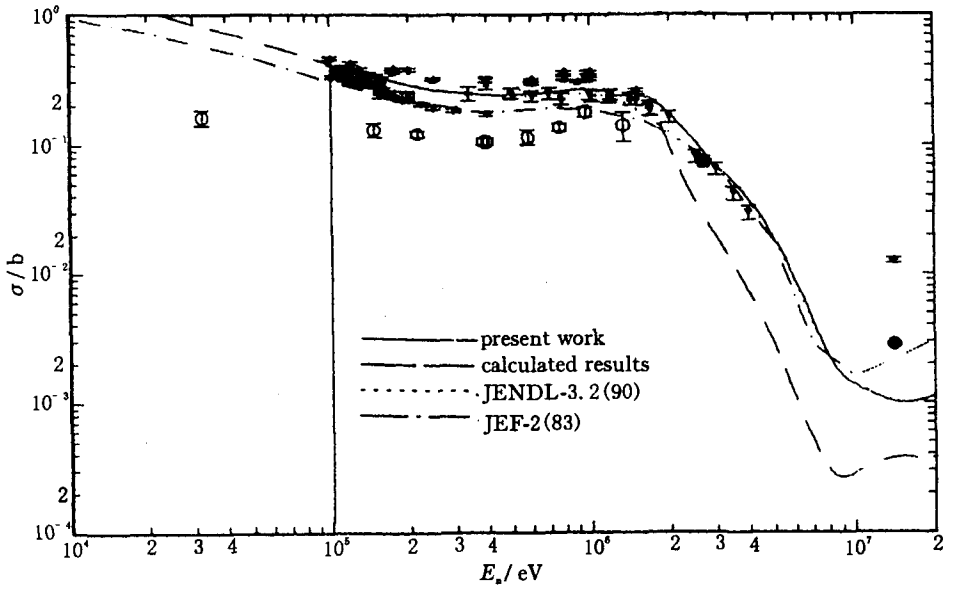

Fig. 6 (n,g) cross section

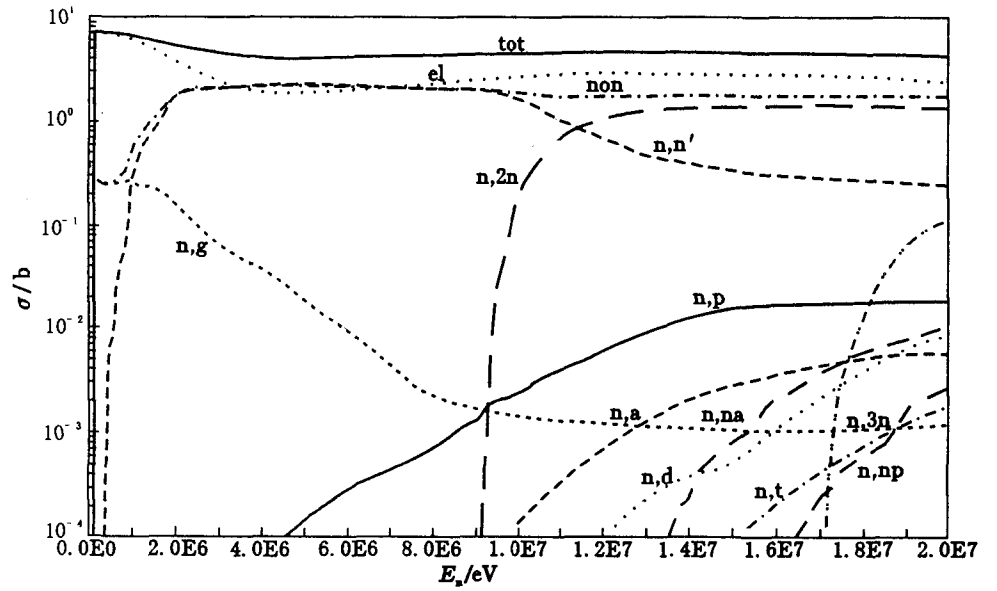

Fig. 7 ^{115}Ln cross section

Reference

[1] J.V.Dukarevich, A.N.Djumin, d.m.kaminker, j, nucl. phys. a,92(2), 433, 1967

[2] G.V.Gorlov, N.S.Lebedeva, V.M.Morozov, j, jadernaja fizika, 6,910, 1967

[3] D.G.Foster jr, D.W.Glasgow, j, phys. pev. c, 3, 576, 1971

[4] M.Divadeenam, E.G.Bilpuch, h.w.newson, j, dissertation abstracts section b, 28,3834, 1968

[5] J.H.Coon,E.R.Graves, h.h.barschall, j, phys. rev., 88, 562, 1952

[6] J.M.Peterson, A.Bratenahl, j.p.stoering, j, phys. rev., 120, 521,1960

[7] A.Bratenahl, J.M.Peterson, j.p.stoering, j. phys, rev., 110, 927,1958

[8] D.W.Miller, R.K.Adair, c.k.bockelman, s.e.darden, j, phys.rev., 88, 83, 1952

[9] R.H.Tabony, K.K.Seth, j, ann. phys., 46, 401, 1968

[10] A.B.Smith, P.T.Guenther, j.f.whalen, j, nucl. phys. a, 415, 1, 1984

[11] W.P.Poenitz, J.F.Whalen, anl-ndm-80, 1983

[12] W.Dilg, H.Vonach, eandc(e)-150, 40, 1972

[13] V.Giordano, C.Manduchi, m.t.russo, et al., j, nucl. phys. a,302, 83, 1978

[14] N.T.Kashukreev, G.A.Stanev, V.T.Surdjiisky, et al.,j, atomnaja energija, 42, 373, 1977

[15] R.J.Prestwood, B.P.Bayhurst, j, phys. rev. 121, 1438, 1961

[16] A.Paulsen, H.Liskien, R.Widera, j, atomkernenergie, 26, 34,1975

[17] Li Jianwei, Wu Zhihua, wu songmao, et al., j, chinese j. of nucl. phys., 10(1), 52, 1988

[18] C.M.Buczko, J.C.Sikai, t.chimoye, et al., 91juelic, 656, 1991

[19] Ke Wei, Zhao Wenrong, Yu Weixiang, et al., j, chinese j. of nucl. phys., 11(3), 11, 1989

[20] Lu Hanlin, Wang Dahai, cui yunfeng, et al., j, current science, 9(2), 11, 1975

[21] D.C.Santry, J.P.Butler, j, can. j. phys., 54, 757, 1976

[22] H.O.Menlove, K.L.Coop, H.A.Grench, et al., j, phys. rev., 163,1308, 1967

[23] M.Bormann, C.Abels, W.Carstens, et al., eandc(e)-76, 51, 1967

[24] J.Csikai, Z.Lantos, C.M.Buczko, et al., j, atoms and nuclei, 337, 39, 1990

[25] T.Mavaooat, S.A.Rao, P.K.Kuroda, j. inorg. nucl. chem., 36, 953, 1974

[16] O.Horibe, Y.Mizumoto, T.Kusakabe, et al., c.89wash, 2, 923, 1989

[27] C.Konno, Y.Ikeda, T.Nakamura, neandc(j)-155, 15, 1990

[28] V.N.Levkovskij, G.P.Vinitskaja, G.E.Kovel'skaja, j, jadernaja fizika, 10(1), 44, 1969

[29] B.E.Leshchenko, G.Peto, v.k.maydanyuk, et al., c.87kiev, 3, 327, 1987

[30] J.K.Temperley, D.E.Barnes, brl-1491, 1970

[31] H.G.Blosser, C.D.Goodman, T.H.Handley, et al., j, phys. rev., 100, 429, 1955

[32] W.Nagel, t.nagel, 1966

[33] R.F.Colfman, B.E.Hawker, L.P.O'connor, et al., j, proc. phys. soc., 73, 215, 1959

[34] T.B.Ryves, Ma Hongchang, s.judge, et al., j. of phys., pt. g, 9, 1549, 1983

[35] R.Pepeleik, B.Anders, B.M.Bahal, et al., neandc(e)-262u, (5), 32, 1985
[36] C.Konno, Y.Ikeda, T.Nakamura, neandc(j)-155, 15, 1990
[37] R.Woelfle, S.M.Qaim, H.Liskien, et al., j, radiochimica acta, 50, 5, 1990
[38] J.S.Brzosko, E.Gierlik, A.Soltan, et al., j, acta physica polonica section b, 2, 489, 1971
[39] G.Peto, J.Csikai, V.Long, et al., acta physica slovaca, 25, 185, 1975
[40] A.I.Leipunskij, O.D.Kazachkovskij, et al., second un conf. on the peaceful uses of atomic energy, geneva, 1-13 september 1958 15, 50(2219), 1958
[41] J.H.Gibbons, R.L.Macklin, et al., j, phys. rev., 122, 182, 1961
[42] B.B.Diven, J.Terrell, a.hemmen, et al., j, phys. rev., 120, 556, 1960
[43] W.P.Poenitz, anl-83-4, 239, 1982
[44] J.Hellstroem, j. nucl. energ., 27, 71, 1973
[45] D.Kompe, j, nucl. phys. a, 133, 513, 1969
[46] R.Fischer, M.Uhl, H.Vonach, j, phys. rev. c, 37(2), 578, 1988
[47] Xu Haishan, Xiang Zhenguy, et al., j, physica energiae fortis et physica nuclearis, 14(4), 340, 1990

Evaluation of Neutron Cross Sections for ^{105,108}Pd

Su Weining Zhao Jingwu
(Department of Physics, Nanjing University, Nanjing, 210093)

Introduction

This is a completely new evaluation for the neutron cross sections for two nuclei ^{105,108}Pd. The experimental data of cross sections mainly referd to EXFOR. The partial reaction were evaluated on the basis of experimental data of natural nucleus, because the experimental data are scarce for isotopes ^{105}Pd and ^{108}Pd. They are also compared with ENDF/B-6, BROND-2, JENDL-3.2 and JEF-2.

1 Total Cross Section

Due to no experimental data for ^{105}Pd and ^{108}Pd in the energy range from 0.1 MeV to 15 MeV, the cross sections were evaluated with experimental data of natural nucleus[1~7]. The total cross sections for two nuclei were recommended with

calculated results above 15 MeV, because there are no experimental data. The recommended results were shown in Fig. 1 for ^{105}Pd and Fig. 2 for ^{108}Pd.

2 Elastic Scattering Cross Section

In the energy range from 0.1 MeV to 20 MeV, the elastic scattering cross sections for two nuclei were obtained by subtracting the non-elastic cross section from total cross sections, respectively.

3 Non-elastic Sctering Cross Section

The cross sections for two nuclei were the sum of all cross section of nonelastic channels, respectively.

4 Total Inelastic Cross Section

The cross sections for two nuclei were the sum of all cross sections of the discrete levels and continuum, respectively.

5 Inelastic Cross Sections to the Discrete Levels and Continuum

The inelastic scattering cross sections to 6 discrete levels for ^{105}Pd and 12 discrete levels for ^{108}Pd were calculated with SUNF code.

The continuum part for two nucleus was also recommanded with calculated results.

6 (n,2n) and (n,3n) Cross Sections

Due to no experimental data for two nucleus, the cross sections for two reaction were recommended with calculated results, respectively.

7 (n,p), (n,n'p)+(n,pn') Cross Sections

For (n,p) reaction, the experimental data[8,9] are divergent for ^{105}Pd. The weighted means was taken (See Fig. 3). However, due to no experimental data for ^{108}Pd, the cross section were recommended with calculated results.

For (n,n'p)+(n,pn') reaction, the cross sections for two nuclei were also taken from calculated results.

8 (n,α), (n,n'α)+(n, αn') Cross Sections

For (n, α) reaction, the experimental data of [10~13] are divergent for ^{108}Pd. The weighted means was taken (See Fig. 4). However, due to no experimental data for ^{105}Pd, the cross seection were recommended with calculated results.

For (n,n'α)+(n, αn') reaction, the cross sections for two nucleus were also taken from calculated results.

9 (n,t), (n,^{3}He) and (n,d) Cross Sections

There are no experimental data for the three reactions, the cross sections of three reactions for the two nuclei were taken from calculated results.

10 Capture Cross Section

There are only one experimental data[14] for ^{105}Pd and two experimental data[15~17] for ^{108}Pd in low energy range. The experimental data of natural nucleus[18~24] were taken for high energy range. The recommended results were shown in Fig. 5 for ^{105}Pd and Fig. 6 for ^{108}Pd. In two figures, the big point is for isotope, the small point is for experimental data of natural element.

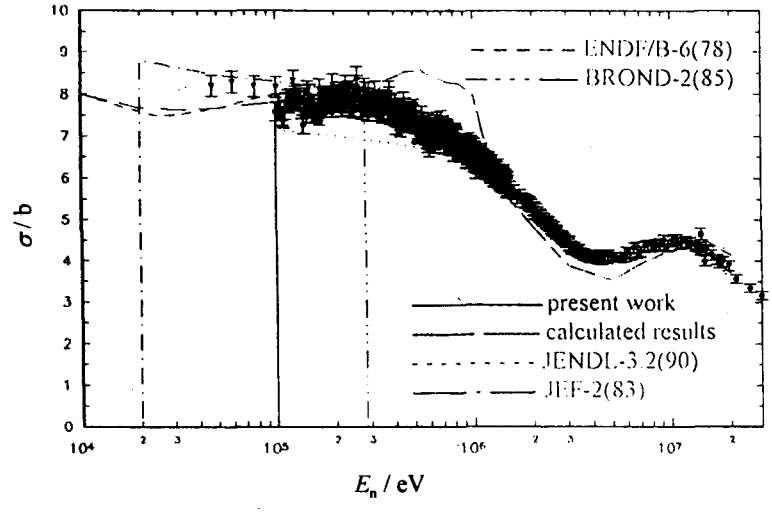

Fig. 1 Total cross section for ^{105}Pd

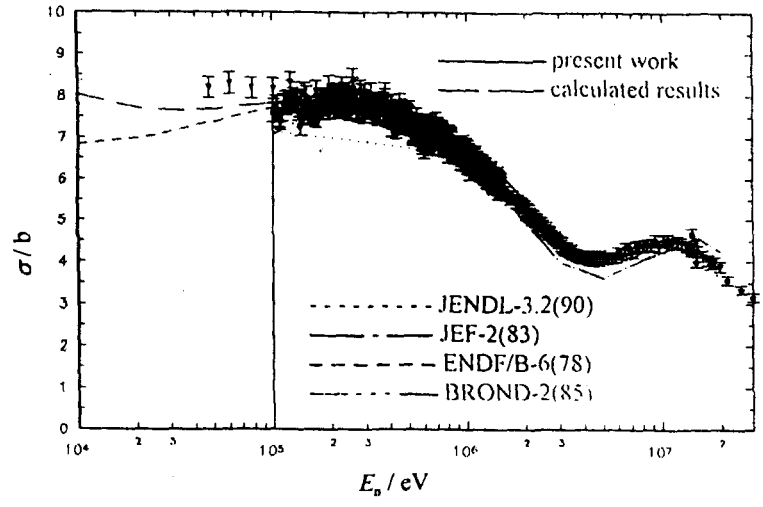

Fig. 2 Total cross section for ^{108}Pd

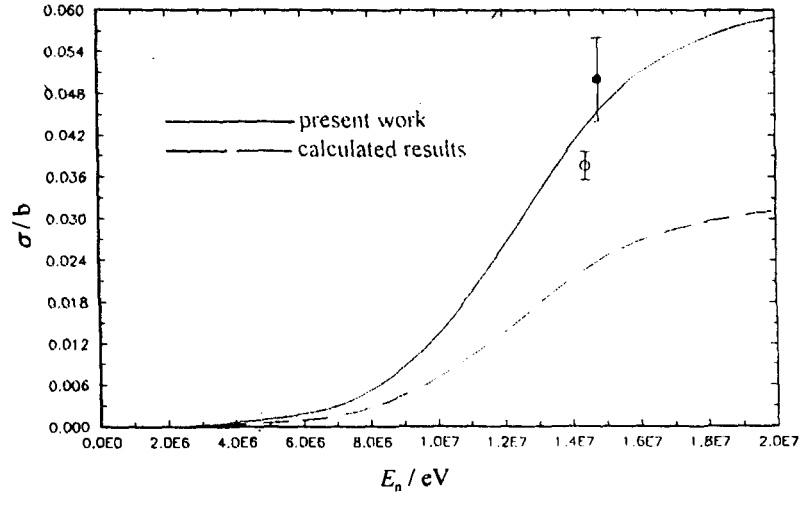

Fig. 3 ^{105}Pd (n,p) cross section

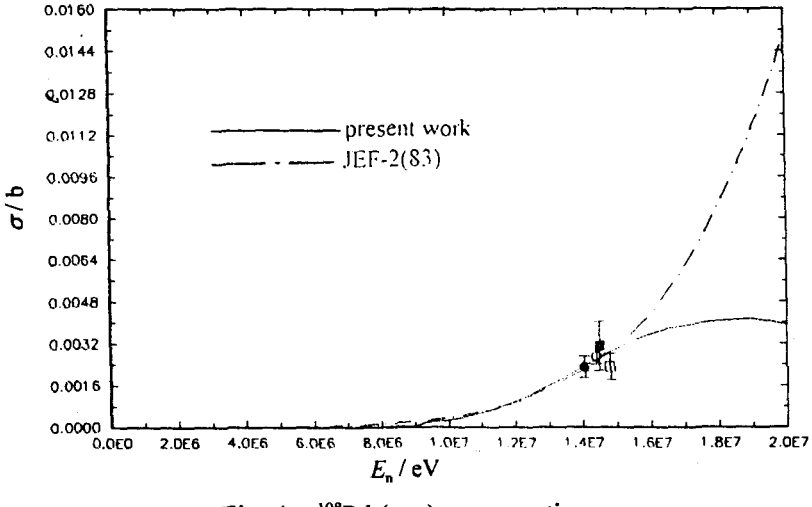

Fig. 4 ^{108}Pd (n,α) cross section

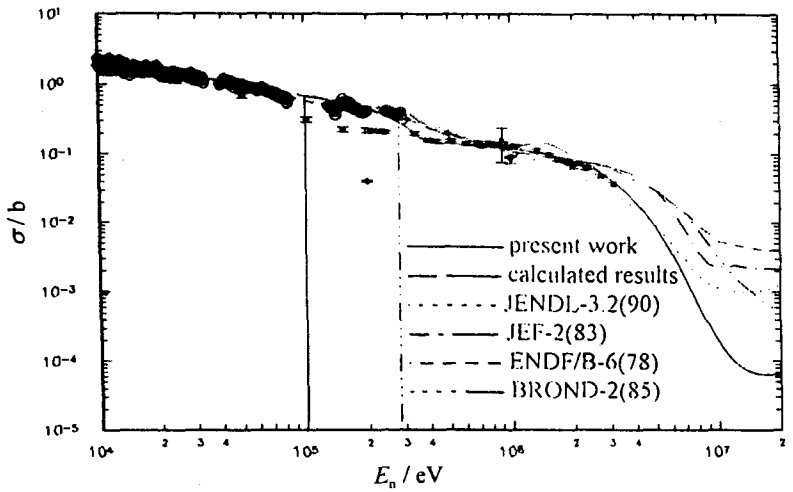

Fig. 5 ^{105}Pd (n,g) cross section

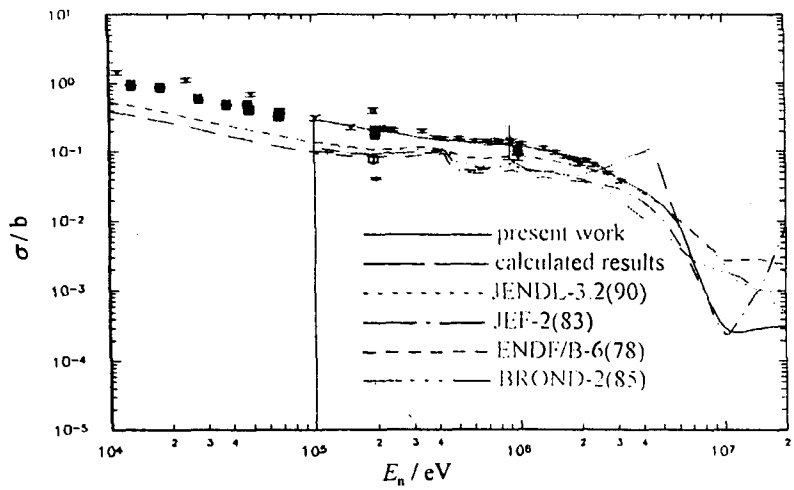

Fig. 6 ^{108}Pd (n,g) cross section

Reference

[1] A.B.Smith, P.Lambropoulos, et al., J, Nucl. Sci. Eng., 49, 389, 1972

[2] J.M.Peterson, A.Bratenahl, et al., J, Phys. Rev., 120, 521, 1960

[3] A.Bratenahl, J.M.Peterson, et al., J, Phys. Rev., 110, 927, 1958

[4] J.Haugsnes, J, Bull. Am. Phys. Soc., 1,187(k2), 1956

[5] A.B.Smith, P.T.Guenther, et al., Anl-ndm-71, 1982

[6] W.P.Poenitz, J.F.Hhalen, Anl-ndm-80, 1983

[7] M.M.Khaletskij, J, Doklady Akademii, nauk sssr, 113(2), 305, 1956

[8] W.D.Lu, N.Ranakumar, et al., J, Phys. Rev. c, 1,358, 1970

[9] R.Prasad, D.C.Sarkar, J, Nuovo Cimento a, 3(3), 467, 1971

[10] W.D.Lu, N.Ranakumar, R.W.Fink, J, Phys. Rev. c, 358, 1970
[11] H.G.Blosser, C.D.Goodman, T.H.Handley, J, Phys. Rev., 110, 531, 1958
[12] S.K.Mukherjee, H.Bakhru, International Conference on Fast Neutron Physics, Bombay, 244, 1963
[13] V.N.Levkovskiy, O.J.Artem'ev, Jadernaja Fizika, 13(5), 923, 1971
[14] R.W.Hockenbury, H.D.Knox, et al., 4th Conf. on Nucl. Cross Sections and Tech., washington d.c., 2, 905, 1975
[15] W.S.Lyon, R.L.Macklin, J, Phys. Rev., 114, 1619, 1959
[16] D.J.Hughes, R.C.Garth, et al., J, Phys. Rev., 91, 1423, 1953
[17] L.W.Wston, K.K.Seth, E.G.Bilp, J, Ann. Phys., 10, 477, 1960
[18] W.P.Poenitz, Specialists' Meeting on Neutron Cross Sections of Fission Product Nuclei, Bologna, 85, 1979
[19] H.Pomerance, J, Phys. Rev., 83, 641, 1951
[20] J.H.Gbbons, R.L.Macklin, et al., J, Phys. Rev., 122, 182, 1961
[21] S.P.Harris, C.O.Muehlhause, et al., J, Phys. Rev., 80, 342, 1950
[22] L.Le sage, R.Sher, Conference on Neutron Cross-section Thchnology, Sdiego, 2, 175, 1966
[23] R.C.Block, G.G.Slaughter, et al., Saclay Conference, Saclay, 203, 1961
[24] D.Kompe, J, Nucl. Phys. a, 133, 513, 1969

Evaluation of Cross Sections for ^{103}Rh

Zhao Jingwu Su Weining
(Department of Physics, Nanjing University, Nanjing, 210093)

Introduction

This is a completely new evaluation for the neutron cross sections. The experimental data mainly referred to EXFOR, and the recommended cross sections are compared with ENDF/B-6, BROND-2, JENDL-3.2 and JEF-2.

1 Total Cross Section

In the energy range 0.1 MeV to 15 MeV, the experimental data were taken from Refs [1~6]. In the region from 15 MeV to 20 MeV (See Fig. 1), the calculated result was recommended.

2 Elastic Scattering Cross Section

In the energy range from 0.1 MeV to 20 MeV, the elastic scattering cross section was obtained by subtracting the non-elastic cross section.

3 Non-elastic Scattering Cross Section

This cross section is the sum of all cross section of nonelastic channels.

4 Total Inelastic Cross Section

The experimental data were taken from Refs. [7~9]. The agreement between the evaluated cross sections and the experiment data is good (See Fig. 2). The cross section is the sum of all cross section of the discrete levels and continuum.

5 Inelastic Cross Sections to the Discrete Levels and Continuum

The inelastic scattering cross sections to 15 discrete levels and continuum part were calculated with SUNF code.

6 (n,2n) and (n,3n) Cross Sections

For (n,2n) reaction, the cross section of ^{103}Rh was measured in Refs [10~15]. The data of Veeser, Frehaut and Mather are adopted (See Fig. 3).

The experimental data of Veeser was adopted to normalize (n,3n) cross section (See Fig. 4).

7 (n,p), (n,n'p)+(n,pn') Cross Sections

Due to no experimental data, the two cross sections were taken from calculated results.

8 (n,α), (n,n'α)+(n, αn') Cross Sections

For (n,α) reaction, the experimental data of [16~18] are divergent. The weighted means is taken to normalize the cross section (See Fig. 5).

There are no experimental data, (n,n'α)+(n, αn') cross section was taken from calculated results.

9 (n,t), (n,^{3}He) and (n,d) Cross Sections

Only one datum[19] was measured for (n,t) cross section. It was used to normalized the calculated cross section (See Fig. 6). The experimental data of [20~24] are divergent. The weighted means was used to normalize (n,^{3}He) cross section (See Fig. 7).

Due to no experimental data, the (n,d) cross section was taken from calculated results.

10 Capture Cross Section

The experimental data of [25~27] were taken to evaluate capture cross section (See Fig. 8).

The present evaluated results are shown in Fig. 9 for all reactions.

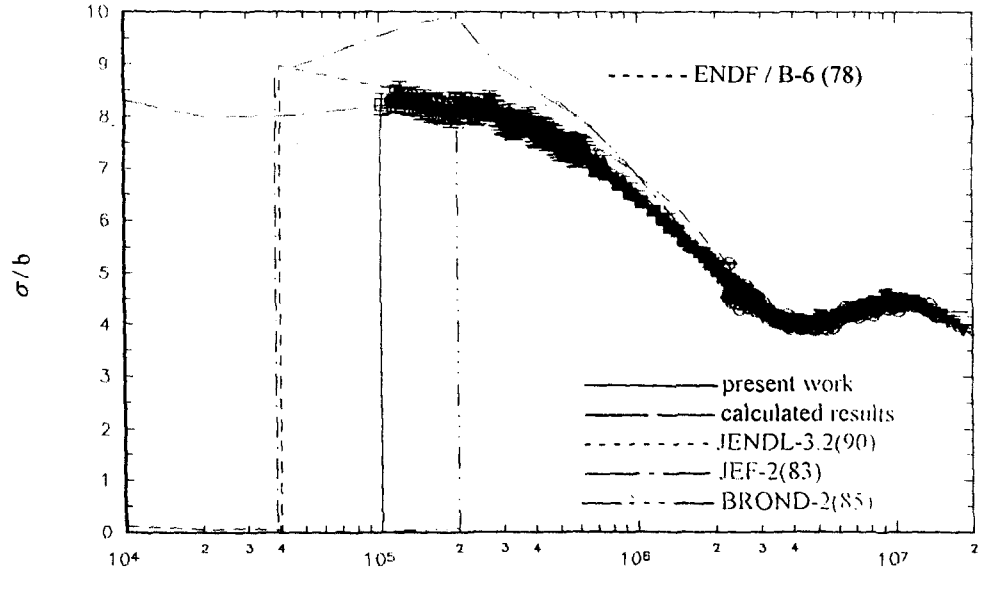

Fig. 1 Total cross section

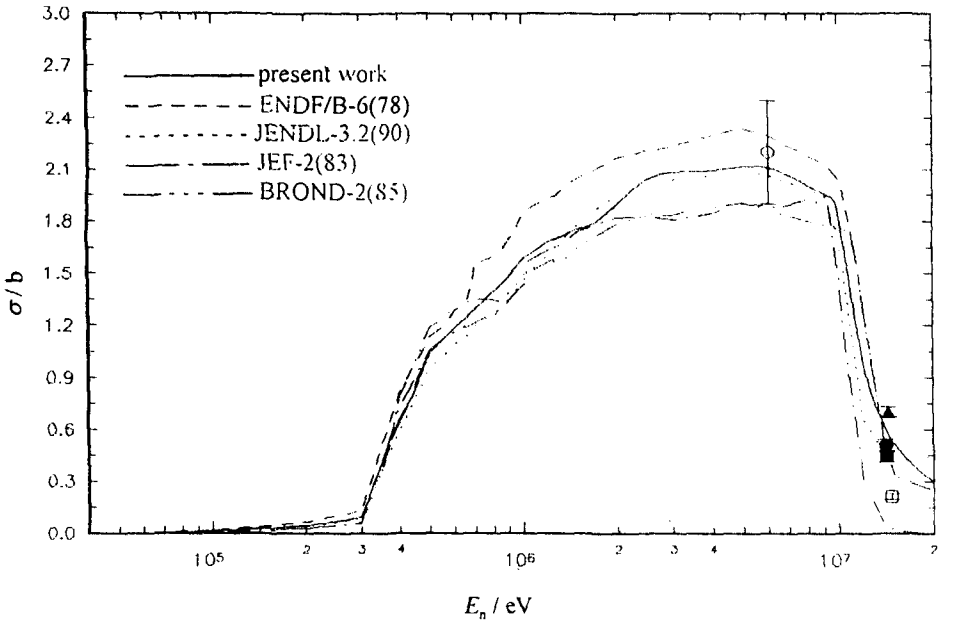

Fig. 2 (n,n') cross section

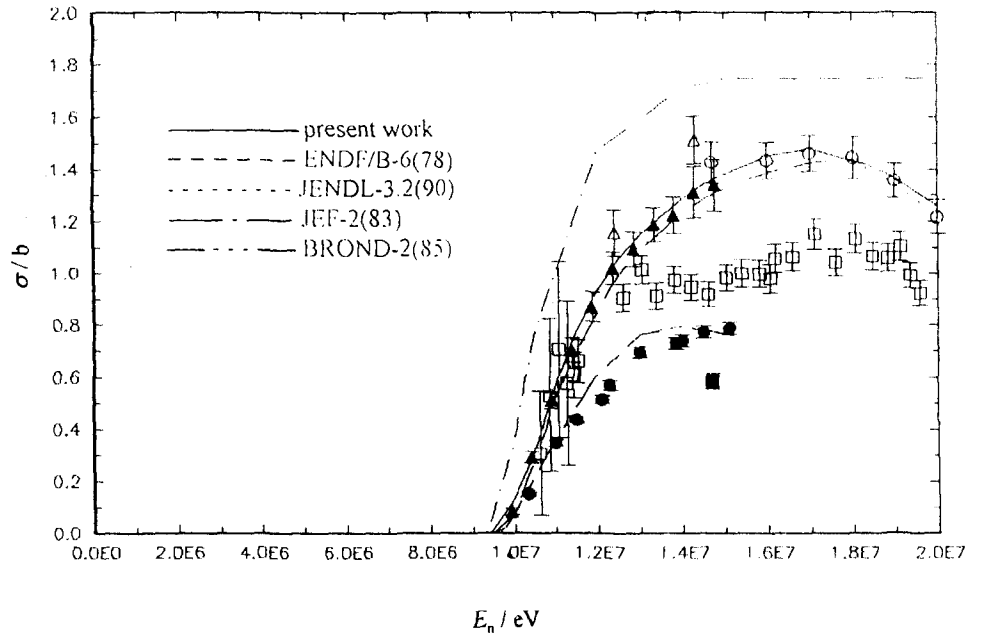

Fig. 3 (n,2n) cross section

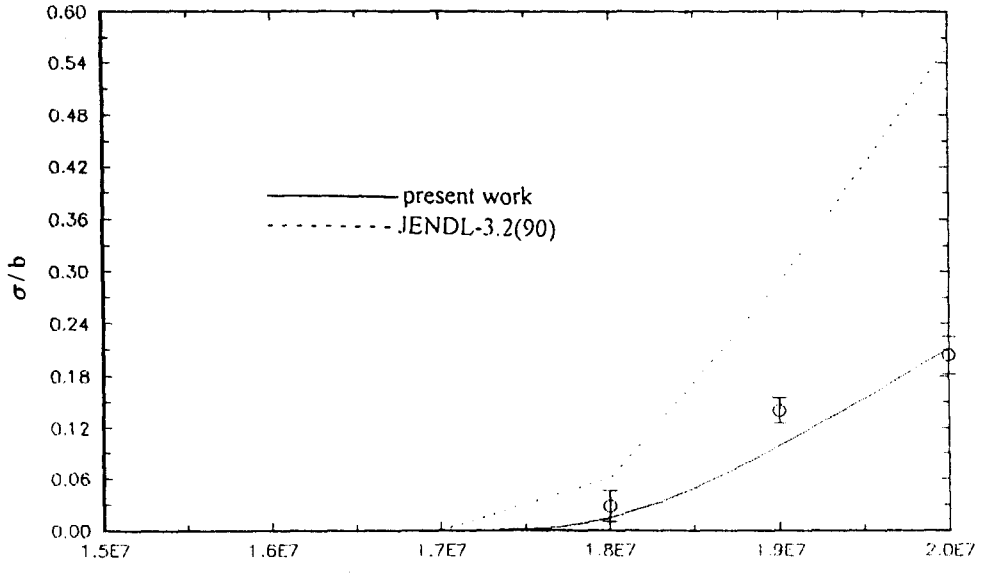

Fig. 4 (n,3n) cross section

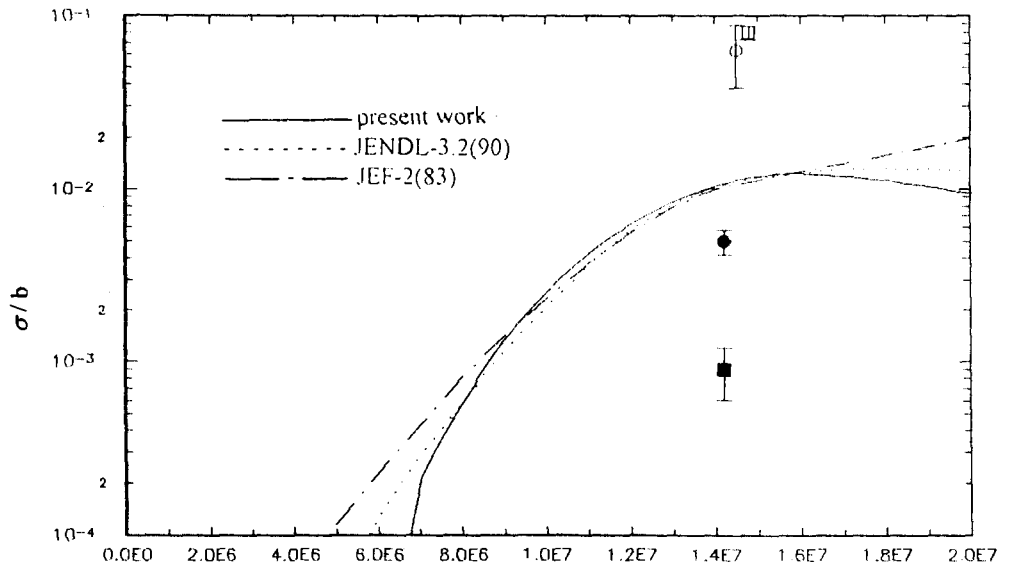

Fig. 5 (n,α) cross section

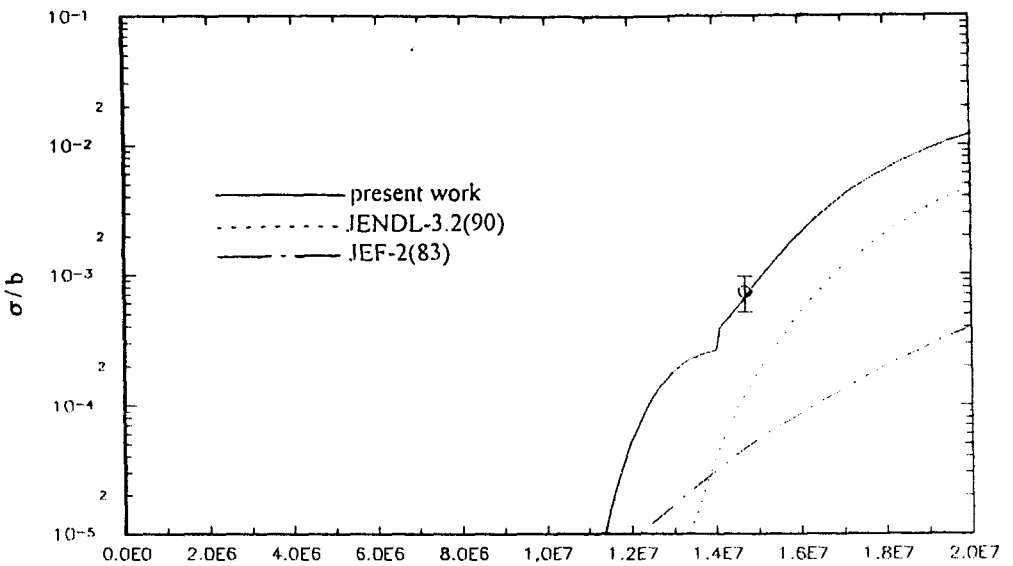

Fig. 6 (n,t) cross section

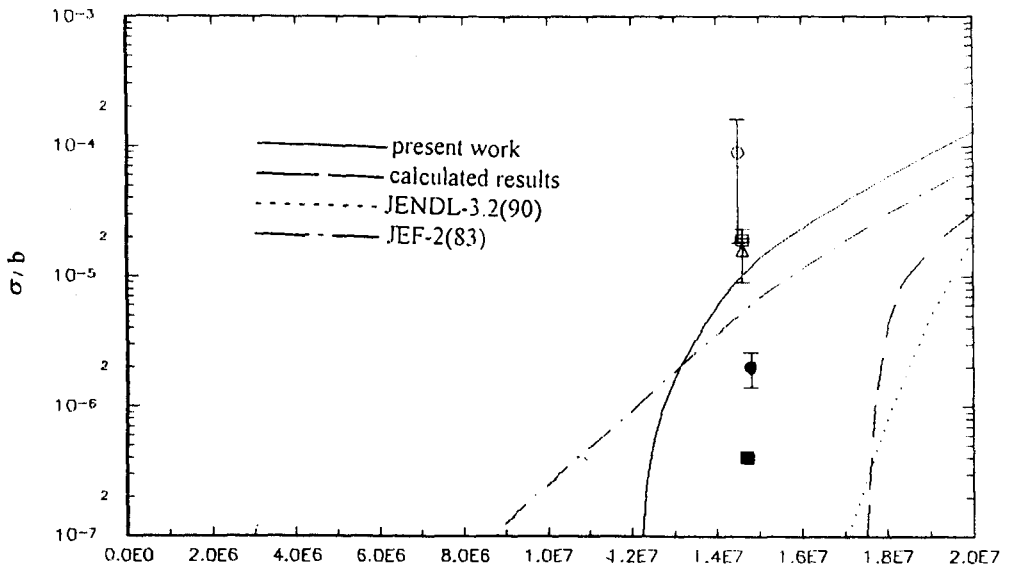

Fig. 7 (n,^{3}He) cross section

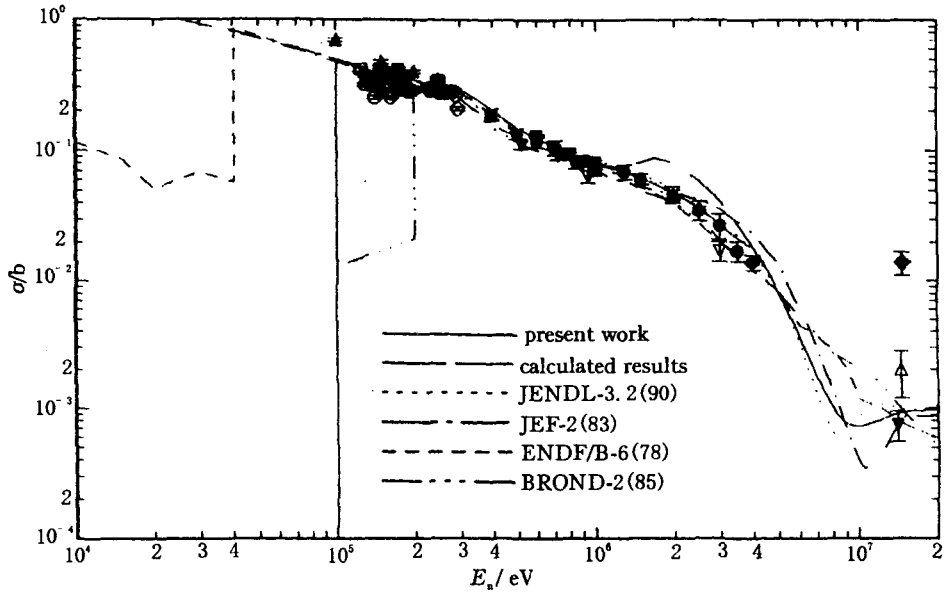

Fig.8 (n,γ) cross section

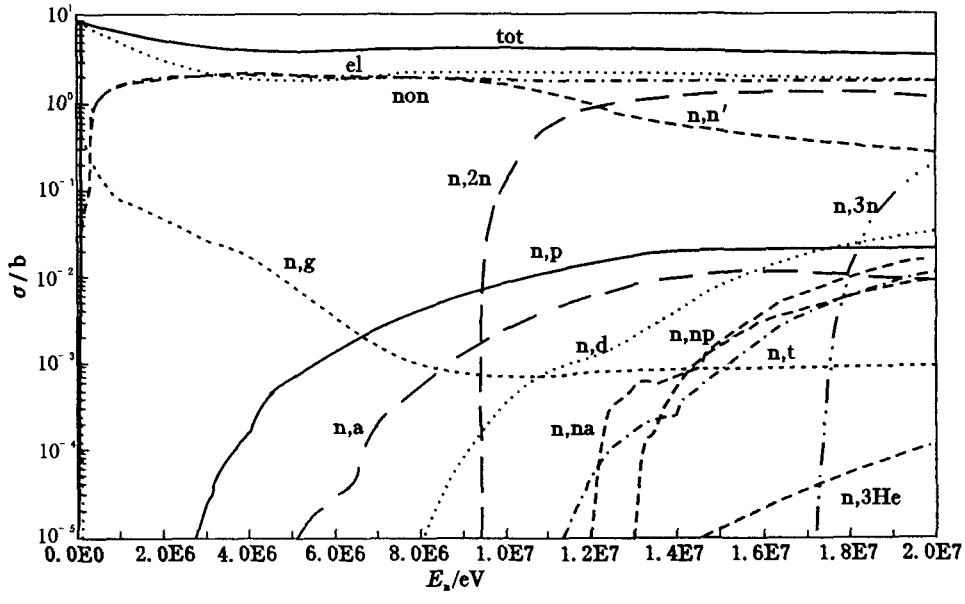

Fig. 9 ^{103}Rh evaluated cross sections

Reference

[1] D.G.Foster JR, DW.Glasgow, J. Phys. Rev. C, 3, 576, 1971

[2] M.Divadeenam, E.G.Bilpuch, H.W.Newson, J. Dissertation Abstracts Section B, 28, 3834, 1968

[3] K.K.Seth, R.H.Tabony, E.G.Bilpuch, et. al., J. Phys. Let., 16, 306, 1965

[4] A.P.Jain, R.E.Chrien, J.A.Moore, et al., J. Phys. Rev. b, 137,83,1965

[5] A.B.Smith, PT.Guenther, J.F.Whalen, J. Nucl. Phys. a, 415, 1, 1984

[6] W.P.Poenitz, J.F.Whalen, R.ANL-NDM-80, 1983

[7] R.M.Wilenzick, K.K.Seth, Pr.Bevington, et. al., J. Nucl. Phys., 62, 511, 1965

[8] T.Nagel, W, Nagel, 1966

[9] E.I.Grigor'ev, G.B.Tarnovskij, V.P.Jaryna, C. 6th All Union Conference on Neutron Physics, Kiev, 2-6 october 1983

[10] LRveeser, E.D.Arthur, P.G.Yo, J. Phys. Rev. c, 16, 1792, 1977

[11] H.A.Tewes,A.A.Caretto, A.E.Mi.R.UCRL-6028-t, 1960

[12] D.G.Vallis, R.AWRE-O-76/66, 1966

[13] A.Paulsen, R.Widera, J. Zeitsch. F. Physik, 238, 23, 1970

[14] J.Frehaut, A.Bertin, R.Bois, et. al. W. Frehaut, 800609, 1980

[15] D.S.Mather, P.F.Bampton, et. al., R. AWRE-O-72/72, 1972

[16] E.B.Paul, R.L.Clarke, J. Can. J. Phys., 31, 267, 1953

[17] M.Bormann, W.Schmidt, V.Schroeder, et. al., J. Nucl. Phys. a, 186, 65, 1972

[18] R.Prasad, D.C.Sarkar, J. Nucl. Phys., 85, 476, 1966

[19] T.Biro, S.Sudar, J.Csikai, et. al., J. Inorg. Nucl. Chem., 37, 1583, 1975

[20] E.T.Bramlitt, R.W.Fink, D.G.Gardner, et. al., J. Phys. Rev., 125, 297, 1962

[21] L.Husain, A.Bari, P.K.Kuroda, J. Inorg. Nucl. Chem., 30, 3145, 1968

[22] P.R.Gray, A.R.Zander, T.G.Ebrey, J. Nucl. Phys., 75, 215, 1966

[23] E.Frevert,J. Acta Physica Austriaca, 20, 304, 1965

[24] M.Diksic, P.Strohal, I.Slauis, J. Inorg. Nucl. Chem., 36, 477, 1974

[25] R.W.Hockenbury, H.D.Knox, et. al., C. 4th Conf. on Nucl. Cross Section and Tech., Washington D.C., 3-7 March 1975, 2, 905, 1975

[26] W.P.Poenitz, C.Specialists' Meeting on Neutron Cross Section of Fission Product Nuclei, Bologna, 12-14 dec. 1979, Publ. as Report rit/fis-ldn(80)1= neandc (e)209, 85, 1979

[27] J.H.Gibbons, R.L.Macklin, et. al., J. Phys. Rev., 122, 182, 1961

[28] R.L.M acklin, J.H.Gibbons, et. al., J. Phys. Rev., 129, 2695, 1963

[29] B.C.Diven, J.Terrell, A.Hemmen, J. Phys. Rev., 120, 556, 1960

[30] R.L.Macklin, J.H.Gibbons, J. Phys. Rev., 159, 1007, 1967

[31] L.W.Weston, K.Kseth, E.G.Bilp, J. Ann. Phys., 10, 477, 1960
[32] F.Rigaud, J.L.Irigaray, et. al., J. Nucl. Phys. a, 173, 551, 1971
[33] F.Rigaud, M.G.Desthuilliers, J. Nucl. Sci. Eng., 55, 17, 1974
[34] C.Lerigoleur, A.Arnaud, et. al., CEA-R-4788, 1976
[35] S.Joly, J.Voignier, G.Grenier, J.Nucl. Sci. Eng., 70,(1), 53, 1979
[36] J.Csikai, G.Peto, M.Buczko, et. al., J. Nucl.Phys., 41, 316, 1963

Evaluation of Cross Sections of Photonuclear Reactions for ^{90,91,92,94,96}Zr Below 30 MeV

Yu Baosheng Han Yinlu Zhang Jingshang
(China Nuclear Data Center, CIAE)

Introduction

The study of the properties of nuclei near to the closed neutron shell at N=50 is a subject of widespread interest. The accurate photonuclear data play an important role in nuclear science and technology. In this work, the experimental data of photonuclear up to 30 MeV for ^{90,91,92,94,96}Zr were evaluated which is impotant to radiation damage, radiation safety, reactor dosimetry. The theoretical calculation were used for supplement to some energy where the measured photonuclear data are scarce. The recommended photonuclear data for ^{90,91,92,94,96}Zr were obtained based on evaluated and calculated data and compared with existing measured data.

1 Evaluation and Analysis of Experimental Data

The natural zirconium consists of five isotopes, i.e. ^{90}Zr (51.45 %), ^{91}Zr (11.22%), ^{92}Zr (17.15 %), ^{94}Zr (17.38 %) and ^{96}Zr (2.8 %). In present work the

cross sections of ^{90,91,92,94,96}Zr(γ,ABS), ^{90,91,92,94,96}Zr(γ,n)+(γ,n+p), ^{90,91,92,94,96}Zr(γ,2n)+(γ,2n+p), ^{90,91,92,94,96}Zr(γ,3n), (γ, n+p), (γ, n+α), (γ, 2n), (γ, 3n), (γ, p), (γ, d), (γ, t), (γ, ^{3}He), (γ, α) ...., and the double differential cross sections of (γ,2n), (γ, 3n), (γ, n+p), (γ, n+α) and (γ, n'$_{continue}$) were evaluated.

The 10 sets of available experimental data[1,2] for photonuclear reaction cross sections of ^{90,91,92,94}Zr are shown in Table 1 from threshold to 30 MeV, which were retrieved from EXFOR master files up to 1998. Among them the 4 sets are mainly for ^{90}Zr, and 2 sets for ^{91}Zr, one set for ^{92}Zr as well as three sets for ^{94}Zr, respectively.

^{90}Zr :

The photonuclear cross sections for ^{90}Zr were first measured by B.L. Berman[1] in gamma energy region of 12.1 to 27.6 MeV in 1967. In order to get accurate photon flux, a xenon-filled transmission ionization chamber between the photon collimator and sample was used to monitor it. The photon beam energy collimated were determined as a function of photon energy by use of NaI γ-ray spectrometer located after neutron detector system. In the giant-resonance region, the photon energy resolution for ^{90}Zr is about 1% (13 to 27 MeV). The enriched ^{90}Zr sample was used, the attenuation of photon flux in the sample were taken into account and the necessary corrections were made. The neutron detector consists of a 2 ft^3 (1 ft=0.3048 m) cube of paraffin moderator with BF_3 counters. An obvious structure of photonuclear cross section corresponding to (γ,n)+(γ,n+p), (γ, 2n)+ (γ, 2n+p) reactions is shown in Fig. 1~2.

Table 1 Collected Data of Photonuclear Reactions for ^{90,91,92,94}Zr

Year	Author	E_n / MeV	nuclide	Detector	Reactions
1967	B.L.Berman	12.1 to 27.6	^{90}Zr	PROPC	(γ, n) + (γ, n+p)
		20.8 to 27.6	^{90}Zr	PROPC	(γ, 2n) + (γ, 2n+p)
		10.8 to 30.2	^{91}Zr	PROPC	(γ, n) + (γ, n+p)
		18.7 to 30.1	^{91}Zr	PROPC	(γ, 2n) + (γ, 2n+p)
		10.0 to 27.8	^{92}Zr	PROPC	(γ, n) + (γ, n+p)
		15.8 to 27.8	^{92}Zr	PROPC	(γ, 2n) + (γ, 2n+p)
		7.8 to 29.0	^{94}Zr	PROPC	(γ, n) + (γ, n+p)
		13.8 to 31.0	^{94}Zr	PROPC	(γ, 2n) + (γ, 2n+p)
		23.3 to 31.0	^{94}Zr	PROPC	(γ, 3n)
1971	A.Lepretre	12.2 to 25.9	^{90}Zr	STANK	(γ, n) + (γ, n+p)
		21.6 to 25.9	^{90}Zr	STANK	(γ, 2n)

PROPC : Paraffin moderator with BF_3 counters

STANK : Gd - loaded liquid scintillator tank

The second measurement of photonuclear cross sections for ^{90}Zr was performed by A. Lepretre using the Ga-loaded liquid scintillation tank(STANK) with natural sample in gamma energy region of 12.2 to 25.5 MeV in 1971. Both of them are in fair agreement. The broadened width and highness of giant resonance peak of A. Lepretre[2] are just slightly bigger than the data measured by B.L. Berman[1]. At that time, there were insufficient signal to noise ratio in this type of STANK, so there is for high back-ground.

The photoabsorption cross section is the sum of (γ,n), (γ,n+p), (γ,2n), (γ, 2n+p), (γ, 3n). The appeared (γ, n)+(γ,n+p), (γ,2n)+ (γ,2n+p) peaks position in the measured data of A. Lepretre consists with the one of the photonuclear (γ,n)+(γ, n+p), (γ, 2n)+ (γ,2n+p) cross sections measured by B.L. Berman[1], however the resolution and the energy region of emitted neutron of B.L. Berman are better and wider than the ones of A. Lepretre. The photonuclear cross section of B.L. Berman, especially the photonuclear (γ,n)+(γ,n+p), (γ,2n)+ (γ,2n+p) cross section can be used to adjust model parameters. These comparisons are shown in Fig. 1~2.

$^{91,92,94}Zr$:

The photonuclear cross sections for ^{91}Zr(γ, n)+(γ, n+p) and (γ, 2n)+(γ, 2n+p) reactions were also measured by B.L. Barman[1] in gamma energy region from 10.8 to 31.0 MeV, for ^{92}Zr(γ,n)+(γ,n+p) and (γ, 2n)+(γ,2n+p) reactions from 10.0 to 27.8 MeV, for ^{94}Zr(γ,n)+(γ,n+p), (γ,2n)+(γ,2n+p) and (γ,3n) from 13.8 to 31.0 MeV, respectively. Therefore, these measured data can also be used to adjust model parameters in calculation for $^{91,92,94}Zr$, respectively.

2 Theoretical calculation and Recommendation

The theoretical calculation for ^{90}Zr was used to fit the adopted experimental data[1,2]. The optical potential parameters for the calculating neutron nuclear data for Zr were obtained from this work.

Then, some parameters concerned were adjusted to make the calculated various photonuclear reaction data, such as (γ, n)+(γ,n+p), (γ, 2n)+(γ, 2n+p) and (γ, 3n) cross sections in good agreement with the experimental data.

The total photoneutron (γ, n) cross section is the sum of the photoneutron from ground, excitation states and continuum state. The level scheme used for theoretical calculation are taken from China Nuclear Parameter Library. The continuum levels were assumed above 2.1506, 3.9755, 2.3569, 1.4640 and

0.9542 MeV for zirconium's isotopes ^{90,91,92,94,96}Zr. The cross sections of (γ,2n) and (γ,3n) reactions were also calculated based on the basis of the experimental data[1,2].

The cross sections of photonuclear reactions were calculated from the threshold to 30 MeV. The theoretically calculated values are in good agreement with the experimental data. Therefore, the calculated data below 30 MeV are recommended and shown in Fig. 1~2.

Based on the available experimental data of photonuclear cross sections for zirconium and its isotopes ^{91}Zr and ^{92,94}Zr, a set of optical potential parameters and photonuclear reaction parameters for ^{92}Zr and ^{92,94}Zr in gamma energy region from the threshold to 30 MeV was obtained, and comparisons of the calculated results with experimental data are shown in Fig. 3~5.

For ^{96}Zr reactions, the model parameters used are the same as those for ^{91,92,94}Zr reaction. The recommended data of photonuclear reactions for ^{96}Zr reactions from threshold to 30 MeV are based on the calculated data.

For ^{90,91,92,94,96}Zr(γ, x) reactions, there are no experimental data. Therefore, the cross sections of changed particle emission for ^{90,92,92,94,96}Zr(γ, p), (γ, d), (γ, t), (γ, ^{3}He), (γ, α) reactions must be calculated theoretically.

The pertinent calculations have already performed using GUNF Code[3]. In present work, the recommended cross sections for γ+ ^{90,91,92,94,96}Zr reactions from threshold to 30 MeV are given in Fig. 6~10.

For the photonuclear double differential cross sections for Zr, the experimental data are very scarce. Therefore, the recommended data come from the theoretical calculations.

Based on the optical potential parameters generated from this work for the calculation of photonuclear reactions of Zr, the double differential cross sections for emission neutrons (γ, 2n), (γ, 3n), (γ, n+p), (γ, n+α) and (γ, $n_{continum}$) with ^{90,91,92,94,96}Zr were calculated and recommended.

Acknowledgments

The authors are indebted to IAEA and CIAE for their supports, and thanks to Drs. Oblozinsky, T. Benson and O. Schwerer for their kind help and suggestions.

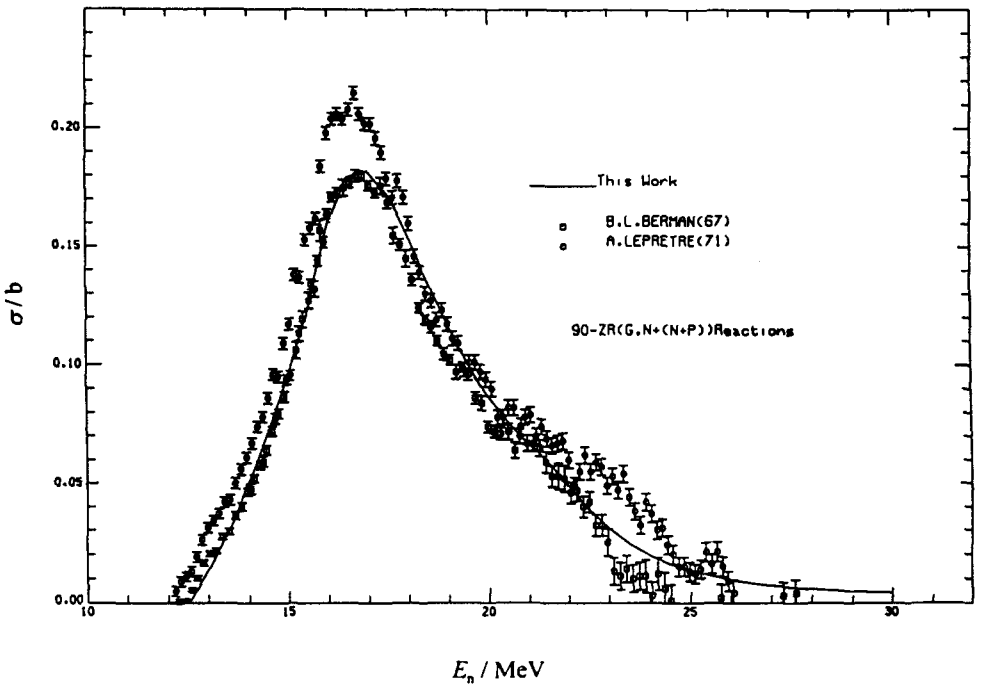

Fig. 1 Comparison of calculated and measured data

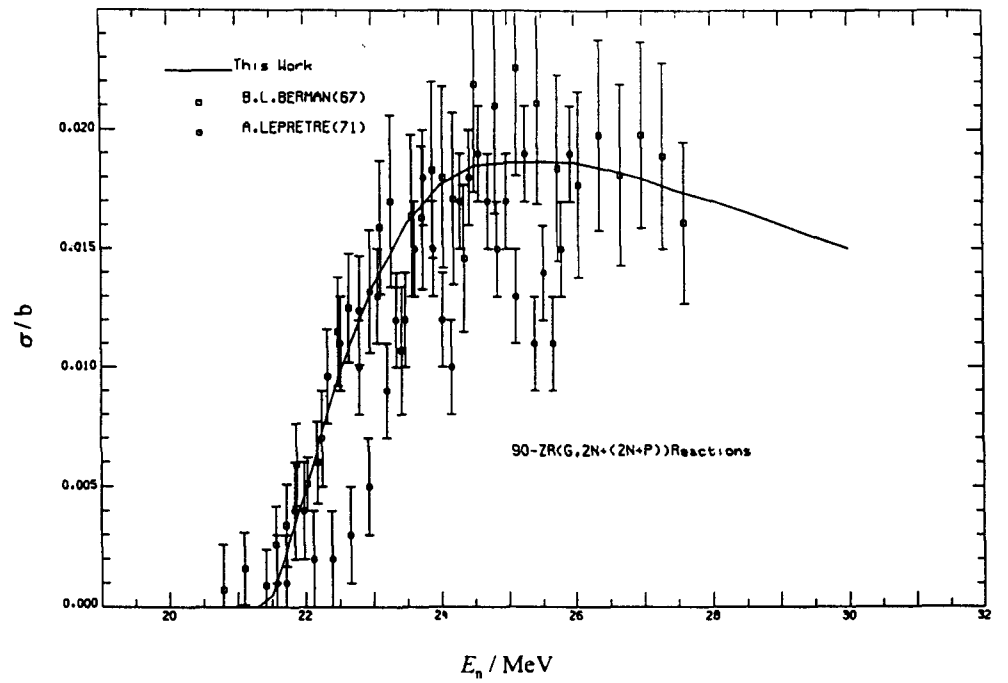

Fig. 2 Comparison of calculated and measured data

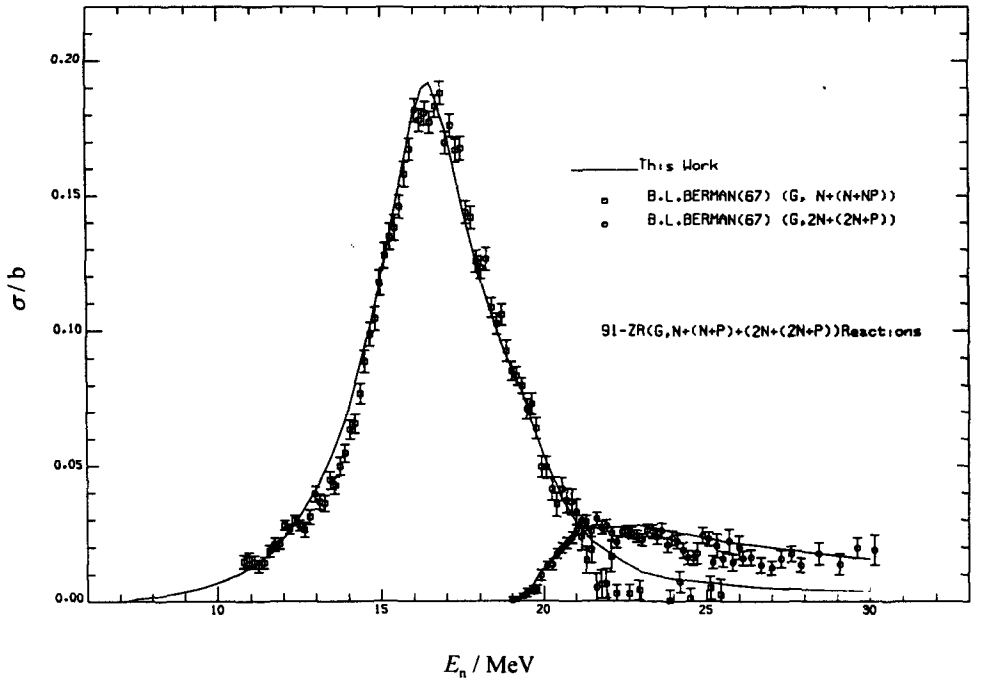

Fig. 3 Comparison of calculated and measured data

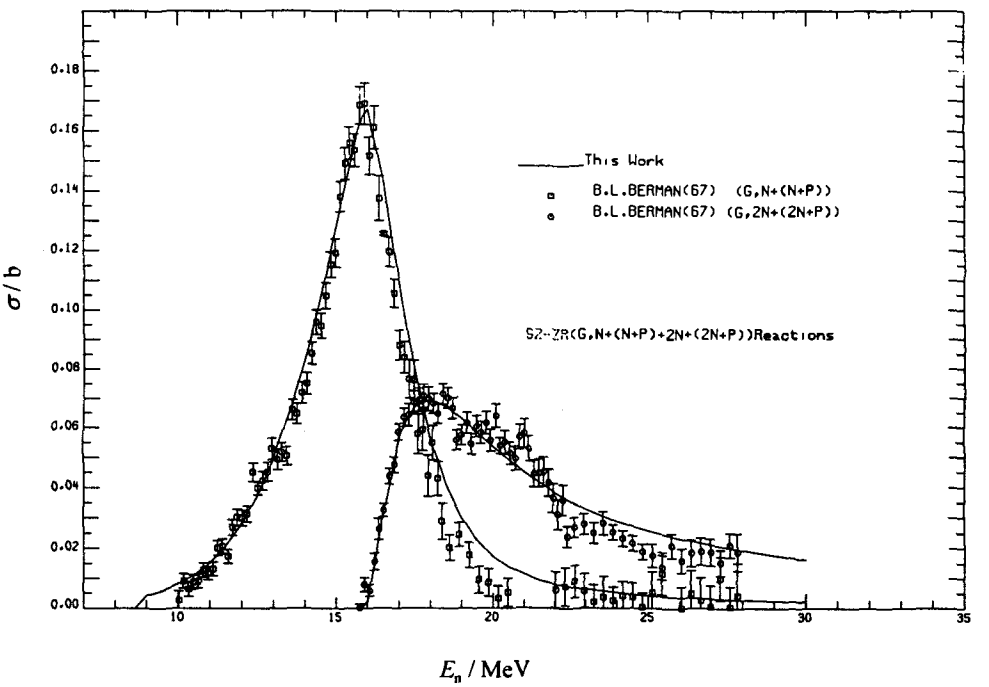

Fig. 4 Comparison of calculated and measured data

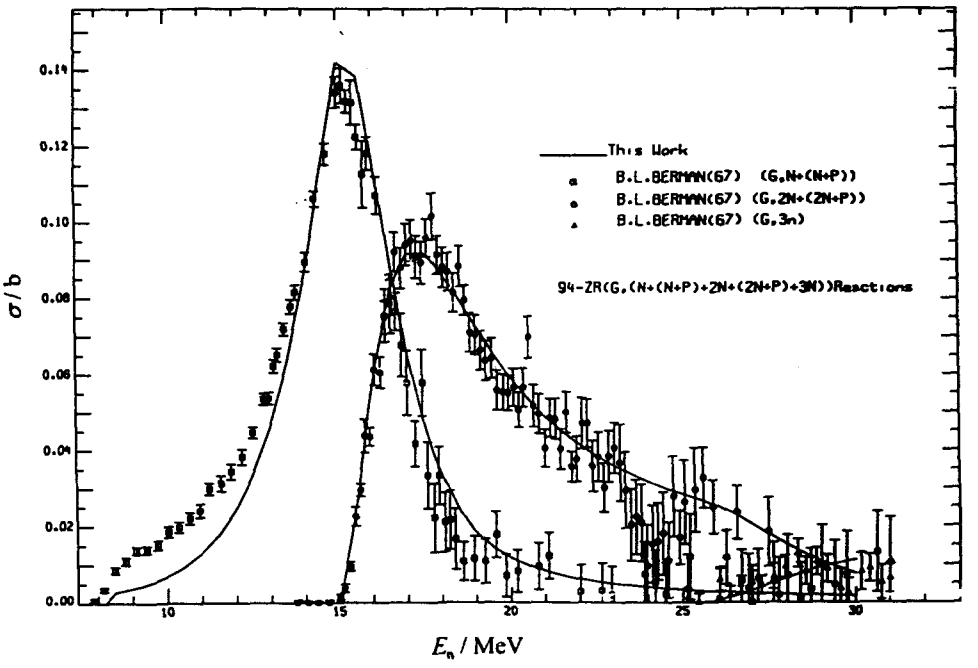

Fig. 5 Comparison of calculated and measured data

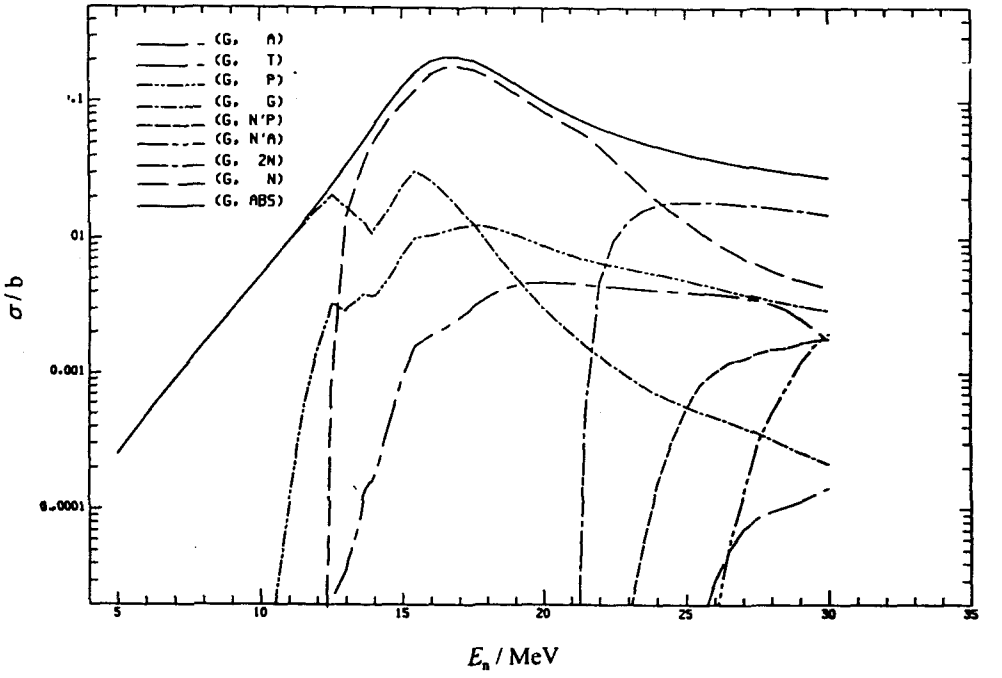

Fig. 6 Recommended data for ^{90}Zr

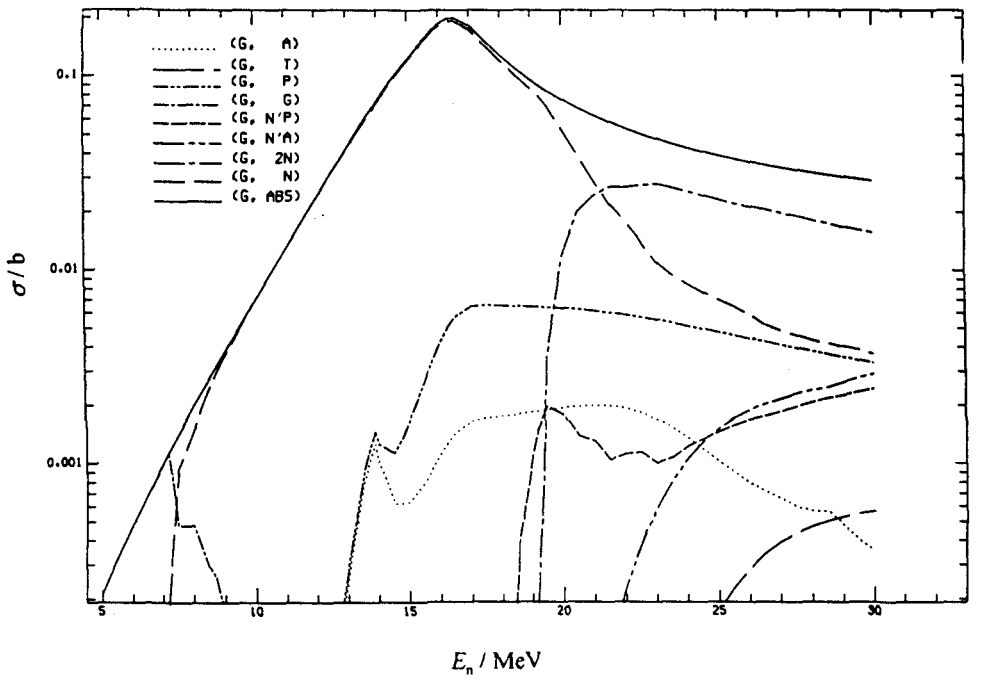

Fig. 7 Recommended data for ^{91}Zr

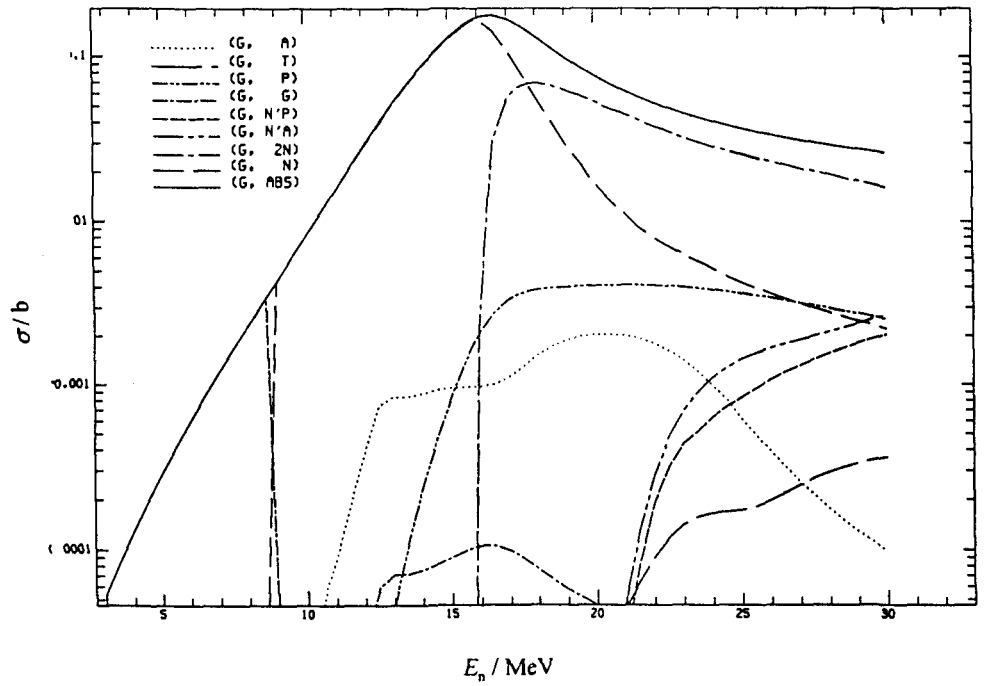

Fig. 8 Recommended data for ^{92}Zr

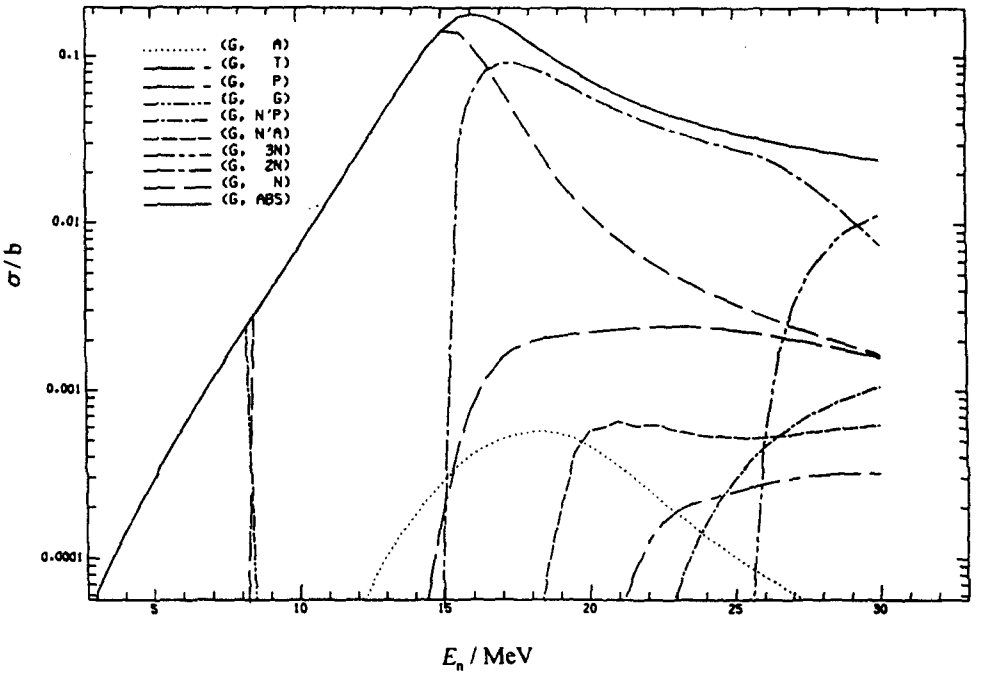

Fig. 9 Recommended data for ^{94}Zr

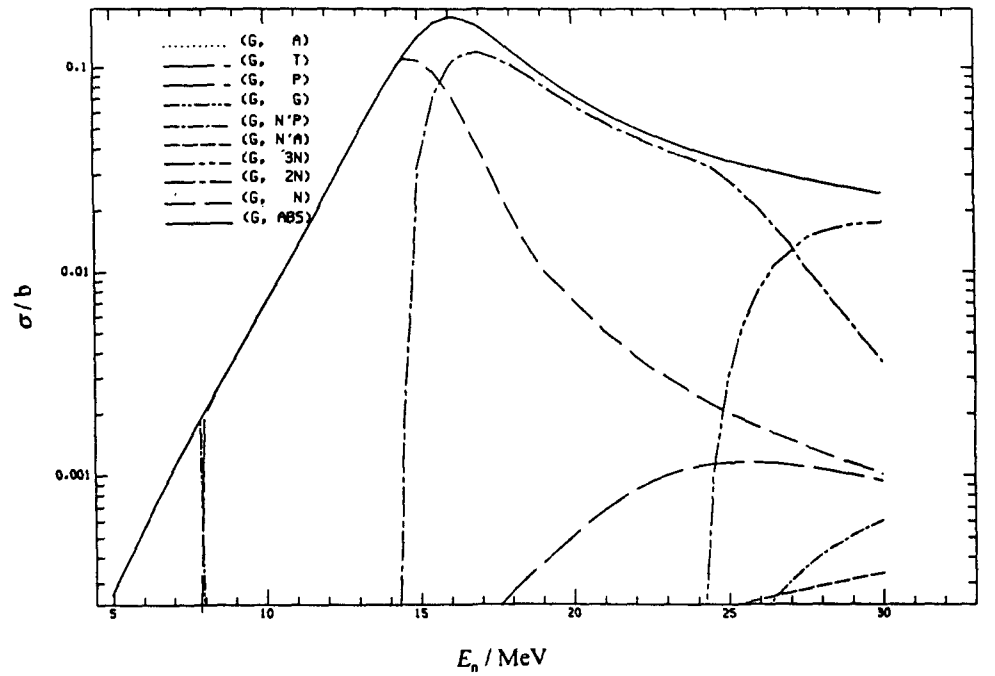

Fig. 10 Recommended data for ^{96}Zr

References

[1] B.L.Berman et al., Phys. Rew.,162,1098(1967)

[2] A.Lepretre et al., Nucl. Phy./A,175,609,(1971)

[3] Zhang Jingshang , GUNF Code, Inter. Report of CEAE(1997)

CN0101617

Thermal Neutron Capture Data Evaluation for A = 1~19

Zhou Chunmei
(China Nuclear Data Center, CIAE, Beijing 102413)

The prompt gamma-ray data of thermal neutron capture for A=1~19 had been evaluated and published in atomic data and nuclear data tables, 26, 511 (1981). Since that time many experimental data of thermal neutron capture have been published. The update of the evaluated prompt gamma-ray data is very necessary for use in high-resolution analytical prompt gamma-ray spectroscopy. The levels, prompt gamma-rays and decay schemes of thermal neutron capture for A=1~19 have been presented. The necessary comments are given in the text.

CN0101618

Nuclear Data Sheets For A = 195

Zhou Chunmei
(China Nuclear Data Center, CIAE, Beijing 102413)

The 1994 Version of Nuclear Data Sheets for A=195 [1] has been updated on the basis of the experimental results from reactions and decays leading to nuclides of

mass number A=195 by the cutoff date noted below. The detailed level schemes and decay schemes, and experimental reaction and decay data on which they are based are summarized and presented for all nuclides with mass number A=195. The experimental data are evaluated; the inconsistencies and discrepancies are noted; and adopted values for levels and γ-ray energies, γ-ray intensities, as well as for other nuclear properties, are presented. The references, JPI arguments, and necessary comments are given in the text.

References

[1] Zhou Chunmei, Nuclear Data Sheets, Vol.71, 367 (1994).

CN0101619

Evaluation of Capture Cross Sections for $^{135\sim138}$Ba

Zhao Jingwu Su weiNing
(Department of Physics, Nanjing University, Nanjing, 210093)

Introduction

There are three sets of evaluated data, for capture cross sections of $^{135\sim138}$Ba from ENDF/B-6, JENDL-3.2 and JEF-2 in 1978, 1990 and 1983, respectively. These data have some difference in the high energy areas and do not agree with recent experimental data. The capture cross sections in the high energy areas are evaluated, and the results are in agreememt with the experimental data very well. The experimental data mainly referred to EXFOR.

1 Experimental Data Analysis

1.1 Experimental data of ^{138}Ba

There were many experimental data for ^{138}Ba. Two set s of data[1,2] with white neutron source were used to evaluate the cross section in the energy range 80 keV to 2.5 MeV. Other experimental data[3~17], whose energy points are less than three, were also used as supplement. For example, references [14] and [15] were used for the cross section nearby 3 MeV.

The data of references [3] and [14] are larger than the actual ones, because the monitor cross sections used are larger . The experimental data of references [12], [13] and [16] are average values over fission neutron source. These data were used for reference only.

The data of references [4~7] and [10] were measured at 14 MeV with activation method. These data are larger than actual cross sections, because of the γ-ray from other reactions, were possibly confused and added to them.

1.2 Experimental data of $^{135\sim137}$Ba

A.R. De L. Musgrove et al.[11] Measured the capture cross sections for $^{135\sim137}$Ba in the energy range 1.0 keV to 100 keV in 1979; P.E. Koehler et al.[18] also measured the cross section for ^{137}Ba in the same energy range with high resolution in 1998. There are no experimental data in other energy range.

2 Recommended Capture Cross Sections

Based on the above experimental data, the neutron capture cross sections were calculated for ^{138}Ba, and the calculated data were smoothed for $^{135\sim137}$Ba. The experimental data were used to correct the calculated result for ^{138}Ba, and the calculated data were smoothed for $^{135\sim137}$Ba. The capture cross sections were recommended on the basis of the experimental data below 5 MeV for ^{138}Ba and below 100 keV for $^{135\sim137}$Ba. The calculated results are recommended in the high energy range. The recommended capture cross sections are shown in Fig. 1~4 for $^{135\sim138}$Ba respectively. The recommended results are in agreement with the experimental data and compared with the data from ENDF/B-6, JENDL-3.2 and JEF-2.

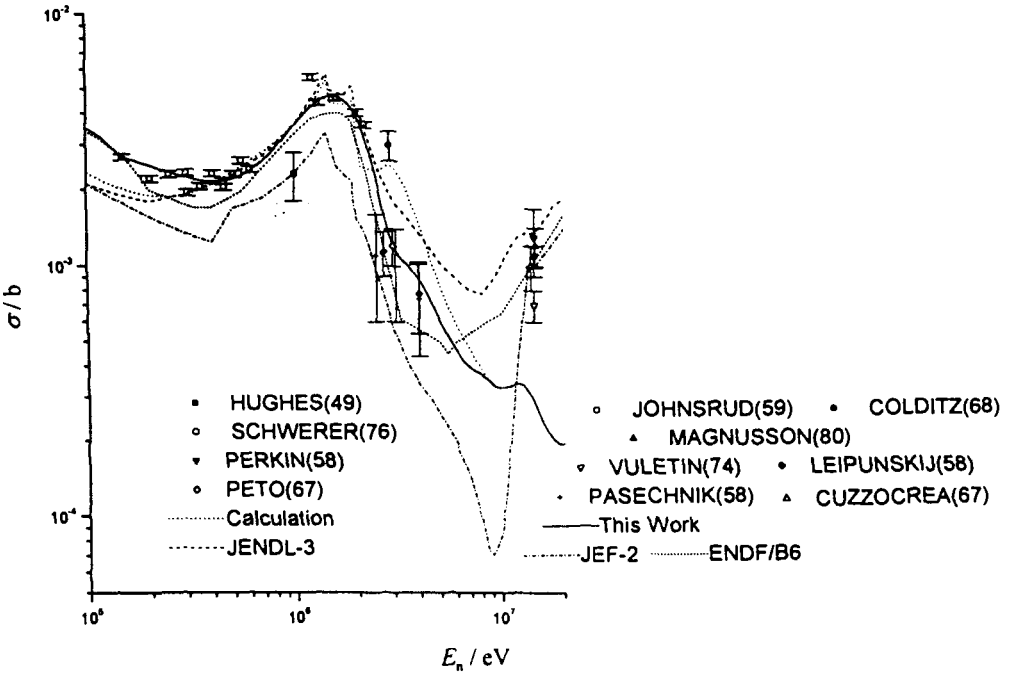

Fig. 1 Capture cross section of ^{138}Ba

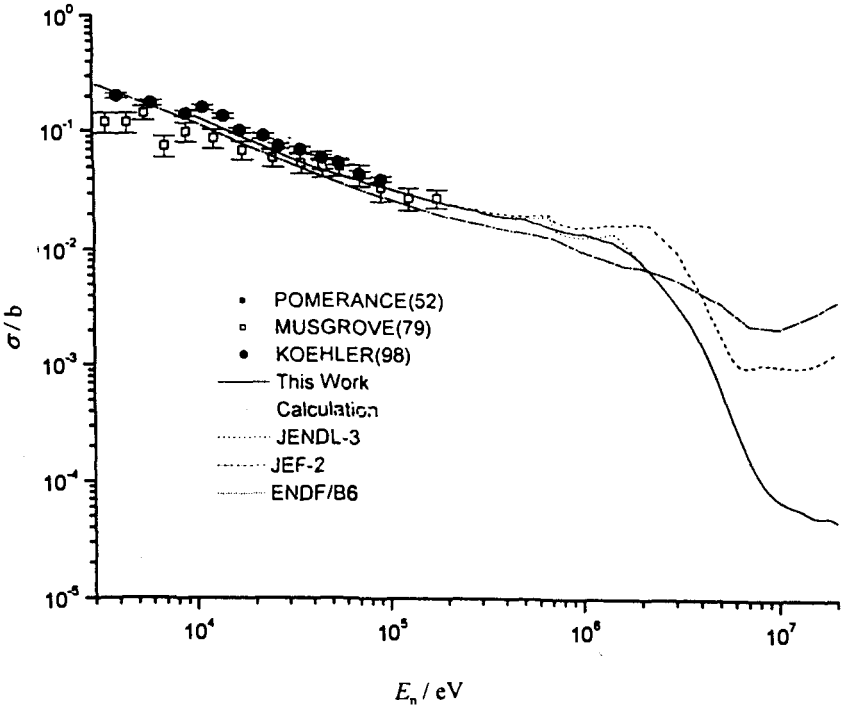

Fig. 2 Capture cross section of ^{137}Ba

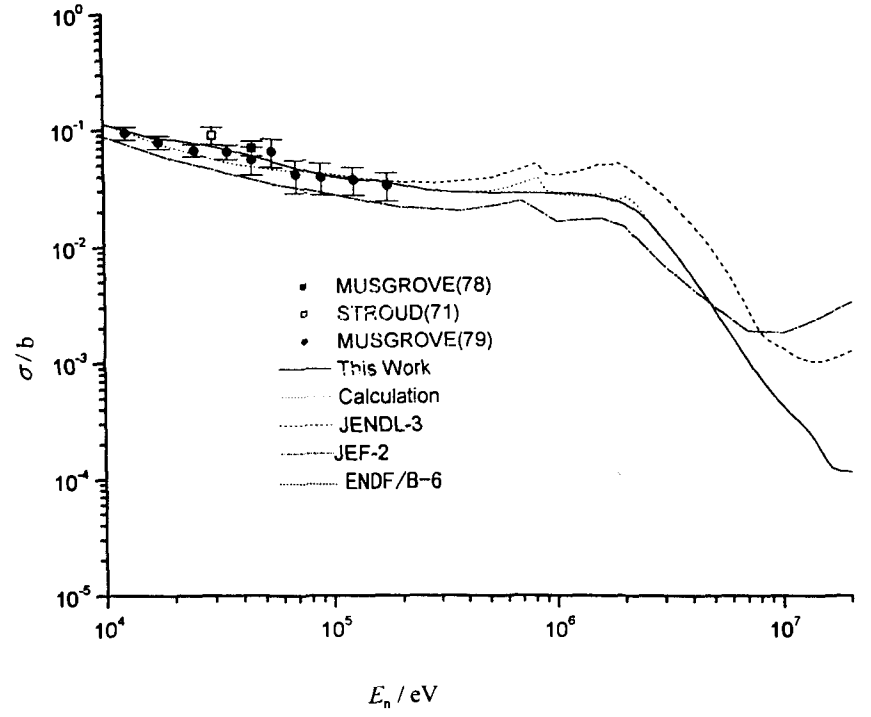

Fig. 3 Capture cross section of ^{136}Ba

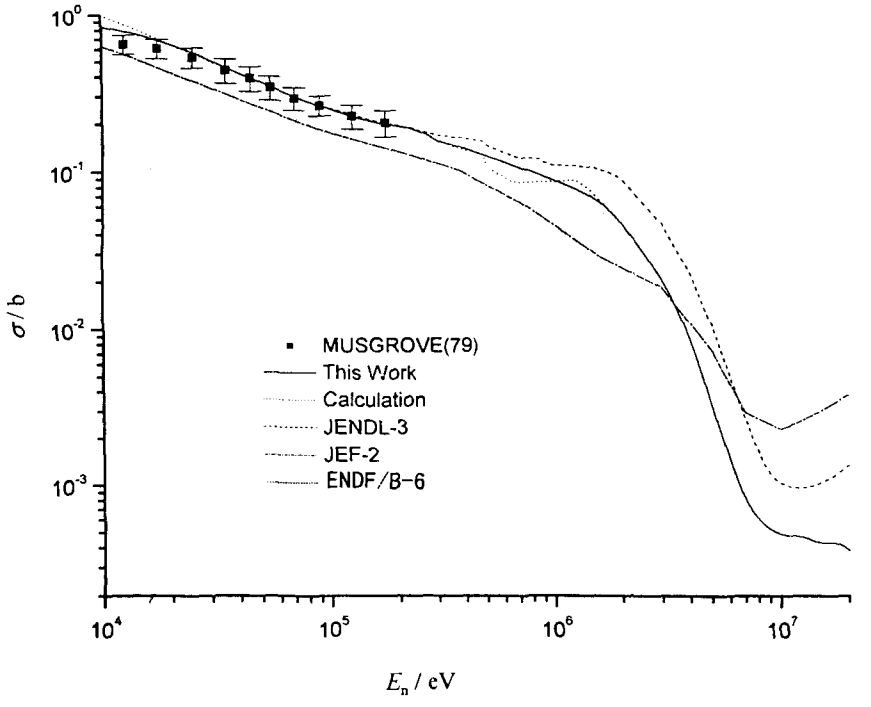

Fig. 4 Capture cross section of ^{135}Ba

Reference

[1] JU.JA.Stavisskij,V.A.Tolstik, et al.,J,Atomnaja Energija, 10,(5),508,1961

[2] A.E.Johnsrud, M.G.Silbert, et al.,J,Phys., 116,927,1959

[3] J.Colditz, P.Hille, J,Osterr. Akad.Wiss. Math.-Naturw.Ki.,Sitzungsber.,105,236,1968

[4] O.Schwer, M.Winkler-Rohatsc, et al., J,Nucl. Phys., A,264, 105, 1976

[5] G.Magnusson, P.Andersson, et al., J, Physica Scripta, 21, (1), 21, 1980

[6] P.Cuzzocrea, S.Notarrigo, et al., J, Nuovo Cimento B, 52, (2), 476,1967

[7] J.L.Perkin, L.P.O'connor, et al., J, Proc. Phys. Soc, 72,505,1958

[8] H.Berr, F.Kaeppeler, J, Phys. Rev. C, 21,534,1980

[9] G.Peto, Z.Milligy, et al., J, Nucl. Energ., 21, 797, 1967

[10] J.Vuletin, P.Kulisic, et al., J,Letter at Nuovo Cimento, 10, 1,1974

[11] A.R.De L.Musgrove, B.J.Allen, et al., J, Australian J, Phys., 32,213, 1979

[12] J.Csikai, Z.Dezso, 3th Conf. on Nucl. Cross-Sections and Tech. Karlsr, 29, 1975

[13] H.Benabdallah, G.Paic, et al., J, Fizika, 17, (2), 191, 1985

[14] A.I.Leipunskij, O.D.Kazachkov, et al., Second UN Conf. on the Peacful Uses of Atomic Energy, U.N.Geneva, 5, 50(2219), 1958

[15] M.V.Pasechnik, I.F.Barchuk, et al., Second UN Conf. on the Peacful Uses of Atomic Energy, U.N.Geneva, 5, 18(2030), 1958

[16] D.J.Hughes, W.D.B.Spatz, J, Phys. Rev., 75, 1781, 1949

[17] H.Von Halban JR, L.Kowarski, J, Nature (NAT), 142, 392, 1998

[18] P.E.Koehler, R.R.Spencer, et al., J, Phys. Rev. C, 57, 4, 1558, 1998

[19] D.B.Stroud, D.M. H.Chan AEC Reports, 9, 1971

IV DATA PROCESSING

Construction of Covariance Matrix for Absolute Fission Yield Data Measurement

Liu Tingjin Sun Zhengjun
(China Nuclear Data Center, Beijing 102413)

Introduction

With the development of reactor physics and computer, now, the covariance data become more and more important in the nuclear engineering applications. For evaluators and experimenters, the information are all given completely only in the case that the covariance matrix is given; because the error, as traditional, is only the diagonal elements of the covariance matrix, describes the accuracy of the data and nothing about the correlation of the data is given. There is the same situation in fission yield data, which are widely used in the radio decay heat calculation, burn-up credit study, radio intensity estimation of fission product and etc.

The purpose of this paper is to provide a tool for experimenters and evaluators to conveniently construct the covariance based on the information of the experiment. The method used is so called as parameter analysis one. The basic method and formula is given in the first section, a practical program is introduced in the second section, and finally, some examples are given in the third section.

1 Basic Method and Formula

1.1 Outline of the Parameter Analysis Method

The measured quantity f is usually a function of a set basic parameters x_k (k=1,2, ...N), which can be measured directly in experiments. Suppose it can be written as

$$f = f(x_1, x_2 \cdots x_N) \tag{1.1}$$

In general case, the parameter x varies with energy E or different products nuclides p, so

$$f_i = f(x_{1i}, x_{2i} \cdots x_{N_i})$$
$$f_j = f(x_{1j}, x_{2j} \cdots x_{N_j})$$

By making Taylor expansion of f_i and f_j at $<x_i>$, $<x_j>$ respectively, neglect the higher order terms, it can be written as

$$f_i = f_{oi} + \sum_{k=1}^{N} \frac{\partial f}{\partial x_k}\Big|_i \Delta x_{ki} \tag{1.2.1}$$

$$f_j = f_{oj} + \sum_{k=1}^{N} \frac{\partial f}{\partial x_k}\Big|_j \Delta x_{kj} \tag{1.2.2}$$

It is obvious that expansions (1.2) are of linear approximation, to make them tenable, the errors of the directly measured quantities Δx_k must be smaller, and the function f should be smooth and no turning points.

From (1.2.1) and (1.2.2), it can be obtained that

$$\begin{aligned} C_{ov}(f_i, f_j) &= \left\langle \left(\sum_{k=1}^{N} \frac{\partial f}{\partial x_k}\Big|_i \Delta x_{ki} \right) \left(\sum_{k'=1}^{N} \frac{\partial f}{\partial x_{k'}}\Big|_j \Delta x_{k'j} \right) \right\rangle \\ &= \sum_{k=1}^{N}\sum_{k'=1}^{N} \frac{\partial f}{\partial x_k}\Big|_i \frac{\partial f}{\partial x_{k'}}\Big|_j \left\langle \Delta x_{ki} \Delta x_{k'j} \right\rangle \\ &= \sum_{k=1}^{N}\sum_{k'=1}^{N} \frac{\partial f}{\partial x_k}\Big|_i \frac{\partial f}{\partial x_{k'}}\Big|_j \rho_{ij}^{kk'} \sigma_{ki} \sigma_{k'j} \\ &= \sum_{k} \frac{\partial f}{\partial x_k}\Big|_i \frac{\partial f}{\partial x_k}\Big|_j \rho_{ij}^{k} \sigma_{ki} \sigma_{k'j} \qquad \text{(Assume } \rho_{ij}^{kk'} = 0, \text{ when } k' \neq k\text{)} \end{aligned} \tag{1.3}$$

Where $\frac{\partial f}{\partial x_k}\Big|_{i(j)}$ is the derivative of function f to parameter x_k and take the value at $(x_k)_{i(j)}$, $\sigma_{ki(j)}$ is the absolute error of k-th parameter x_k at energy point or for nuclide $i(j)$; $\rho_{ij}^{kk'}$ is the correlation coefficient of parameter between parameter x_k at point i and parameter $x_{k'}$ at point j, and ρ_{ij}^{k} is the correlation coefficient of parameter x_k between points i and j.

It can be seen from the Eq. 1.3 that the covariance matrix of the indirectly measured quantity can be constructed if the calculation formula, the errors and correlation coefficients of the directly measured parameters concerned are known. In general case, it is easier for experimenters themselves to know the expression formula and the errors of the parameters, but it is more difficult for them to give the correlation coefficients of the parameters at different points, because this is not familiar with and less concerned traditionally for them.

1.2 Calculation Formula of Absolute Fission Yield Measurement

The fission yield can be calculated for absolute measurement with Ge(Li) method:

$$Y = N\lambda \Big/ \left[\sum_{i=1}^{I} n_{f_i} (1 - e^{-\lambda \Delta T_i}) e^{-\lambda T_{ci}} \right] \left[e^{-\lambda t_1} - e^{-\lambda t_2} \right] E_\eta \cdot E_P \cdot E_S \cdot E_\Omega \cdot E_\tau \qquad (1.4)$$

Where

N is the total count of radioactivity, e.g. the area under peak measured;

λ is the radio decay constant of the nuclide to be measured;

n_{fi} is the fission rate in the i-th time interval;

ΔT_i is the i-th time interval of irradiation;

T_{ci} is the time from the end of i-th irradiation to the end of irradiation;

t_1 is the cooling time, namely the time from the end of irradiation to the beginning of the measurement;

t_2 the time from the end of irradiation to the end of measurement;

E_η is the efficiency of the γ detector;

E_P is the branch ratio;

E_S is the correction factor for γ self-absorption;

E_Ω is the correction factor for geometry;

E_τ is the correction factor for pules pile.

Suppose the fission rate n_{fi} is a constant during the irradiation (case 1), then the Eq.1.4 becomes

$$Y = N\lambda/(1-e^{-\lambda T})n_f\left(e^{-\lambda t_1}-e^{-\lambda t_2}\right)E_\eta \cdot E_P \cdot E_S \cdot E_\Omega \cdot E_\tau \qquad (1.5)$$

Where T is the irradiation time.

This is tenable from the view point of covariance study. In fact, it is true for most of the cases, for example the irradiation neutrons are thermal, those with fission spectrum or from ^{252}Cf neutron source. For the 14 MeV neutron irradiation, it is also true when the accelerator runs under well conditions.

In the case that, comparing with the half-life of the nuclide to be measured, the irradiation time is long enough (case 2), for example $T/T_{1/2} \geq 5$, then

$$e^{-\lambda T} \to 0$$

and Eq. 1.5 becomes

$$Y = N\lambda/\left(e^{-\lambda t_1}-e^{-\lambda t_2}\right)n_f \cdot E_\eta \cdot E_P \cdot E_S \cdot E_\Omega \cdot E_\tau \qquad (1.6)$$

Suppose, comparing with the half-life of the nuclide to be measured, the cooling time t_1 and measured time t_2 are short enough(case 3), for example, $t_1 / T_{1/2}$, $t_2 / T_{1/2} <$ 0.1, then

$$e^{-\lambda t_1} \approx 1-\lambda t_1, \qquad e^{-\lambda t_2} \approx 1-\lambda t_2$$

and Eq. 1.6 becomes

$$Y = N/\left(t_2-t_1\right)n_f \cdot E_\eta \cdot E_P \cdot E_S \cdot E_\Omega \cdot E_\tau \qquad (1.7)$$

1.3 Calculation Formula of Covariance Matrix for Absolute Fission Yield Measurement

Rewrite the formulas mentioned- above as a unified form

$$Y = N/F(\lambda)\, n_f \cdot E_\eta \cdot E_P \cdot E_S \cdot E_\Omega \cdot E_\tau \qquad (1.8)$$

Where

$$F(\lambda)=\begin{cases}\lambda/(1-\mathrm{e}^{-\lambda T})(\mathrm{e}^{-\lambda t_1}-\mathrm{e}^{-\lambda t_2}) & (1.9.1)\ \text{(case 1)}\\ \lambda/(\mathrm{e}^{-\lambda t_1}-\mathrm{e}^{-\lambda t_2}) & (1.9.2)\ \text{(case 2)}\\ 1/(t_2-t_1) & (1.9.3)\ \text{(case 3)}\end{cases}$$

Take the logarithm in two sides of the Eq. (1.8), and then take the derivative to each parameters and taking the values at points i and j, then the relative covariance matrix elements are obtained:

$$V_{ij}^{\mathrm{R}}=\frac{Cov(y_i,y_j)}{y_i y_j}=f_i(\lambda)f_j(\lambda)\delta_{\lambda i}\delta_{\lambda j}\rho_{ij}^{\lambda}+\sum_k \delta_{x_{ki}}\delta_{x_{kj}}\rho_{ij}^{xk} \qquad (1.10)$$

Where i, j mean different energy points for the same nuclide or different nuclides at the same energy point, and

$$x_k = n_{\mathrm{f}},\ E_\eta,\ E_P,\ E_S,\ E_\Omega \text{ and } E_\tau$$

$$F(\lambda)=\begin{cases}1-\dfrac{\lambda T}{1-\mathrm{e}^{-\lambda T}}-\lambda\dfrac{t_2\mathrm{e}^{-\lambda t_2}-t_1\mathrm{e}^{-\lambda t_1}}{\mathrm{e}^{-\lambda t_1}-\mathrm{e}^{-\lambda t_2}} & (1.11.1)\ \text{(case 1)}\\ 1-\lambda\dfrac{t_2\mathrm{e}^{-\lambda t_2}-t_1\mathrm{e}^{-\lambda t_1}}{\mathrm{e}^{-\lambda t_1}-\mathrm{e}^{-\lambda t_2}} & (1.11.2)\ \text{(case 2)}\\ 0 & (1.11.3)\ \text{(case 3)}\end{cases}$$

Correspondingly, the absolute covariance matrix

$$V_{ij}^{\mathrm{A}}=V_{ij}^{\mathrm{R}}\cdot Y_i Y_j \qquad (1.12)$$

and the correlation coefficient matrix

$$V_{ij}^{\mathrm{C}}=V_{ij}^{\mathrm{A}}\Big/\sqrt{V_{ii}^{\mathrm{A}}V_{jj}^{\mathrm{A}}} \qquad (1.13)$$

2 Practical Program

A practical program FYCCA was developed for experimenter or evaluator to conveniently calculate the covariance matrix of fission yield data by just inputting the errors of each directly measurable parameters, which they are familiar with.

The correlation coefficients of each directly measurable parameters are given on the basis of the general case in the experiments and included in the code. These coefficients are listed in Table 1 for different nuclides and different energy points. The arguments for given values are also indicated in the table.

There are some flags N_1, N_2, N_3 in the input data to distinguish the different cases for the calculation. N_1 is to indicate whether fission yield or yield covariance or both of them will be calculated; N_2 is for selecting the calculation formula as given above, in another word, to what extent of the approximation the covariance will be calculated; N_3 is to define i, j for different nuclide (at same energy point) or at different energy points (for same nuclide). In the different cases the corresponding parameters are read from the input data file.

Table 1 The correlation coefficients of each directly measurable parameters

Quantity	$i,j^{1)}$	$i,j^{2)}$	comments
N total count under γ peak	0	0	statistical
n_f fission rate	1.0	0	the same in same measurement, no relation for different nuclides
λ decay constant	0	1.0	the same for same nuclide, no relation for different nuclides
E_η γ-detector efficiency	0.5	1.0	the same for same γ energy, medium range correlation for different γ energy
E_p branch ratio	0	1.0	The same for same nuclide, no relation for different nuclides
E_S correction factor for self-absorvition	0.5	1.0	relate to thickness of U sample and γ energy
E_Ω correction factor for pulse pile	0.5	0.5	relate to geometry andγ energy
E_τ correction factor for pulse pile	0.5	1.0	relate to measurement system

(1) different nuclides at same energy point

(2) different energy points for same nuclide

The output data include absolute covariance matrix, relative covariance matrix, correlation coefficient matrix and the error of the yield in the traditional meaning.

The constructed matrix must be symmetry and positive definite in mathematics. It is easy to prove the symmetry of the matrix that

$$
\begin{aligned}
Cov(f_i, f_j) &= \left\langle \left(\sum_{k=1}^{N} \frac{\partial f}{\partial x_k}\Big|_i \Delta x_{ki} \right) \left(\sum_{k'=1}^{N} \frac{\partial f}{\partial x_{k'}}\Big|_j \Delta x_{k'j} \right) \right\rangle \\
&= \left\langle \left(\sum_{k'=1}^{N} \frac{\partial f}{\partial x_{k'}}\Big|_j \Delta x_{k'j} \right) \left(\sum_{k=1}^{N} \frac{\partial f}{\partial x_k}\Big|_i \Delta x_{ki} \right) \right\rangle \\
&= Cov(f_j, f_i)
\end{aligned}
\tag{2.1}
$$

In physics, it is obvious that the correlation between points i, j and j, i is the same.

The positive definite of the matrix is checked in the code by using the method of calculating its eigenvalues λ_i. To reduce the calculation error, the eigenvalues are calculated for the correlation coefficient matrix $\boldsymbol{V}^{\mathrm{C}}$, instead of the absolute covariance matrix $\boldsymbol{V}^{\mathrm{A}}$, because

$$
\boldsymbol{V}^{\mathrm{A}} = \boldsymbol{E}^{+} \cdot \boldsymbol{V}^{\mathrm{C}} \cdot \boldsymbol{E} \tag{2.2}
$$

where the error matrix is defined as

$$
\boldsymbol{E} = \begin{pmatrix}
\sigma_1 & 0 & \cdots & 0 \\
0 & \sigma_1 & \cdots & 0 \\
\cdots & \cdots & \cdots & \cdots \\
0 & \cdots & \cdots & \sigma_N
\end{pmatrix} \tag{2.3}
$$

they have the same positive definite feature and the elements of correlation coefficient matrix are all larger than -1 and equal to or smaller than 1.

If the matrix constructed is not positive definite, it means that it is unreasonable in physics, which may be caused by taking some unreasonable parameters. In this case, some parameters must be changed and calculated again.

3 Example

An example is given below to show what input data are needed, if the code works well, and whether the results are reasonable. The example was taken from Ref.[1], in which the fission yields were absolutely measured by using Ge(Li) detector γ spectrum method for product nuclides ^{95}Zr, ^{103}Ru, ^{131}I, ^{132}I, ^{140}Ba at fission and thermal spectrum energy points.

The input data are listed in Table 2, which were collected and compiled from the paper [1].

Table 2 Input data for calculating fission yield covariance of the example

nuclide	δ_{n_f}%	δ_{E_τ}%	δ_{E_s}%	δ_{E_p}%	δ_{E_η}%	δ_λ%	thermal		fission	
							δ_{N_i}%	Y	δ_{N_i}%	Y
^{95}Zr	1.5	0.2	0.3	1.2	1.5	0.2	0.98	6.37	1.02	6.31
^{103}Ru	1.5	0.2	0.3	3.4	3.5	0.2	1.05	3.08	0.89	3.66
^{131}I	1.5	0.2	0.4	5.0	2.3	0.2	0.57	3.18	0.72	4.04
^{132}I	1.5	0.2	0.3	6.0	3.0	0.2	1.56	3.55	1.67	3.97
^{140}Ba	1.5	0.2	0.3	5.0	1.2	0.2	0.92	6.20	0.47	6.34

The calculated covariance matrices are given for different nuclides in Table 3 at thermal energy point and Table 4 at fission spectrum. The matrices are given for different energy points in Table 5. The errors given in Tables 3 and 4 are, in factor, the same with given by original authors, the differences are caused by different combination method of systematical and statistical errors. They were directly summed by original authors, but they were sum of squares in present case.

It can be seen from Table 3, 4 and 5 that the correlation is not so strong for different nuclides, but is quite large for same nuclide. The correlation mainly comes from the errors of detector's efficiency, γ branch ratio and fission number (see Table 2). Because the correlation coefficients for different nuclides at same energy points are 1.0 for fission number n_f, 0.5 for detector's efficiency and 0.0 for branch ratio, but for same nuclide at different energy points they are 0.0, 1.0, 1.0 respectively (see Table 1), whatever the errors of the efficiency and branch ratio in most cases are larger than fission number, so the correlation of same nuclide is larger than different nuclides.

Table 3 Calculated covariance matrices for different nuclides at thermal energy point

1) Relative Covariance matrix

	^{95}Zr	^{103}Ru	^{131}I	^{132}I	^{140}Ba
^{95}Zr	7.0304E−04	4.9400E−04	4.0550E−04	4.5650E−04	3.2150E−04
^{103}Ru		2.7293E−03	6.3550E−04	7.5650E−04	4.4150E−04
^{131}I			3.3065E−03	5.7800E−04	3.7100E−04
^{132}I				4.9814E−03	4.1150E−04
^{140}Ba					2.9666E−03

2) Absolute Covariance matrix

	^{95}Zr	^{103}Ru	^{131}I	^{132}I	^{140}Ba
^{95}Zr	2.8527E-02	9.6921E-03	8.2141E-03	1.0323E-02	1.2697E-02
^{103}Ru		2.5891E-02	6.2243E-03	8.2716E-03	8.4309E-03
^{131}I			3.3437E-02	6.5250E-03	7.3146E-03
^{132}I				6.2778E-02	9.0571E-03
^{140}Ba					1.1404E-01

3) Correlation coefficient matrix

	^{95}Zr	^{103}Ru	^{131}I	^{132}I	^{140}Ba
^{95}Zr	1.0000E+00	3.5663E-01	2.6596E-01	2.4394E-01	2.2262E-01
^{103}Ru		1.0000E+00	2.1155E-01	2.0517E-01	1.5516E-01
^{131}I			1.0000E+00	1.4242E-01	1.1846E-01
^{132}I				1.0000E+00	1.0704E-01
^{140}Ba					1.0000E+00

4) Error

	^{95}Zr	^{103}Ru	^{131}I	^{132}I	^{140}Ba
Relative	2.6515E-02	5.2242E-02	5.7502E-02	7.0579E-02	5.4467E-02
Absolute	1.6890E-01	1.6091E-01	1.8286E-01	2.5055E-01	3.3769E-01

Table 4 Calculated covariance matrices for different nuclides at fission spectrum

1) Relative Covariance matrix

	^{95}Zr	^{103}Ru	^{131}I	^{132}I	^{140}Ba
^{95}Zr	7.1104E-04	4.9400E-04	4.0550E-04	4.5650E-04	3.2150E-04
^{103}Ru		2.6982E-03	6.3550E-04	7.5650E-04	4.4150E-04
^{131}I			3.3258E-03	5.7800E-04	3.7100E-04
^{132}I				5.0169E-03	4.1150E-04
^{140}Ba					2.9041E-03

2) Absolute Covariance matrix

	^{95}Zr	^{103}Ru	^{131}I	^{132}I	^{140}Ba
^{95}Zr	2.8311E-02	1.1409E-02	1.0337E-02	1.1436E-02	1.2862E-02
^{103}Ru		3.6144E-02	9.3968E-03	1.0992E-02	1.0245E-02
^{131}I			5.4283E-02	9.2704E-03	9.5026E-03
^{132}I				7.9071E-02	1.0357E-02
^{140}Ba					1.1673E-01

3) correlation coefficient matrix

	^{95}Zr	^{103}Ru	^{131}I	^{132}I	^{140}Ba
^{95}Zr	1.0000E+00	3.5665E-01	2.6369E-01	2.4170E-01	2.2373E-01
^{103}Ru		1.0000E+00	2.1214E-01	2.0561E-01	1.5772E-01
^{131}I			1.0000E+00	1.4150E-01	1.1938E-01
^{132}I				1.0000E+00	1.0781E-01
^{140}Ba					1.0000E+00

4) Error

	^{95}Zr	^{103}Ru	^{131}I	^{132}I	^{140}Ba
Relative	2.6665E-02	5.1944E-02	5.7670E-02	7.0830E-02	5.3890E-02
Absolute	1.6826E-01	1.9012E-01	2.3299E-01	2.8120E-01	3.4166E-01

Table 5 Calculated covariance matrices for same nuclide at different energy points

Nuclide	Energy	V^R		V^A		V^C	
^{95}Zr	T	7.0304E-04	3.8200E-04	2.8527E-02	1.5354E-02	1.0000E+00	5.4029E-01
	F		7.1104E-04		2.8311E-02		1.0000E+00
^{103}Ru	T	2.7293E-03	2.3940E-03	2.5891E-02	2.6987E-02	1.0000E+00	8.8220E-01
	F		2.6982E-03		3.6144E-02		1.0000E+00
^{131}I	T	3.3065E-03	3.0490E-03	3.3437E-02	3.9171E-02	1.0000E+00	9.1944E-01
	F		3.3258E-03		5.4283E-02		1.0000E+00
^{132}I	T	4.9814E-03	4.5130E-03	6.2778E-02	6.3604E-02	1.0000E+00	9.0276E-01
	F		5.0169E-03		7.9071E-02		1.0000E+00
^{140}Ba	T	2.9666E-03	2.6570E-03	1.1404E-01	1.0444E-01	1.0000E+00	9.0522E-01
	F		2.9041E-03		1.1673E-01		1.0000E+00

Note: V^R relative covariance matrix

V^A absolute covariance matrix

V^C correlation coefficient matrix

T thermal energy

F fission spectrum

4 Conclusion

With present method, so called parameter analysis, and program the covariance matrix can be constructed conveniently for absolutely measured fission yield, just inputting the errors of directly measurable parameters, which are familiar with for experimenters or evaluators. The correlation coefficients of the parameters are included in the code and needn't be input. As shown by the example, constructed matrices including the errors of the yields are reasonable.

The authors would like to express their appreciation to Prof. Li Ze and Associate Prof. Liu Yonghui for their beneficial discussion on the measurement of fission yield.

Reference

[1] Wang Yusheng et al., Jour. of Nucl. and Radiochemistry,2,(1),9(1980).

V BENCHMARK TESTING

Thermal and Fast Reactor Benchmark Testing of ENDF/B-6.4

Liu Guisheng
(China Nuclear Data Center, CIAE)

Introduction

In 1995 and 1996, CNDC made homogeneous fast and thermal reactor benchmark testing of CENDL-2 and B-6.2(ENDF/B-6 version 2), respectively[1, 2]. It proved that ^{238}U data of CENDL-2 are better than those of B-6.2.

For fast reactor benchmarks, B-6.2 shows 1~2 % larger k_{eff} than CENDL-2 for the cores with ^{238}U fuel and reflector. The difference is mainly caused by ^{238}U data, especially its inelastic data. The inelastic scattering cross sections of ^{238}U from B-6.2 makes the fast neutron spectrum hardened and increases of neutron production rate. In thermal reactor benchmark testing, the k_{eff} values calculated using B-6.2 for both lattice assembly TRX-1 and TRX-2 with metal uranium fuel rod are underestimated from 0.6 % to 1 %. And for BAPL-UO_2-1, -2 and -3 with uranium oxide fuel rod lattice, the k_{eff} values calculated using B-6.2 are underestimated by about 0.2 % to 0.5 %.

Last year, CNDC received new version of B-6.4 (ENDF/B version 4). In order to understand the state of development of ENDF/B-6, it is necessary to carry out fast and thermal reactor benchmark testing of B-6.4 again.

The benchmark testing for B-6.4 was done with the same benchmark experiments and calculating method as for B-6.2[1, 2]. The effective multiplication factors k_{eff}, central reaction rate ratios of fast assemblies and lattice cell reaction rate ratios of thermal lattice cell assemblies were calculated and compared with testing results of B-6.2 and CENDL-2.

It is obvious that ^{238}U data files are most important for the calculations of large fast reactors and lattice thermal reactors. However, ^{238}U data in the new version of

ENDF/B-6 have not been renewed. Only data of ^{235}U, ^{27}Al, ^{14}N and ^{2}D have been renewed in ENDF/B-6.4. Therefor, it will be shown that the thermal reactor benchmark testing results are remarkably improved and the fast reactor benchmark testing results are not been improved.

1 Thermal Reactor Benchmark Testing

1.1 Multigroup Constant Generations and Benchmark Calculations

NSLINK code system[3] were used to process B-6.4 and generating 123 group cross sections in AMPX master library format. A modified code system[4] PASC-1 was used in the calculations. The first step, it calculates a lattice-cell spectrum of 123 groups in P_3 S_8 for heterogeneous assembly or infinite medium spectrum for homogeneous assembly and produces spectrum averaging cross section set of 48 groups. The second step, it is used for critical calculations. For heterogeneous assembly, the experimental total buckling is used to account for leakage correction. The calculated integral parameters include k_{eff} and lattice-cell reaction rate ratios ρ^{28}, δ^{25}, δ^{28} and C*.

1.2 Effective Multiplication Factors

Table 1 presents the calculated k_{eff} values of 13 thermal reactor benchmark assemblies for B-6.4 obtained by CNDC along with the values of k_{eff} published for benchmark testing of B-6.2 and CENDL-2. In fact, new version data of ^{27}Al, ^{14}N and ^{2}D were changed only in the high energy region, and the variances between old and new versions do not affect the calculated results for thermal benchmarks testing.

In Table 1 all of the testing results for B-6.2 indicate that the calculated values of k_{eff} are underestimated notably. Naturally, the data of some important nuclides, for example, ^{238}U and ^{235}U in ENDF/B-6 library, should be reevaluated. In fact, ^{238}U data are most important but it has never been changed from B-6.2 to B-6.4. For ^{235}U in the B-6.4 the data files of σ_t, σ_f, σ_c and σ_e below 1 keV were changed and ν_f values below 10 keV were increased by 0.082 %, as compared with that of B-6.2. The variance between two versions results in increasing the calculated k_{eff} values.

For different assemblies the variances of the calculated values of k_{eff} are different. Let Δk_{eff} express the calculated value of k_{eff} using B-6.4 decreased by using B-6.2. For the light water moderated assemblies the Δk_{eff} values of TRX-1 and TRX-2 are less than these of BAPL-UO_2-1, -2 and -3. And the Δk_{eff} values of ZEEP-1, -2 and -3 with heavy water moderator are the biggest, compared with these assemblies with light water moderator. That is to say, k_{eff} is gradually increased with

that spectrum of assembly softens. It is the reason that the more neutrons are absorbed in the light-water moderated system. Therefor, the increments of Δk_{eff} for assemblies ZEEP-1,-2 and -3 with heavy-water moderator are from 0.31% to 0.25%, respectively, and they are about two times larger than that for the others with light-water moderator.

Table 1 Results of k_{eff} Calculations

Assembly	CENDL-2	ENDF/B6.4	ENDF / B - 6 . 2					Δk_{eff}
	CNDC Sn, 123 g Ref. 2	CNDC Sn, 123 g this work	CNDC Sn, 123 g Ref. 2	ORNL Sn,123g Ref. 5	LANL Sn, 69g Ref. 6	JAERI MC Ref. 7	KAERI WIMS Ref. 8	
ORNL-1	0.9995	0.9978	0.9971	0.9965	0.9969	—	—	0.0007
ORNL-2	0.9990	0.9973	0.9968	0.9964	0.9967	—	—	0.0005
ORNL-3	0.9959	0.9943	0.9938	0.9935	—	—	—	0.0005
ORNL-4	0.9973	0.9957	0.9952	0.9950	—	—	—	0.0005
ORNL-10	0.9944	0.9932	0.9928	0.9961	0.9972	—	—	0.0004
TRX-1	0.9968	0.9923	0.9909	0.9894	0.9869	0.9919	0.9908	0.0014
TRX-2	0.9993	0.9947	0.9939	0.9915	0.9891	0.9925	0.9924	0.0008
BAPL-UO_2-1	0.9998	0.9966	0.9949	0.9975	0.9949	—	0.9952	0.0017
BAPL-UO_2-2	1.0007	0.9975	0.9957	0.9971	0.9959	—	0.9951	0.0018
BAPL-UO_2-3	1.0027	0.9992	0.9979	0.9972	0.9974	—	0.9960	0.0013
ZEEP-1	1.0019	1.0029	0.9998	—	—	—	—	0.0031
ZEEP-2	1.0001	1.0008	0.9981	—	—	—	—	0.0027
ZEEP-3	0.9987	0.9994	0.9969	—	—	—	—	0.0025

Note: $\Delta k_{eff} = k_{eff}(B6.4) - k_{eff}(B6.2)$

^{238}U data play an important role in thermal reactor calculations because its contents in the fuel rod of lattice-cell assembly are more than 96 % for light-water moderator system and 99 % for heavy-water moderator system, respectively. It is obvious that improving calculation results are essentially impossible when data of ^{238}U are neverre-evaluated .

1.3 Lattice Cell Reaction Rate Ratios

The lattice cell reaction rate ratios ρ^{28}, δ^{25}, δ^{28} and C^* of five lattice assemblies with light water moderator were calculated using B-6.4. The calculated results together with B-6.2 from CNDC[2] and KAERI[8] are given in Table 2.

Table 2 Calculation results of lattice-cell reaction rate ratios (C / E)

Assembly	ρ^{28} epithermal / thermal ^{238}U capture				δ^{25} epithermal / thermal ^{235}U fission			
	CENDL-2	ENDF / B-6.2		ENDF/B-6.4	CENDL-2	ENDF / B-6.2		ENDF/B-6.4
	CNDC	CNDC	KAERI	CNDC	CNDC	CNDC	KAERI	CNDC
TRX-1	1.0533	1.0448	1.0490	1.0343	1.0049	1.0102	0.9960	1.0034
TRX-2	1.0342	1.0248	1.0390	1.0177	0.9899	0.9945	0.9530	0.9881
BAPL-UO_2-1	1.0475	1.0373	1.0360	1.0257	0.9957	1.0000	0.9640	0.9926
BAPL-UO_2-2	1.0813	1.0704	1.0710	1.0571	1.0021	1.0065	0.9710	0.9990
BAPL-UO_2-3	1.0451	1.0374	1.0350	1.0236	1.0054	1.0094	0.9810	1.0023
	δ^{28} ^{238}U fission / ^{235}U fission				C^* ^{238}U capture / ^{235}U fission			
TRX-1	1.0148	1.0433	1.0610	1.0389	1.0039	1.0113	1.0150	1.0042
TRX-2	0.9812	1.0025	1.0026	0.9999	0.9919	0.9998	1.0050	0.9955
BAPL-UO_2-1	0.9977	0.9782	1.0000	0.9721	—	—	—	—
BAPL-UO_2-2	0.9174	0.9353	0.9570	0.9300	—	—	—	—
BAPL-UO_2-3	0.9223	0.9381	0.9650	0.9340	—	—	—	—

Table 2 shows that the lattice cell reaction rate ratios of calculation value to experimental value, that is C / E, for TRX-1 and -2 using B-6.4 are obviously improved, compared with using B-6.2. For example, the values of ρ^{28} for TRX-1 and -2 are decreased by 1% and 0.7%, respectively. Both of δ^{25} for two assemblies are decreased by 0.7%. δ^{28} and C^* are also improved. For assemblies with UO_2 fuel rods, however, improvements of values of δ^{25} are not obvious, except ρ^{28}. It seems that values of δ^{28} become a little bad.

In order to analyze these results conveniently lattice cell spectrum average cross sections and fluxes of six groups are calculated. The sixth group among them is the thermal group and the cut-off of thermal energy is 0.625 eV. The data of ^{235}U and ^{238}U cross sections and fluxes of fifth and sixth group from B-6.4 and B-6.2 are listed in Table 3, respectively.

First of all, it is found from Table 3 that both of the calculated thermal or epithermal average flux for same assembly using B-6.4 are decreased, as compared with using B-6.2. Besides, there are large differences in the calculated spectra for different assemblies. It can be seen that the changes of lattice cell parameters come from the changes of ^{235}U cross sections and flux spectrum from B-6.2 to B-6.4. And the changes are different for different assemblies.

^{235}U fission cross sections in the thermal energy region are increased 0.41 barn for TRX-2 and 0.528 barn for BAPL-UO_2-1. And its epithermal fission cross sections are decreased about 0.2 barn for all four assemblies. The differences of

thermal fluxes for assemblies between B-6.4 and B-6.2, however, are small, therefore δ^{25} (epithermal / thermal ^{235}U fission) using B-6.4 is decreased 0.7% and is more close to experimental value.

Table 3 Comparison of lattice cell average fluxes and thermal and epithermal cross sections between B-6.2 andB-6.4

Assembly	TRX-1		TRX-2		BAPL-UO_2-1		BAPL-UO_2-3	
Lattice cell pitch	1.806/cm		2.174/cm		1.5578/cm		1.8057/cm	
E Upper /eV	1.324E3	0.625	1.324E3	0.625	1.324E3	0.625	1.324E3	0.625
E Lower /eV	0.625	1E-5	0.625	1E-5	0.625	1E-5	0.625	1E-5
B-6.4 average flux	5.7904	6.0753	5.4859	9.2544	7.5588	8.5173	6.6825	11.5766
B-6.2 average flux	5.7935	6.0852	5.4879	9.2640	7.5610	8.5284	6.6837	11.5864
$^{B\text{-}6.4}$flux − $^{B\text{-}6.2}$flux	−0.0031	−0.0099	−0.0020	−0.0096	−0.0022	−0.0111	−0.0012	−0.0098
^{235}U B-6.4 σ_c/b	15.196	56.075	15.300	56.913	16.007	63.690	16.172	66.438
^{235}U B-6.2 σ_c/b	14.048	56.101	14.157	56.973	14.796	63.732	14.962	66.514
$\Delta_c = {}^{B\text{-}6.4}\sigma_c - {}^{B\text{-}6.2}\sigma_c$	+1.148	−0.026	+1.143	−0.060	+1.211	−0.042	+1.210	−0.076
^{235}U B-6.4 σ_f/b	28.519	329.962	28.693	335.485	29.618	374.053	29.874	390.583
^{235}U B-6.2 σ_f/b	28.715	329.469	28.890	335.075	29.815	373.525	30.074	390.121
$\Delta_f = {}^{B\text{-}6.4}\sigma_f - {}^{B\text{-}6.2}\sigma_f$	−0.196	+0.493	−0.197	+0.410	−0.197	+0.528	−0.200	+0.462
^{238}U B-6.4 σ_c/b	1.0773	1.6252	1.7533	1.6394	2.2915	1.8313	2.4233	1.8983
^{238}U B-6.2 σ_c/b	1.0778	1.6253	1.7539	1.6395	2.2920	1.8314	2.4237	1.8984
$\Delta_c = {}^{B\text{-}6.4}\sigma_c - {}^{B\text{-}6.2}\sigma_c$	−0.0005	−0.0001	−0.0006	−0.0001	−0.0005	−0.0001	−0.0004	−0.0001

^{235}U thermal capture cross sections are decreased 0.026 barns for TRX-1 and 0.076 barns for BAPL-UO_2-3, and its epithermal capture cross sections are increased about 1.148 and 1.121 barns. It results in a decrement of epithermal fluxes. Owing to the difference of spectrum, for the same assembly the average ^{238}U capture cross sections using B-6.4 have decrement, though the data of ENDF/B-6 have not been changed. Consequently, ρ^{28} (epithermal / thermal ^{238}U capture) obtained using B-6.4 is decreased about 1% and is more close to experimental value. The most obvious improvement is ρ^{28}. It is natural that C^* is improved.

Furthermore, all σ_e values of ^{235}U in the thermal and epithermal regions are decreased by tens mb. All the σ_t values of ^{235}U in the thermal and epithermal regions are also increment because of the increment of thermal σ_f and epithermal σ_c.

2. Fast Reactor Benchmark Testing

2.1 Multigroup Constant Generations and Benchmark Calculations

NSLINK code system was applied to processing B-6.4 and generating 175 group library with VITAMIN-J energy group structure in AMPX master library format.

The PASC-1 code system was used in the calculations. Firstly, it performs a resonance self-shielding calculation based on the Bondarenko method and generates problem-dependent master data set. Then, it calculates k_{eff} and central reaction rate ratios with 175 groups in P_3 S_{32} .

2.2 Effective Multiplication Factors

In the fast reactor benchmarks testing, only the data files of ^{235}U and ^{241}Pu have been changed from B-6.2 to B-6.4. The variances of ^{241}Pu data matters little to testing results, because its content is too small in fast reactor concerned. The changes of cross section data of ^{235}U are merely arisen below 2 keV. Considering fast reactors the flux above this energy is much higher than that below this energy, so that there are no obvious changes for the recalculated reactor parameters.

Table 4 presents the calculated k_{eff} values of nine homogeneous assemblies for B-6.4 obtained by CNDC along with the values of k_{eff} published for benchmark testing of B-6.2[1],[5],[6],[7],[9]. As expected, the calculated k_{eff} values are almost the same with the two libraries of different versions. That is to say, there is no any improvement for the fast reactor testing results from B-6.2 to B-6.4.

It is well known that the results for uranium fuel system from CENDL-2 are better than those from B-6.4. The data of ^{238}U from CENDL-2 used in calculations gives good results for all of uranium fuel assemblies with hard and soft spectra. The k_{eff} value of BIG-10 for B-6.4 or B-6.2 was overestimated by 2%, because the calculated spectrum is too hard.

In fast reactor benchmark testing, both B-6.4 and B-6.2 show 1~2% larger k_{eff} than CENDL-2 for the cores with ^{238}U fuel and reflector. The difference is mainly caused from ^{238}U data, especially its inelastic data. Inelastic scattering cross sections of ^{238}U from ENDF/B-6 make harder fast neutron spectrum and increases neutron production rate. Consequently, it leads the k_{eff} value to a increment. Dr. Takano gave

the same conclusion as our results for B-6.2[7]. Therefor, It is to say the data of ^{238}U of CENDL-2 is much better than that of ENDF/B-6.

Table 4 Results of k_{eff} calculations for fast reactor benchmark testing

ASSEMBLY	CENDL-2	B-6.4	ENDF / B-6.2				
	CNDC	CNDC	CNDC	ORNL	LANL	M. Caro	JAERI
	Ref. 1	This work	Ref. 1	Ref. 5	Ref. 6	Ref. 9	Ref. 7
GODIVA	1.00003	0.99946	0.99946	0.9960	0.9983	0.9954	0.9965
FLATTOP-25	1.00142	1.00782	1.00785	1.0018	1.0030	1.0007	1.0073
BIG-10 C	0.99541	1.01576	1.01576	1.0171	1.0105	1.0063	1.0149
C / E	0.99940	1.01984	1.01984	—	—	—	—
JEZEBEL	1.00430	1.00053	1.00056	0.9970	0.9989	0.9960	0.9972
JEZEBEL-Pu	1.00391	1.00181	1.00261	0.9980	0.9981	0.9893	0.9987
FLATTOP-Pu	1.00066	1.00883	1.00886	1.0029	1.0055	1.0025	1.0041
JEZEBEL-23	0.99463	0.99458	0.99458	0.9934	0.9940	0.9929	0.9933
FLATTOP-23	1.00187	1.00645	1.00645	1.0032	1.0041	1.0026	1.0028
THOR	1.00925	1.00721	1.00721	—	—	1.0056	1.0059

2.3 Central Reaction Rate Ratios

Table 5 represents the results of central reaction rate ratios of nine assemblies which were calculated by CNDC for B-6.2, B-6.4 and CENDL-2. The reaction rates are all relative to that of fission of ^{235}U. The C/E represents a ratio of calculation value to experimental value.

It is clear that there are no obvious variations in the calculated results between B-6.2 and B-6.4, except F28. For assembly JEZEBEL-Pu F28 is underestimated by 0.24% for B-6.4, compared with B-6.2. It arises from the variations of ^{241}Pu data in both of ENDF/B-6 libraries. The variations from B-6.2 to B-6.4 do not result in a obvious difference of two calculation values of F28 for JEZEBEL, because the nuclear density of ^{241}Pu is only 0.000117(nuclei/b-cm), about twelve times less than JEZEBEL-Pu.

Considering calculation results for CENDL-2, very satisfactory results were obtained for three uranium fuel assemblies. Especially, F28 and C28 for BIG-10 are much better than that from both of ENDF/B-6 libraries. F28 of BIG-10 using B-6.4 or B-6.2 is about 5 percent larger than experimental value but C28 is about 5 percent less than it, but the results for other assemblies with harder spectra are satisfactory.

Table 5 Central Reaction Rate Ratios (*C/E*)

Assembly	Exp.	CENDL-2	B-6.2	B-6.4	Assembly	Exp.	CENDL-2	B-6.2	B-6.4
GODIVA	F28 .1647	0.9866	0.9879	0.9879	JEZEBEL	F28 .2137	0.9708	0.9839	0.9836
	F49 1.402	0.9971	0.9883	0.9883		F49 1.448	0.9941	0.9818	0.9812
	F 37 0.837	0.9719	0.9883	0.9883		F37 0.962	0.9828	0.9874	0.9873
	F 23 1.590	0.9999	1.0002	1.0002		F23 1.578	1.0016	0.9987	0.9987
FLATTOP -25	F 28 0.149	0.9993	0.9968	0.9966	JEZEBEL -Pu	F28 0.206	0.9861	0.9941	0.9917
	F 49 1.370	1.0020	0.9953	0.9953		F37 0.920	1.0116	1.0164	1.0157
	F 37 0.760	0.9937	1.0141	1.0141	FLATTOP -Pu	F28 0.180	0.9733	0.9909	0.9908
	F 23 1.600	0.9920	0.9936	0.9936		F 37 0.840	0.9821	0.9987	0.9986
BIG-10	F 28 .0373	1.0046	1.0512	1.0512	JEZEBEL -23	F 28 .2131	1.0588	1.0560	1.0558
	C28 0.110	1.0032	0.9475	0.9473		F 37 0.977	0.9821	1.0256	1.0257
	F 49 1.185	0.9704	0.9948	0.9948	FLATTOP -23	F 28 0.191	1.0473	1.0453	1.0455
	F 37 0.316	0.9410	1.0639	1.0639		F 37 0.890	1.0111	1.0331	1.0330
	F 23 1.580	0.9850	0.9954	0.9954	THOR	F 28 0.195	0.9620	0.9760	0.9759
						C28 0.083	0.8471	0.8413	0.8413
						F 37 0.920	0.9512	0.9548	0.9548

Note : F28, ratio of ^{238}U fission rate to ^{235}U fission rate,
C28, ratio of ^{238}U capture rate to ^{235}U fission rate,
F49, ratio of ^{239}Pu fission rate to ^{235}U fission rate,
F37, ratio of ^{237}Np fission rate to ^{235}U fission rate,
F23, ratio of ^{233}U fission rate to ^{235}U fission rate.

3. Conclusions

To sum up, some conclusions can be obtained :

(1) Obvious improvement has been made in the thermal reactor benchmark testing of B-6.4, but the calculated values of k_{eff} are still 0.0017 lower for homogeneous assemblies, 0.0045 for TRX-1 and -2 and 0.0032 for BAPL-UO_2-1, -2 and -3, respectively, less than that of CENDL-2.

(2) For fast reactor benchmarks testing of B-6.4, there is no any improvement, as compared with B-6.2, both of ENDF/B versions show 1~2% larger k_{eff} than that of CENDL-2 for the cores or reflectors with ^{238}U fuel. The results from CENDL-2 are much better than those from Both ENDF/B-6.

(3) For the ^{235}U data of B-6.4, the values of σ_f in the thermal energy region and ν_f values below 10 keV are increased, compared with that of B-6.2. The variances between two versions result in the increase calculated k_{eff} values for thermal reactor benchmark testing but yet it does not avail for fast reactor benchmark testing of B-6.4.

(4) The σ_c values of ^{235}U in the epithermal energy region are increased, so that epithermal neutron flux is decreased, the calculated values of lattice cell parameter ρ^{28} are improved and δ^{25} values are decreased. The calculated values of energy spectrum indexes, however, are not improved for fast reactor benchmark testing of B-6.4.

(5) Owing to the ^{238}U inelastic cross sections of both ENDF/B-6 libraries make neutron spectrum of nuclear assembly hardened and underestimate neutron moderating power, the neutron production rate in the high energy region is remarkably overestimated and number of neutrons in the low energy region is remarkably underestimated. Consequently, k_{eff} for thermal reactor calculations is underestimated and is overestimated for fast reactor calculations . Owing to that ^{238}U data play an important role in thermal reactor or large fast reactor calculations, it is obvious that improving calculation results are essentially impossible without renewing data of ^{238}U.

(6) The recent experiments about $^{238}U(n,n')$ seem to indicate that the data of ^{238}U in ENDF/B-6 are not the best, and all these activities will lead to significant changes of the data for ^{238}U[10].

Reference

[1] Liu Guisheng, Homogeneous Fast Reactor Benchmark Testing of CENDL-2 and ENDF/B-6, INDC(CPR)-034 / L, p. 107 (1995).

[2] Liu Guisheng, Thermal Reactor Benchmark Testing of CENDL-2 and ENDF/B-6,INDC(CPR)-040 / L, p. 87 (1996).

[3] P. F. A. de Leege, IRI-131-091-003, Delft University, Netherlands, 1991.

[4] Liu Guisheng et al., Chinese Journal of Nuclear Science and Engineering, Vol. 13 No.3, p. 9, Sep., 1993.

[5] R. Q. Wright et al., Proceedings Inter. Conf. on Nucl. Data for Sci. and Tech.,Vol. 2, p. 815, Gatlinburg, Tennessee, May 9~13, 1994.

[6] R. E. MacFalane, ibid., p. 786, 1994.

[7] H. Takano et al., Proceedings Inter. Conf. on Nucl. Data for Sci. and Tech.,p. 1122, Trieste, Italy, May 19~24, 1997.

[8] Jung-do- Kim et al., (KAERI), INDC(JPN)-157 / L, p. 394 (1992).

[9] M. Caro et al., Proceedings Inter. Conf. on Nucl. Data for Sci. and Tech., p. 214,Berlin, Germany, May 13~17, 1991.

[10] Chao Yungan, private Communication from Westinghouse Company in U.S.A (1998).

VI NUCLEAR ACTIVITIES

Activities and Cooperation on Nuclear Data in China During 1998

Liu Tong
(China Nuclear Data Center, IAE)

1 Meetings Held in China during 1998

1) The Meeting on Evaluation and Calculation of Neutron Data for Fission Nuclides, Jan. 12-14, Beijing.
2) The Symposium of Benchmark Testing Working Group, Apr. 25-28, Yangzhou.
3) The Symposium of Nuclear Data Measurement Working Group, May. 11-15, Zhejiang.
4) The Joint Symposium of Nuclear Data Evaluation working Group and Nuclear Data working Group, Sep. 13-15, Chengdu.

2 The International Meetings and Workshops in Nuclear Data Field Attended by Staff of CNDC in 1998

1) Workshop on Nuclear Reaction Data and Nuclear Reactors Physics Design and Safety, Feb. 23-Mar. 19, Fan Sheng, Ge Zhigang, Rong Jian, ICTP.
2) IAEA Advisory Group Meeting on the Coordination of the Nuclear Reaction Data Centers, May. 11-15, Liu Tong, Vienna .
3) The meeting of NEA. Working Party on International Evaluation Cooperation, June 15-19, Liu Tingjin, Belgium.
4) The second Research Coordination Meeting on Compilation and Evaluation of Photo-Nuclear Data for Applications, June 21-30, Yu Baosheng, USA.

5) The 3rd Research Co-ordination Meeting on Development of Reference Charged Particle Cross Section Database for Medical Radioisotope Production, Sep. 26~Oct. 4, Zhuang Youxiang, Belgium.
6) The Fifth College on Microprocessor-Based Read-Time System in Physics, Oct. 8~Nov. 16, Shu Nengchuan, ICTP.
7) The Coordinate Meeting on Nuclear Structure and Decay Data, Dec. 14-17, Zhou Chunmei, Vienna.

3 The Foreign Scientists in Nuclear Data Field Visited CNDC/CIAE in 1998

Dr. A. Hasegawa, JAERI/NDC, Japan, Nov. 25~31.
Dr. E.T. Cheng, San Diego, USA, Nov. 31

4 Staff of CNDC Worked or Working in Foreign Country

Zhuang Youxiang, Nuclear Data Evaluation Lab of KAERI, half a year,
Han YinLu, Nuclear Data Evaluation Lab. of KAERI, scheduled one year,
Huang Xiaolong, Nuclear Data Center in JAERI, scheduled one year,
Zhang Baocheng, Engineering Development Company (EDC) in Japan, scheduled one year.

CINDA INDEX

Nuclide	Quantity	Energy/ eV		Lab	Type	Documentation					Author, Comments
		Min	Max			Ref	Vol	Page	Date		
^{6}Li	(n,t)	3.67+6	4.42+6	BJG	Expt	Jour CNDP	21	1	Jun	99	Zhang Guohui+, T, DA, SIG, CRV
^{39}K	(n,α)	4.41+6	6.52+6	BJG	Expt	Jour CNDP	21	11	Jun	99	Zhang Guohui+, IC, DA/DE, SIG, CRV
^{63}Cu	(n,2n)	Thrsh	2.0+7	SIU	Eval	Jour CNDP	21	59	Jun	99	Ma Gonggui, SIG
	(n,γ)	Thrsh	2.0+7	SIU	Eval	Jour CNDP	21	59	Jun	99	Ma Gonggui, SIG
	Evaluation	1.0-5	2.0+7	SIU	Eval	Jour CNDP	21	59	Jun	99	Ma Gonggui, SIG, DA, DE
^{65}Cu	(n,2n)	Thrsh	2.0+7	SIU	Eval	Jour CNDP	21	83	Jun	99	Ma Gonggui, SIG, DA, DE
	(n,γ)	Thrsh	2.0+7	SIU	Eval	Jour CNDP	21	83	Jun	99	Ma Gonggui, SIG, DA, DE
^{Nat}Cu	(n,2n)	Thrsh	2.0+7	SIU	Eval	Jour CNDP	21	83	Jun	99	Ma Gonggui, SIG, DA, DE
	(n,γ)	Thrsh	2.0+7	SIU	Eval	Jour CNDP	21	83	Jun	99	Ma Gonggui, SIG, DA, DE
^{69}Ga	Calculation	1.0+3	2.0+7	AEP	Theo	Jour CNDP	21	52	Jun	99	Zhang Songbai+, MDL, CALC, SIG, DA, DE
^{71}Ga	Calculation	1.0+3	2.0+7	AEP	Theo	Jour CNDP	21	52	Jun	99	Zhang Songbai+, MDL, CALC, SIG, DA, DE
^{83}Kr	Calculation	1.0+3	2.0+7	NKU	Theo	Jour CNDP	21	40	Jun	99	Cai Chonghai, MDL, CALC, SIG, DA, DE
^{84}Kr	Calculation	1.0+3	2.0+7	NKU	Theo	Jour CNDP	21	40	Jun	99	Cai Chonghai, MDL, CALC, SIG, DA, DE
^{85}Kr	Calculation	1.0+3	2.0+7	NKU	Theo	Jour CNDP	21	40	Jun	99	Cai Chonghai, MDL, CALC, SIG, DA, DE
^{86}Kr	Calculation	1.0+3	2.0+7	NKU	Theo	Jour CNDP	21	40	Jun	99	Cai Chonghai, MDL, CALC, SIG, DA, DE
^{90}Zr	γ-reaction	1.0-5	3.0+7	AEP	Eval	Jour CNDP	21	108	Jun	99	Yu Baosheng
^{91}Zr	γ-reaction	1.0-5	3.0+7	AEP	Eval	Jour CNDP	21	108	Jun	99	Yu Baosheng
^{92}Zr	γ-reaction	1.0-5	3.0+7	AEP	Eval	Jour CNDP	21	108	Jun	99	Yu Baosheng
^{94}Zr	γ-reaction	1.0-5	3.0+7	AEP	Eval	Jour CNDP	21	108	Jun	99	Yu Baosheng
^{96}Zr	γ-reaction	1.0-5	3.0+7	AEP	Eval	Jour CNDP	21	108	Jun	99	Yu Baosheng
^{93}Nb	(n,2n)		1.4+7	LNZ	Expt	Jour CNDP	21	6	Jun	99	Li Gongping+, ACTIC, CS, TBL
^{103}Rh	Evaluation	1.0-5	2.0+7	NAN	Eval	Jour CNDP	21	100	Jun	99	Zhao Jingwu+, SIG, DA, DE
^{105}Pd	Evaluation	1.0-5	2.0+7	NAN	Eval	Jour CNDP	21	95	Jun	99	Su Weuning+, SIG, DA, DE

CINDA INDEX

Nuclide	Quantity	Energy/ eV		Lab	Type	Documentation				Author, Comments
		Min	Max			Ref	Vol	Page	Date	
^{108}Pd	Evaluation	1.0-5	2.0+7	NAN	Eval	Jour CNDP	21	95	Jun 99	Su Weuning+, SIG, DA, DE
^{115}In	Evaluation	1.0-5	2.0+7	NAN	Eval	Jour CNDP	21	88	Jun 99	Zhao Jingwu+, SIG, DA, DE
^{140}Ce	Evaluation	1.0-5	2.0+7	AEP	Eval	Jour CNDP	21	70	Jun 99	Yu Baosheng+, SIG, DA, DE
^{141}Ce	Evaluation	1.0-5	2.0+7	AEP	Eval	Jour CNDP	21	70	Jun 99	Yu Baosheng+, SIG, DA, DE
^{142}Ce	Evaluation	1.0-5	2.0+7	AEP	Eval	Jour CNDP	21	70	Jun 99	Yu Baosheng+, SIG, DA, DE
^{144}Ce	Evaluation	1.0-5	2.0+7	AEP	Eval	Jour CNDP	21	70	Jun 99	Yu Baosheng+, SIG, DA, DE
^{135}Ba	Evaluation	1.0+4	2.0+7	NAN	Eval	Jour CNDP	21	118	Jun 99	Zhao Jingwu+, SIG
^{136}Ba	Evaluation	1.0+4	2.0+7	NAN	Eval	Jour CNDP	21	118	Jun 99	Zhao Jingwu+, SIG
^{137}Ba	Evaluation	1.0+4	2.0+7	NAN	Eval	Jour CNDP	21	118	Jun 99	Zhao Jingwu+, SIG
^{138}Ba	Evaluation	1.0+4	2.0+7	NAN	Eval	Jour CNDP	21	118	Jun 99	Zhao Jingwu+, SIG
^{151}Eu	Calculation	1.0+3	2.0+7	AEP	Theo	Jour CNDP	21	35	Jun 99	Ge Zhigang, MDL, CALC, SIG, DA, DE
^{153}Eu	Calculation	1.0+3	2.0+7	AEP	Theo	Jour CNDP	21	35	Jun 99	Ge Zhigang, MDL, CALC, SIG, DA, DE
^{154}Eu	Calculation	1.0+3	2.0+7	AEP	Theo	Jour CNDP	21	35	Jun 99	Ge Zhigang, MDL, CALC, SIG, DA, DE
^{155}Eu	Calculation	1.0+3	2.0+7	AEP	Theo	Jour CNDP	21	35	Jun 99	Ge Zhigang, MDL, CALC, SIG, DA, DE
^{235}U	Calculation	1.0+3	2.0+7	NKU	Theo	Jour CNDP	21	16	Jun 99	Cai Chonghai+, MDL, CALC, SIG, DA, DA/DE γ Emission

图书在版编目（CIP）数据

中国核科技报告 CNDC-0024 CNIC-01373：核数据进展通讯 No.21：英文/刘挺进等著. —北京：原子能出版社，1999.7

ISBN 7-5022-2033-X

I. 中… II. 刘… III. 核技术-研究报告-中国-英文 IV. TL-2

中国版本图书馆 CIP 数据核字 (1999) 第 24352 号

原子能出版社出版发行

责任编辑：李曼莉

社址：北京市海淀区阜成路 43 号 邮政编码：100037

中国核科技报告编辑部排版

核科学技术情报研究所印刷

开本：787×1092 mm 1/16 印张 9 字数 144 千字

1999 年 7 月北京第一版 1999 年 7 月北京第一次印刷

印数：1—800

定价：10.00 元